

UC San Diego

UC San Diego Electronic Theses and Dissertations

Title

Ichthyoliths as a paleoceanographic and paleoecological proxy and the response of open-ocean fish to Cretaceous and Cenozoic global change

Permalink

<https://escholarship.org/uc/item/60d8q1w2>

Author

Sibert, Elizabeth Claire

Publication Date

2016

Peer reviewed|Thesis/dissertation

UNIVERSITY OF CALIFORNIA, SAN DIEGO

Ichthyoliths as a paleoceanographic and paleoecological proxy
and the response of open-ocean fish to Cretaceous and Cenozoic global change

A dissertation submitted in partial satisfaction of the
requirements for the Degree Doctor of Philosophy

in

Oceanography

by

Elizabeth Claire Sibert

Committee in charge:

Professor Richard D. Norris, Chair
Professor Lin Chao
Professor Peter J. S. Franks
Professor Philip A. Hastings
Professor Lisa A. Levin

2016

Copyright

Elizabeth Claire Sibert, 2016

All Rights Reserved

The dissertation of Elizabeth Claire Sibert is approved, and it is acceptable in quality and form for publication on microfilm and electronically:

Chair

University of California, San Diego

2016

DEDICATION

For Midnight

I love you forever, my little bear

TABLE OF CONTENTS

SIGNATURE PAGE	iii
DEDICATION	iv
TABLE OF CONTENTS	v
LIST OF FIGURES	viii
LIST OF TABLES	xi
ACKNOWLEDGEMENTS	xii
VITAE	xx
ABSTRACT OF THE DISSERTATION	xxi
CHAPTER 1 Introduction to the Dissertation	1
1.1 Introduction	2
1.2 Outline of the Dissertation	9
1.3 References	14
CHAPTER 2 Methods for isolation and quantification of microfossil fish teeth and elasmobranch dermal scales (ichthyoliths) from marine sediments	21
2.1 Abstract	22
2.2 Introduction	22
2.3 Methods for ichthyolith isolation and concentration	27
2.3.1 Carbonates	29
2.3.2 Pelagic clays	33
2.3.3 Silica-dominated sediments	34
2.3.4 Organic-rich sediments	37
2.3.5 Comments about ichthyolith-specific washing and picking techniques	39
2.4 Results and Discussion	41
2.4.1 Ichthyolith Accumulation Rates	41
2.4.2 Ichthyolith Community Metrics	46
2.5 Conclusions	49
2.6 References	50
2.7 Acknowledgements	55
CHAPTER 3 Resilience of Pacific pelagic fish across the Cretaceous/Palaeogene mass extinction	56
3.1 Abstract	57
3.2 Introduction	57
3.3 Results and Discussion	57
3.4 Methods	60
3.5 Acknowledgements	60
3.6 References	60
3.7 Supplementary Information	61
3.8 Supplementary Materials and Methods	62
3.9 Supplementary Discussion	70
3.10 Supplementary References	75
3.11 Supplementary Figures	77

CHAPTER 4	No evidence for productivity-driven dwarfing in pelagic fish communities following the Cretaceous-Paleogene Mass Extinction.....	94
4.1	Abstract.....	95
4.2	Introduction.....	96
4.3	Methods.....	98
4.4	Results and Discussion	99
4.5	Conclusion	105
4.6	References.....	106
4.7	Acknowledgements.....	109
CHAPTER 5	New Age of Fishes initiated by the Cretaceous– Paleogene mass extinction.....	110
5.1	Abstract.....	111
5.2	Introduction.....	111
5.3	Results.....	112
5.4	Discussion.....	113
5.5	Conclusions.....	115
5.6	Materials and Methods.....	115
5.7	Acknowledgements.....	116
5.8	References.....	116
5.9	Supporting Information.....	117
CHAPTER 6	A two-pulsed radiation of pelagic fishes following the K/Pg mass extinction.....	124
6.1	Abstract.....	125
6.2	Introduction.....	126
6.3	Methods.....	129
6.3.1	DSDP Site 596 lithology and ichthyolith isolation.....	129
6.3.2	Fish Tooth Morphology and Morphotypes.....	131
6.3.3	Morphospace Analyses	135
6.3.4	Estimation of evolutionary rates	136
6.4	Results.....	138
6.4.1	Stratigraphic Ranges of ichthyoliths.....	138
6.4.2	Ichthyolith abundance and sampling	141
6.4.3	Origination and extinction rates.....	143
6.4.4	Changes in Morphospace Occupation	148
6.5	Discussion.....	150
6.6	Conclusion	156
6.7	References.....	157
6.8	Appendix I: A novel coding scheme for quantifying the morphological variation of tooth-type ichthyoliths.....	163
6.8.1	Introduction.....	163
6.8.2	Coding System	165
6.8.3	Morphotype Designation	175
6.9	Appendix II: Rules used for removing potentially reworked teeth from analysis.....	176
6.9.1	Conservative reworking rules	178

6.9.2	Liberal reworking rules.....	179
6.10	Acknowledgements.....	180
CHAPTER 7	85 million years of Pacific Ocean gyre ecosystem structure: long-term stability marked by punctuated change.....	181
7.1	Abstract.....	182
7.2	Introduction.....	182
7.3	Cretaceous Ocean.....	183
7.4	Palaeogene Ocean.....	184
7.5	Modern Ocean.....	185
7.6	Conclusion.....	186
7.7	Methods.....	187
7.8	References.....	187
7.9	Supplementary Methods.....	189
7.10	Acknowledgements.....	197
CHAPTER 8	Conclusion to the Dissertation.....	198
8.1	Major Findings.....	199
8.2	A Cenozoic Age of Fishes.....	206
8.3	The future of ichthyolith work.....	207
8.4	References.....	209

LIST OF FIGURES

Figure 2-1: An assortment of large (>106µm fraction) denticles (elasmobranch scales; left) and fish teeth (right) from DSDP Site 596, a red clay core in the South Pacific.	23
Figure 2-2: A flowchart showing the steps for sediment processing for efficient and effective ichthyolith isolation from a variety of sediment types.....	29
Figure 2-3: Paleocene-aged ichthyoliths from ODP Site 1262, stained with Alizarin Red S.	36
Figure 2-4: Examples of select taxonomically identifiable fossil ichthyoliths and modern counterparts.....	45
Figure 3-1: Map of the sites included in this study and relative changes in ichthyolith accumulation across the boundary.	58
Figure 3-2: Global pattern of ichthyolith accumulation rates through the K/Pg mass extinction.....	58
Figure 3-3: Central Pacific (ODP Site 1209) comparison of mass accumulation rates for different trophic groups through the K/Pg mass extinction.	59
Figure 3-4: Figure S1. ODP Site 1209 shipboard measurements of dry bulk density and GRA (gamma ray attenuation).....	77
Figure 3-5: Figure S2. Relationship between GRA density and dry bulk density for ODP Hole 1209A.....	78
Figure 3-6: Figure S3. Dry bulk density calculated from GRA (gamma ray attenuation) and observed GRA to dry bulk relationship	79
Figure 3-7: Figure S4. Sedimentary mass accumulation rate (MAR) comparison between constant and variable dry bulk density.....	80
Figure 3-8: Figure S5. Ichthyolith mass accumulation rate (MAR) comparison between constant and variable dry bulk density.....	81
Figure 3-9: Figure S6. Relationship between total Fe and % carbonate for ODP Site 1209 based on published XRF Fe counts and % carbonate values from multiple sources.	82
Figure 3-10: Figure S7. % Carbonate as calculated from XRF Fe counts and the relationship between ln(Fe) and % carbonate.	83
Figure 3-11: Figure S8. Carbonate mass accumulation rate (MAR) comparison between constant % carbonate and variable % carbonate.....	84
Figure 3-12: Figure S9. Foraminiferal sized grain mass accumulation rate (MAR) comparison of proportion of non-carbonate grains in clay fraction only or all size fractions.....	85
Figure 3-13: Figure S10. Foraminiferal sized grain mass accumulation rate (MAR) comparison between Hull et al. (2011) and this study.....	86
Figure 3-14: Figure S11. Nannofossil sized grain mass accumulation rate (MAR) comparison between Hull et al. (2011) and this study.....	87
Figure 3-15: Figure S12. Mass accumulation rates (MAR) for (a) nannoplankton, (b) foraminifera, and (c) ichthyoliths, calculated using the Westerhold et al. (2008) age model solution 1 and the Hilgen et al. (2010) age model with variable dry bulk density.	88

Figure 3-16: Figure S13. Mass accumulation rates (MAR) for (a) Gubbio, Italy, and (b) ODP 1209, Shatsky Rise comparing age models.....	89
Figure 3-17: Figure S14. Extended version of Main Figure 2: ichthyolith accumulation rate at all sites considered in this study, including data generated by Shackleton (1984) from Walvis Ridge, DSDP Site 527 in the South Atlantic.	90
Figure 3-18: Figure S15. Fish MAR at Shatsky Rise compared to iron counts of Westerhold et al. (2008).....	91
Figure 3-19: Figure S16. Comparison of ichthyolith mass and sample large tooth count data.....	92
Figure 4-1: Ichthyolith accumulation rate (IAR) for ODP Site 1209 and ODP Site 1262.	101
Figure 4-2: Kernel density plots showing the percent large (>63µm) teeth in each assemblage, split by site and time bin.....	103
Figure 4-3: Absolute (top; a,c) and relative (bottom; b,d) abundance of each size class of ichthyoliths found in the Pacific (1209; top; a-b) and Atlantic (1262; top; c-d). 105	
Figure 5-1: Ichthyolith accumulation, ratio of teeth to denticles, and abundance of size classes across the K/Pg boundary for the North and South Pacific	113
Figure 5-2: Paleomap showing the ratio of fish teeth to shark denticles from the Cretaceous and Paleocene from six sites around the world’s oceans.	113
Figure 5-3: An extended record from the South Pacific Ocean (DSDP Site 596) of various ichthyolith community metrics	114
Figure 5-4: Figure S1. Representative tooth-size histograms and ichthyolith assemblages from the South Pacific (DSDP Site 596).	119
Figure 5-5: Figure S2. Size structure of ichthyoliths at South Pacific (DSDP Site 596) and North Pacific (ODP Site 886).	120
Figure 5-6: Figure S3. Results of bootstrapped shark tooth simulation 6, showing the spread of ratios calculated for each of 5,000 simulations. (A) Cretaceous ratios in each simulation.	121
Figure 6-1: Example tooth assemblage from DSDP Site 596.....	130
Figure 6-2: Example tooth with outline and measurements.	131
Figure 6-3: A schematic representation of the different character-states described in our tooth morphology system.....	133
Figure 6-4: Stratigraphic range chart of all ichthyolith morphotypes.....	138
Figure 6-5: Morphotypes that went extinct at the K/Pg.....	139
Figure 6-6: Range duration for morphotypes which originated at each time bin.	141
Figure 6-7: Total tooth accumulation at DSDP Site 596.	142
Figure 6-8: Plots comparing sampling intensity to morphotype observation.	143
Figure 6-9: Origination and extinction rate estimates using the Boundary Crosser calculations (top; Foote 2000) and a set of capture-mark-recapture models (bottom).....	145
Figure 6-10: A fish tooth NMDS morphospace showing the extant morphotypes within four time bins: the Cretaceous (>66 Ma; blue), the Early Paleocene, (66-60 Ma; green), the Late Paleocene (55-60 Ma; pink), and the Eocene (55-42 Ma; brown).	149

Figure 6-11: NMDS-based Morphospace occupation of tooth morphotypes which either (a) originated or (b) went extinct during each time bin	150
Figure 6-12: An example of the novel Late Paleocene/Early Eocene curved flanged tooth morphotype group.....	153
Figure 6-13: Multivariate variance of tooth disparity through time.	155
Figure 6-14: Stratigraphic range charts of all ichthyolith morphotypes for each of the three levels of reworking considered.	177
Figure 7-1: 85 million year accumulation records from (a) DSDP Site 596 in the South Pacific and (b) ODP Site 886 in the North Pacific.	183
Figure 7-2: Direct comparison of North Pacific (green open circles) and South Pacific (blue closed circles) ichthyolith accumulation for (a) the Cretaceous, (b), the Oligocene, and (c), the Miocene.	184
Figure 7-3: 85 million year relative and absolute abundance of elasmobranch denticles.	184
Figure 7-4: A cartoon illustration of the three ocean ecosystem states described in this paper.....	186
Figure 7-5: Figure S1: Sediment mass accumulation rate for DSDP Site 596, based on Zhou and Kyte 1992 (black triangles).	192
Figure 7-6: Figure S2: Ichthyolith Accumulation Rate calculated for DSDP Site 596 using the interpolated sediment MAR values (red dots), and the Neogene average MAR value (open black circles).	192
Figure 7-7: Figure S3: Sediment MAR versus Ichthyolith accumulation.	193
Figure 7-8: Figure S4: Age-depth plot for DSDP Site 596.....	194
Figure 7-9: Figure S5: Total ichthyolith (red dots), tooth (green open circles), and denticle (blue solid triangles) accumulation rates for DSDP Site 596, showing the abnormally high values during the interval of 23-19 Ma.	194
Figure 7-10: Figure S6: Ichthyoliths per gram for DSDP Site 596.	195
Figure 7-11: Figure S7: Age-depth model for ODP Site 886, showing constant sedimentation rate, with two major hiatuses in the record.....	195
Figure 7-12: Figure S8: Total ichthyoliths per gram sediment at ODP Site 886.....	196

LIST OF TABLES

Table 5-1: Table S1. Global ichthyolith assemblage ratios used for Fig. 5-2.	121
Table 5-2: Table S2. Results from simulated presence of shark teeth.....	122
Table 6-1: Teeth removed from analysis under conservative reworking dataset rules (10 total).	178
Table 6-2: Teeth removed from analysis under liberal reworking dataset rules (14 total).	179

ACKNOWLEDGEMENTS

My time here at Scripps has truly been one of the greatest adventures of my life. It is hard to even begin to thank everyone who has helped create such a positive, supportive environment for me as I traversed this path of discovery, science, and life.

First and foremost, I must thank Dick Norris. While every PhD student has an advisor, I must say that Dick transcends the status of “advisor”, and has truly been a mentor to me, helping me grow not only as a researcher, but as a person. Throughout my entire time here, Dick has been incredibly supportive all of my ideas, trials, and work. Dick’s unending enthusiasm, joy, and knowledge of the natural world are truly contagious, and it has been an honor and privilege to learn from him. In addition to being a wonderful research mentor, I am eternally grateful to Dick for granting me the opportunity to be his teaching assistant for SIO 104: Paleobiology and the History of Life. Over the 4 years that we taught the class, Dick’s encouragement, feedback, and enthusiasm have helped me to become a better teacher and mentor. Somewhere between the labs, the lectures, and the field trips, I think we created an unforgettable class. Finally, I must thank Dick’s propensity to say “yes”. From the very first “yes” to the 19-year-old Elizabeth who walked into the lab and said “can I volunteer? I’ll do anything”, which eventually led to the project that would become my dissertation, to the opportunities which he has helped me to develop and achieve as a PhD student, Dick has been a constant pillar of support, and for this, I am incredibly grateful.

I am grateful to have had a supportive and inquisitive committee, which has helped me to develop and stretch my scientific thinking. I thank Lisa Levin, whose thoughtful reviews and questions have returned me to the fundamentals of modern

ecology, and helped to place my research in paleobiology within the framework of the known natural world. In addition to introducing me to the basics of biological oceanography, I am grateful to Peter Franks for patiently helping me to translate my thoughts into equations, and for his support in both personal and professional realms. From Phil Hastings, I learned the basics of fish biology, behavior, and ecology. Lin Chao introduced me to the idea that evolution can be represented mathematically, and has helped me to develop my statistical thinking, and to further explore the mathematical properties of my data. I also want to thank David Woodruff, who sadly passed away in 2015, for his support and enthusiasm about this project, and his help in clarifying the ecological implications of my research, and his service on my doctoral committee.

I have been particularly lucky in my collaborations, and would like to thank my “unofficial” committee members, who have each played an important role in my development as a researcher. First and foremost, I must thank Celli Hull. Celli has been integral to this project from the very beginning, when she (then in the final year of her PhD) and Dick took a chance on a young undergraduate volunteer to try this “fish tooth thing”. Over the years, Celli has been more than a research mentor to me: she has been a true friend and an inspiration, who I continue to look up to today. Her ideas and enthusiasm are infectious, and I am always energized and excited about my work after talking with her. Celli’s support has come in both practical and intangible forms, from sharing her equipment and software to make my analysis of fish tooth morphology possible, to lending an ear when I need someone to talk to. They say your advisor is a bit like your academic parent, and Celli has truly filled her role as an academic “big sister”.

I have also been lucky enough to spend several months as a visiting scholar in two different labs while working on what ultimately became Chapter 6 of this dissertation. I would like to thank Matt Friedman, for opening his lab to me at Oxford University, and for helping me to develop the model for fish tooth morphology presented in this thesis. Matt has been incredibly supportive of the project, and I thank him for saying “yes” when I emailed to ask if he’d be interested in helping to solve the puzzle, and for his continued support, intellectually and academically over the past 2 years. I also thank Gene Hunt, at the Smithsonian National Museum of Natural History, for sponsoring and supporting me during the summer of 2015 as a predoctoral fellow with his research group. Gene’s mathematical insights and direction have opened me to many new directions in macroevolution. I particularly want to thank both Matt and Gene for their patience in helping me (try to) learn the various statistical methods and ways of thinking, and for their efforts to wrangle all of the “moving parts” of my dataset.

My interest in the field of paleobiology was sparked by Jeremy Jackson’s paleobiology and the history of life course: Jeremy’s class opened my eyes to the concepts of deep time, macroevolution, and the many uses of the fossil record. It taught me the value of knowing a system’s history, to better understand where we came from. Paul Dayton also played a formative role in my appreciation not just of Earth’s history, but for the history of the Scientific Literature, and for the philosophy of scientific inquiry. Both Jeremy and Paul have been staunch supporters as I have navigated the academic world, and thank them for the perspectives which I have gained through our interactions.

Navigating the logistics of doing a PhD is a challenge on the best of days. I am grateful for the expertise, support, and help of the wonderful folks in the Scripps

Graduate and Undergraduate Offices, past and present: Denise Darling, Adam Peterson, Gilbert Bretado, Maureen McGreevy, Maureen McCormack, Gayle Artura, Christine Co, Josh Reeves, and Sid Eads. I particularly thank Adam Petersen and the rest of the Scripps Student Symposium founding committee for their help in organizing such an incredible event, and Josh Reeves for his assistance every year dealing with the logistics of Paleobiology. I would also have been lost without the GRD support staff: Anne Cressey, Jan Hess, Laura Schafer, Megan Smith, and Monica Bailey have helped me with keys, mailing packages, grant applications, and all of my sometimes seemingly endless logistical questions. I am indebted to Leanne Elder for her help and support during my time at Yale, and the Yale Department of Geology and Geophysics computer gurus, who helped to ensure that my data were safe and able to be processed from a distance.

I have been blessed by wonderful labmates, mentors, and mentees. I was welcomed into Dick's lab as an undergraduate by his cadre of smart, driven, and kind female PhD students, who offered me their mentorship and their friendship. Seeing them succeed has shown me that it really is possible, and I am grateful to all of them for being my role models, friends, and colleagues. In particular, I thank Jessica Carilli for giving me my first research experience, and introducing me to the idea of historical ecology and drilling back in time to get an ecological baseline. Over the past 8 years, Jess has truly become a mentor and friend, and I learn so much from her perspectives both about science and life. Jill Leonard-Pingel taught me the basics of paleontology and how to work with fossils, and passed on her paleobiology labs to me. Jill's superb teaching truly set the bar for me, and her kindness has helped me to gain the confidence to always strive to improve my own teaching. I thank Sandy Kirtland Turner for always being willing to

listen and think about my data, and for her incredible and deep understanding of global carbon cycling, and for sharing her office with me her last year here. Katie Cramer has been a wonderful colleague and co-author, always willing to discuss data and analyses. Katie's perspective on modern and historical ecology has kept me from getting too bogged down in the deep-time record, and somehow she always manages to help me feel better about research and life when I talk to her.

I have had the honor of working with a whole bunch of talented undergraduate and Master's students throughout my dissertation. Together, they have helped me to generate a considerable amount of data, taught me how to be a better mentor, and even become friends. Christopher Ladwig, Matthias Scheer, Tiffani Horiguchi, Matthew Howard, Eric Schwab, Summer Buckley, and Teng Gao all generously volunteered their time to help with various aspects of the fish tooth project. Lana Graves, Raquel Bryant, Jacques Lyakov, and Betty Foreman have done independent study projects, advancing ichthyolith research in their own right. Jose Cuevas's enthusiasm for both research and science communication is an inspiration, and our Age of Fishes video was really fun to make. Doug Tomczik's Master's work on fish at the PETM has helped to shape my own ichthyolith work. And finally, I want to thank Michelle Zill. Michelle began as an independent study student, and I have had the privilege of watching her grow and develop intellectually through her Master's degree project. Michelle has become a wonderful friend, and I am so glad to have had the opportunity to work with her both in the lab and as co-TAs for my last year of Paleobiology, as well as on outreach activities.

I thank Jasmeet Dhaliwal for field assistance in Italy – it is always best to have a field partner who has integral skills which I lack, and Jasmeet's command of both driving

a stick shift car and speaking Italian made the entire thing possible. My Biological Oceanography cohort, without whom I wouldn't have made it through my first year and departmental, and the rest of the graduate students at Scripps, have all helped to shape my experiences. I also thank Rishi Sugla for being a great officemate and fellow Norris Lab PhD student, and the rest of the Norris Lab, past and present, for their support, intellectual curiosity, and friendship through the years.

My time here at Scripps has been financially supported by a number of grants and fellowships, big and small. I have been supported primarily by an NSF Graduate Research Fellowship, and through TA stipend support through the graduate office. I have been able to travel to numerous conferences to present data and meet new colleagues, through the generous support of many donors to the Scripps graduate fellowship funds. None of my work would have been possible without the support of the International Ocean Discovery Program (IODP), who have sent me thousands of pieces of sediment to dissolve in my quest for fish teeth. I was supported for 3 months on a Peter Buck Predoctoral Fellowship through The Smithsonian National Museum of Natural History, and have attended several short-course through workshop-specific NSF grants. My field work was supported through a Lewis and Clark Fund for Field Research in Astrobiology, administered through the American Philosophical Society.

Finally, I want to take a moment to thank everyone who has helped keep me sane, healthy, and generally happy through my PhD. The Thunderkittens, Cat Nickels and Ali Freibott, and Sara Shen have been my rocks through this whole experience, and I am incredibly grateful for their friendship, love, and support. Brian House, my wonderful roommate and partner in crime, thank you for making my life so much more interesting. I

also want to thank Dr. Stacie San Miguel for keeping me healthy and functional enough to stay in graduate school, even when my body had other plans. Devon Ayres has been more than a friend, even from halfway around the world, and I am so glad that our paths crossed. My circus family, both at Aerial Revolution and UCSD has been paramount in helping me maintain balance, both figuratively and literally in my life. Thank you, too, to my family, who encouraged my early interest in oceanography and allowed me to follow my passion. And to those who are not listed here, it is only because I am running out of space. I thank you for being part of my life at Scripps and in San Diego. My world is richer having known you.

Finally, I must thank all of my coauthors: Pincelli Hull, Katie Cramer, Philip Hastings, Jose Cuevas, Lana Graves, Gene Hunt, Matt Friedman, and of course, my advisor, Richard Norris, for their input and participation in the projects that comprised my PhD, and the reviewers and editors at Nature Geoscience, PNAS, and Proceedings of the Royal Society B, for their time and effort in preparing my manuscripts for publication.

Below is the content of the dissertation which is either published or submitted for publication. I was the primary investigator and author on all manuscripts in this dissertation.

Chapter 2, in full, has been submitted for publication as: Sibert, E. C., Cramer, K. L., Hastings, P. A., and Norris, R. D. “Methods for isolation and quantification of microfossil fish teeth and elasmobranch dermal denticles (ichthyoliths) from marine sediments”. The dissertation author was the primary investigator and author of this manuscript.

Chapter 3, in full, is a reprint of materials as it appears in Sibert, E. C., Hull, P. M., and Norris, R. D. (2014). “Resilience of Pacific Pelagic Fish following the Cretaceous/Palaeogene Mass Extinction” in *Nature Geoscience*, v. 7, no. 9, p. 667-670. DOI:10.1038/ngeo2227. The dissertation author was the primary investigator and author of this manuscript.

Chapter 4, in full, is in preparation for publication as: Sibert, E. C., and Norris, R. D. “No evidence for productivity-driven dwarfing in pelagic fish communities following the Cretaceous-Paleogene Mass Extinction”. The dissertation author was the primary investigator and author of this manuscript.

Chapter 5, in full, is a reprint of materials as it appears in Sibert, E. C., and Norris, R. D. (2015). “New Age of Fishes initiated by the Cretaceous/Paleogene Mass Extinction” in the *Proceedings of the National Academy of Sciences*, v.112, no. 28, p. 8537-8542. DOI:10.1073/pnas.1504985112. The dissertation author was the primary investigator and author of this manuscript.

Chapter 6 is in preparation for publication as Sibert, E. C., Friedman, M., Hull, P. M., Hunt, E., and Norris, R. D. “A two-pulsed radiation of pelagic fishes following the K/Pg mass extinction”. The dissertation author was the primary investigator and author of this manuscript.

Chapter 7, in full, is a reprint of materials as it appears in as: Sibert E, Norris R, Cuevas J, Graves L. (2016) “Eighty-five million years of Pacific Ocean gyre ecosystem structure: long-term stability marked by punctuated change” in the *Proceedings of the Royal Society B*, v.283: 20160189. <http://dx.doi.org/10.1098/rspb.2016.0189>. The dissertation author was the primary investigator and author of this manuscript.

VITAE

- 2011 Bachelor of Science, Biology, University of California, San Diego
- 2011-2016 NSF Graduate Research Fellowship, University of California, San Diego
- 2012-2015 Teaching Assistant, Paleobiology, University of California, San Diego
- 2013 Master of Science, Oceanography, Scripps Institution of Oceanography, University of California, San Diego
- 2015 Visiting Scholar, Department of Earth Sciences, Oxford University, UK
- 2015 Smithsonian Pre-Doctoral Fellow, Smithsonian National Museum of Natural History, Washington, D.C.
- 2016 Research Assistant, University of California, San Diego
- 2016 Doctor of Philosophy, Oceanography, Scripps Institution of Oceanography, University of California, San Diego
- 2016-2019 Junior Fellow, Harvard Society of Fellows, Harvard University

PUBLICATIONS

- Sibert, E. C., Norris, R. D., Cuevas, J. M., and Graves, L. G. (2016). “85 million years of Pacific Ocean Gyre ecosystem structure: long-term stability marked by punctuated change”: *Proceedings of the Royal Society B*, **283**: 20160189. <http://dx.doi.org/10.1098/rspb.2016.0189>.
- Sibert, E. C., and Norris, R. D. (2015) New Age of Fishes initiated by the Cretaceous–Paleogene mass extinction: *Proceedings of the National Academy of Sciences*, v. 112, no. 28, p. 8537-8542.
- Sibert, E. C., Hull, P. M., and Norris, R. D. (2014) Resilience of Pacific pelagic fish across the Cretaceous/Palaeogene mass extinction: *Nature Geoscience*, v. 7, no. 9, p. 667-670.
- Bagulayan, A., Bartlett-Roa, J. N., Carter, A. L., Inman, B. G., Keen, E. M., Orenstein, E. C., Patin, N. V., Sato, K. N. S., Sibert, E. C., and Simonis, A. E. (2012) Journey to the Center of the Gyre: The Fate of the Tohoku Tsunami Debris Field: *Oceanography*, v. 25, no. 2, p. 200.

ABSTRACT OF THE DISSERTATION

Ichthyoliths as a paleoceanographic and paleoecological proxy
and the response of open ocean fish to Cretaceous and Cenozoic global change

by

Elizabeth Claire Sibert

Doctor of Philosophy in Oceanography

University of California, San Diego, 2016

Professor Richard D. Norris, Chair

Ichthyoliths, isolated fossil fish teeth and shark dermal scales preserved in deep-sea sediment cores, can reveal how marine vertebrate consumers (sharks and fish) have responded to major global change events in Earth's history. In this dissertation, I first develop methods for the isolation and curation of ichthyoliths from a variety of marine sediment types. I then use ichthyoliths to assess how (1) total fish production, (2) pelagic

fish community structure, and (3) fish evolution have responded to select global change events in Earth's history.

The Cretaceous/Paleogene (K/Pg) Mass Extinction 66 million years ago (Ma) catalyzed the diversification of fish in the open ocean. Cretaceous oceans (>66 Ma) were relatively devoid of fish teeth, and at the K/Pg, fish abundance declined only in the Atlantic Ocean, while in the Pacific, fish abundance stayed constant or increased immediately following the extinction. Yet the event caused a global shift in the marine vertebrate community, with the relative abundance of teeth increasing compared to that of denticles in marine sediments. Further, the size structure of the fish tooth assemblages shifted towards larger, rather than smaller individuals, suggesting that the group was resilient to the extinction event. Bony fishes rose to ecological dominance in the open ocean following the K/Pg extinction, rapidly radiating in morphological diversity after the extinction, while other open ocean groups lagged behind. Extreme global warmth in the Early Eocene (~52-48 Ma) is associated with an increase in fish and shark abundance, but not diversity. Fish abundance broadly follows global temperature gradients in the Paleogene (66-20 Ma), with the highest abundance of fish in the warmest part of the Cenozoic. The most recent 20 million years is characterized by highly variable ichthyolith production and low abundances of sharks and other elasmobranchs in the gyres. This shift is temporally correlated with the diversification of open-ocean whales and seabirds, groups which may have out-competed sharks for fish prey in the modern open ocean. Together, these results show that that fishes were consistently able to adapt to Cenozoic global change, both ecologically and evolutionarily, allowing the Cenozoic to truly become an "Age of Fishes".

CHAPTER 1

Introduction to the Dissertation

1.1 Introduction

While we can project future ecological change and potential consequences of environmental perturbations using ecosystem and climate models, a lot can be learned about the earth system simply by looking at its history. Modern, anthropogenic global change will have considerable effects on marine ecosystems (Doney et al., 2012). Even now, shifts in ocean chemistry, temperature, and circulation are changing distributions of organisms (Doney et al., 2009; Field et al., 2006; Prince and Goodyear, 2006). However, the planet has undergone numerous profound shifts in climate since it formed some 4.5 billion years ago. In the past 100 million years, Earth has experienced global oceanic anoxia (Jenkyns, 1980; Leckie et al., 2002; Schlanger and Jenkyns, 1976), mass extinctions (Bambach, 2006; D'Hondt, 2005; Hull and Darroch, 2013; Raup and Sepkoski Jr, 1982; Schulte et al., 2010; Thomas, 2007), extreme greenhouse-induced warming (Aze et al., 2014; Bowen et al., 2015; Cramer et al., 2009; Sluijs et al., 2013; Zachos et al., 2001; Zachos et al., 2008; Zachos et al., 2003), ocean acidification (Honisch et al., 2012; Zachos et al., 2005), a transition from an ice-free greenhouse to an icehouse earth with permanently glaciated poles (Diester-Haass and Zahn, 1996; Liu et al., 2009), and glacial/interglacial cycles that define the modern climate system (Archer et al., 2000). While none of these events is a perfect analog to our modern anthropogenic greenhouse experiment, they can provide insight into the mechanisms that drive the structure and function of marine ecosystems, and in turn suggest how they might fare in the face of modern global change (Norris et al., 2013).

Traditionally, the history of the oceans, and the response of different biological groups to global change events has been revealed through analysis of the unicellular

protist microfossil record – foraminifera, diatoms and calcareous nannofossils. The deep-sea fossil record can reveal a temporally complete view of before, during, and after these climate and biotic events, providing a series of natural experiments to study the macroecological and evolutionary responses of ecosystems and past life to global change. However, the corresponding responses of higher parts of open-ocean food webs, such as fish, sharks, and other marine vertebrates, to environmental change is mostly unknown.

Fishes are a ubiquitous part of modern marine ecosystems and significant in terms of biomass, biodiversity, and ecosystem function. Fishes are a paraphyletic group defined as aquatic vertebrates which have gills for their entire life cycle, and which also have fins, rather than limbs, if any appendages are present (Nelson, 2006). This includes the jawless fishes (e.g. lampreys and hagfish), the cartilaginous fishes (e.g. sharks and rays), and bony fishes (including both lungfish and ray-finned fishes), as well as a host of now extinct fossil lineages of aquatic, gilled vertebrates such as the placoderms. It is important to note that this definition is not taxonomically significant. Tetrapods, which share a common ancestor with bony fishes, and would therefore be included in the clade, are excluded from the colloquial definition of the group. Modern fishes are incredibly diverse, comprising approximately 50% of all extant vertebrate diversity, with over 33,000 described species (Nelson, 2006). Ray-finned fishes have been particularly successful, diversifying rapidly in the past 100 million years to become the dominant vertebrates in the ocean (Friedman and Sallan, 2012; Near et al., 2013; Near et al., 2012). This dissertation primarily considers fishes from two major clades: the Elasmobranchii, including sharks, skates, and rays, and Actinopterygii, or ray-finned fishes, the predominant fish groups in the oceans today and over the past 85 million years.

The highly-resolved record of marine microplankton in deep-sea sediment cores (Coxall et al., 2006; Gibbs et al., 2012; Thomas, 2007) stands in stark contrast to the traditional vertebrate fossil record (Friedman, 2009; Friedman and Sallan, 2012; Sallan and Galimberti, 2015). The fossil record of fishes is sparsely populated, temporally discontinuous, and biased towards species living in lacustrine and shallow marine environments most likely to be uplifted and exposed to land-based paleontologists, making it difficult to study how these diverse and important animals have responded to rapid global change events. The fish fossil record also largely ignores the open ocean and deep sea, which are rarely uplifted and exposed on land.

However, preserved in the deep-sea sedimentary record, alongside the record of microfossil plankton and environmental proxies, is an extensive, temporally continuous, and novel fossil record of marine vertebrates. Ichthyoliths are the isolated bony remains of ocean-dwelling fishes. The most-often preserved ichthyoliths include durable, calcium-phosphate fish teeth and dermal scales (denticles) shed from elasmobranch skin. Ichthyoliths are found in nearly all sediment types, including those previously considered unfossiliferous as they are highly resistant to dissolution, and the most robust part of the fish (Doyle and Riedel, 1979). Despite some use of ichthyoliths as biostratigraphic markers (e.g. Doyle, 1983; Doyle et al., 1985; Johns et al., 2006), the majority of ichthyolith-based studies have simply used the largest teeth as carriers of isotopes such as neodymium (Martin and Haley, 2000; Scher and Martin, 2004; Thomas et al., 2014), strontium (Gleason et al., 2002), and rare earth elements (Huck et al., 2016) for paleoceanographic reconstructions, ignoring any taxonomic affinity or ecological relevance of the organisms that produced the fossils.

Fishes are a product of an efficient and functional marine ecosystem. For example, in an upwelling ecosystem, with large phytoplankton, a short food web will dominate, with a large proportion of fixed carbon being converted to fish biomass, while in a nutrient-starved ecosystem, a long, complex microbe-dominated food web will retain the majority of the fixed carbon within the microbial loop, producing considerably less fish biomass (Iverson, 1990; Moloney et al., 1991; Ryther, 1969). As the number of fish is proportional to the number of teeth, to a first-order approximation, regions of higher primary productivity or dominated by shorter food webs will yield a higher abundance of teeth in the sediments. Therefore, the flux of ichthyoliths to the sediment is a function of both net primary production and ecosystem structure, and may be indicative of overall export production of an oceanic ecosystem.

However, the biology of the fishes present in an ecosystem may influence the abundance of ichthyoliths preserved on the seafloor. Since many ray-finned fish resorb and regenerate their teeth rather than shed them continuously (Bemis et al., 2005), many teeth reaching the seafloor are likely from individuals which have recently died. Thus, a species which sheds teeth over its lifetime could account for a greater proportion of the teeth on the seafloor. An observed shift in ichthyolith abundance could be due to a demographic shift in the relative abundance of species which shed or resorb their teeth, as opposed to a change in total fish biomass. In addition, as most preserved ichthyoliths are extremely small, less than 63 μ m, most are likely either pharyngeal teeth or from juveniles. Fish with larger jaws may therefore produce more small teeth, or alternatively may produce larger teeth, but at lower abundances. However, inter-specific variation in tooth production and abundance is large, so a shift in the dominant species in a region could

alter the abundance of teeth in sediments, without an associated change in fish biomass in the ecosystem. Still, another explanation for changes in total flux of ichthyoliths to the seafloor is generation time of the fish that produce them. Each deep-sea sediment sample represents a fixed interval of time, usually between 10,000 and 100,000 years for the samples used in this dissertation. In two ecosystems with equal standing biomass of fish, the ecosystem with a faster generation time will produce more individuals over a fixed interval of time, and thus more teeth have the potential to be deposited on the seafloor. However, substantial or abrupt changes in ichthyolith abundance that are driven by demographic changes in the fish population, rather than increases in total abundance of fishes, would likely be detectable as changes in the size structure of the tooth assemblage. By comparing both ichthyolith abundance and assemblage size structure in concert, we can begin to tease apart these effects.

Elasmobranch-sourced ichthyoliths are considerably less abundant than ray-finned fish ichthyoliths in the vast majority of deep-sea sediments. While sharks continually lose teeth, shark teeth are both large (>1-2 mm), and are extremely rare in ichthyolith assemblages, possibly reflecting the large body size and long life spans of many shark taxa. However, sharks are covered in mineralized dermal denticles, which are 100-300 μm in size, with hundreds in a square cm of shark skin, and are well represented in many ichthyolith assemblages. The abundance of denticles, not their size, scales with the surface area of the elasmobranch: thus, the abundance of denticles in an ichthyolith assemblage is a function both of numerical abundance, and body size of the elasmobranchs present in the community. However, two small sharks will produce more denticles than a single shark with twice the biomass, because surface area (cm^2) does not

scale linearly with biovolume (cm^3) or length. Thus shifts in the abundance of denticles in the fossil record are more reflective of elasmobranch abundance than individual elasmobranch biomass. Further, the number of denticles on a single elasmobranch is several orders of magnitude larger than the number of teeth they will shed in a lifetime, so it is unsurprising that the majority of elasmobranch-sourced ichthyoliths preserved in the marine microfossil record are denticles.

Finally, to sample the deep-time ichthyolith record in the deep sea it is necessary to drill many tens or hundreds of meters into deep-sea sediments, a difficult and expensive process. The sediment samples represent one small spot in the ocean, which may be subject to local processes, such as changes in fish migration patterns, rather than preserving a signal of global or basin-wide significance. This bias is addressed by comparing records from multiple ocean basins, or from multiple sites within a basin, to see whether patterns are consistent across both space and time. I have partly dealt with this problem of picking representative samples of ocean environments by focusing this dissertation on gyre ecosystems, allowing for cross-site comparisons, but note that there is considerable potential for ichthyolith studies in non-gyre environments. Further, as a single sediment sample may represent many thousands of years of time, migrations of mobile organisms, such as fish, will be time-averaged in the sedimentary record, effectively erasing any shorter-term changes in the distribution or occurrence of fishes. It is worthwhile noting, however, that a decline in ichthyolith abundance at a gyre site does not necessarily translate to a global decline in fish or sharks: it may be that the ichthyolith-producing individuals have simply shifted to a different habitat, such as a

coastal upwelling zone, and spend less time in the region we are investigating for ichthyoliths.

While this dissertation is limited in scope to ichthyoliths from gyre sediments, reflecting primarily open-ocean habitats, with some deep-sea and benthic species, it lays the groundwork for the field of ichthyolith micropaleontology, contributing methods, interpretations, and discoveries using this novel microfossil group. The types of questions examined, and methods developed in this dissertation can be expanded and applied to many other paleoceanographic or paleoclimate events. Further, there are many potential applications beyond the field of paleoceanography, including conservation paleobiology (e.g. Cramer et al., in review), limnology, and even archaeology.

In this dissertation, I lay the foundations for using ichthyoliths as a paleoceanographic and paleontological proxy for fish, as both a metric for ecosystem structure and function across events in Earth's history, and for assessing pattern and process in fish evolution. The ichthyolith record lends itself to multiple scales of ecological and macroevolutionary inquiry. This dissertation focuses on three scales of fish and ecosystem evolution, with a focus on specific case-study events in Earth's history: 1) ecosystem production, or how much fish biomass was produced, 2) community structure: concerning the relative abundances of different types and size classes of ichthyoliths, and 3) individual ichthyoliths: how have different ichthyolith morphotypes and groups changed through time, and what insights can this offer into the tempo and mode of fish evolution in the open ocean?

1.2 Outline of the Dissertation

In this dissertation, I develop ichthyoliths for use as a paleoceanographic and paleontological proxy, to elucidate patterns in fish production, community structure, and evolution. I then apply the proxy to a series biotic and climate events and transitions over the past 85 million years of Earth's history.

In **Chapter 2**, I outline a methodological framework for isolating ichthyoliths from marine sediments. These methods expand upon preliminary work by (Doyle and Riedel, 1979), including acid dissolution of carbonate sediments. I introduce several new techniques that can be applied to ichthyolith isolation, including the use of Alizarin Red S stain, a calcium-specific stain that binds to ichthyoliths, giving them a pink color that increases their visual identification in otherwise difficult-to-process samples. I further describe calculations for ichthyolith flux, a metric called ichthyolith accumulation rate (IAR), and outline many other potential uses of ichthyoliths beyond the applications in this dissertation.

In **Chapters 3-6**, I focus on the impacts of the Cretaceous-Paleogene (K/Pg) mass extinction event on the marine fish community. In **Chapter 3**, I calculate IAR across the K/Pg at five different locations around the world, and find that in the Pacific Ocean, fish flux is resilient across the extinction, either remaining stable, or increasing above Cretaceous levels after the extinction. This is in contrast to the Atlantic and Tethys Sea, both of which show a decrease in IAR in the immediate aftermath of the extinction (Sibert et al., 2014). This is consistent with a model of post-extinction ecosystem recovery dynamics which has emerged in recent years, where the ocean basins had different responses to the extinction event: the Atlantic Ocean showed greater declines in

production and a longer recovery from the extinction event than the Pacific (Alegret and Thomas, 2009; Hull and Norris, 2011; Hull et al., 2011; Jiang et al., 2010). **Chapter 3** was published in full as Sibert, E. C., Hull, P. M., and Norris, R. D. (2014). *Resilience of Pacific pelagic fish across the Cretaceous/Palaeogene mass extinction in Nature Geoscience* v. 7, no. 9, p. 667-670.

This paper is followed up in **Chapter 4**, where I directly compared IAR between the South Atlantic and North Pacific basins with the fish community structure. I found that despite differences in total IAR and patterns of IAR across the K/Pg, the relative fish community structure, as defined by the relative abundance of different size classes of teeth, was stable across the extinction. There is no evidence for dwarfism following the event at either location, which has been observed in many shallow marine fossil groups and unicellular plankton. The assemblages both shifted towards larger teeth at approximately 62 Ma in both ocean basins. This suggests that the drivers of community structure in small pelagic fish are independent of total net primary production. Further, the K/Pg did not cause even a short-term change in community structure, suggesting that fishes were able to maintain their ecological roles in the post-extinction ecosystem, possibly contributing to their success in the aftermath. Further, as the shift in tooth assemblage size structure occurred nearly 4 million years after the extinction, independent of a major global change event or shift in export production, this suggests that changes in the size structure of the fish community are driven primarily by evolutionary processes, rather than shifts in primary production.

In **Chapter 5**, I show that the mass extinction triggered a permanent change in the relative abundance of elasmobranch denticles as compared to fish teeth in ichthyolith

assemblages: denticles remained stable or decreased in absolute abundance, while teeth increased, beginning a new regime of pelagic vertebrate structure. Further, the maximum tooth size increased 3-fold following the extinction event, suggesting that large fishes were evolutionarily released and able to diversify in pelagic environments. Molecular clock data have suggested that there was a radiation of ray-finned fishes during the Late Cretaceous and early Paleogene (Miya et al., 2013; Near et al., 2012), often referred to as the “New Age of Fishes”. This study showed that the Cretaceous-Paleogene extinction fundamentally and instantaneously (in geologic time) changed the structure of pelagic vertebrate communities, and catalyzed the diversification and rise to ecological dominance of ray-finned fishes in modern open ocean environments (Sibert and Norris, 2015). **Chapter 5** was published in full as Sibert, E. C., and Norris, R. D. (2015) *New Age of Fishes initiated by the Cretaceous–Paleogene mass extinction* in the *Proceedings of the National Academy of Sciences*, v. 112, no. 28, p. 8537-8542.

In **Chapter 6**, I consider ichthyoliths as individual fossils, rather than in aggregate as either an accumulation rate or community structure metric. Using ichthyoliths preserved in a red-clay core from the South Pacific Gyre, I develop a morphological scheme for quantifying variation in tooth morphology, and use this to define 136 individual tooth morphotypes which were present during the interval of 73 to 42 million years ago (Ma), with unprecedented temporal resolution for a vertebrate study. This interval includes the K/Pg extinction (66 Ma) and the Early Eocene Climate Optimum (53-50 Ma), two very significant periods of global change. I then investigate whether these environmental events had any effect on the morphological variation or macroevolutionary patterns in the ichthyolith community. I use several rate-calculation

techniques, including traditional paleontological metrics (Foote, 2000), and also apply capture-mark-recapture theory (Liow and Nichols, 2010), to evaluate speciation and extinction rates. I show that there were two pulses of radiation in the Paleocene, but none during the late Cretaceous or Early to Middle Eocene. The first pulse of origination corresponds with the period of high abundances of large teeth observed in **Chapter 5**, and the second occurs approximately 4 million years later, near the end of the Paleocene. I use non-metric multidimensional scaling to generate a morphospace of ichthyolith shape disparity during these intervals of radiation, and find that the first radiation includes teeth that are distinctly different in morphology from the Cretaceous fauna, while the second radiation yields fish assemblages which occupy a morphospace similar to that of the Cretaceous, with several notable novel expansions, and is maintained into the Eocene greenhouse world. This suggests that following the Cretaceous-Paleogene extinction, open-ocean fishes evolved rapidly, first with a disaster fauna of novel and morphological distinct morphotypes that went extinct as the ecosystem continued to stabilize following the K/Pg event. A second wave of radiation, which included more “typical” tooth morphologies then populated the oceans, and was stable across several major climate events over the next 10 million years, including the Paleocene Eocene Thermal Maximum, the Early Eocene Climate Optimum, and into the Middle Eocene. While there was net extinction in the Eocene, the morphospace occupation of fish teeth did not decline considerably. These results suggest that the Cretaceous/Paleogene extinction event was a driver in fish evolutionary processes, while later climate events, including the establishment of the extreme “greenhouse world” of the Early Eocene did

not have a major effect on the ecology of fish communities, at least at the resolution of the tooth-based morphological groups.

Finally, in **Chapter 7**, I compile several ichthyolith records, spanning the interval of 85 Ma to present in the Pacific gyres, to assess the structure and function of pelagic ecosystems on long timescales. I use metrics of fish production, as measured by ichthyolith accumulation, and fish community structure, as measured by the relative abundance of teeth and denticles in the ichthyolith assemblages, and find that over the past 85 million years, there have been three distinct ichthyolith community structures, each lasting tens of millions of years, and marked by a punctuated change unrelated to global climate events or trends. The Cretaceous Ocean (>85-66 Ma) had large numbers of elasmobranchs, but comparatively few fish, and relatively stable levels of ichthyolith accumulation. The Paleogene Ocean, which lasted from 66-20 Ma, and began at the K/Pg extinction (**Chapter 5**), showed a considerable increase in fish but not elasmobranchs. In addition, IAR in the Paleogene increased and decreased in concert with global bottom-water temperature, with relatively low variance, while the assemblage structure did not change, suggesting that ecosystem structure and function were decoupled in the Paleogene Ocean.

Approximately 20 Ma, this stable regime abruptly changed: elasmobranch fossils nearly disappeared from the assemblages, and IAR became highly variable, varying in value by over an order of magnitude on <500,000 year time intervals, considerably faster than the millions-of-years of smooth increases and decreases in IAR observed in the Paleogene. There is no known notable global change event to have driven this abrupt and distinct shift, however, this Modern Ocean state, defined by the onset of high levels of

variance in primary production and fish productivity, is correlated to the rise of large, migratory pelagic predators, including tunas, seabirds, open-ocean-dwelling whales, and pinnipeds. It is possible that as the intensity of the icehouse climate increased, the delivery of nutrients to the open ocean reached a threshold that caused a change in planktonic ecosystem structure, leading to highly variable primary productivity, high levels of variance in the total abundance of prey-fish, and thus a loss of larger megafauna in the open ocean. **Chapter 7**, was published in full as Sibert, E. C., Norris, R. D., Cuevas, J. M., and Graves, L. G. (2016). *85 million years of Pacific Ocean Gyre ecosystem structure: long-term stability marked by punctuated change in the Proceedings of the Royal Society B*. v.283: 20160189.

Together these chapters represent the first effort to quantify and use ichthyoliths as a proxy for fishes and the open-ocean ecosystem, and provide unprecedented insights into the evolution, structure, and function of open-ocean ecosystems and fish evolution through geologic time.

1.3 References

- Alegret, L., and Thomas, E., 2009, Food supply to the seafloor in the Pacific Ocean after the Cretaceous/Paleogene boundary event: *Marine Micropaleontology*, v. 73, no. 1-2, p. 105-116.
- Archer, D., Winguth, A., Lea, D., and Mahowald, N., 2000, What caused the glacial/interglacial atmospheric pCO₂ cycles?: *Reviews of Geophysics*, v. 38, no. 2, p. 159-189.
- Aze, T., Pearson, P. N., Dickson, A. J., Badger, M. P. S., Bown, P. R., Pancost, R. D., Gibbs, S. J., Huber, B. T., Leng, M. J., Coe, A. L., Cohen, A. S., and Foster, G. L., 2014, Extreme warming of tropical waters during the Paleocene–Eocene Thermal Maximum: *Geology*, v. 42, no. 9, p. 739-742.

- Bambach, R. K., 2006, Phanerozoic biodiversity mass extinctions: *Annual Review of Earth and Planetary Sciences*, v. 34, p. 127-155.
- Bemis, W. E., Giuliano, A., and McGuire, B., 2005, Structure, attachment, replacement and growth of teeth in bluefish, *Pomatomus saltatrix* (Linnaeus, 1766), a teleost with deeply socketed teeth: *Zoology*, v. 108, no. 4, p. 317-327.
- Bowen, G. J., Maibauer, B. J., Kraus, M. J., Rohl, U., Westerhold, T., Steimke, A., Gingerich, P. D., Wing, S. L., and Clyde, W. C., 2015, Two massive, rapid releases of carbon during the onset of the Palaeocene-Eocene thermal maximum: *Nature Geosci*, v. 8, no. 1, p. 44-47.
- Coxall, H. K., D'Hondt, S., and Zachos, J. C., 2006, Pelagic evolution and environmental recovery after the Cretaceous-Paleogene mass extinction: *Geology*, v. 34, no. 4, p. 297-300.
- Cramer, B. S., Toggweiler, J. R., Wright, J. D., Katz, M. E., and Miller, K. G., 2009, Ocean overturning since the Late Cretaceous: Inferences from a new benthic foraminiferal isotope compilation: *Paleoceanography*, v. 24, no. 4, p. PA4216.
- Cramer, K. L., O'Dea, A., Leonard-Pingel, J. S., Clark, T. R., Zhao, J.-x., and Norris, R. D., in review, Prehistorical and historical decline of Caribbean reef ecosystems linked to loss of herbivores.
- D'Hondt, S., 2005, Consequences of the Cretaceous/Paleogene mass extinction for marine ecosystems: *Annual Review of Ecology, Evolution, and Systematics*, v. 36, p. 295-317.
- Diester-Haass, L., and Zahn, R., 1996, Eocene-Oligocene transition in the Southern Ocean: History of water mass circulation and biological productivity: *Geology*, v. 24, no. 2, p. 163.
- Doney, S. C., Fabry, V. J., Feely, R. A., and Kleypas, J. A., 2009, Ocean Acidification: The Other CO₂ Problem: *Annual Review of Marine Science*, v. 1, p. 169-192.
- Doney, S. C., Ruckelshaus, M., Duffy, J. E., Barry, J. P., Chan, F., English, C. A., Galindo, H. M., Grebmeier, J. M., Hollowed, A. B., Knowlton, N., Polovina, J., Rabalais, N. N., Sydeman, W. J., and Talley, L. D., 2012, Climate change impacts on marine ecosystems: *Ann Rev Mar Sci*, v. 4, p. 11-37.
- Doyle, P. S., 1983, Ichthyolith stratigraphy in the Pacific, *Eos, Transactions, American Geophysical Union, Volume 64*: Washington, American Geophysical Union, p. 741-742.

- Doyle, P. S., and Riedel, W. R., 1979, Ichthyoliths: present status of taxonomy and stratigraphy of microscopic fish skeletal debris, La Jolla, CA, Scripps Institution of Oceanography, University of California, San Diego, Scripps Institution of Oceanography Reference Series.
- Doyle, P. S., Riedel, W. R., Heath, G. R., Burckle, L. H., D'Agostino, A. E., Bleil, U., Horai, K.-i., Jacobi, R. D., Janecek, T. R., Koizumi, I., Krissek, L. A., Monechi, S., Lenotre, N., Morley, J. J., Schultheiss, P. J., and Wright, A. A., 1985, Ichthyolith biostratigraphy of western North Pacific pelagic clays, Deep Sea Drilling Project Leg 86: Initial Reports of the Deep Sea Drilling Project, v. 86, p. 349-366.
- Field, D. B., Baumgartner, T. R., Charles, C. D., Ferreira-Bartrina, V., and Ohman, M. D., 2006, Planktonic foraminifera of the California Current reflect 20th-century warming: *Science*, v. 311, no. 5757, p. 63-66.
- Foote, M., 2000, Origination and extinction components of taxonomic diversity: general problems: *Paleobiology*, v. 26, no. sp4, p. 74-102.
- Friedman, M., 2009, Ecomorphological selectivity among marine teleost fishes during the end-Cretaceous extinction: *Proceedings of the National Academy of Sciences of the United States of America*, v. 106, no. 13, p. 5218-5223.
- Friedman, M., and Sallan, L. C., 2012, Five hundred million years of extinction and recovery: a Phanerozoic survey of large-scale diversity patterns in fishes: *Palaeontology*, v. 55, no. 4, p. 707-742.
- Gibbs, S. J., Bown, P. R., Murphy, B. H., Sluijs, A., Edgar, K. M., Palike, H., Bolton, C. T., and Zachos, J. C., 2012, Scaled biotic disruption during early Eocene global warming events: *Biogeosciences*, v. 9, no. 11, p. 4679-4688.
- Gleason, J. D., Moore, T. C., Rea, D. K., Johnson, T. M., Owen, R. M., Blum, J. D., Hovan, S. A., and Jones, C. E., 2002, Ichthyolith strontium isotope stratigraphy of a Neogene red clay sequence: calibrating eolian dust accumulation rates in the central North Pacific: *Earth and Planetary Science Letters*, v. 202, no. 3-4, p. 625-636.
- Honisch, B., Ridgwell, A., Schmidt, D. N., Thomas, E., Gibbs, S. J., Sluijs, A., Zeebe, R., Kump, L., Martindale, R. C., Greene, S. E., Kiessling, W., Ries, J., Zachos, J. C., Royer, D. L., Barker, S., Marchitto, T. M., Moyer, R., Pelejero, C., Ziveri, P., Foster, G. L., and Williams, B., 2012, The Geological Record of Ocean Acidification: *Science*, v. 335, no. 6072, p. 1058-1063.

- Huck, C. E., van de Flierdt, T., Jiménez-Espejo, F. J., Bohaty, S. M., Röhl, U., and Hammond, S. J., 2016, Robustness of fossil fish teeth for seawater neodymium isotope reconstructions under variable redox conditions in an ancient shallow marine setting: *Geochemistry, Geophysics, Geosystems*, p. n/a-n/a.
- Hull, P. M., and Darroch, S. A. F., 2013, Mass extinctions and the structure and function of ecosystems: *Paleontological Society Papers*, v. 19, p. 115-156.
- Hull, P. M., and Norris, R. D., 2011, Diverse patterns of ocean export productivity change across the Cretaceous-Paleogene boundary: New insights from biogenic barium: *Paleoceanography*, v. 26, no. 26, p. 3205.
- Hull, P. M., Norris, R. D., Bralower, T. J., and Schueth, J. D., 2011, A role for chance in marine recovery from the end-Cretaceous extinction: *Nature Geoscience*, v. 4, p. 856–860.
- Iverson, R. L., 1990, Control of Marine Fish Production: *Limnology and Oceanography*, v. 35, no. 7, p. 1593-1604.
- Jenkyns, H. C., 1980, Cretaceous Anoxic Events - From Continents to Oceans: *Journal of the Geological Society*, v. 137, no. MAR, p. 171-188.
- Jiang, S. J., Bralower, T. J., Patzkowsky, M. E., Kump, L. R., and Schueth, J. D., 2010, Geographic controls on nannoplankton extinction across the Cretaceous/Palaeogene boundary: *Nature Geoscience*, v. 3, no. 4, p. 280-285.
- Johns, M. J., Barnes, C. R., and Narayan, Y. R., 2006, Cenozoic ichthyolith biostratigraphy; Tofino Basin, British Columbia: *Canadian Journal of Earth Sciences = Revue Canadienne des Sciences de la Terre*, v. 43, no. 2, p. 177-204.
- Leckie, R. M., Bralower, T. J., and Cashman, R., 2002, Oceanic anoxic events and plankton evolution: Biotic response to tectonic forcing during the mid-Cretaceous: *Paleoceanography*, v. 17, no. 3.
- Liow, L. H., and Nichols, J. D., 2010, Estimating rates and probabilities of origination and extinction using taxonomic occurrence data: capture-mark-recapture (CMR) approaches: *Alroy and Hunt*, p. 81-94.
- Liu, Z., Pagani, M., Zinniker, D., DeConto, R., Huber, M., Brinkhuis, H., Shah, S. R., Leckie, R. M., and Pearson, A., 2009, Global cooling during the Eocene-Oligocene climate transition: *Science*, v. 323, no. 5918, p. 1187-1190.
- Martin, E., and Haley, B., 2000, Fossil fish teeth as proxies for seawater Sr and Nd isotopes: *Geochimica Et Cosmochimica Acta*, v. 64, no. 5, p. 835-847.

- Miya, M., Friedman, M., Satoh, T. P., Takeshima, H., Sado, T., Iwasaki, W., Yamanoue, Y., Nakatani, M., Mabuchi, K., and Inoue, J. G., 2013, Evolutionary origin of the scombridae (tunas and mackerels): members of a paleogene adaptive radiation with 14 other pelagic fish families: *Plos One*, v. 8, no. 9, p. e73535.
- Moloney, C. L., Field, J. G., and Lucas, M. I., 1991, The size-based dynamics of plankton food webs. II. Simulations of three contrasting southern Benguela food webs: *Journal of plankton research*, v. 13, no. 5, p. 1039-1092.
- Near, T. J., Dornburg, A., Eytan, R. I., Keck, B. P., Smith, W. L., Kuhn, K. L., Moore, J. A., Price, S. A., Burbrink, F. T., Friedman, M., and Wainwright, P. C., 2013, Phylogeny and tempo of diversification in the superradiation of spiny-rayed fishes: *Proceedings of the National Academy of Sciences*, v. 110, no. 31, p. 12738-12743.
- Near, T. J., Eytan, R. I., Dornburg, A., Kuhn, K. L., Moore, J. A., Davis, M. P., Wainwright, P. C., Friedman, M., and Smith, W. L., 2012, Resolution of ray-finned fish phylogeny and timing of diversification: *Proceedings of the National Academy of Sciences of the United States of America*, v. 109, no. 34, p. 13698-13703.
- Nelson, J. S., 2006, *Fishes of the World*, New York, NY, Wiley, 600 p.:
- Norris, R., Turner, S. K., Hull, P., and Ridgwell, A., 2013, Marine ecosystem responses to Cenozoic global change: *Science*, v. 341, no. 6145, p. 492-498.
- Prince, E. D., and Goodyear, C. P., 2006, Hypoxia-based habitat compression of tropical pelagic fishes: *Fisheries Oceanography*, v. 15, no. 6, p. 451-464.
- Raup, D. M., and Sepkoski Jr, J. J., 1982, Mass extinctions in the marine fossil record: *Science*, v. 215, no. 4539, p. 1501-1503.
- Ryther, J. H., 1969, Photosynthesis and fish production in the sea: *Science*, v. 166, no. 3901, p. 72-76.
- Sallan, L., and Galimberti, A. K., 2015, Body-size reduction in vertebrates following the end-Devonian mass extinction: *Science*, v. 350, no. 6262, p. 812-815.
- Scher, H. D., and Martin, E. E., 2004, Circulation in the Southern Ocean during the Paleogene inferred from neodymium isotopes: *Earth and Planetary Science Letters*, v. 228, no. 3-4, p. 391-405.
- Schlanger, S. O., and Jenkyns, H. C., 1976, Cretaceous oceanic anoxic events; causes and consequences: *Geologie en Mijnbouw. Netherlands Journal of Geosciences*, v. 55, no. 3-4, p. 179-184.

- Schulte, P., Alegret, L., Arenillas, I., Arz, J. A., Barton, P. J., Bown, P. R., Bralower, T. J., Christeson, G. L., Claeys, P., Cockell, C. S., Collins, G. S., Deutsch, A., Goldin, T. J., Goto, K., Grajales-Nishimura, J. M., Grieve, R. A. F., Gulick, S. P. S., Johnson, K. R., Kiessling, W., Koeberl, C., Kring, D. A., MacLeod, K. G., Matsui, T., Melosh, J., Montanari, A., Morgan, J. V., Neal, C. R., Nichols, D. J., Norris, R. D., Pierazzo, E., Ravizza, G., Rebolledo-Vieyra, M., Reimold, W. U., Robin, E., Salge, T., Speijer, R. P., Sweet, A. R., Urrutia-Fucugauchi, J., Vajda, V., Whalen, M. T., and Willumsen, P. S., 2010, The Chicxulub Asteroid Impact and Mass Extinction at the Cretaceous-Paleogene Boundary: *Science*, v. 327, no. 5970, p. 1214-1218.
- Sibert, E. C., Hull, P. M., and Norris, R. D., 2014, Resilience of Pacific pelagic fish across the Cretaceous/Palaeogene mass extinction: *Nature Geosci*, v. 7, no. 9, p. 667-670.
- Sibert, E. C., and Norris, R. D., 2015, New Age of Fishes initiated by the Cretaceous–Paleogene mass extinction: *Proceedings of the National Academy of Sciences*, v. 112, no. 28, p. 8537-8542.
- Sluijs, A., van Roij, L., Harrington, G. J., Schouten, S., Sessa, J. A., LeVay, L. J., Reichart, G. J., and Slomp, C. P., 2013, Extreme warming, photic zone euxinia and sea level rise during the Paleocene/Eocene Thermal Maximum on the Gulf of Mexico Coastal Plain; connecting marginal marine biotic signals, nutrient cycling and ocean deoxygenation: *Climate of the Past Discussions*, v. 9, no. 6, p. 6459-6494.
- Thomas, D. J., Korty, R., Huber, M., Schubert, J. A., and Haines, B., 2014, Nd isotopic structure of the Pacific Ocean 70–30 Ma and numerical evidence for vigorous ocean circulation and ocean heat transport in a greenhouse world: *Paleoceanography*, v. 29, no. 5, p. 2013PA002535.
- Thomas, E., 2007, Cenozoic mass extinctions in the deep sea; what perturbs the largest habitat on Earth?: *Special Paper - Geological Society of America*, v. 424, p. 1-23.
- Zachos, J., Pagani, M., Sloan, L., Thomas, E., and Billups, K., 2001, Trends, rhythms, and aberrations in global climate 65 Ma to present: *Science*, v. 292, no. 5517, p. 686-693.
- Zachos, J. C., Dickens, G. R., and Zeebe, R. E., 2008, An early Cenozoic perspective on greenhouse warming and carbon-cycle dynamics: *Nature*, v. 451, no. 7176, p. 279-283.

Zachos, J. C., Röhl, U., Schellenberg, S. A., Sluijs, A., Hodell, D. A., Kelly, D. C., Thomas, E., Nicolo, M., Raffi, I., and Lourens, L. J., 2005, Rapid acidification of the ocean during the Paleocene-Eocene thermal maximum: *Science*, v. 308, no. 5728, p. 1611-1615.

Zachos, J. C., Wara, M. W., Bohaty, S., Delaney, M. L., Petrizzo, M. R., Brill, A., Bralower, T. J., and Premoli-Silva, I., 2003, A transient rise in tropical sea surface temperature during the Paleocene-Eocene Thermal Maximum: *Science*, v. 302, no. 5650, p. 1551-1554.

CHAPTER 2

Methods for isolation and quantification of microfossil fish teeth and elasmobranch dermal scales (ichthyoliths) from marine sediments

2.1 Abstract

Ichthyoliths—microfossil fish teeth and shark dermal scales (denticles)—are found in nearly all marine sediments. Their small size and relative rarity compared to other microfossil groups means that they have been largely ignored by the paleontology and paleoceanographic communities, except as carriers of certain isotope systems. Yet, when properly concentrated, ichthyoliths are sufficiently abundant to reveal patterns of fish abundance and diversity at unprecedented temporal and spatial resolution, in contrast to the typical millions of years-long gaps in the vertebrate body fossil record. In addition, ichthyoliths are highly resistant to dissolution, making it possible to reconstruct whole fish communities over highly precise and virtually continuous timescales. Here we present methods to isolate and utilize ichthyoliths preserved in the sedimentary record to track fish community structure and ecosystem productivity through geological and historical time periods. These include techniques for isolation and concentration of these microfossils from a wide range of sediments, including deep-sea and coral reef carbonates, clays, shales, and silicate-rich sediments. We have also developed a novel protocol for ichthyolith staining using Alizarin Red S to easily visualize and distinguish small teeth from debris in the sample. Finally, we discuss several metrics for quantification of ichthyolith community structure and abundance, and their applications to reconstruction of ancient marine food webs and environments.

2.2 Introduction

Microfossils are an integral part of the fossil record. While they are small, the high abundances of microfossils can provide unique insights into evolutionary patterns

(e.g. (Hull and Norris, 2009; Hunt, 2004; Hunt et al., 2010; Thomas and Gooday, 1996)), the responses of taxa to global change events (Alegret and Thomas, 2009; Hull et al., 2011; Sibert et al., 2014; Sibert and Norris, 2015; Thomas, 2003, 2007), and dynamics of ecosystems over geological and historical timescales (Cramer et al., in review; Sibert et al., 2014). Here we present a methodological framework for working with ichthyoliths, a valuable but understudied microfossil resource. Literally translated as “fish-stones”, ichthyoliths are the microfossil calcium phosphate remains of marine vertebrates – mostly teeth and dermal denticles (Figure 2-1), although some well-preserved samples have a high abundance of bone fragments as well. The majority of tooth-type ichthyoliths are thought to be from ray-finned fishes (Actinopterygii), however there is also a well-preserved record of dermal scales (denticles), representing sharks and rays (Elasmobranchii).

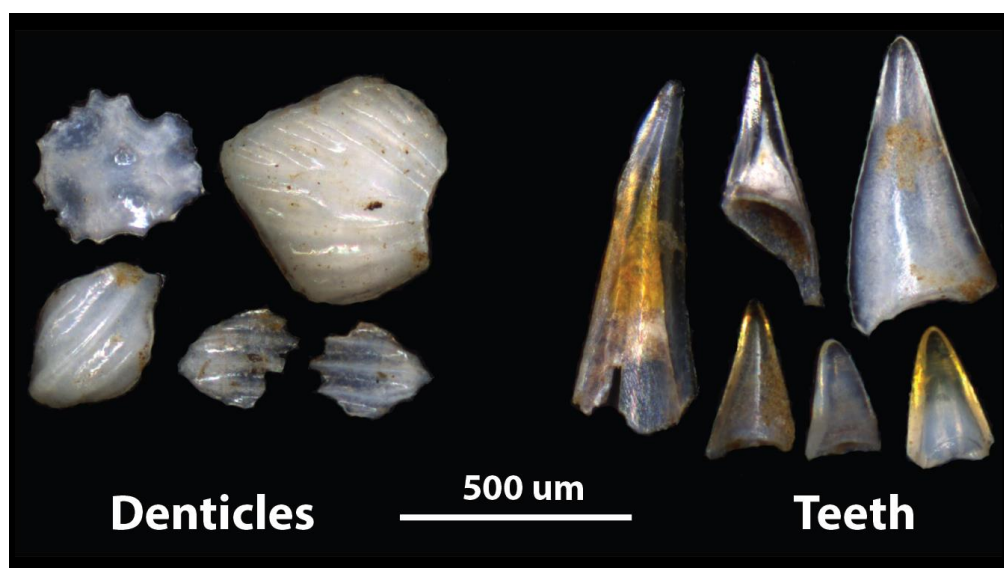


Figure 2-1: An assortment of large (>106µm fraction) denticles (elasmobranch scales; left) and fish teeth (right) from DSDP Site 596, a red clay core in the South Pacific. These ichthyoliths are approximately 52 million years old. Image was taken on the Hull Lab Imaging System, Yale University. Scale bar is 500µm.

While ichthyoliths have a rich history of study in the Paleozoic (Maisey, 1984; Turner, 2004; Turner and Anonymous, 2002), younger ichthyoliths (Late Mesozoic and Cenozoic) have largely been ignored by the paleontology community, excepting large shark teeth (Cappetta and Schultze, 2012), as the majority of stem diversity for living clades was established by the Mesozoic. However, the Cretaceous and Cenozoic ichthyolith record can reveal important information about the role of fishes in aquatic ecosystems, and their response to global change events (Sibert et al., 2014; Sibert and Norris, 2015). As ichthyoliths are found in nearly all sediment types, including those of the open ocean which is rarely preserved on land, pelagic ichthyoliths represent a fossil record virtually untouched by traditional paleoichthyology. While Paleozoic and Mesozoic ichthyolith studies have focused on the taxonomic identification of ichthyoliths to better understand the evolutionary trajectories of elasmobranchs and fishes, the Late Cretaceous and Cenozoic ichthyolith record, with its high abundances of fossils can also reveal patterns in relative and absolute abundances of marine vertebrates within the ecological or environmental context of the time periods (Sibert et al., 2014; Sibert and Norris, 2015). Recent records of ichthyoliths have the potential for identification to extant taxa, and can show changes in functional and taxonomic groups over prehistorical and historical time periods resulting from environmental and/or anthropogenic change (Cramer et al., in review). Although the methods presented here have been developed and tested with deep-sea sediments and near-modern coral reef sediments, we believe that they can be translated to other marine and lacustrine records.

Cretaceous and Cenozoic ichthyoliths have been used as carriers of several isotopic proxies, including Neodymium (Martin and Haley, 2000; Scher and Martin, 2004), a water-mass tracer, and Strontium, which can be used both as a weathering proxy, and for rough dating of sediments (Gleason et al., 2004; Gleason et al., 2002; Gleason et al., 2008; Ingram, 1995). The field of ichthyolith biostratigraphy was developed in the early 1970s, and used to date fossil-poor pelagic red clays (Doyle, 1983; Doyle et al., 1988; Doyle and Riedel, 1979b; Doyle and Riedel, 1985). An updated ichthyolith biostratigraphy for the Eastern North Pacific was developed in 2006 (Johns et al., 2005; Johns et al., 2006). The value of ichthyoliths in biostratigraphy lies in their being extremely dissolution-resistant; indeed, due to their calcium-phosphate composition, ichthyoliths are one of the last microfossil groups remaining in marine sediments exposed to corrosive deep ocean water. They are found in nearly all sediment types, including red clays (Doyle and Riedel, 1979b) which have historically been ignored in paleoceanographic and paleobiological studies as they are often otherwise barren of microfossils.

Despite being relatively common in marine sediments, ichthyoliths have been overlooked by much of the scientific community, overshadowed by the physically larger, more abundant, and better understood foraminifera for studies of biological responses to ancient climate and environmental change (Cifelli, 1969; Frerichs, 1971; Hallock and Schlager, 1986; Hull et al., 2011; Kelly et al., 1998; Smit, 1982). While understanding the response of these unicellular organisms to climate and biotic events provides insight into the sensitivity of marine ecosystems to global change, unicellular algae and protists are only the base of a complex marine ecosystem, which support a diverse array of

consumers, including marine vertebrates. Since the biomass of fishes is dependent on both the total amount of primary production, and the efficiency with which that energy is transferred up the food web (Iverson, 1990; Moloney and Field, 1991), the abundance of ichthyoliths potentially serves as a proxy of paleo-ecosystem structure and function. Quantification of the changes in abundance of vertebrates from the ichthyolith record can reveal how the upper trophic levels of past food webs respond to environmental and anthropogenic disturbances. Moreover, there are typically excellent chronologies and relatively continuous sedimentation rates in many deep-sea sedimentary sequences (e.g. (Hilgen, 1991; Hilgen et al., 2010; Westerhold et al., 2008)). Thus, it is possible to capture unusually detailed histories of vertebrates, as compared to the typical temporal and spatial fragmentation of the terrestrially exposed body-fossil record. In recent, shallow marine sediments, ichthyoliths have the promise of revealing changes in both diversity and abundance of fishes and sharks in coastal systems – making it possible to reconstruct fish community responses to overfishing, reef environmental decline and anthropogenic climate change (Jackson et al., 2001).

Fishes are one of the most diverse and ecologically successful vertebrate clades (Friedman and Sallan, 2012; Near et al., 2013; Nelson, 2006), and are a hallmark of a healthy marine ecosystem. The presence and abundance of fish biomass is an indicator of how efficiently an ecosystem is functioning, in terms of transferring energy from the base of the food web to the upper tiers (Iverson, 1990; Sprules and Munawar, 1986). On modern coral reefs, the abundance of coral-associated fishes is a reliable indicator of coral abundance and growth, and intensive algal grazing by herbivorous fishes facilitates coral dominance (Bellwood and Wainwright, 2002; Randall, 1961). Thus the ichthyolith

record, in conjunction with other microfossil and geochemical records, can provide insight into ecosystem response and resilience to climatic, biotic, and even anthropogenic perturbations (Cramer et al., in review; Sibert et al., 2014; Sibert and Norris, 2015). Lastly, understanding how this group of consumers has responded to global change events may also yield insights into the mechanisms behind Cenozoic marine vertebrate evolution and the development of the vast diversity of fish clades (Betancur-R et al., 2013; Broughton et al., 2013; Near et al., 2013; Near et al., 2012; Nelson, 2006). Here, we provide a detailed methodological framework for the isolation, concentration, and analysis of ichthyoliths as a paleoceanographic, paleoecological, and paleontological resource.

2.3 Methods for ichthyolith isolation and concentration

It is usually impractical to sort through disaggregated sediments for ichthyoliths due to their small size and rarity compared to other microfossils such as benthic and planktonic foraminifera and other coarse-grained sediment clasts. Since metrics of ichthyolith accumulation (abundance) and community structure rely on the quantification of all ichthyoliths in a sample, as opposed to a randomly sampled subset, it is necessary to concentrate the full ichthyolith assemblage from a raw sediment sample. Processing a sediment sample for ichthyoliths is a balance between efficient concentration (typically by disaggregation of sediment and washing through a fine sieve), and minimization of potential loss of teeth by dissolution, fragmentation or adherence onto surfaces such as paintbrushes, splitters, vials, or other surfaces during processing and picking. While calcium phosphate (bio-apatite) is resistant to dissolution, care must be taken to

counteract potential destruction and loss of ichthyoliths when using methods of acid preparation or bleach-mediated disaggregation of sediments. Once washed, ichthyoliths are picked out of the remaining sediments using a high-power dissection microscope and extremely fine paintbrush.

A challenge in working with ichthyoliths is their small size: the vast majority of teeth in pelagic sediments are only retained on a 38 μ m screen (passing through the typical 63 μ m sieves used for most foraminifera research). Modern reef fish teeth are somewhat larger, retained on 63 μ m screens, however they are some of the smallest-sized components of reef sediments. As a practical matter, most pelagic fish teeth are conical or triangular, and will slip through the larger 63 μ m sieve. We have found that upwards of 50-80% of the total ichthyolith assemblage in pelagic sediments is represented by the 38-63 μ m fraction. It is likely that using a sieve smaller than 38 μ m would yield additional ichthyoliths, as the majority of teeth in our samples are in the 38-63 μ m fraction, however the <38 μ m fraction presents significant technical challenges for reflected-light microscope-based work. We present methods for isolation of ichthyoliths from a variety of sediment types (Figure 2-2) and discuss the specifics of each protocol.

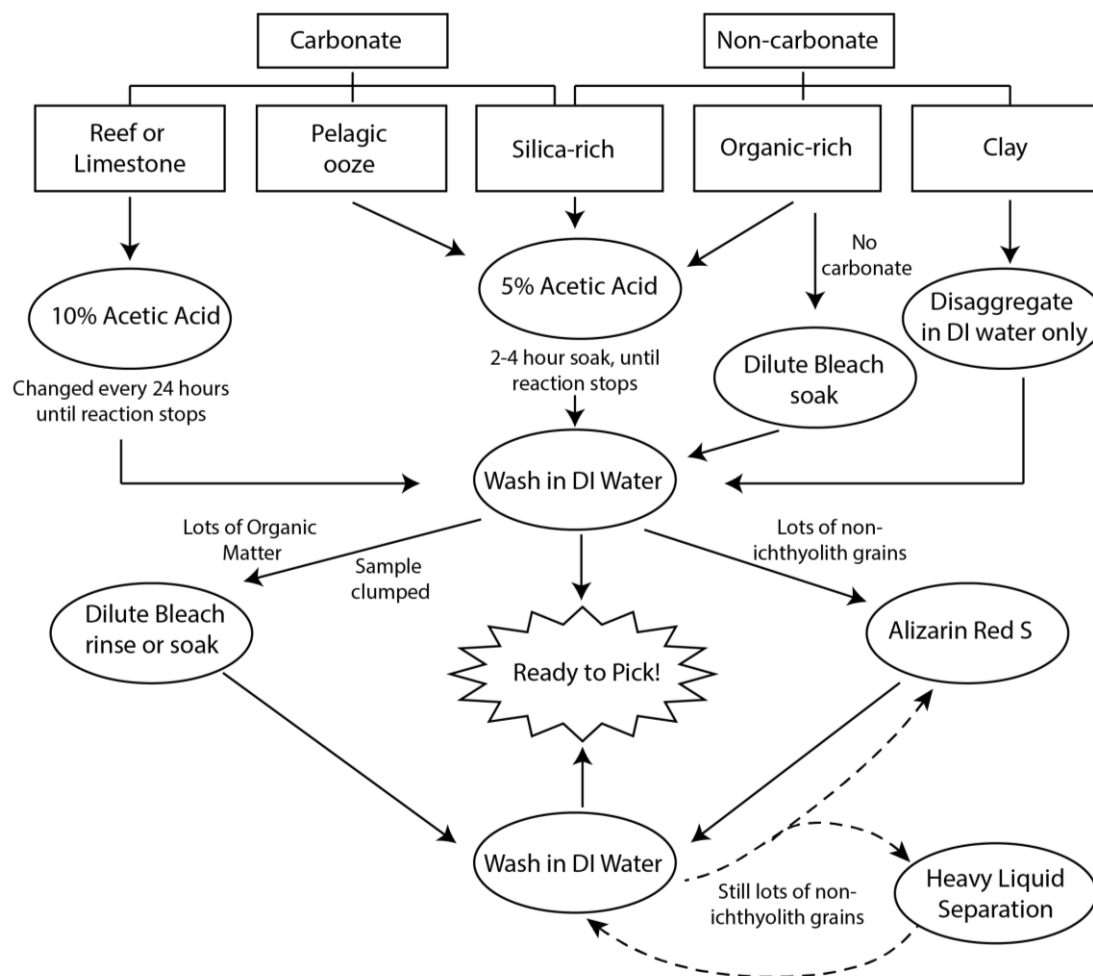


Figure 2-2: A flowchart showing the steps for sediment processing for efficient and effective ichthyolith isolation from a variety of sediment types. Sediment types are in boxes, while processing steps are shown in ovals.

2.3.1 Carbonates

Acid-resistant calcium phosphate ichthyoliths are generally extracted from marine carbonates by acid dissolution of the calcium carbonate fraction. In deep-sea sediments, carbonate-hosted ichthyolith assemblages can then be placed on the highly resolved time scales derived from analysis of other microfossil groups, magnetic reversals or astrochronologies (Sibert et al., 2014). In near-modern coral reef sediments, high-

precision Uranium-Thorium dating of coral skeletons can provide extremely well-resolved chronologies of fish communities over prehistorical and historical time (Cramer et al., in review). These precise time scales provide estimates of sedimentation rate and mass accumulation rate which can be used to estimate fish and elasmobranch abundance or productivity. Combined with the rich abundance of microfossil plankton, a well-studied carbonate section can yield information about many components of an ecosystem through an interval of interest, giving environmental and ecological context to an ichthyolith record (Sibert et al., 2014).

Deep-sea carbonate ooze and chalk. Simply picking ichthyoliths out of the coarse fraction of carbonate sediments is time consuming, and often leads to poor data quality, as the small teeth can easily be missed during the picking process due to the high abundance of foraminifera and siliceous microfossils. To concentrate ichthyoliths effectively and address these issues, samples are dried to a constant weight, and then dissolved in 5-10% acetic acid. Acid is added to the samples in 100-200 ml intervals until no carbonate remains, usually after ~2-5 hours. Samples are stirred every 20-30 minutes, and the reaction is considered complete when no bubbles are released when adding acid or stirring. We find that between 30 and 80 ml of acid is needed per gram of dry sediment to completely dissolve all of the carbonate in a sample, depending both on the concentration of acid used, and the percent-carbonate composition of the sediments. We do not observe any etching or other damage to ichthyoliths during this process, and indeed, due to their high abundance and exceptional preservation in red clays, it is likely that this limited exposure to weak acetic acid does not damage ichthyoliths. However, to avoid any potential destruction of ichthyoliths, acid exposure should be limited and dilute

acid should be used. Once dissolved, the sample is washed over a 38 μm screen and the residue is transferred to filter paper in a funnel and dried in a 50°C oven.

Although it is destructive of the calcareous fossils, dissolution of bulk carbonate samples for ichthyoliths as outlined above, is by far the most effective method. It also yields the highest data quality, as every transfer of the sample between containers leads to some loss of ichthyoliths. Bulk dissolution followed by washing also uses the least amount of water per sample. However, if it is imperative to preserve certain carbonate microfossils in a sample, such as larger benthic foraminifera for a stable isotope record, or foraminifera from a critical interval, we propose a double-washing procedure: the first wash is carried out with de-ionized water only, to retain the coarse fraction of carbonates >38 μm . All material below a specific size threshold (e.g. 150 μm or 250 μm , study-specific) is then dissolved to concentrate the smaller ichthyoliths. We have found that ichthyoliths are selectively lost in sample splitters due to static adhesion, and recommend against their use. As the volume of coarse-grained carbonate sediment is relatively small, it is feasible, although time consuming, to pick out all of the teeth in the >150 μm or >250 μm calcareous residues. In this case, it is most important that the processing method be internally consistent for an entire sample set, and the potential biases recognized when comparing absolute ichthyolith abundance values to other records. Additionally, large teeth (>150 μm) are relatively rare in pelagic sediments and, if ignored or under counted, will not greatly bias the total ichthyolith accumulation rate. Indeed, it is also possible to count only the fraction subjected to acid treatment since the fine fractions retain the vast majority of teeth in a given sample; however in this case, information on the maximum size of teeth, or the change in abundance of specific large teeth and denticles, which are

almost exclusively $>100\mu\text{m}$ will be missed (Sibert and Norris, 2015) . Therefore, the exact method employed will depend on the goals of the study, and it is most important to maintain consistency in processing method throughout the entire record.

Limestones. Lithified limestone also yields ichthyoliths in the acid-insoluble fraction, however the processing is slightly different from that used for deep-sea carbonate sediments. Limestones should be broken up into $\sim 1\text{cm}$ pieces, to increase surface area exposed to acid, while preserving the microfossils. Our approach comprises barely covering samples with 10% acetic acid – we have found that 5% is ineffective for the majority of limestones – and changing acid every 24 hours. When changing the acid, the sample is washed over a stack of sieves with all pieces of limestone $>150\mu\text{m}$ returned to fresh acid, and all residues $<150\mu\text{m}$ but $>38\mu\text{m}$ retained to pick through for ichthyoliths. The process takes approximately 5-12 washes, depending on the degree of lithification of the rock, and the size of the original limestone fragments.

Coral reef sediments. Modern reef sediments are comprised almost entirely of carbonate grains from calcifying organisms including corals, mollusks, echinoderms, foraminifera, calcareous algae, sponges, and crustaceans. To preserve these other taxonomic groups, which are mostly $>500\mu\text{m}$, only the fraction $<500\mu\text{m}$ of these cores is digested in acid and picked through for ichthyoliths, the majority of which are $<250\mu\text{m}$. Due to the larger carbonate grains in predominately sand-sized reef sediments, approximately 50 ml of 10% acetic acid is required for each $\sim 200\text{g}$ sample (dry weight). Two to four applications of approximately 200ml of acid are added every 24 hours. When gentle stirring of acid and residues fails to cause further reaction and residues darken due to dominance of organic material following elimination of carbonates, samples are

transferred to a 63 μ m sieve and washed with DI water until the water leaving the sieve runs clear. To eliminate organic debris that causes excessive clumping of ichthyoliths and highly abundant but acid-insoluble siliceous sponge spicules, samples are treated with 25ml chlorine bleach poured directly onto sieve following an initial rinse, left for approximately 1 minute, then rinsed with DI water and lightly agitated until water runs clear below the sieve. The samples are then transferred to filter paper in a funnel and dried at 50°C. In contrast to pelagic sediments, where the majority of ichthyoliths are within the 38-63 μ m fraction, the vast majority of ichthyoliths preserved in reef sediments are >63 μ m, so the larger sieve size is used to facilitate washing the larger sample volumes necessary in these high sedimentation rate systems (Cramer et al., in review).

2.3.2 *Pelagic clays*

Pelagic clays yield, by far, the greatest abundance of ichthyoliths: the slow sedimentation rate below the carbonate compensation depth, and small grain size means that ichthyoliths are highly concentrated, and are typically extremely well-preserved. However, the slow sedimentation rate and lack of other biostratigraphically well-calibrated microfossils mean that clays often have poor age constraints, and there may be very little paleoenvironmental context within single cores.

To isolate ichthyoliths from pelagic clay, the samples are dried completely to enable the calculation of ichthyolith accumulation rates. We have found that many pelagic clay samples fail to achieve stable dry weights for many weeks, perhaps because of water bound in clays. However, once the samples are completely dried, they are simply disaggregated in de-ionized water, washed over a 38 μ m sieve, transferred to filter

paper in a funnel and dried in a 50°C oven. These residues, in the best circumstance, may contain only fish teeth and dermal denticles, however in other cases may also contain micro-Manganese nodules, siliceous microfossils, terrigenous sediment clasts, or clumps of Fe-oxides.

2.3.3 *Silica-dominated sediments*

Siliceous sediments, whether from quartz silt or biogenic opal, create distinctive challenges in the isolation and quantification of ichthyoliths. Silica is insoluble and thus increases the volume of the acid-insoluble coarse-fraction containing ichthyoliths. Additionally, many quartz grains have a significant visual similarity to tiny ichthyoliths at first glance, making picking a challenge. We have found two methods to be effective in isolation of teeth in siliceous sediments—the use of alizarin red S, a calcium-specific stain to color ichthyoliths and make them visible against a backdrop of translucent silica, and, when absolutely necessary, the deployment of heavy liquids to remove most of the low density siliceous sediment relative to ichthyoliths.

Alizarin Red S. Visual differentiation of fish teeth from other small triangular sediment grains can often be confounded at small size fractions (<63µm). However, Alizarin Red S (1,2-dihydroxyanthraquinone, C₁₄H₈O₄), a calcium-specific dye commonly used in clearing-and-staining fish (Song and Parenti, 1995; Taylor, 1967) stains just the ichthyoliths (Figure 2-3), leaving the silica grains untouched. Alizarin is a pH sensitive dye, which turns a deep purple in basic solution, and when in contact with calcium, will adhere to it, leaving a pink or red color. Alizarin Red S is not a panacea: it will also dye all calcium carbonate grains in a particular sample, and thus is used most

effectively after the carbonate fraction has been removed from a sample via acid dissolution (see Figure 2-2). We modified a clearing-and-staining protocol for fishes, based on both a published protocol (step 9, ref. (Song and Parenti, 1995)), and the protocol used by Scripps Marine Vertebrate Collection, to use a 1% potassium hydroxide (KOH) solution with enough Alizarin to turn the solution a deep purple (a surprisingly small amount). The KOH/Alizarin Red S solution is added to the post-acid, washed and dried residue, often in its plastic or glass storage vial. The volume of Alizarin + KOH solution needed is dependent on the amount of residue: generally, just a few drops of the solution, enough to cover the sample residue in its container, is more than sufficient to produce the desired effect. This is left for 24-48 hours, and then washed over a 38 μ m screen, transferred to filter paper in a funnel, and dried overnight in a 50°C oven before picking. This technique is extremely effective, staining >95% of the ichthyoliths in a sample a pink color (Figure 2-3). The intensity of the color is dependent on both the concentration of dye, and the length of time in solution. The Alizarin staining protocol requires exposure to toxic chemicals (KOH) and a second wash, which can increase the amount of teeth lost to processing, so it is generally best saved for particularly challenging residues, where silica consistently confounds counts of small ichthyoliths, and used consistently within a single record.



Figure 2-3: Paleocene-aged ichthyoliths from ODP Site 1262, stained with Alizarin Red S. The scale bar is 500 μ m, with teeth >106 μ m in the upper row and teeth <106 μ m in the lower. Note that in the coloring effect is present in all teeth, however the degree of staining varies.

Heavy Liquid Separation. Heavy liquids have been historically used to isolate calcium phosphate conodonts from acid-prepared limestone and the methods have been described extensively elsewhere (Leiggi and May, 2005). This procedure can effectively separate ichthyoliths from biogenic silica and quartz silt, however heavy liquids are expensive and toxic, making them a last resort for ichthyolith isolation. We have used both sodium metatungstate hydrate ($\text{Na}_6\text{W}_{12}\text{O}_{39} \cdot x\text{H}_2\text{O}$) and LST solution (heteropolytungstate) as heavy liquids since both are non-toxic and have low viscosity at room temperature. Both liquids have the disadvantage of being relatively expensive (~\$1000/liter), and can be destroyed by contamination with calcium. Therefore, the use

of heavy liquids on samples containing calcium carbonate grains should be avoided. We use a heavy liquid density of about 2.3-2.4 g/cm³, to capture most of the biogenic silica or 2.85 g/cm³ to separate ichthyoliths from quartz silt.

In our practice, heavy liquid of suitable density is poured into a 25-50 mL tube containing the prepared sample residues, and mixed until the sample is completely wetted; sufficient heavy liquid should be added to the tube so that the silica can float. The tube is capped and centrifuged for five minutes at 1000-1500 rpm to concentrate the ichthyoliths in the bottom of the tube. The light fraction is scooped or poured off the top of the liquid. Both the light and heavy fractions are rinsed in de-ionized water over a 38µm screen, retaining the rinse solution, then transferred to filter paper in a funnel and dried in at 50°C oven. The heavy liquid is recovered and cleaned by passing it through a 0.4µm filter in a vacuum filtration system. The dilute, filtered heavy liquid is placed in an oven to evaporate the rinse water and restore its density.

2.3.4 *Organic-rich sediments*

While the majority of deep-sea sediments are carbonate or silica-dominated, there are many distinct horizons, such as the Mediterranean sapropels (Cramp and O'Sullivan, 1999), which are organic-rich, and ichthyolith concentration using other methods is hampered. In addition, modern coral reef sediments, though carbonate dominated, may still have considerable amounts of organic matter, as they are recently buried and fairly shallow. This leads to sediment clumping and adds extra challenges to sample processing. To address this, samples are first disaggregated and dissolved in weak acid, following the carbonate deep-sea sediments protocol, and washed over a 38µm sieve. However, in

many cases, this does not sufficiently concentrate ichthyoliths and may leave numerous organic-rich clumps of sediment remaining. Once the sample has been thoroughly washed, a rise while on the sieve with dilute (5-10%) bleach solution promotes disaggregation and dissolution of the remaining organic matter. However, it is important to note that bleach and acetic acid produce chlorine gas when mixed, so caution is advised to ensure that the sample is sufficiently rinsed from acid before any bleach is used.

In the case where disaggregation of organic-rich sediments does not occur with the addition of de-ionized water or acetic acid, an additional short soak in bleach, hydrogen peroxide (H₂O₂), Borax™, Calgon™, or OxiClean™ are a potential alternatives, although prolonged exposure can damage the ichthyoliths. Most commercial grades of bleach contain perfume and colorants besides pure sodium hypochlorate, and various formulations produce different results. For instance, in work with Turonian black shales from Ocean Drilling Program Site 1259, we achieved the best disaggregation using pure commercial bleach, rather than making a dilute mixture (Bice and Norris, 2005). In our experience, commercial grades of bleach vary in their content of sodium hypochlorate from 5.25% to 6%. Dilution lowers the pH of bleach solutions, potentially increasing the etching of microfossils with sustained contact and may reduce the effectiveness of the solution for breaking down organic-rich sediments. However, prolonged exposure to bleach at any concentration is potentially damaging to the organic components in ichthyoliths, and should be limited if possible.

Isolating Modern Ichthyoliths. Similar to removing organic material from sediments, flesh can be removed from jaws or skin patches of modern specimens to

isolate taxonomically known fish teeth and shark scales. In this case, the jaw (for fish teeth) or a patch of skin (for shark denticles) is dissected from a modern specimen and placed in dilute (5-10%) bleach until all flesh is dissolved, usually 1-4 hours. Since bleach will attack the organic compounds in teeth and bone as well as the softer tissues, we recommend removing the ichthyoliths from the bleach and washing the newly isolated modern ichthyoliths as soon as is practical. These isolated modern ichthyoliths are then washed over a 38 μ m screen and dried in at 50°C oven.

2.3.5 Comments about ichthyolith-specific washing and picking techniques

Traditional uses of ichthyoliths, for biostratigraphy or as carriers of isotopes, do not require that all teeth be retained and accounted for in a sample. However, to assess the ichthyolith accumulation rate, ichthyolith community structure, and the role of fishes within an ecosystem through time, all of the ichthyoliths within a certain size range must be quantified. The methods presented here aim to improve the fidelity of isolation and concentration of ichthyoliths, to make this robust quantification both possible and repeatable. Due to their small size and unusual shape, care must be taken when handling the concentrated ichthyolith residue to avoid losing any teeth. As most teeth are triangular, they tend to stick point-down into the sieve when washing. Running water up through the back of the sieve, a technique often used when separating biological samples, will help to dislodge any teeth that are stuck point-down.

Earlier ichthyolith work mounted tooth residues in optical medium and viewed them using transmitted light microscopy (Doyle, 1983; Doyle et al., 1977; Doyle and Riedel, 1979a, b; Doyle and Riedel, 1985). Transmitted light imaging is particularly

useful for observing the details of the interior of the pulp cavity and the structure of the enamel cap and so may have value for identification of teeth to taxonomic group (Doyle and Riedel, 1979b; Johns, 1993). Strewn slides made by embedding the entire sample residue in Canada Balsam or Norland optical medium can also be used to count the abundance of extremely small teeth, which can be re-located by use of a England Finder, similar to the study of calcareous nannoplankton. However, there are a number of disadvantages of embedding teeth in a mounting medium, including the formation of bubbles in the pulp cavity, the difficulty in achieving standard orientations given the very small size of many teeth, and the three-dimensional aspect of large teeth in contrast with the narrow depth of field in transmitted light microscopy. An alternative approach is to pick ichthyoliths with a fine paint brush and mount them with water soluble glue on cardboard micropaleontology slides. This method retains the most options for quantifying ichthyoliths. It also ensures that teeth are not overlooked in original count analyses. Once picked, these assemblage slides are a resource which can be worked with directly, or easily be used for many other imaging techniques, including transmitted light microscopy, scanning electron microscopy, and even microCT or nanoCT scanning. This also leaves the ichthyoliths accessible for geochemical analyses.

For pelagic sediments in particular, the small size of ichthyoliths presents a challenge to conventional picking using the techniques typically applied to foraminifera or ostracods: the majority of ichthyoliths are translucent and nearly invisible to the naked eye, making them difficult to place in a storage slide once picked out of the residue. Indeed, we have found that for ichthyoliths $<106\mu\text{m}$, it is necessary to use a microscope when placing the picked ichthyoliths into storage slides. We use standard gridded

micropaleontology brass picking trays and a fine-tipped natural hair brush wetted with water to separate ichthyoliths from the remainder of the residue. The sample can be sieved before picking so that the relatively coarse fraction can be picked separately from the fine fraction. Alternatively, for pelagic sediments with exceptionally small teeth, only the coarse fraction ($>63\mu\text{m}$) may be picked and the finer fraction ($38\text{-}63\mu\text{m}$) may be left for counting with a clicker or counting machine, or prepared for transmitted light observation in a mounted slide. Placing the smallest fraction in a mounting medium for transmitted light observation is not severely limiting, as long as there is no clumping in the residue and ichthyoliths are not severely outnumbered by insoluble sediment clasts, since the very smallest teeth are presently difficult to identify to morphological or taxonomic group and have little value for geochemical analysis. For picking the coarse fraction, one approach is to use a pair of microscopes set up side-by-side – one to pick through the residue on a gridded tray, and a second to place the teeth into slides for storage. This setup eliminates the need to change the microscope's focus or move the picking tray when transferring ichthyoliths to a micropaleontological slide.

2.4 Results and Discussion

2.4.1 Ichthyolith Accumulation Rates

Once isolated and quantified, ichthyoliths provide a unique view of fish production and community dynamics through time. However, changes in sedimentation rate, composition, and density can have a profound effect on the absolute abundance of ichthyoliths in a sample, which bias any estimations of fish production or flux. To correct

for this, we calculate an ichthyolith accumulation rate (IAR; eq. 1), yielding a metric of ichthyolith flux of ichthyoliths falling to a fixed area of seafloor over a fixed time interval. Thus, changes in IAR can be interpreted as increases or decreases in total ichthyolith production, a proxy for overall fish production (Sibert et al., 2014). IAR in pelagic sediments is calculated as:

Ichthyolith Accumulation Rate = Abundance * Dry Bulk Density * Sedimentation Rate

$$\left(\frac{\text{Ichthyoliths}}{\text{cm}^2 * \text{kyr}}\right) = \frac{\text{ichthyoliths}}{\text{gram}} * \frac{\text{grams}}{\text{cm}^3} * \frac{\text{cm}}{\text{kyr}}$$

In the case of sediments from reef matrix cores which have large fragments of subfossil coral or mollusk shell (>2mm), IAR is calculated by normalizing by the weight of sediments in the size fraction <2mm (where the vast majority of teeth are found) and the number of years represented by a sample. The number of years in a sample was computed from U/Th-derived sediment accumulation rates. This produces an ichthyolith abundance accumulation rate (AAR):

$$\text{AAR} = \left(\frac{\text{Ichthyoliths}}{\text{gram} * \text{year}}\right) = \frac{\text{ichthyoliths}}{\text{sample}} / \frac{\text{years}}{\text{sample}} / \text{grams}$$

This calculation of IAR or AAR normalizes for sedimentation rate and changes in lithology. Therefore, we can compare the flux of ichthyoliths to the sea floor between sites with very different background sedimentation rates, such as between open ocean gyre sites and those from the high-productivity equatorial oceans. We can also correct for variations in sedimentation rate time in a single site that result from changes in fish production, sediment delivery, or carbonate dissolution. However, the calculation of IAR is highly sensitive to the accuracy of the time scale used to estimate sedimentation rate. Bulk density is also a component of IAR, but contributes relatively little to variation in

IAR in pelagic sediments (Sibert et al., 2014). An exception is where there are major changes in lithology, such as from carbonates to claystone or calcareous ooze to limestone; in these cases accurate measurement of bulk density and sedimentation rate can be important in the calculation of IAR.

Sample size. The size fractions quantified can be study-specific, to balance between statistical confidence in the data (enough ichthyoliths available), time committed by the researcher, and preservation of other microfossils. We have found through our work that for pelagic marine carbonates, where sedimentation rate is 1-2 cm/kyr, quantification of all ichthyoliths $>38\mu\text{m}$ in a 10-20cc sample is necessary for sufficiently robust abundances of >30 -100 teeth/sample. The same sample volume in pelagic red clay can yield thousands of teeth, and statistically significant samples of several hundred teeth may be found in the $>106\mu\text{m}$ fraction. In contrast, in coastal sediments and reef carbonates, the high degree of dilution of ichthyoliths by other grains and higher sedimentation rates can require much larger sample volumes to obtain statistically representative ichthyolith samples. For example, in our work in modern Caribbean reef sediments, we routinely sample volumes of 400cc (about 200g dry weight) to recover 2-232 teeth (mean=74 teeth) and 0-5 denticles per sample.

While the abundance of fish may be an indicator of primary or export productivity of an ecosystem, this is not the only signal recorded in the ichthyolith record. The overall efficiency of a marine food web is determined by how many trophic steps are needed to transfer the carbon fixed by primary producers up to higher-order consumers such as fish. In a large phytoplankton-dominated system, such as a modern upwelling zone, a modest total production will yield abundant fish with only 1-2 trophic steps. In contrast, a system

dominated by small phytoplankton (such as cyanobacteria in the open ocean) with the same absolute primary production may require 5-7 trophic steps to produce a single fish (Moloney and Field, 1991; Moloney et al., 1991). While both of these ecosystems may have similar levels of primary production, the former will produce several orders of magnitude more fish biomass than the latter (Iverson, 1990), and thus should have a significantly higher ichthyolith accumulation rate. Indeed, a substantial portion of observed IAR patterns could be accounted for not by changing net primary production, but instead by small shifts in the relative abundance of certain size classes of phytoplankton. This food web imprint can also be exacerbated by changes in the efficiency of energy transfer between trophic levels due to increases or decreases in metabolic rates of the organisms. IARs may also be affected by changes in habitat: for example, in coral reef sediments, abundances of teeth from coral-associated taxa are tightly coupled with reef accretion rates (Cramer et al., in review).

IAR is also influenced by the production of ichthyoliths by individuals. Species which put considerable effort into growing their teeth and have low turnover, or resorb teeth rather than shedding them (Bemis et al., 2005), could produce fewer ichthyoliths than a species which produces numerous, but oftentimes less sturdy teeth which are regularly shed, such as parrotfish teeth (Figure 2-4). The majority of the ichthyolith accumulation rate signal is driven by the smallest teeth, which likely are derived from a combination of small species, juvenile fish and the pharyngeal jaw tooth battery. At present we are unsure about the relative contribution of teeth from these different sources, but we suspect that most teeth preserved in sediments are biased toward those with dissolution-resistant enamel caps. The excellent preservation of enamel relative to

dentine is likely to bias the tooth record toward oral teeth and those of species with robust dentitions, and mitigate against relatively lightly calcified pharyngeal teeth and the teeth of some midwater species where an elongate pulp cavity can run almost the full length of the teeth (Fink, 1981). Long-term trends in changes in ichthyolith abundance, particularly with shifts in the size structure of the assemblage, over 10s of millions of years, may reflect an evolutionary shift in fish community composition (Sibert and Norris, 2015), though not necessarily a change in overall productivity or food web dynamics.

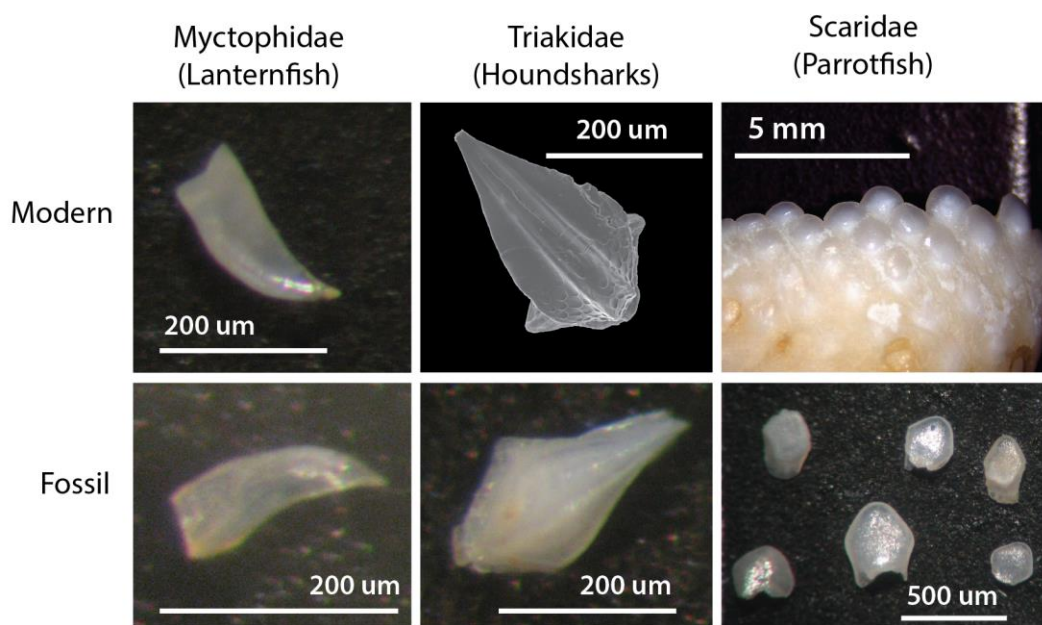


Figure 2-4: Examples of select taxonomically identifiable fossil ichthyoliths and modern counterparts. All modern ichthyoliths were isolated from specimens in the Scripps Marine Vertebrate Collection. The fossil Myctophidae and Triakidae specimens are from ODP Site 1262, and are 62 million years old. The Scaridae modern teeth are from Smithsonian National Museum of Natural History’s Fish Collection and subfossil teeth are from coral reef sediment cores taken off of the coast of Bocas del Toro, Panama, and are approximately 1200 years old.

2.4.2 *Ichthyolith Community Metrics*

While taxonomic identifications of most ancient ichthyoliths is presently elusive, a considerable amount of information about marine vertebrate community composition can be obtained by considering the composition of whole ichthyolith assemblages, which represent snapshots of the entire community, rather than occurrences of a single species or morphotype. Since ichthyoliths are abundant in most sediment samples, we can evaluate how the relative abundances of different marine vertebrate groups have changed through time.

Teeth vs. Denticles. Due to similarity in their chemical compositions, both shark dermal scales (denticles) and fish teeth are preserved in the ichthyolith record. They are easily differentiated visually, as the majority of teeth are triangular or conical and have a distinctive tooth-like shape, while denticles are irregularly shaped – typically flattened, button-shaped or scalloped. While the majority of denticles preserved in the ichthyolith record have been chipped, or preserve only the crown of the scale, they are distinctive from teeth and readily recognizable as denticles (Figure 2-1). The absolute abundances of teeth and denticles through time can be used to study the response of different trophic level organisms to global change (Sibert and Norris, 2015).

Ichthyolith functional group and taxonomic composition. Individual ichthyolith size is also informative of evolutionary patterns. While fish tooth size is not necessarily correlated directly with body size (e.g., deep-sea viperfish of the family Stomiidae have fanglike teeth that are nearly the length of their head), it is an indicator of diet. For example, long, pointed teeth are more likely to be used for handling larger or more active prey. The size structure of an ichthyolith assemblage, quantified either

through changes in relative abundance of different size fractions or by measuring the length of individual teeth (Sibert and Norris, 2015), can reveal evolutionary or ecological trends. For example, following the Cretaceous-Paleogene extinction, the maximum size of the largest teeth in an assemblage in open ocean sediments tripled from pre-extinction values, suggesting that there was a radiation of fishes preferring larger prey following the extinction event (Sibert and Norris, 2015).

While some ichthyoliths are taxonomically identifiable (Figure 2-4), the majority remain unidentified to taxonomic group at this stage. Teeth from modern Caribbean reef sediments have a greater variety of tooth morphotypes than those from pelagic sediments and can be divided into diet categories such as predators (raptorial or canine teeth), herbivores (incisiform teeth), and durophagous invertivores (molariform teeth), producing a record of fish trophic structure through time (Cramer et al., in review).

Utilizing a fish tooth reference collection for modern Caribbean reef fish (www.ichthyolith.ucsd.edu), it is also possible to identify several distinctive tooth types to family level. Pelagic ichthyoliths also have discrete morphological characters, such as the shape and structure of the pulp cavity, which have been studied in depth for biostratigraphy, and we believe that identification of either taxonomic affinity or ecological group will also become possible for pelagic fishes as research progresses.

Ichthyolith Taphonomy. While ichthyoliths are generally resistant to the dissolution effects that damage other microfossil groups, there are several taphonomic processes that can affect the preservation of ichthyoliths. As many teeth have an extensive, hollow pulp cavity, larger teeth are prone to splitting due to mechanical forces, either during preservation or sediment processing. However, as the large teeth most likely

to break are relatively rare in a sample, it is quite often straightforward to piece a single large tooth back together following a fracture. We have also observed iron and manganese oxides growing in the pulp cavity of teeth which can cause splintering. These same oxides can also grow around teeth, hiding them from observation. When this relatively rare phenomenon occurs, we often find some teeth which have just begun to be covered in the coarse fraction, and can therefore either account for the bias (if there are relatively few nodules in the sample) or consider removing the sample from quantitative analysis. Finally, some parts of ichthyoliths are more durable than others. For example, the crowns of denticles are much more likely to be preserved than the subcutaneous base, and the more heavily enameled tooth tips preserve more often as well. Despite these taphonomic biases, the ichthyolith record is generally well-preserved.

Future Applications of Ichthyoliths. While we have addressed several applications of the ichthyolith record here, there are numerous other potential applications. For example, taxonomically identifiable pelagic ichthyoliths can provide significantly better fossil calibration ages for molecular clock estimates of divergence in open ocean lineages, which have a poor body fossil record. Comparison of ichthyolith records with other biological groups present in the same core (e.g. ichthyoliths and coral community composition in the Caribbean, or fish and foraminifera in the open ocean) can reveal trophic or community dynamics through time. IAR or community composition metrics can also be compared to geochemical proxies, to assess the effects of local or global change on fish population or community ecology. Establishing the natural abundance, structure, and variability of fish communities in coastal, reef, or even lake settings, on historic or pre-historic timescales can provide a baseline for separating

anthropogenic pressures and climate impacts on economically significant fish stocks.

Finally, archaeological middens may have considerable amounts of ichthyoliths, which could offer insight into how ancient humans interacted with marine resources.

2.5 Conclusions

Ichthyoliths represent an important and understudied microfossil group that preserves the record of fishes and sharks at unprecedented temporal resolution.

Quantification of the relative and absolute abundance of ichthyoliths through time can reveal changing patterns in fish production, food web stability, and ecosystem structure through Earth's history (including the Anthropocene) and across global change events.

Accurate quantification of these trends in ichthyolith accumulation and assemblage

structure relies on quantification of all ichthyoliths in each discrete sample. We have

presented a methodological framework for isolation and quantification of ichthyoliths

from most marine sediment types ranging from coral reefs to the open ocean, however

these methods can also be applied to lacustrine or other marine deposits. We have further

presented a novel protocol for staining ichthyoliths pink for easier and more accurate

visual identification using Alizarin Red S. The applications of the ichthyolith record

include more traditional biostratigraphy and geochemistry, alongside fish production,

evolution, and ancient food web reconstruction. Taxonomic or ecological identification of

ichthyoliths will further reveal patterns in fish evolution, shed light on the development

and rise to dominance of the most diverse group of vertebrates on the planet, and reveal

the full magnitude of change in fish communities resulting from past and present human

activities.

2.6 References

- Alegret, L., and Thomas, E., 2009, Food supply to the seafloor in the Pacific Ocean after the Cretaceous/Paleogene boundary event: *Marine Micropaleontology*, v. 73, no. 1-2, p. 105-116.
- Bellwood, D. R., and Wainwright, P. C., 2002, The history and biogeography of fishes on coral reefs: *Coral reef fishes: dynamics and diversity in a complex ecosystem*, p. 5-32.
- Bemis, W. E., Giuliano, A., and McGuire, B., 2005, Structure, attachment, replacement and growth of teeth in bluefish, *Pomatomus saltatrix* (Linnaeus, 1766), a teleost with deeply socketed teeth: *Zoology*, v. 108, no. 4, p. 317-327.
- Betancur-R, R., Broughton, R. E., Wiley, E. O., Carpenter, K., López, J. A., Li, C., Holcroft, N. I., Arcila, D., Sanciangco, M., and Cureton, J., 2013, The tree of life and a new classification of bony fishes: *PLoS Curr*, v. 5, p. 1-33.
- Bice, K. L., and Norris, R. D., Data report: Stable isotope ratios of foraminifers from ODP Leg 207, Sites 1257, 1258, and 1260 and a cleaning procedure for foraminifers in organic-rich shales, *in* *Proceedings Proc. Ocean Drill. Program Sci. Results2005, Volume 207*.
- Broughton, R. E., Betancur, R., Li, C., Arratia, G., and Ortí, G., 2013, Multi-locus phylogenetic analysis reveals the pattern and tempo of bony fish evolution: *PLoS Curr*, v. 5, no. 5.
- Cappetta, H., and Schultze, H., 2012, Mesozoic and Cenozoic Elasmobranchii: teeth, chondrichthyes: *Handbook of Palaeoichthyology E*, v. 3.
- Cifelli, R., 1969, Radiation of Cenozoic planktonic foraminifera: *Systematic Biology*, v. 18, no. 2, p. 154-168.
- Cramer, K. L., O'Dea, A., Leonard-Pingel, J. S., Clark, T. R., Zhao, J.-x., and Norris, R. D., in review, Prehistorical and historical decline of Caribbean reef ecosystems linked to loss of herbivores.
- Cramp, A., and O'Sullivan, G., 1999, Neogene sapropels in the Mediterranean: a review: *Marine Geology*, v. 153, no. 1-4, p. 11-28.
- Doyle, P. S., 1983, Ichthyolith stratigraphy in the Pacific, *Eos, Transactions, American Geophysical Union, Volume 64: Washington, American Geophysical Union*, p. 741-742.

- Doyle, P. S., Boillot, G., Winterer, E. L., Meyer, A. W., Applegate, J., Baltuck, M., Bergen, J. A., Comas, M. C., Davies, T. A., Dunham, K. W., Evans, C. A., Girardeau, J., Goldberg, D., Haggerty, J. A., Jansa, L. F., Johnson, J. A., Kasahara, J., Loreau, J.-P., Luna, E., Moullade, M., Ogg, J. G., Sarti, M., Thurow, J., and Williamson, M. A., 1988, Remarks on Cretaceous-Tertiary ichthyolith stratigraphy in the Atlantic, Ocean Drilling Program Leg 103: Proceedings of the Ocean Drilling Program, Scientific Results, v. 103, p. 445-458.
- Doyle, P. S., Dunsworth, M. J., and Riedel, W. R., 1977, Reworking of ichthyoliths in eastern tropical Pacific sediments: *Deep-Sea Research*, v. 24, no. 2, p. 181-198.
- Doyle, P. S., and Riedel, W. R., 1979a, Cretaceous to Neogene ichthyoliths in a giant piston core from the central North Pacific: *Micropaleontology*, v. 25, no. 4, p. 337-364.
- Doyle, P. S., and Riedel, W. R., 1979b, Ichthyoliths: present status of taxonomy and stratigraphy of microscopic fish skeletal debris, La Jolla, CA, Scripps Institution of Oceanography, University of California, San Diego, Scripps Institution of Oceanography Reference Series.
- Doyle, P. S., and Riedel, W. R., 1985, *Cenozoic and Late Cretaceous ichthyoliths*, Cambridge, United Kingdom (GBR), Cambridge Univ. Press, Cambridge, Plankton stratigraphy.
- Fink, W. L., 1981, Ontogeny and phylogeny of tooth attachment modes in actinopterygian fishes: *Journal of Morphology*, v. 167, no. 2, p. 167-184.
- Frerichs, W. E., 1971, Evolution of planktonic foraminifera and paleotemperatures: *Journal of Paleontology*, p. 963-968.
- Friedman, M., and Sallan, L. C., 2012, Five hundred million years of extinction and recovery: a Phanerozoic survey of large-scale diversity patterns in fishes: *Palaeontology*, v. 55, no. 4, p. 707-742.
- Gleason, J., Moore Jr, T., Johnson, T., Rea, D., Owen, R., Blum, J., Pares, J., and Hovan, S., 2004, Age calibration of piston core EW9709-07 (equatorial central Pacific) using fish teeth Sr isotope stratigraphy: *Palaeogeography, Palaeoclimatology, Palaeoecology*, v. 212, no. 3, p. 355-366.
- Gleason, J. D., Moore, T. C., Rea, D. K., Johnson, T. M., Owen, R. M., Blum, J. D., Hovan, S. A., and Jones, C. E., 2002, Ichthyolith strontium isotope stratigraphy of a Neogene red clay sequence: calibrating eolian dust accumulation rates in the central North Pacific: *Earth and Planetary Science Letters*, v. 202, no. 3-4, p. 625-636.

- Gleason, J. D., Thomas, D. J., Moore, T. C., Blum, J. D., Owen, R. M., and Haley, B. A., 2008, Early to middle Eocene Arctic paleoceanography from Nd-Sr isotope study of fossil fish debris, Lomonosov Ridge: *Geochimica Et Cosmochimica Acta*, v. 72, no. 12, p. A314-A314.
- Hallock, P., and Schlager, W., 1986, Nutrient excess and the demise of coral reefs and carbonate platforms: *Palaios*, p. 389-398.
- Hilgen, F., 1991, Astronomical calibration of Gauss to Matuyama sapropels in the Mediterranean and implication for the geomagnetic polarity time scale: *Earth and Planetary Science Letters*, v. 104, no. 2-4, p. 226-244.
- Hilgen, F. J., Kuiper, K. F., and Lourens, L. J., 2010, Evaluation of the astronomical time scale for the Paleocene and earliest Eocene: *Earth and Planetary Science Letters*, v. 300, no. 1-2, p. 139-151.
- Hull, P. M., and Norris, R. D., 2009, Evidence for abrupt speciation in a classic case of gradual evolution: *Proceedings of the National Academy of Sciences of the United States of America*, v. 106, no. 50, p. 21224-21229.
- Hull, P. M., Norris, R. D., Bralower, T. J., and Schueth, J. D., 2011, A role for chance in marine recovery from the end-Cretaceous extinction: *Nature Geoscience*, v. 4, p. 856-860.
- Hunt, G., 2004, Phenotypic variation in fossil samples: modeling the consequences of time-averaging: *Paleobiology*, v. 30, no. 3, p. 426-443.
- Hunt, G., Wicaksono, S. A., Brown, J. E., and MacLeod, K. G., 2010, Climate-Driven Body-Size Trends in the Ostracod Fauna of the Deep Indian Ocean: *Palaeontology*, v. 53, p. 1255-1268.
- Ingram, B. L., 1995, High-resolution dating of deep-sea clays using Sr isotopes in fossil fish teeth: *Earth and Planetary Science Letters*, v. 134, no. 3, p. 545-555.
- Iverson, R. L., 1990, Control of Marine Fish Production: *Limnology and Oceanography*, v. 35, no. 7, p. 1593-1604.
- Jackson, J. B. C., Kirby, M. X., Berger, W. H., Bjorndal, K. A., Botsford, L. W., Bourque, B. J., Bradbury, R. H., Cooke, R., Erlandson, J., Estes, J. A., Hughes, T. P., Kidwell, S., Lange, C. B., Lenihan, H. S., Pandolfi, J. M., Peterson, C. H., Steneck, R. S., Tegner, M. J., and Warner, R. R., 2001, Historical overfishing and the recent collapse of coastal ecosystems: *Science*, v. 293, no. 5530, p. 629-638.
- Johns, M., 1993, Taxonomy and biostratigraphy of Middle and Upper Triassic ichthyoliths from northeastern British Columbia: *Master's thesis*: University of Victoria.

- Johns, M. J., Barnes, C. R., and Narayan, Y. R., 2005, Cenozoic and Cretaceous ichthyoliths from the Tofino Basin and western Vancouver Island, British Columbia, Canada: *Palaeontologia Electronica*, v. 8, p. no. 2, 202.
- Johns, M. J., Barnes, C. R., and Narayan, Y. R., 2006, Cenozoic ichthyolith biostratigraphy; Tofino Basin, British Columbia: *Canadian Journal of Earth Sciences = Revue Canadienne des Sciences de la Terre*, v. 43, no. 2, p. 177-204.
- Kelly, D. C., Bralower, T. J., and Zachos, J. C., 1998, Evolutionary consequences of the latest Paleocene thermal maximum for tropical planktonic foraminifera: *Palaeogeography, Palaeoclimatology, Palaeoecology*, v. 141, no. 1, p. 139-161.
- Leiggi, P., and May, P., 2005, *Vertebrate paleontological techniques*, Cambridge University Press.
- Maisey, J., 1984, Higher elasmobranch phylogeny and biostratigraphy: *Zoological Journal of the Linnean Society*, v. 82, no. 1- 2, p. 33-54.
- Martin, E., and Haley, B., 2000, Fossil fish teeth as proxies for seawater Sr and Nd isotopes: *Geochimica Et Cosmochimica Acta*, v. 64, no. 5, p. 835-847.
- Moloney, C. L., and Field, J. G., 1991, The size-based dynamics of plankton food webs. I. A simulation model of carbon and nitrogen flows: *Journal of plankton research*, v. 13, no. 5, p. 1003-1038.
- Moloney, C. L., Field, J. G., and Lucas, M. I., 1991, The size-based dynamics of plankton food webs. II. Simulations of three contrasting southern Benguela food webs: *Journal of plankton research*, v. 13, no. 5, p. 1039-1092.
- Near, T. J., Dornburg, A., Eytan, R. I., Keck, B. P., Smith, W. L., Kuhn, K. L., Moore, J. A., Price, S. A., Burbrink, F. T., Friedman, M., and Wainwright, P. C., 2013, Phylogeny and tempo of diversification in the superradiation of spiny-rayed fishes: *Proceedings of the National Academy of Sciences*, v. 110, no. 31, p. 12738-12743.
- Near, T. J., Eytan, R. I., Dornburg, A., Kuhn, K. L., Moore, J. A., Davis, M. P., Wainwright, P. C., Friedman, M., and Smith, W. L., 2012, Resolution of ray-finned fish phylogeny and timing of diversification: *Proceedings of the National Academy of Sciences of the United States of America*, v. 109, no. 34, p. 13698-13703.
- Nelson, J. S., 2006, *Fishes of the World*, New York, NY, Wiley, 600 p.:

- Randall, J. E., 1961, Overgrazing of algae by herbivorous marine fishes: *Ecology*, v. 42, no. 4, p. 812.
- Scher, H. D., and Martin, E. E., 2004, Circulation in the Southern Ocean during the Paleogene inferred from neodymium isotopes: *Earth and Planetary Science Letters*, v. 228, no. 3-4, p. 391-405.
- Sibert, E. C., Hull, P. M., and Norris, R. D., 2014, Resilience of Pacific pelagic fish across the Cretaceous/Paleogene mass extinction: *Nature Geosci*, v. 7, no. 9, p. 667-670.
- Sibert, E. C., and Norris, R. D., 2015, New Age of Fishes initiated by the Cretaceous–Paleogene mass extinction: *Proceedings of the National Academy of Sciences*, v. 112, no. 28, p. 8537-8542.
- Smit, J., 1982, Extinction and evolution of planktonic foraminifera after a major impact at the Cretaceous/Tertiary boundary: *Geological Society of America Special Papers*, v. 190, p. 329-352.
- Song, J., and Parenti, L. R., 1995, Clearing and staining whole fish specimens for simultaneous demonstration of bone, cartilage, and nerves: *Copeia*, p. 114-118.
- Sprules, W. G., and Munawar, M., 1986, Plankton Size Spectra in Relation to Ecosystem Productivity, Size, and Perturbation: *Canadian Journal of Fisheries and Aquatic Sciences*, v. 43, no. 9, p. 1789-1794.
- Taylor, W. R., 1967, An enzyme method of clearing and staining small vertebrates.
- Thomas, E., 2003, Extinction and food at the seafloor: A high-resolution benthic foraminiferal record across the initial Eocene thermal maximum, Southern Ocean site 690: *Geological Society of America Special Papers*, v. 369, p. 319-332.
- Thomas, E., 2007, Cenozoic mass extinctions in the deep sea; what perturbs the largest habitat on Earth?: *Special Paper - Geological Society of America*, v. 424, p. 1-23.
- Thomas, E., and Gooday, A. J., 1996, Cenozoic deep-sea benthic foraminifers: Tracers for changes in oceanic productivity?: *Geology*, v. 24, no. 4, p. 355-358.
- Turner, S., 2004, Early vertebrates: analysis from microfossil evidence: *Recent advances in the origin and early radiation of vertebrates*, p. 65-94.
- Turner, S., and Anonymous, 2002, Stages in the origin of vertebrates; analysis from actual fossil evidence, *Journal of Vertebrate Paleontology*, Volume 22: Norman, University of Oklahoma, p. 116.

Westerhold, T., Roehl, U., Raffi, I., Fornaciari, E., Monechi, S., Reale, V., Bowles, J., and Evans, H. F., 2008, Astronomical calibration of the Paleocene time: *Palaeogeography, Palaeoclimatology, Palaeoecology*, v. 257, no. 4, p. 377-403.

2.7 Acknowledgements

We thank Jeff Williams, Kim McComas, Diane Pitassy, HJ Walker, Marcos Alvarez, Felix Rodriguez, Maria Pinzon Concepcion, and Arcadio Castillo for help with developing the modern Caribbean reef fish tooth reference collection, Arisa Sanderson for help with isolating and identifying teeth from coral reef cores, and Brian Oller, Carolina Carpenter, Summer Buckley, and Matti-pohto Siltanen for help processing reef sediments. ECS is supported on an NSF Graduate Research Fellowship. KLC was supported by Smithsonian Institution MarineGEO Postdoctoral Fellowship and UC San Diego Frontiers of Innovation Scholars Postdoctoral Fellowship. No permits were required for the described study, which complied with all relevant regulations.

Chapter 2, in full, has been submitted for publication as: Sibert, E. C., Cramer, K. L., Hastings, P. A., and Norris, R. D. "Methods for isolation and quantification of microfossil fish teeth and elasmobranch dermal denticles (ichthyoliths) from marine sediments". The dissertation author was the primary investigator and author of this manuscript.

CHAPTER 3

Resilience of Pacific pelagic fish across the Cretaceous/Palaeogene mass extinction

Resilience of Pacific pelagic fish across the Cretaceous/Palaeogene mass extinction

Elizabeth C. Sibert^{1*}, Pincelli M. Hull² and Richard D. Norris¹

Open-ocean ecosystems experienced profound disruptions to biodiversity and ecological structure during the Cretaceous/Palaeogene mass extinction about 66 million years ago³. It has been suggested that during this mass extinction, a collapse of phytoplankton production rippled up the food chain, causing the wholesale loss of consumers and top predators³⁻⁵. Pelagic fish represent a key trophic link between primary producers and top predators, and changes in their abundance provide a means to examine trophic relationships during extinctions. Here we analyse accumulation rates of microscopic fish teeth and shark dermal scales (ichthyoliths) in sediments from the Pacific Ocean and Tethys Sea across the Cretaceous/Palaeogene extinction to reconstruct fish abundance. We find geographic differences in post-disaster ecosystems. In the Tethys Sea, fish abundance fell abruptly at the Cretaceous/Palaeogene boundary and remained depressed for at least 3 million years. In contrast, fish abundance in the Pacific Ocean remained at or above pre-boundary levels for at least four million years following the mass extinction, despite marked extinctions in primary producers and other zooplankton consumers in this region. We suggest that the mass extinction did not produce a uniformly dead ocean or microbially dominated system. Instead, primary production, at least regionally, supported ecosystems with mid-trophic-level abundances similar to or above those of the Late Cretaceous.

The Cretaceous/Palaeogene (K/Pg) event precipitated an 80–95% species-level extinction of calcareous nannoplankton (primary producers) and planktonic foraminifera (primary consumers), decimating part of the base of the open-ocean food web. This loss of productivity is thought to have driven extinction at higher trophic levels². For instance, ~34% extinction at the genus level has been inferred for sharks and rays, with the highest losses among coastal and surface ocean groups⁶. The K/Pg event also produced a major shift in coastal bony fish functional diversity with particularly large losses among predatory fishes with ecologies similar to modern tuna, billfish and jacks^{7,8}. Complete extinction of mosasaurs, plesiosaurs and ammonites further suggests that the extinction reverberated to the top of the food web^{3,9}. Whereas the response of well-fossilized plankton and megafauna to the K/Pg mass extinction has been well studied^{1,6,10,11}, the ecological and evolutionary response of the trophic link between the two groups, the mid-level consumers such as small-bodied fishes, is relatively unknown (as discussed in refs 7,8).

Ichthyoliths have an excellent, but underappreciated, fossil record that spans the K/Pg boundary in the deep ocean¹². Teeth are typically small (most abundant in the <150 µm sieve fraction)

and so are likely to represent small pelagic species or juveniles, whereas rarer denticles may come from sharks with a range of body sizes. Unlike most microfossils, ichthyoliths are composed of calcium phosphate, which is highly resistant to dissolution¹³. Ichthyoliths are thus found in nearly all sediment types, including pelagic red clays¹³. An analysis of stratigraphic ranges of teeth in Pacific red clay suggests that the K/Pg extinction of tooth morphotypes was slight in contrast to the marked extinction of top pelagic predators^{6,7}. A stage-level biostratigraphic compilation of ichthyolith morphological diversity throughout the Pacific Ocean shows extinction of only 5 of 42 morphotypes between the Late Cretaceous and the early Palaeocene (a ~12% loss; ref. 13). The low level of extinction of tooth morphotypes suggests that few basic trophic groups of fishes were lost among small pelagic taxa. However, these data indicate little about the magnitude of loss of fish taxa at the boundary, because the samples represent several million years of time-averaging. In addition, in modern fishes tooth shape can evolve rapidly among closely related species, and convergence is common in fishes exploiting similar prey¹⁴.

We produced high-resolution time series of pelagic fish tooth abundance, in the North Pacific (Ocean Drilling Program (ODP) Site 886), Central Pacific (ODP Site 1209, Shatsky Rise), South Pacific (Deep-Sea Drilling Program (DSDP) Site 596) and the Tethys Sea (Bottaccione Gorge, Gubbio, Italy; Fig. 1). The absolute abundance of fish tooth remains is presented as an ichthyolith mass accumulation rate (MAR). Ichthyolith MAR accounts for changes in the sedimentation rate and density of deep-sea sediments, and provides an approximation for the relative abundance of pelagic fish in the overlying water column (Methods and Supplementary Information and Supplementary Figs 1–15). Our data sets use slightly different timescale and MAR metrics, based on the material and lithology of the site (Methods and Supplementary Information and Supplementary Figs 1–15). As a result, although absolute ichthyolith abundances are not equivalent across sites, the patterns and trends are comparable (Fig. 2).

Ichthyolith accumulation from the South Pacific Ocean (DSDP Site 596, Fig. 2c) increases across the boundary from an average of 41.8 ichthyoliths cm⁻² Myr⁻¹ in the last one million years of the Maastrichtian to 59.6 ichthyoliths cm⁻² Myr⁻¹ in the first million years of the Danian (two-sample *t*-test, *P* = 0.03; counts of ichthyoliths in the >106 µm fraction). The age model is based on cobalt accumulation rate and strontium isotope chronologies calibrated to the K/Pg boundary, which is placed at a prominent iridium anomaly and impact debris horizon^{15,16}. Teeth are preserved in red clay with a sedimentation rate of ~0.25 m Myr⁻¹, so it is possible that a brief decline in fish abundance could be masked

¹Scripps Institution of Oceanography, University of California, San Diego, La Jolla, California 92093, USA, ²Department of Geology and Geophysics, Yale University, New Haven, Connecticut 06520, USA. *e-mail: esibert@ucsd.edu

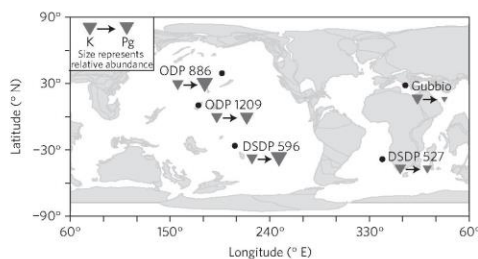


Figure 1 | Map of the sites included in this study and relative changes in ichthyolith accumulation across the boundary. The map shows the locations of the five sites from this study. The triangles underneath each site represent the relative change in ichthyolith accumulation from before (left) to after (right) the K/Pg boundary. The size of the triangles reflects average ichthyolith accumulation for the one million years before and after the boundary. See Methods for the source of the plate reconstruction.

by bioturbation. Still it is clear that there was no long-term decline in the export of fish remains to the deep sea following the mass extinction.

In the North Pacific Ocean (ODP Site 886C, Fig. 2a), ichthyolith accumulation is relatively constant in the Maastrichtian, at about $105 \text{ ichthyoliths cm}^{-2} \text{ Myr}^{-1}$ (counts of ichthyoliths in the $>106 \mu\text{m}$ fraction). There is a substantial ($5\times$) increase in ichthyolith accumulation in the half-million years following the boundary, after which ichthyolith accumulation stabilizes at nearly twice the Cretaceous level at $180 \text{ ichthyoliths cm}^{-2} \text{ Myr}^{-1}$ (two-sample t -test, $P = 3 \times 10^{-9}$). Here the chronology is based on magnetostratigraphy, biostratigraphy and strontium isotope stratigraphy, tied to the K/Pg iridium anomaly; the record stops 64 million years ago (Ma) owing to a hiatus¹⁷. Together the North Pacific (ODP 886C) and South Pacific (DSDP 596) indicate that Pacific pelagic fish abundance was relatively unaffected, or even increased, following the K/Pg mass extinction.

In the Central Pacific (ODP Site 1209, Shatsky Rise, Fig. 2b) ichthyolith MAR (based on both ichthyolith weights and counts) is also relatively unchanged across the K/Pg boundary (Fig. 2a), with the possible exception of a 62 kyr interval coincident with the deposition of impact debris. Contamination by impact tektites prevents us from estimating ichthyolith weights at the K/Pg boundary, but counts of teeth and denticles (measured as ichthyoliths per square centimetre per million years) show no significant drop associated with the extinction horizon (Fig. 3a). Counts of fish ichthyoliths ($>600 \mu\text{m}$ and $>63 \mu\text{m}$) and total ichthyolith mass (tooth weight $>38 \mu\text{m}$) are significantly correlated (Supplementary Fig. 16), supporting our interpretation of little or no change in ichthyolith accumulation rates immediately across the K/Pg boundary at Shatsky Rise (Fig. 2). This Central Pacific record adds key support for the similar patterns observed in the North and South Pacific, as it has the best constrained age model for calculating accumulation rates.

There are two primary astronomical timescales for Site 1209, and both suggest that ichthyolith MAR was relatively stable immediately across the boundary (Supplementary Information and Supplementary Fig. 13). Between 65.65 Ma and 65.71 Ma (Fig. 2a), the Westerhold Option 1 (refs 18,19) age model suggests that there is a sharp increase in ichthyolith MAR (measured as ichthyolith weight) to an average of $0.31 \text{ g cm}^{-2} \text{ Myr}^{-1}$ and confirmed by repeated sampling. From 65.6 to 62.1 Ma fish flux oscillates between $0.06 \text{ g cm}^{-2} \text{ Myr}^{-1}$ and $0.42 \text{ g cm}^{-2} \text{ Myr}^{-1}$ (average = $0.21 \text{ mg cm}^{-2} \text{ kyr}^{-1}$). The alternative Hilgen *et al.* age model²⁰ also shows no drop in ichthyolith weight across the boundary, but the sustained spike in ichthyolith abundance in the earliest Danian suggested by the Westerhold Option 1 age model¹⁸ disappears (Supplementary Figs 12 and 13). We note that a post-boundary increase in fish debris accumulation, similar to that implied by the Westerhold Option 1 age model¹⁸, is observed in the South Pacific (Site 596) and North Pacific (Site 886C) as well (Fig. 2), suggesting that this pattern may be robust and record a Pacific-wide boom in ichthyolith accumulation during the first million years of the Danian.

One notable difference among the Pacific records is the degree of variability in ichthyolith accumulation rates, particularly in

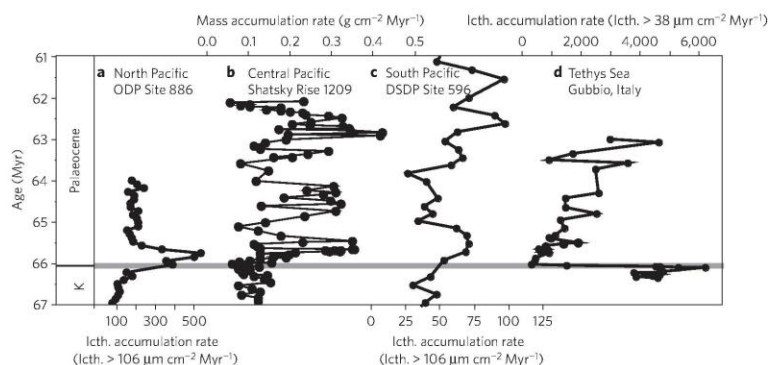


Figure 2 | Global pattern of ichthyolith accumulation rates through the K/Pg mass extinction. a–d. Ichthyolith accumulation in the North Pacific (ODP Site 886; ichthyoliths $>106 \mu\text{m cm}^{-2} \text{ Myr}^{-1}$), age model based on compilation of biostratigraphy, magnetostratigraphy, strontium isotopes and iridium anomaly¹⁷ (a), the Central Pacific (Shatsky Rise, ODP Site 1209; $\text{g cm}^{-2} \text{ Myr}^{-1}$ of $>38 \mu\text{m}$ fish debris), age model after Westerhold solution 1 (ref. 18) and shipboard biostratigraphy²⁹ (b), the South Pacific (DSDP Site 596; ichthyoliths $>106 \mu\text{m cm}^{-2} \text{ Myr}^{-1}$), age model based on cobalt accumulation¹⁵ (c), and the Tethys Sea (Gubbio, Italy; ichthyoliths $>38 \mu\text{m cm}^{-2} \text{ Myr}^{-1}$), age model based on bio- and magnetostratigraphy^{21,22} (d). All age models use GTS 2012 ages for the K/Pg boundary and biostratigraphic and magnetostratigraphic datums³⁰.

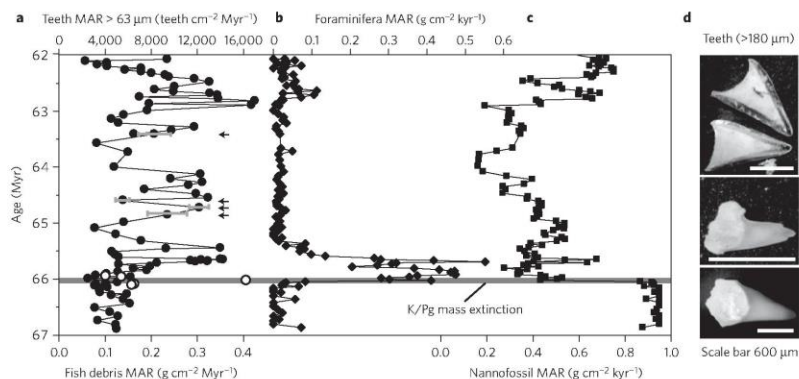


Figure 3 | Central Pacific (ODP Site 1209) comparison of mass accumulation rates for different trophic groups through the K/Pg mass extinction. **a–c**, Ichthyolith MAR (filled circles indicate $\text{g cm}^{-2} \text{ Myr}^{-1}$ for the $>38 \mu\text{m}$ fraction; open circles indicate $\text{teeth cm}^{-2} \text{ Myr}^{-1}$ for the $>63 \mu\text{m}$ fraction; **a**), foraminiferal MAR ($\text{g cm}^{-2} \text{ kyr}^{-1}$; ref. 10; **b**) and calcareous nannofossil MAR ($\text{g cm}^{-2} \text{ kyr}^{-1}$; ref. 10; **c**). The horizontal grey line is the K/Pg boundary. **d**, Examples of large fish teeth from the Palaeocene (scale bar = $600 \mu\text{m}$). The arrows in **a** indicate replicated samples (Supplementary Discussion); error bars are 95% confidence intervals. Timescale after Westerhold *et al.* solution 1 (ref. 18) and shipboard age model²⁹ updated to GTS 2012 (ref. 30).

North Pacific ODP Site 1209. The observed variability is not a simple function of sedimentation rates, because both ODP Site 1209 (with the highest sedimentation rates) and DSDP Site 596 (with the lowest) show distinct cycles in ichthyolith MAR. In addition, these differences in variability among sites are clear only in the Palaeocene portion of the record. We suggest that differences in Palaeocene variability in fish MAR may reflect a real, and in some cases prolonged, change in fish production initiated by the K/Pg extinction, but this conclusion remains to be verified in comparably long records of Cretaceous ichthyolith accumulation.

In contrast to the Pacific Ocean, there is an abrupt collapse in ichthyolith accumulation in the Tethys Sea (Gubbio, Italy, Fig. 2d), followed by a slow 'recovery' period of 3 million years (Fig. 2d). The standard age model based on biostratigraphy and magnetostratigraphy^{21,22} shows that ichthyolith abundance drops from approximately $4,672 \text{ ichthyoliths cm}^{-2} \text{ Myr}^{-1}$ in the latest Cretaceous to just $589 \text{ ichthyoliths cm}^{-2} \text{ Myr}^{-1}$ in the earliest Palaeocene, a nearly 88% decrease in ichthyolith abundance. An alternative helium-age model for this site²³ reveals at least a 50% decline in ichthyolith accumulation at the boundary (Supplementary Fig. 13b), and compresses the recovery into a 700,000 year period. Thus, regardless of age model, there is a large, abrupt and sustained reduction in ichthyolith abundance at Gubbio in the Tethys Sea. The collapse and slow recovery of ichthyolith accumulation that we observe in the Tethys was also reported, in a low-resolution ichthyolith record from the South Atlantic at DSDP Site 527 (Supplementary Fig. 16; ref. 24). Considered jointly, both the Atlantic and Tethys basins show a marked decline in fish production consistent with traditional expectations for a collapse of mid to upper trophic levels in pelagic food webs that contrasts directly with our findings in the Pacific.

Our results suggest that the mass extinction did not cause a uniformly dead ocean or one lacking a robust zooplankton community, but instead generated diverse responses of fish in different ocean environments and geographic regions. Fish production in the Tethys and perhaps the South Atlantic was suppressed much longer than in the open Pacific Ocean. Although there is a well-known global extinction and drop in export production of calcareous plankton, this evidently is not a reflection

of the entire community of primary producers^{25,26}, because Pacific pelagic fish were able to find sufficient food to maintain populations at levels comparable to or higher than pre-extinction communities. Previous work has found similar geographic heterogeneity in other aspects of pelagic ecosystems^{10,25}. Export production indicated by both biogenic barium and benthic foraminifer communities suggests that Pacific primary production did not fall after the mass extinction²⁶. Our results show that pelagic fish, at least, seem to have either been able to switch to the new resources or to have been replaced by Danian fish groups that were equally productive as those of the Late Cretaceous in the Pacific Ocean, even in the face of major changes in lower trophic levels.

There are also large inter-ocean differences in the pace and dynamics of the ecological recovery from the mass extinction. All three Pacific records show an early Danian increase in ichthyolith accumulation (Fig. 2), which coincides with evidence for increased export productivity^{25–27}. Our Central Pacific and South Pacific records also show two other periods of increased ichthyolith accumulation in the early Palaeocene, one from approximately 65 to 64 Ma, and one that begins at approximately 63 Ma. These increases in fish debris accumulation coincide with a major diversification of planktonic foraminifera and the recovery of nannofossil mass accumulation rates in Central Pacific Site 1209 (Fig. 3; refs 10,28). It seems that marked extinction and loss of productivity in calcareous algae was not devastating to the entire food web, at least in the Pacific Ocean. This is possibly because other groups of non- (or poorly) fossilized primary producers were able to sustain comparable levels of new production in the immediate aftermath of the extinction in the Pacific²⁷. In contrast, the decline in fish remains, biogenic barium and benthic foraminifer assemblages lasts for hundreds of thousands to millions of years in the Atlantic and Tethys. The duration of this inter-basinal contrast suggests that differences between the ocean basins are not purely the direct results of the extinction but are reinforced by geographic differences in productivity of ecosystems following the extinction. Our findings support an emerging view of the end-Cretaceous mass extinction^{10,11,25–27} where there is considerable variation in the effects of the extinction both among trophic groups and between ocean regions as well as in the timing of the recovery of ecosystem structure and function.

Methods

Ichthyolith isolation methods varied between sites owing to lithological differences. At all sites, samples were dissolved in 5% acetic acid and washed over a 38 µm sieve to isolate the ichthyoliths. Sample size varied by site and lithology: 10 g in pelagic carbonate oozes at ODP 1209, 5–10 g red clay at DSDP 596 and ODP 886, 100 g limestone at Gubbio. For Gubbio, the limestone was broken up into ~1 cm³ chunks and dissolved in 5–10% acetic acid (bath changed every 24 h) until no carbonate remained in the >150 µm fraction. At Shatsky Rise, after dissolution, samples were visually checked to confirm that the remaining material was entirely fish debris. Then the pure fish debris residue was weighed to calculate MAR using two astronomically tuned timescales for ODP Site 1209 in the Palaeocene^{18,20}, shipboard sedimentation rates in the Late Cretaceous⁹, and variable dry bulk density (Supplementary Information and Supplementary Figs 1–5). Measurement reproducibility of ichthyolith weights is good based on replicate measurements of splits of samples (Supplementary Information). Additional debris (non-ichthyolith) in the non-carbonate fraction at DSDP Site 596, ODP 886 and Gubbio precluded a weight-based assessment of fish MAR. Instead, ichthyoliths were manually picked from the >106 µm (DSDP 596 and ODP 886) and >38 µm (Gubbio, owing to low abundance of large ichthyoliths) size fractions, and counted. The DSDP 596 timescale is based on a cobalt accumulation model¹⁵ and tied to the K/Pg Boundary. The ODP Site 886 timescale is based on a compilation of radiolarian biostratigraphy and strontium isotopes, and is also tied to the K/Pg boundary¹⁷. The age model for Gubbio was constructed using bio- and magnetostratigraphy^{21,22} and tied to the boundary. We also computed the Gubbio fish MAR using a published helium isotope stratigraphy (Supplementary Fig. 13; ref. 23). All sites were calibrated using the Geologic Time Scale 2012 (GTS 2012; ref. 30). See the Supplementary Information for a discussion of other factors considered in our interpretation including preservation, sediment mixing, the MAR of the non-biogenic fraction, and age model accuracy.

Data. The 66.0 Ma palaeo-continent reconstruction was generated using the ODSN plate reconstruction service (www.odsn.de/odsn/services/paleomap/paleomap.html). Supplementary data are available online through <http://www.nature.com/ngeo/index.html> or at <http://dx.doi.org/10.1594/PANGAEA.834235>.

Received 5 June 2014; accepted 18 July 2014;
published online 24 August 2014

References

- Coxall, H. K., D'Hondt, S. & Zachos, J. C. Pelagic evolution and environmental recovery after the Cretaceous-Paleogene mass extinction. *Geology* **34**, 297–300 (2006).
- D'Hondt, S. Consequences of the Cretaceous/Paleogene mass extinction for marine ecosystems. *Annu. Rev. Ecol. Syst.* **36**, 295–317 (2005).
- D'Hondt, S., Donaghay, P., Zachos, J. C., Luttenberg, D. & Lindinger, M. Organic carbon fluxes and ecological recovery from the Cretaceous-Tertiary mass extinction. *Science* **282**, 276–279 (1998).
- Hsu, K. J. & McKenzie, J. A. A 'Strangelove' ocean in the earliest Tertiary. *Geophys. Monogr.* **32**, 487–492 (1985).
- Kump, L. R. Interpreting carbon-isotope excursions—Strangelove oceans. *Geology* **19**, 299–302 (1991).
- Kriwet, J. & Benton, M. J. Neoselachian (Chondrichthyes, Elasmobranchii) diversity across the Cretaceous-Tertiary boundary. *Palaeogeogr. Palaeoclimatol. Palaeoecol.* **214**, 181–194 (2004).
- Friedman, M. Ecomorphological selectivity among marine teleost fishes during the end-Cretaceous extinction. *Proc. Natl Acad. Sci. USA* **106**, 5218–5223 (2009).
- Friedman, M. & Sallan, L. C. Five hundred million years of extinction and recovery: A Phanerozoic survey of large-scale diversity patterns in fishes. *Palaeontology* **55**, 707–742 (2012).
- Ward, P. D., Kennedy, W. J., Macleod, K. G. & Mount, J. F. Ammonite and inoceramid bivalve extinction patterns in Cretaceous Tertiary boundary sections of the Biscay region (southwestern France, northern Spain). *Geology* **19**, 1181–1184 (1991).
- Hull, P. M., Norris, R. D., Bralower, T. J. & Schueth, J. D. A role for chance in marine recovery from the end-Cretaceous extinction. *Nature Geosci.* **4**, 856–860 (2011).
- Jiang, S. J., Bralower, T. J., Patzkowsky, M. E., Kump, L. R. & Schueth, J. D. Geographic controls on nannoplankton extinction across the Cretaceous/Paleogene boundary. *Nature Geosci.* **3**, 280–285 (2010).
- Doyle, P. S. & Riedel, W. R. *Cenozoic and Late Cretaceous Ichthyoliths* (Cambridge Univ. Press, 1985).
- Doyle, P. S. & Riedel, W. R. *Ichthyoliths: Present Status of Taxonomy and Stratigraphy of Microscopic Fish Skeletal Debris* Vol. 79–16 (Scripps Institution of Oceanography, University of California, 1979).
- Rüber, L., Verheyen, E. & Meyer, A. Replicated evolution of trophic specializations in an endemic cichlid fish lineage from Lake Tanganyika. *Proc. Natl Acad. Sci. USA* **96**, 10230–10235 (1999).
- Zhou, L. & Kyte, E. T. Sedimentation history of the South Pacific pelagic clay province over the last 85 million years inferred from the geochemistry of Deep Sea Drilling Project Hole 596. *Paleoceanography* **7**, 441–465 (1992).
- Zhou, L., Kyte, E. T. & Bohor, B. F. Cretaceous/Tertiary boundary of DSDP Site 596, South Pacific. *Geology* **19**, 694–697 (1991).
- Snoeckx, H., Rea, D., Jones, C. & Ingram, B. Eolian and silica deposition in the central North Pacific: Results from Sites 885/886. *Proc. Ocean Drill. Program, Sci. Results* **145**, 219–230 (1995).
- Westerhold, T. et al. Astronomical calibration of the Paleocene time. *Palaeogeogr. Palaeoclimatol. Palaeoecol.* **257**, 377–403 (2008).
- Westerhold, T., Röhl, U. & Laskar, J. Time scale controversy: Accurate orbital calibration of the early Paleocene. *Geochim. Geophys. Geosyst.* **13**, Q06015 (2012).
- Hilgen, F. J., Kuiper, K. F. & Lourens, L. J. Evaluation of the astronomical time scale for the Paleocene and earliest Eocene. *Earth Planet. Sci. Lett.* **300**, 139–151 (2010).
- Silva, I. P. Upper Cretaceous–Paleocene magnetic stratigraphy at Gubbio, Italy II. Biostratigraphy. *Geol. Soc. Am. Bull.* **88**, 371–374 (1977).
- Roggenthien, W. M. & Napoleone, G. Upper Cretaceous–Paleocene Magnetic Stratigraphy at Gubbio, Italy: 4. Upper Maastrichtian–Paleocene Magnetic Stratigraphy. *Geol. Soc. Am. Bull.* **88**, 378–382 (1977).
- Mukhopadhyay, S., Farley, K. & Montanari, A. A short duration of the Cretaceous-Tertiary boundary event: Evidence from extraterrestrial helium-3. *Science* **291**, 1952–1955 (2001).
- Shackleton, N. J. Accumulation rates in Leg 74 sediments. *Initial Rep. Deep Sea Drill. Proj.* **74**, 621–644 (1984).
- Alegret, L., Thomas, E. & Lohmann, K. C. End-Cretaceous marine mass extinction not caused by productivity collapse. *Proc. Natl Acad. Sci. USA* **109**, 728–732 (2012).
- Hull, P. M. & Norris, R. D. Diverse patterns of ocean export productivity change across the Cretaceous-Paleogene boundary: New insights from biogenic barium. *Paleoceanography* **26**, PA3205 (2011).
- Sepúlveda, J., Wendler, J. E., Summons, R. E. & Hinrichs, K. U. Rapid resurgence of marine productivity after the Cretaceous-Paleogene mass extinction. *Science* **326**, 129–132 (2009).
- Berggren, W. A. & Norris, R. D. Biostratigraphy, phylogeny and systematics of the Paleocene trochospiral planktic foraminifera. *Micropaleontology* **43**, 280–280 (1997).
- Shipboard Scientific Party. Site 1209. In Bralower, T. J. et al., Proc. ODP, Init. Repts., 198 (Ocean Drilling Program), 1102 (2012).
- Gradstein, F. M., Ogg, J. G. & Schmitz, M. *The Geologic Time Scale 2012* Vol. 2 (Elsevier, 2012).

Acknowledgements

This work was financially supported by a NASA Exobiology grant NNX07AK62G (to R.D.N.) and supported by the Ocean Drilling Program (special thanks to F. Rumford). Field work for collection and processing of Gubbio samples was funded by a Lewis and Clark Fund for Exploration and Field Research in Astrobiology by the American Philosophical Society in 2012 to E.C.S. Assistance in the field was provided by J. Dhaliwal.

Author contributions

R.D.N. and P.M.H. conceived the study; E.C.S. developed the methods, collected field samples, and generated and analysed the data; all authors contributed to the writing of the manuscript.

Additional information

Supplementary information is available in the online version of the paper. Reprints and permissions information is available online at www.nature.com/reprints. Correspondence and requests for materials should be addressed to E.C.S.

Competing financial interests

The authors declare no competing financial interests.

Resilience of Pacific pelagic fish across the Cretaceous/Palaeogene mass extinction

Elizabeth C Sibert^{1*}, Pincelli M Hull², and Richard D Norris¹

¹Scripps Institution of Oceanography, University of California, San Diego, La Jolla, CA, USA

²Department of Geology and Geophysics, Yale University, New Haven, CT, USA

*To whom correspondence should be addressed. E-mail: esibert@ucsd.edu

This PDF file includes:

ESM Materials and Methods: 2-9

ESM Discussion: 10-15

References: 15-16

Figures S1-S16

ESM MATERIALS AND METHODS

Sampling Details

Sample density and spacing was as follows: ~50 kyr sample spacing (~10 cm resolution) between 67.1 and 62.1 Ma at ODP Site 1209, Shatsky Rise; ~200 kyr sample spacing (5 cm resolution) between 67 and 61 Ma at DSDP Site 596 ~100 kyr sample spacing (5 cm resolution) between 67 and 63.8 Ma at ODP 886, and 10-20 cm resolution, (~20-50 kyr sample spacing) between 66.3 and 62.9 Ma at Gubbio, Italy. At Shatsky Rise, where shipboard data allowed for refined estimates of dry bulk density, high-resolution variable dry bulk densities were calculated based on the relationship between shipboard gamma ray attenuation density (measured approximately every 2 cm) and dry bulk density measurements (measured approximately every meter). At Shatsky Rise, we tested the importance of this resolved dry bulk density and the use of a constant dry bulk density throughout (as was done at the other sites: Gubbio, DSDP 596, and DSDP 527) and found that it was inconsequential for our interpretation (see below). For the cross trophic-level comparison at Shatsky Rise (Fig. 3), MAR of foraminifera and nannoplankton was calculated as in Hull et al. 2011¹, but used a variable dry bulk density and variable percent carbonate (Figs. S1-S11). This updated calculation had no appreciable affect on K-Pg boundary trends for any of the MAR calculations.

Calculation of Mass Accumulation Rates

Our results and inferences depend on the accurate calculation of group-specific mass accumulation rates (e.g., flux) across the K-Pg boundary interval and on the inference that the mass accumulation rate of fossils reflects the living abundance of organisms. We address both issues here in turn.

Mass accumulation rates describe the relative mass of a given sedimentary component per unit time (kyr) and area (cm²). Accurate time estimates are notoriously difficult to constrain in deep time and particularly around extinction horizons, so it is notable that ODP Site 1209 Shatsky Rise is one of three sites used to calculate a global cyclostratigraphic age model of the Paleocene². This age model provides the best time constraint on the timing of extinction and recovery available for any mass extinction event. At Shatsky Rise, the cyclostratigraphic age model does not extend into the latest Cretaceous; latest Cretaceous ages are instead calculated from shipboard age models³. A second astronomical age model (Hilgen et al. 2010⁴, left unchanged our inferences regarding major changes in mass accumulation rates of foraminifera and nannofossils (see also Fig. S12a,b). For ichthyolith MARs, the Hilgen et al. age model supports a very slight (~15%, less than variation in tooth abundance in the late Cretaceous) reduction in ichthyolith accumulation in the early Danian lasting approximately 1,000,000 years (Fig. S12c).

In order to directly compare the effect of the two different age models, Westerhold et al. (2008) and Hilgen et al. (2010), on our interpretation of ichthyolith MAR, we have shifted the Westerhold et al. (2008) age model to a K-Pg boundary age of 66.04 Ma in accordance with GTS 2012. It is worth noting that this approach is only valid for comparing the relative effects of cyclostratigraphic age model interpretation in a floating framework as the Westerhold et al. (2008) and Hilgen et al. (2010) age models attribute a different amount of time to the Paleocene epoch (see discussion in Westerhold et al. 2012⁵). As this debate is still ongoing with regards to the duration of the Paleocene, we have used these age models in a relative sense as end-members. While other solutions presented in Westerhold et al. 2008 (Soln. 3, in particular) have

K-Pg boundary ages closer to GTS 2012, the greatest difference in the attribution of relative time amongst the possible Westerhold et al. (2008) age models and the Hilgen et al. (2010) age model in the very earliest Paleocene is between the two models we contrast: Westerhold et al. (2008) Soln 1 and Hilgen et al. (2010). We present and interpret our ichthyolith results for site 1209 with the Westerhold et al. (2008) age model because the Westerhold et al. linear sedimentation rates in the earliest Danian (grey boxes in Fig. S12) yielded a fish MAR record that looks strikingly like the record from DSDP 596. This second record (DSDP 596) provides independent support for our Pacific interpretations, as does the third Pacific record at ODP 886, which also has a large spike in the earliest Danian.

Sedimentary mass accumulation rate (MAR) is simply the linear sedimentation rate (cm/kyr) multiplied by the sediment dry bulk density (g/cm^3). At ODP Site 1209 Shatsky Rise, point samples of dry bulk density were typically measured once per section (that is, approximately every 1.5 meters)³, excepting a ~14 meter gap in dry bulk density measurements across the K-Pg boundary (Fig S1). Given this boundary gap and the relatively consistent dry bulk measurements of 1.2 g/cm^3 in the surrounding late Cretaceous and early Paleocene sediments (Fig. S1), we previously used a constant dry bulk density value of 1.2 g/cm^3 to calculate mass accumulation rates at Shatsky Rise¹. Here we update this calculation by using the relationship between the high-resolution down core logging of gamma-ray attenuation (Fig. S1, GRA), and dry bulk density (Fig. S2, also from ref. 3) to interpolate the dry bulk density measurements to a similar 3-cm resolution (Fig. S3a). Dry bulk density estimates for ichthyolith (Fig. S3b) and carbonate (Fig. S3c) mass accumulation rate calculations were taken from this GRA-based calculation of dry bulk density. Over the interval in question (61 - 67 Ma) dry bulk density was quite stable

(mean = 1.17 g/cm³, median = 1.17 g/cm³, range = 0.97 – 1.33 g/cm³, standard deviation = 0.07 g/cm³). MAR calculations with variable dry bulk densities varied at most by 23% (or 0.159 g/cm³) from the MARs calculated with a constant dry bulk density of 1.2 g/cm³ (Fig. S4). It is notable that all large deviations (>10%) in sedimentary mass accumulation rates between the constant-density and variable-density calculation occur within a narrow boundary window (approximately 64.88-66 Ma). However, these dry bulk density deviations are all calculated from gamma ray attenuation values –an indirect measure of dry bulk density with accompanying assumptions⁶ – alone.

With accurate time constraints for linear sedimentation rates and high resolution dry bulk density estimates, the mass accumulation rate of ichthyoliths is calculated simply as the fraction of ichthyoliths (gram of non-carbonate/gram of sample) multiplied by the sedimentary mass accumulation rate (MAR) (Fig. S5). The choice of dry bulk density (constant or variable) also has some affect on the inferred MAR of ichthyoliths across the K-Pg boundary, with the largest deviations (excepting one outlier) in fish tooth mass accumulation rates falling with the same boundary window lacking a dry bulk density calibration of GRA (Fig. S5).

To estimate the standard error in our fish debris MAR calculations, we split four of our 30 cc samples into three chunks and measured the concentration of fish debris in each sample. We found a mean fish debris MAR of 0.14 to 0.29 g/cm²/myr, with a standard error of 0.009 to 0.023 g/cm²/myr. These measurements suggest that variation in fish debris MAR is highly reproducible. Error bars based upon these estimates of standard error are shown in Fig. 3a in the main text and are marked by small arrows.

Determining the MAR of planktonic foraminifera and calcareous nannofossils is more complicated and requires splitting sedimentary components into the non-carbonate fraction, the small, nannofossil-sized carbonate fraction, and the large, foraminiferal-sized carbonate fraction and then using these relative percentages to determine the mass accumulation rate of each group. We first determine the relative contribution of carbonate to non-carbonate components in Shatsky Rise sediments. Empirical measurements of percent carbonate are of relatively low resolution between 57.5-66 Ma. Thus, we use the relationship of percent carbonate to sedimentary iron content (measured as $\ln(\text{Fe total counts})$ by X-ray fluorescence, XRF, previously published in Hull and Norris 2011⁷) to calculate a high-resolution record of sedimentary percent carbonate (Fig. S6). Given the relatively low amount of variance in percent carbonate explained by XRF Fe ($r^2 = 0.49$), we avoid over interpreting the high resolution oscillations in Fe by applying a 7-point running median to the inferred percent carbonate values (Fig. S7). This serves to eliminate the high frequency oscillations in calculated percent carbonate and improves the relationship between observed and calculated percent carbonate from an r^2 of 0.489 to an r^2 of 0.552. In a previous study we used a constant percent carbonate value (95% carbonate) to calculate mass accumulation rates¹. The use of constant percent carbonate versus the Fe-interpolated percent carbonate has a relatively minor effect on total carbonate MARs (Fig. S8; maximum difference of 5% or 0.043 $\text{g/cm}^2/\text{kyr}$) and, in the case of our previously published carbonate MAR¹, act to neatly oppose the bias introduced by using a constant dry bulk density (compare Figs S4 and S8).

Sediment smear slides consistently identify the non-carbonate fraction at Shatsky Rise as being comprised of clay-sized minerals, with rare iron oxides, pyrite infills and quartz⁸. The lithological unit description for the Paleocene and late Cretaceous also describe a non-carbonate fraction comprised of clay minerals³:

Subunit IIB extends from 198mbsf to the KT boundary at 235.2 mbsf in Hole 1209A. It primarily comprises very pale orange (10YR 8/2) nannofossil ooze and pale yellowish brown (10YR 6/2) nannofossil ooze with clay. These two major lithologies tend to alternate on a meter scale with very gradational contacts. There are also several centimeter-scale horizons characterized by darker more clay-rich lithologies with more abrupt contacts. ... Minor amounts of pyrite are also present, primarily as foraminiferal infill. The base of Unit II, the K/T boundary, is marked by a thin, nondistinct horizon. The sediments both above and below this horizon are white (N9) to very pale orange (10YR 8/2) nannofossil ooze. ... Lithologic Unit III consists predominantly of a uniform white (N9) to very pale orange (10YR 8/2) nannofossil ooze with carbonate content in excess of 96 wt%. [3]

We thus assume that the non-carbonate fraction of total sedimentary MAR is comprised of just small, nannofossil sized sediments, as opposed to a range of sediment sizes spanning the size range of both nannofossils and foraminifera. Whether the non-carbonate fraction is considered equally distributed across foraminiferal and nannofossil sized grains (as assumed in Hull et al.¹) or is considered to be almost entirely comprised of roughly nannofossil-sized grains (i.e., clay; as we assume here), is of relatively small effect (>8%) on the calculation of foraminiferal and nannofossil mass accumulation rates (Fig. S9, see also discussion and Supplementary figure 12 in Hull et al.¹).

High resolution grain size analysis was used to subdivide sediments at Shatsky Rise into foraminiferal and nannofossil sized components as described at length in Hull et al.¹, using a Malvern Mastersizer particle size analyzer (e.g., optical measurement of grain size between 0.1 and 1000 μm , see Bralower et al.⁹ for explanation of use on K-Pg boundary sediments). Traditionally, the size distribution of calcareous microfossils has been measured using the weight of sieve size fractions, a method that has relatively coarse size binning but avoids some of the

uncertainties associated with optical grain size analyzers. We previously examined the relationship between sieve size fractions versus Malvern Mastersizer measurements for splitting foraminiferal from nannofossil sized grains¹. There we found a one-to-one relationship between the two methods (significant linear regression with confidence intervals on the slope bracketing one, and confidence intervals on the intercept bracketing zero) for sediments with less than 27% foraminiferal sized grains (e.g., all but eight samples analyzed). If the eight samples with the highest % foraminifera were included then the slope of the relationship increased to 1.15. This shift in the relationship with the inclusion of the eight foraminifera-rich samples likely reflects the relatively high abundance of grains in those samples that fall clearly within the foraminiferal size range (between 15 and 38 μm) but would be assigned to nanoplankton in traditional sieve size analyses (see details in supplemental materials to Hull et al.¹).

Here our calculation of the MAR of foraminifera and nannofossils differs from our previously published numbers (i.e., those in ref. 1) by using a variable dry bulk density, variable percent carbonate, and a non-carbonate fraction entirely attributed to the nannofossil size fraction. Each change does individually affect the calculated mass accumulation rate of foraminifera and nanoplankton (see above discussion and Figs S4, S8, and S9); however, the main patterns of a K/Pg boundary crash in nannofossil MARs coincident with a burst in planktonic foraminiferal MARs, are entirely unaffected (Figs S10a and S11a). The assumptions of the calculation *do* have a large effect on absolute MARs observed at specific time intervals (Figs S10b, c, and S11b,c), but these effects do not change the large scale trends observed and interpreted here and in previous work (i.e., Hull et al.¹). Rather, they tend to have a relatively large effect on MARs for

samples with low MAR of foraminifera and /or nannoplankton or for samples with relatively poor constraints on the variable values used to calculate and attribute carbonate MARs.

As compared to Shatsky Rise, our ability to constrain bulk density and mass accumulation rates at the other sites is considerably less resolved. This is unlikely to have much of an effect on our main conclusions from DSDP 596, ODP 886, or Gubbio, Italy. DSDP 596 and ODP 886 are both red clay sites throughout this interval, so compositional changes are not expected to affect dry bulk density measurements. The age model at DSDP 596 is by far the least constrained (based only on cobalt accumulation rates and the boundary iridium anomaly). However, the similarity of patterns between DSDP 596 and ODP 1209, provides us with some confidence that we are correctly interpreting the Pacific pattern. At Gubbio, an independent helium age model¹⁰ supports the decline in fish MAR across the K/Pg boundary (Fig. S13a) although the recovery interval implied is much shorter than suggested by the magneto-biostratigraphy chronology. DSDP 527 (included in Fig. S14e), at Walvis Ridge, is the least certain site due both to the sampling scheme, in which there is a large variation in sample size across the boundary. At Walvis, the smallest raw samples are an order of magnitude smaller than the largest and it is in these samples that the lowest number of teeth were counted, raising questions of sampling limitations. In addition, there is a large change in lithology across the Walvis Ridge K-Pg boundary, that is not accounted for in the current sampling MAR bulk density

SI DISCUSSION

Issues of Preservation

Three preservational factors could have a dominant influence on our inferences regarding patterns in the mass accumulation rate of nannofossils, planktonic foraminifera, and ichthyoliths at the K-Pg boundary.

First, carbonate preservation can play a dominant role in the mass accumulation rates of planktonic foraminifera and nannofossils in deep sea sediments¹¹⁻¹⁴. An increase or decrease in the MAR of calcareous fossils could simply reflect changing preservation conditions rather than changes in the standing population size of living organisms. This factor is of such great importance that it was explored at length (with independent preservation proxies) in a previous study on MARs of planktonic foraminifera and nannofossils across the K-Pg boundary at Shatsky Rise¹. There, we found a change in preservation unlikely to fully account for the main patterns observed: an increase in foraminiferal MAR coincident with large decrease in nannofossil MAR. We refer interested readers to the detailed supplement of Hull et al.¹ for a full treatment of this topic.

Second, the interpretation of no prolonged change in small pelagic fish abundance across the K-Pg boundary are all dependent upon age models. However, where we have multiple independent age models, our basic conclusions about either no change (in the Pacific Site 1209 record) or a dramatic drop in fish MAR (Gubbio) are supported by the available data. In addition, our record from DSDP 596 uses an entirely different approach to calculated sedimentation rates (i.e., cobalt

accumulation) and our ichthyolith records there also support our finding of no decline in MAR. DSDP 596 is a red clay site, leaving the clay sedimentation rates unaffected by the large changes in carbonate deposition rates across the boundary.

Third, variations in fish tooth abundance could reflect differential preservation of teeth. We discount this hypothesis because teeth are among the most robust fossils of any group of organisms in the oceans, typically being the only fossil component to survive seafloor dissolution in pelagic red clay sequences. Teeth can be destroyed by mechanical processes (which in our experience reduce teeth to shards of enamel), but the abundance of small, often quite delicate, specimens in our samples, suggests that mechanical sorting and fragmentation are not a dominant process in our record. Additionally, a lack of indications of traditional chemical degradation such as pitting or splintering of the teeth suggests that they are not subject to large amounts of chemical degradation. A comparison between ichthyolith MAR and XRF Fe at Shatsky Rise supports this interpretation (Fig. S15). With the Westerhold age model, there is little concordance between ichthyolith MAR and Fe counts, arguing against a preservation related control. For the Hilgen age model, there is some similarity between the two records but only if the first (K-Pg to 252 rncd) and second (252 rncd and shallower) half of the record are considered separately. Thus, for both age models, the independent dynamics of ichthyolith MAR and Fe counts provides an additional line of evidence against a dominant preservation control on the records. Finally, the contrasting patterns of ichthyolith MARs between sites, discounts the possibility that a widespread change in deep-sea chemistry is driving the various records.

Non-Carbonate Components

One concern with using bulk ichthyolith abundance at ODP 1209, Shatsky Rise as a proxy of the abundance of small pelagic fishes is that the weight of the non-carbonate fraction $>38\mu\text{m}$ could be affected by the deposition of biotic or abiotic materials from organisms other than small fishes. Visual checks of all samples rule out an influence from siliceous microfossils such as radiolaria. Abiotic materials are present in the ODP Site 1209 K-Pg boundary sample (abundant tektites) and several samples in a heavily condensed interval contain unidentifiable clumps of insoluble sediment (not biologic in origin). Both the sample with tektites and the samples with sediment clumps are excluded from Figs. 2 and 3 of the main text.

To check for the potential effects of biotic, non-fish related fossils driving our results and interpretations, we counted the number of teeth ($>63\mu\text{m}$) in five samples spanning the K-Pg boundary. These counts confirm our major conclusion of no change in fish abundance across the K-Pg boundary. Our calculation of fish tooth count MAR shows a single point spike at the boundary (where MAR doubles over the youngest Cretaceous data point), but we suspect that this point may be biased by the abrupt change in sedimentation rates at the K-Pg boundary between the shipboard, latest Cretaceous³ and the Westerhold et al., earliest Danian² age models. We have no direct means of correcting this potential age-model artifact, but in any case this problem only affects a single sample containing the K-Pg impact ejecta. However, we think the data do not contradict our contention that there was no prolonged drop in fish export production at the K-Pg boundary.

A second concern with comparing total ichthyolith MAR flux (MAR of the non-carbonate fraction $>38\mu\text{m}$) from the North Pacific to fish tooth counts from other sites is that these two types of measurements ($>38\mu\text{m}$ NCF and tooth counts) may not be comparable. Rough counts of the very largest fish teeth ($>180\mu\text{m}$ in at least one dimension) at Shatsky Rise suggest that, to a first order, the $>38\mu\text{m}$ NCF fraction and tooth counts both follow the same signal (presumably the flux of fish remains to the deep sea) (Fig. S16), a result discussed at length within the main manuscript. In addition, the other sites used in the study had non-carbonate fractions that were not pure fish debris. In these sites, individual ichthyoliths were picked directly from the $>38\mu\text{m}$ washed residues, and ichthyolith accumulation rate was calculated based on ichthyoliths/gram dry sediment rather than the total ichthyolith mass used at Shatsky Rise. For these picked sites, we aimed to process sample volumes large enough to obtain at least 50 ichthyoliths per sample, to insure that the patterns we observed were robust. In the case of DSDP Site 596 and ODP Site 886, the $>106\mu\text{m}$ size fraction consistently yielded the minimum number of ichthyoliths. The smaller size fractions were not counted at DSDP Site 596 and ODP Site 886, as they greatly increased processing times and generally trended along with the $>106\mu\text{m}$ fraction in test samples. At Gubbio, teeth were sufficiently rare to necessitate picking all ichthyoliths $>38\mu\text{m}$ despite large raw samples of $>100\text{g}$. Shackleton's Walvis Ridge record, which we have considered briefly in the manuscript (DSDP Site 527)¹⁵ considers ichthyoliths $>63\mu\text{m}$, presumably because this is the size fraction retained for foraminifera work. In our work at Shatsky Rise (ODP Site 1209), we split the samples into size fractions to weigh them, and found that the overall size structure of the samples was relatively constant during the Danian. Considering just the larger or smaller size fractions yielded the same trends as the whole $>38\mu\text{m}$ sample for Shatsky Rise. Therefore, we think that while the raw counts and associated

ichthyolith MARs are not numerically comparable, the overall patterns and relative cross-site patterns are robust.

Mixing across the K-Pg boundary

The K-Pg boundary at Shatsky Rise has distinct evidence of bioturbation (like many otherwise complete marine K-Pg boundaries) with boundary-crossing burrows⁸, evidence for Cretaceous nannofossils mixed up into the early Paleocene¹⁶ and stratigraphically spread out boundary ejecta and impact-associated elements (e.g., Hull et al.¹⁷). Small sedimentary components (like nannofossils and fine grained boundary clays) are normally mixed further than large sediment grains (like foraminifera and fish teeth)¹⁸⁻¹⁹. Thus we assume that the boundary mixing is unlikely to have a large effect on our inferences of boundary changes in fish tooth accumulation beyond ~20cm spanning the boundary at Shatsky Rise –e.g., the range of heavily remixed Cretaceous nannofossils and the spread of the iridium anomaly. In contrast, mixing in the slowly accumulating red clays of DSDP 596 and ODP 886 could serve to obliterate a short-lived decline in fish tooth accumulation rates. However, if such a decline occurred, then a large increase (above Cretaceous MAR) would be needed to give the overall pattern of no boundary change with a slight increase in the early Danian. At Gubbio, although boundary mixing is known to occur it would only affect the few centimeters on either side of the boundary. Here, our interpretation of the sustained drop in ichthyolith accumulation at Gubbio is unlikely to be overprinted by such local scale effects.

A previous record from DSDP Site 527 on Walvis Ridge in the South Atlantic supports the inference of a decline in fish abundance inferred at Gubbio. Using data collected by

Shackleton¹⁵, recalibrated to the GTS2012 timescale, we found that at DSDP 527 accumulation of ichthyoliths drops from 2534 ichthyoliths/cm²/myr in the Latest Cretaceous to approximately 974 ichthyoliths/cm²/myr. This represents a nearly 60% decline across the boundary, which does not return to pre-extinction levels for nearly 4 million years (Fig. S13a, S14e). However, it is worth noting that ichthyolith accumulation levels in the earliest Danian are comparable to those of the Maastrichtian approximately 2 million years before the boundary, and accumulation rates reach similar lows throughout the Paleogene. The highly variable sample size used in the Walvis Ridge study combined with a large change in lithology (and dry bulk density) make this supporting evidence from Walvis Ridge tentative at present, and as such it was excluded from the main manuscript.

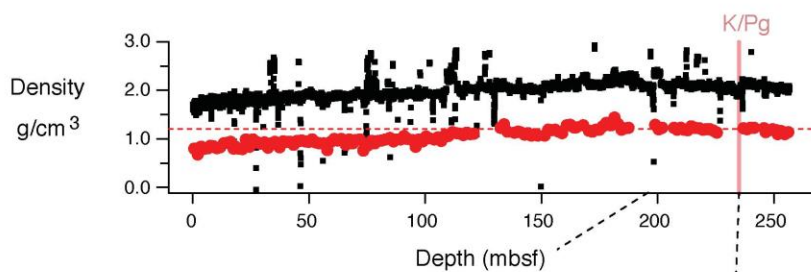
REFERENCES

- 1 Hull, P. M., Norris, R. D., Bralower, T. J. & Schueth, J. D. A role for chance in marine recovery from the end-Cretaceous extinction. *Nat Geosci*, 856–860 (2011).
- 2 Westerhold, T. *et al.* Astronomical calibration of the Paleocene time. *Palaeogeography, Palaeoclimatology, Palaeoecology* **257**, 377-403 (2008).
- 3 Bralower, T. J. *et al.* Site 1209. *Proceedings of the Ocean Drilling Program, Part A: Initial Reports* **198**, 105 (2002).
- 4 Hilgen, F. J., Kuiper, K. F. & Lourens, L. J. Evaluation of the astronomical time scale for the Paleocene and earliest Eocene. *Earth Planet Sc Lett* **300**, 139-151 (2010).
- 5 Westerhold, T., Röhl, U. & Laskar, J. Time scale controversy: Accurate orbital calibration of the early Paleogene. *Geochemistry, Geophysics, Geosystems* **13** (2012).
- 6 Blum, P. Physical properties handbook: a guide to the shipboard measurement of physical properties of deep-sea cores. *ODP Tech. Note* **26** (1997).
- 7 Hull, P. M. & Norris, R. D. Diverse patterns of ocean export productivity change across the Cretaceous-Paleogene boundary: New insights from biogenic barium. *Paleoceanography* **26**, 3205 (2011).
- 8 Bralower, T. J. *et al.* Leg 198 Summary. *Proceedings of the Ocean Drilling Program, Part A: Initial Reports* **198**, 148 (2002).
- 9 Bralower, T. *et al.* Grain size of Cretaceous-Paleogene boundary sediments from Chicxulub to the open ocean: Implications for interpretation of the mass extinction event. *Geology* **38** (2010).

- 10 Mukhopadhyay, S., Farley, K. & Montanari, A. A short duration of the Cretaceous-Tertiary boundary event: Evidence from extraterrestrial helium-3. *Science* **291**, 1952-1955 (2001).
- 11 Broecker, W. S. & Clark, E. CaCO₃ size distribution: A paleocarbonate ion proxy? *Paleoceanography* **14**, 596-604 (1999).
- 12 Broecker, W. S. & Clark, E. Reevaluation of the CaCO₃ size index paleocarbonate ion proxy. *Paleoceanography* **16**, 669-671 (2001).
- 13 Chiu, T. C. & Broecker, W. S. Toward better paleocarbonate ion reconstructions: New insights regarding the CaCO₃ size index. *Paleoceanography* **23** (2008).
- 14 Naik, S. S. & Naidu, P. D. Evaluation of the CaCO₃ dissolution proxies in sediment cores from above the lysocline. *Quaternary International* **213**, 69-73 (2010).
- 15 Shackleton, N. J. Accumulation Rates in Leg 74 sediments. *Initial Reports of the Deep Sea Drilling Project* **74**, 621-644 (1984).
- 16 Bown, P. Selective calcareous nannoplankton survivorship at the Cretaceous-Tertiary boundary. *Geology* **33**, 653-656 (2005).
- 17 Hull, P. M., Franks, P. J. S. & Norris, R. D. Mechanisms and models of iridium anomaly shape across the Cretaceous-Paleogene boundary. *Earth Planet Sc Lett* **301**, 98-106 (2011).
- 18 Thomson, J. *et al.* Radiocarbon age offsets in different-sized carbonate components of deep-sea sediments. *Radiocarbon* **37**, 91-101 (1995).
- 19 Wheatcroft, R. A. Experimental tests for particle size-dependent bioturbation in the deep ocean. *Limnol Oceanogr* **37**, 90-104 (1992).

Figure S1. ODP Site 1209 shipboard measurements [2] of dry bulk density and GRA (gamma ray attenuation). (a) All measurements (dry bulk density in red, GRA in black), and (b) Paleocene measurements in ODP Hole 1209A. K/Pg boundary in pink; Paleocene bounds indicated in black dashed lines; 1.2 g/cm³ dry bulk density indicated in red dashed line; and depth indicated as meters below sea floor (mbsf).

a All shipboard ODP Hole 1209A dry bulk and GRA density measurement



b Paleocene ODP Hole 1209A dry bulk and GRA density measurement

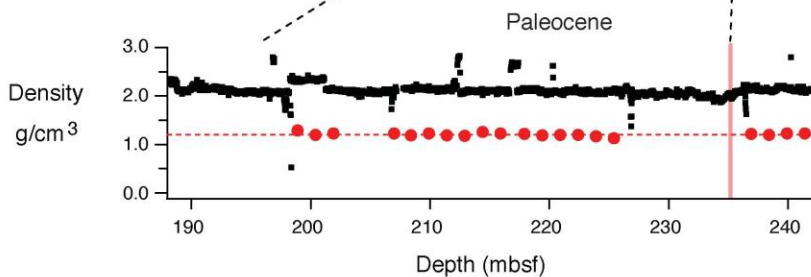


Figure S2. Relationship between GRA density and dry bulk density for ODP Hole 1209A (all shipboard measurements [3]). GRA density interpolated down to depth intervals of dry bulk density. Linear regression between GRA and dry bulk density determined for GRA density values less than 2.1 g/cm³, as the high scatter of values for GRA densities greater than 2.1 g/cm³ strongly influence the regression. Dry bulk densities calculated from the regression of GRA densities below 2.1 g/cm³ better approximate direct measurements of dry bulk density in the Paleocene (median residual = 0.032) than calculations based on the regression on all values (median residual = 0.089).

$$\text{Dry Bulk Density} = -1.305 + (1.199 \times \text{GRA Density})$$

$r^2 = 0.93$, $P < 0.001$ (for points included in regression; e.g. points with GRA values < 2.1 g/cm³)

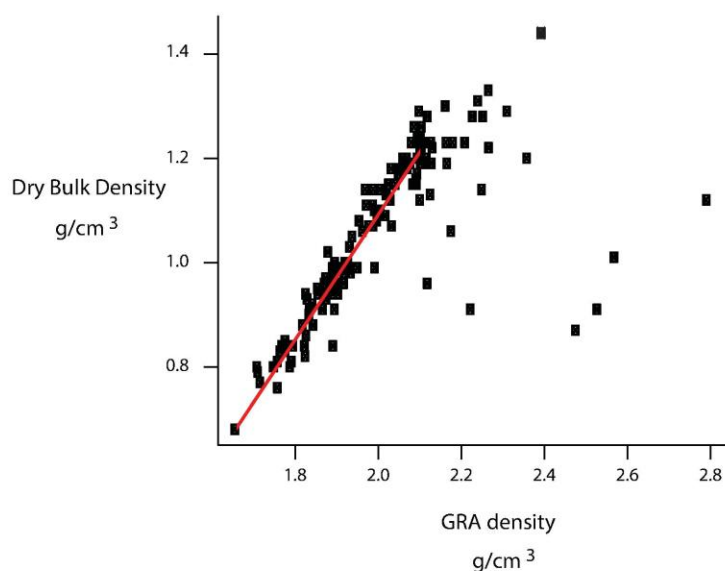


Figure S3. Dry bulk density calculated from GRA (gamma ray attenuation) and observed GRA to dry bulk relationship. (a) Direct dry bulk measurements (light blue) over calculated dry bulk values (black), (b) interpolated dry bulk values for fish MAR calculations (orange) over calculated dry bulk values (black), and (c) interpolated dry bulk values for calcareous MAR calculations (yellow) over calculated dry bulk values (black). K/Pg boundary in pink; Paleocene bounds indicated in black dashed lines; 1.2 g/cm^3 indicated in red dashed line; and depth indicated as revised meters composite depth (rmcd). One outlier (c, boxed in red) calculated dry bulk density was replaced in all downstream calculations by the average of the surrounding two values.

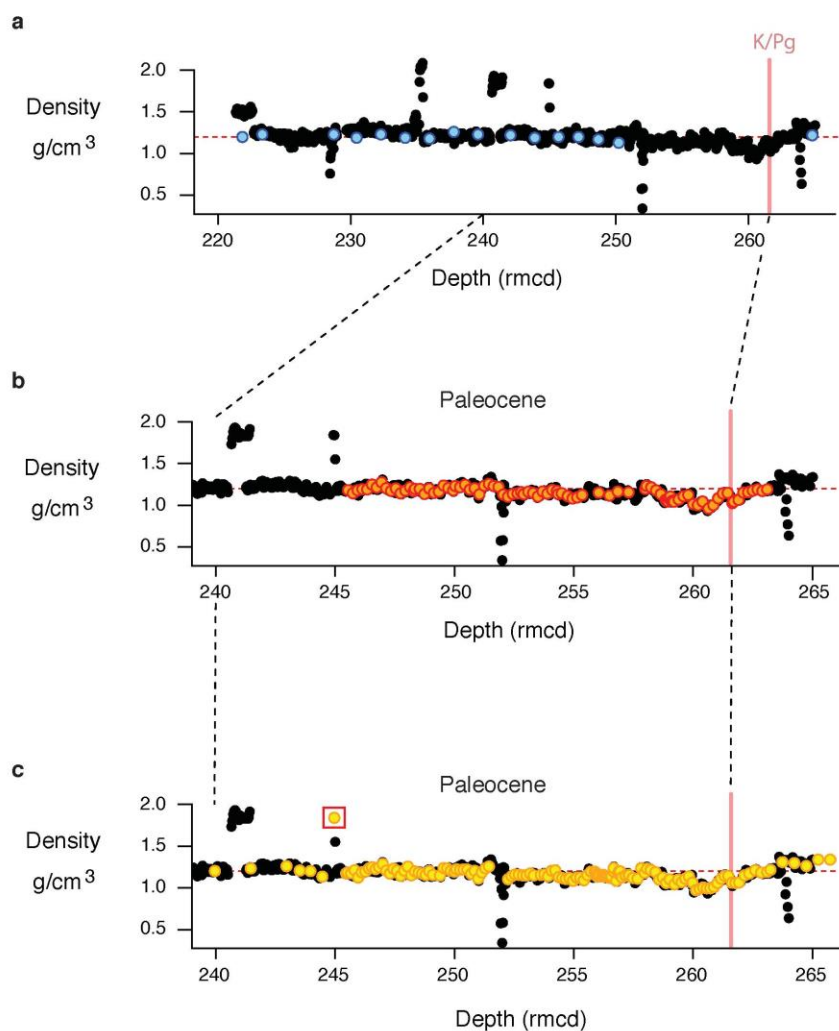


Figure S4. Sedimentary mass accumulation rate (MAR) comparison. (a) Sedimentary MAR calculated with a constant dry bulk density (1.2 g/cm^3 , black) and with a variable GRA-based dry bulk density (red). Difference in sedimentary MAR between constant-density MAR and variable-density MAR shown in (b) as the difference in MAR, and in (c) as the percent difference relative to the variable-density MAR values. K/Pg boundary in pink; no difference indicated in red dotted line in b and c; and age in millions of years using the Westerhold et al. (2008) age model.

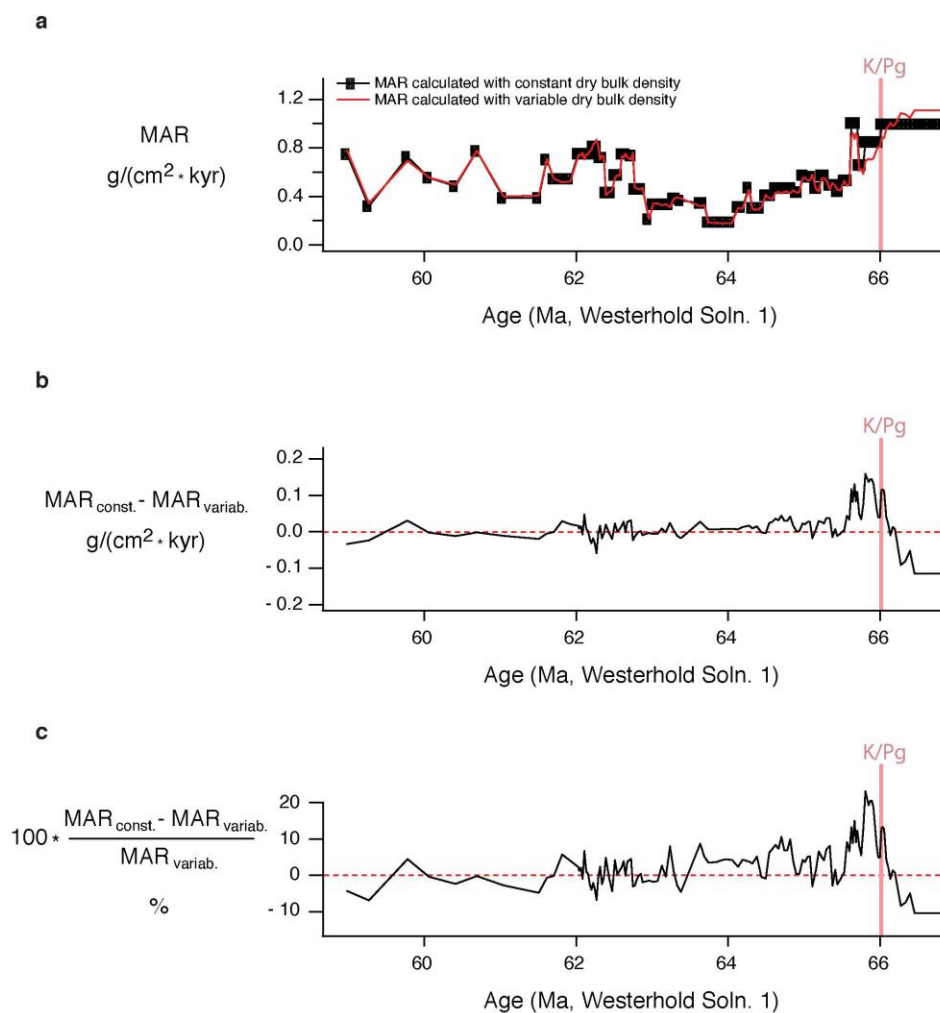
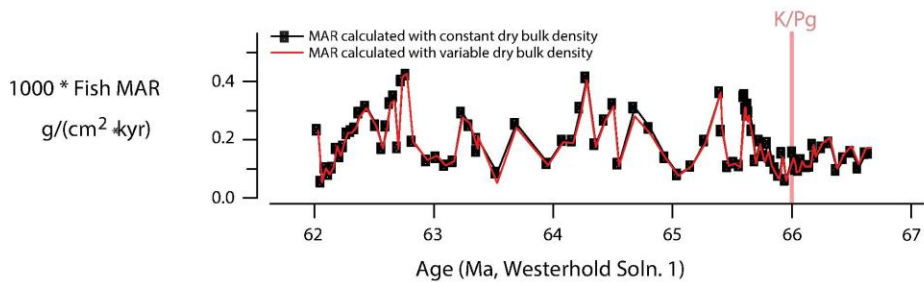
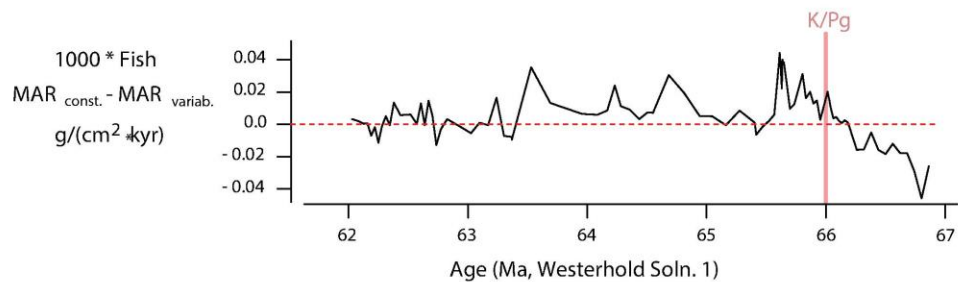


Figure S5. Ichthyolith mass accumulation rate (MAR) comparison. (a) Ichthyolith MAR calculated with a constant dry bulk density (1.2 g/cm³, black) and with a variable GRA-based dry bulk density (red). Difference in ichthyolith MAR between constant-density MAR and variable-density MAR shown in (b) as the difference in MAR, and in (c) as the percent difference relative to the variable-density MAR values. K/Pg boundary in pink; no difference indicated in red dotted line in b and c; and age in millions of years using the Westerhold et al. (2008) age model.

a



b



c

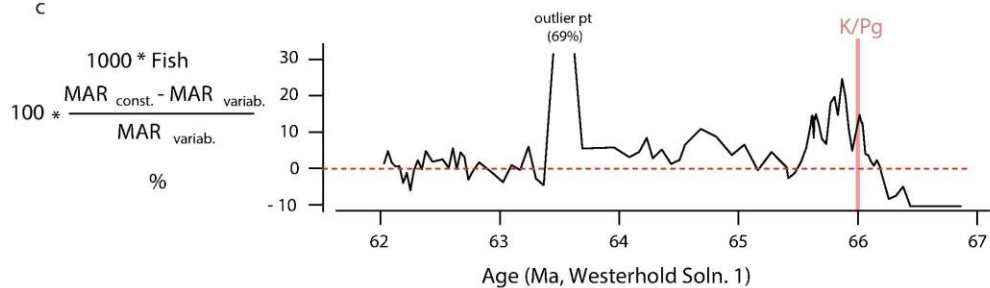


Figure S6. Relationship between total Fe and % carbonate for ODP Site1209 based on published XRF Fe counts [7] and % carbonate values from multiple sources. Fe counts interpolated down to match the depth intervals of the percent carbonate measurements. Linear regression used to determine the relationship between $\ln(\text{Fe})$ and percent carbonate.

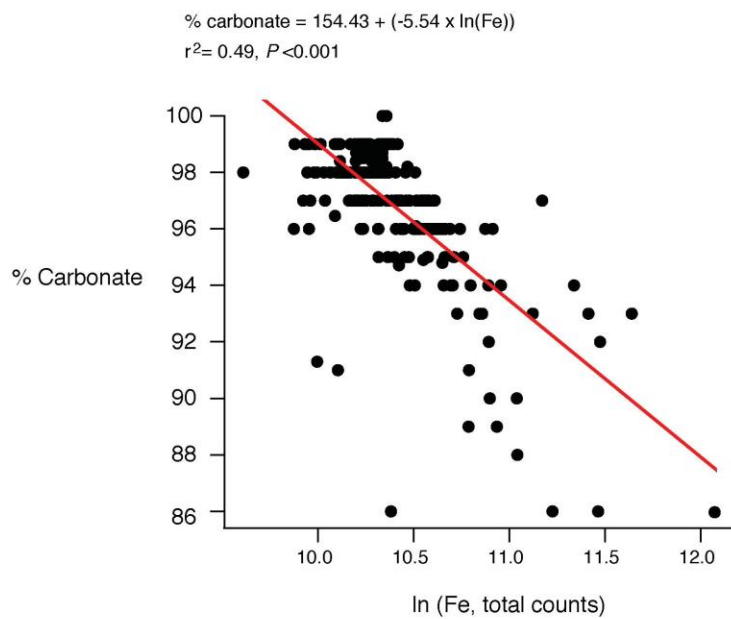


Fig. S7. % Carbonate as calculated from XRF Fe counts and the relationship between $\ln(\text{Fe})$ and % carbonate. Full XRF % Carbonate dataset shown in black; 7-point running mean of data in red. 7-pt running mean used in all downstream % carbonate calculations. Note: all calculated % carbonate values over 100% are replaced by 100% for dependent calculations.

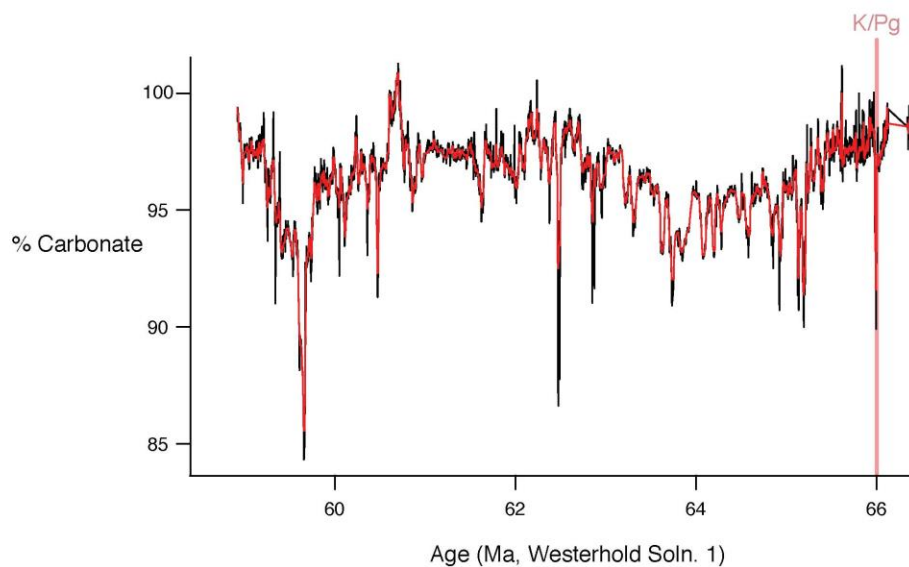


Figure S8. Carbonate mass accumulation rate (MAR) comparison. (a) Carbonate MAR calculated by multiply sedimentary MAR (variable density) by a constant % carbonate (95%, black) or a Fe-based variable % carbonate (red). Difference in carbonate MAR between constant and variable % carbonate shown in (b) as the difference in carbonate MARs, and in (c) as the percent difference relative to the variable-% carbonate MAR values. K/Pg boundary in pink; no difference indicated in red dotted line in b and c; and age in millions of years using the Westerhold et al. (2008) age model.

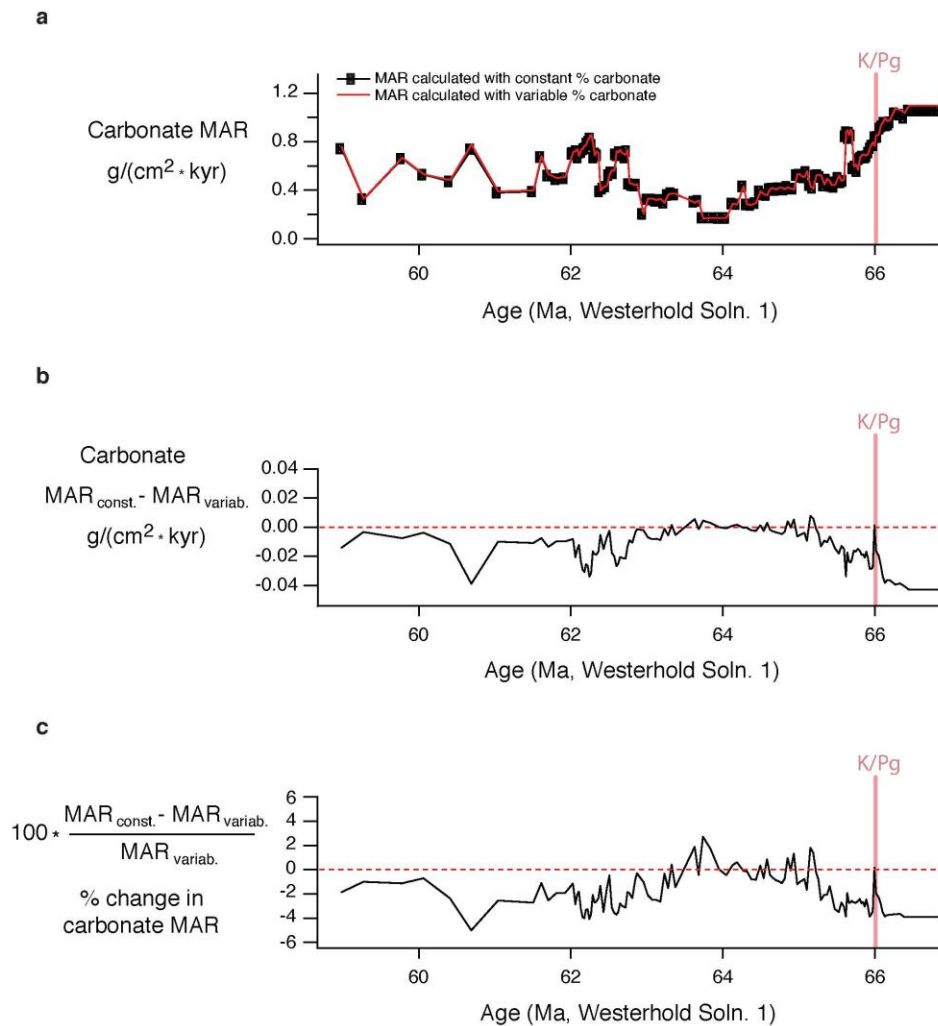


Figure S9. Foraminiferal sized grain mass accumulation rate (MAR) comparison.
(a) Foraminiferal MAR calculated with the assumption that non-carbonate grains are found across all size classes (black) or just within the clay fraction (red). Difference in foraminiferal MAR between all versus clay sized non-carbonates shown in (b) as the difference in MARs, and in (c) as the percent difference relative to clay-sized non-carbonates calculation. K/Pg boundary in pink; no difference indicated in red dotted line in b and c; and age in millions of years using the Westerhold et al. (2008) age model.

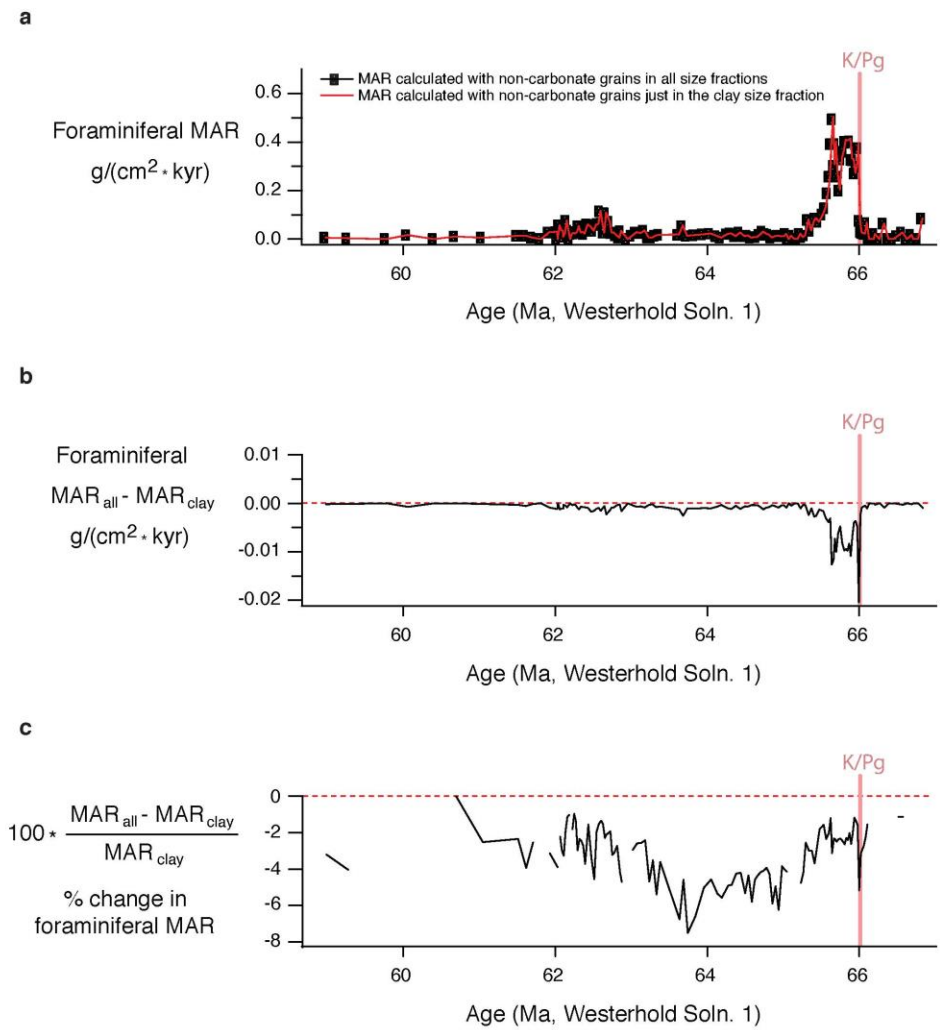


Figure S10. Foraminiferal sized grain mass accumulation rate (MAR) comparison.
(a) Foraminiferal MAR calculated in previous work (Hull et al. [3], black) and in this study (red). Difference in foraminiferal MAR between the previous and current study shown in (b) as the difference in MARs, and in (c) as the percent difference relative to the current calculation. K/Pg boundary in pink; no difference indicated in red dotted line in b and c; and age in millions of years using the Westerhold et al. (2008) age model.

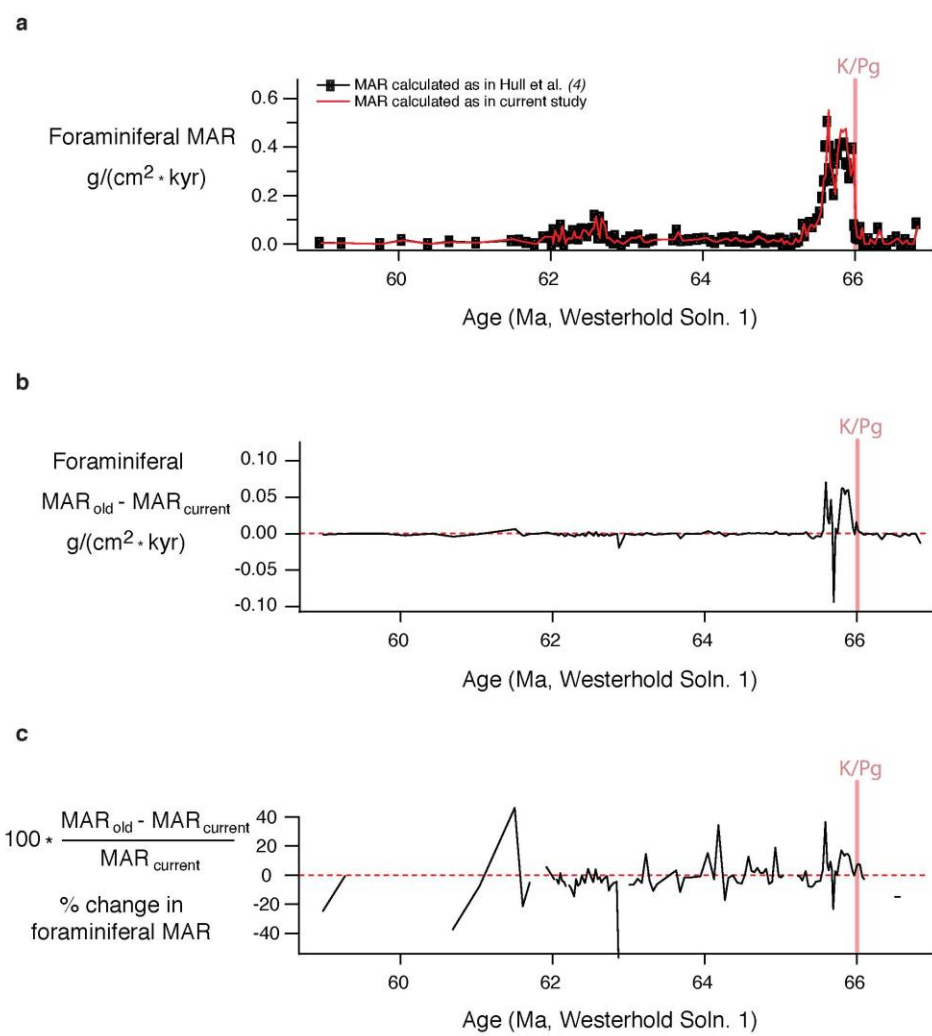


Figure S11. Nannofossil sized grain mass accumulation rate (MAR) comparison.
(a) Nannofossil MAR calculated in previous work (Hull et al. [3], black) and in this study (red). Difference in nannofossil MAR between the previous and current study shown in (b) as the difference in MARs, and in (c) as the percent difference relative to the current calculation. K/Pg boundary in pink; no difference indicated in red dotted line in b and c; and age in millions of years using the Westerhold et al. (2008) age model.

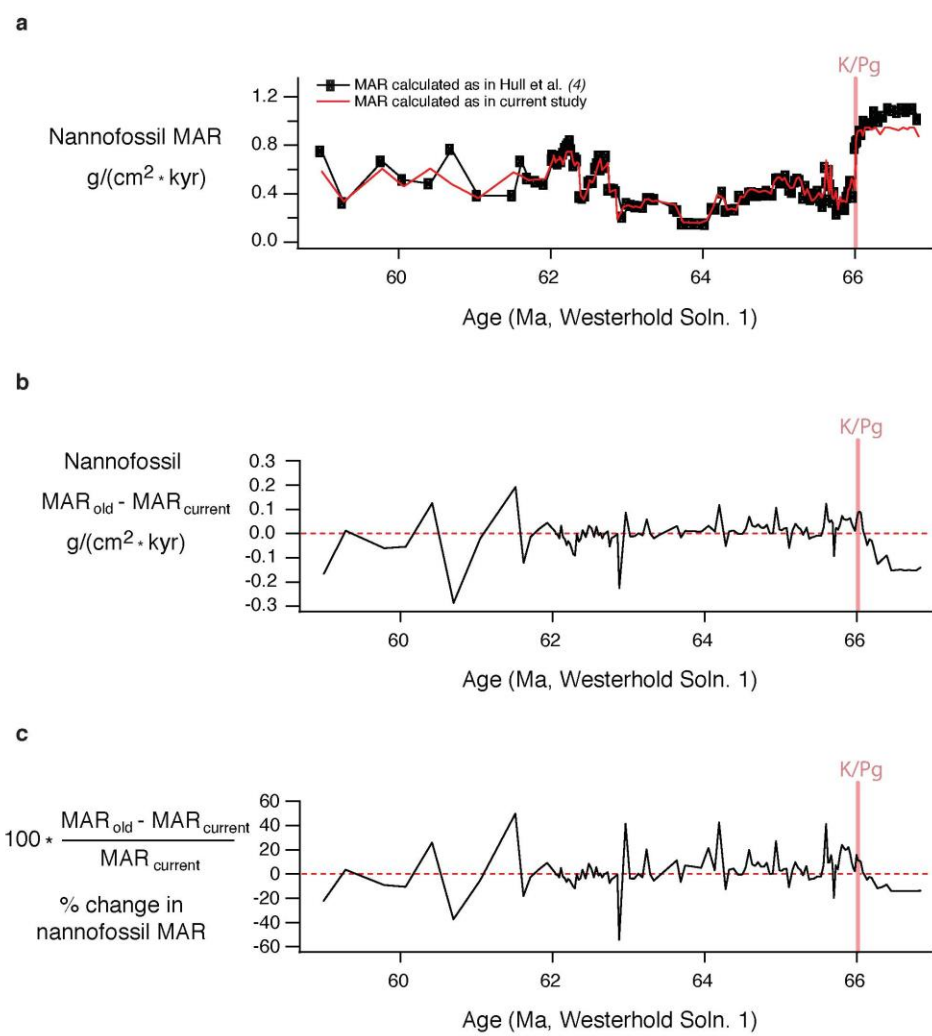


Figure S12. Mass accumulation rates (MAR) for (a) nannoplankton, (b) foraminifera, and (c) ichthyoliths, calculated using the Westerhold et al. (2008) age model solution 1 (black line with circles) and the Hilgen et al. (2010) age model with a variable dry bulk density. Late Cretaceous sedimentation rates calculated using shipboard age models¹ in both cases. The critical interval (grey box) is where age model differences affect the interpretation of ichthyolith accumulation rates.

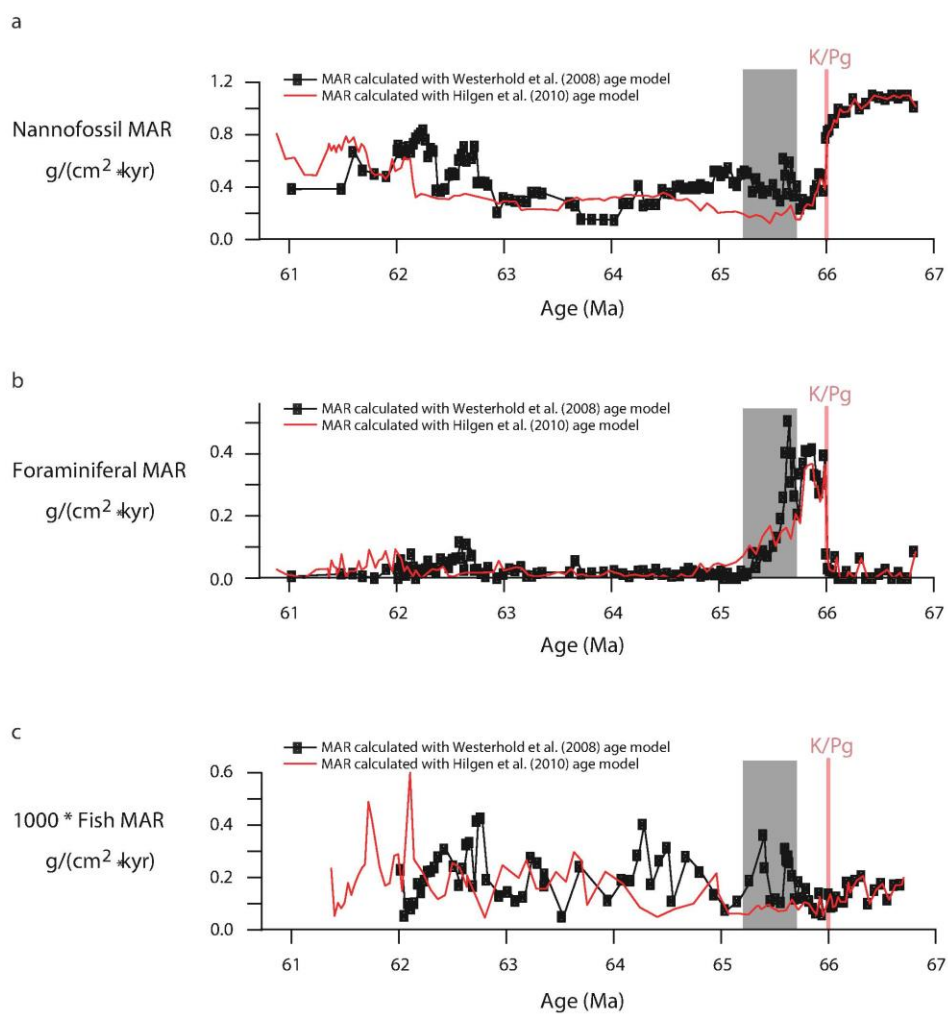
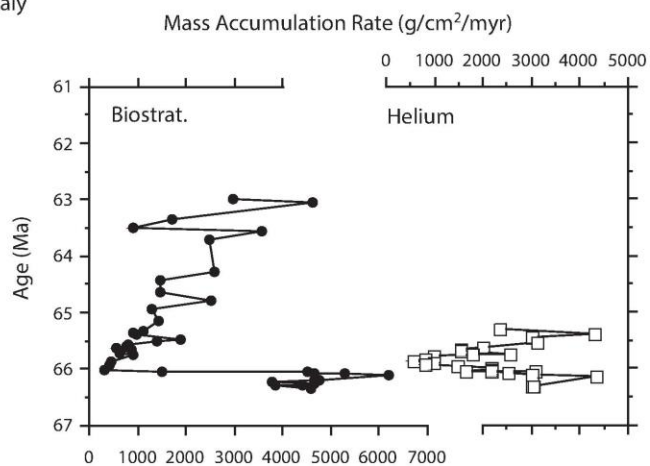


Figure S13. Mass accumulation rates (MAR) for (a) Gubbio, Italy, and (b) IODP 1209, Shatsky Rise, comparing two age models and their effect on boundary mass accumulation rates.

a Gubbio, Italy



b ODP 1209, N. Pacific

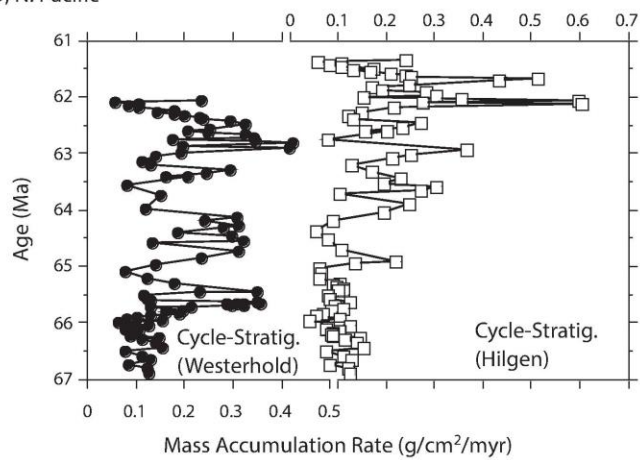


Figure S14. Extended version of Main Figure 2: Ichthyolith accumulation rate at all sites considered in the study, including data generated by Shackleton (1984) from Walvis Ridge, DSDP Site 527 in the South Atlantic. Data generated by this study are represented in (a) - (d). We note that while there may be a decline in ichthyolith accumulation across the K/Pg boundary in the South Atlantic (as has been interpreted), sample spacing and sample size are relatively poor. The data presented here is a restatement of Shackleton's data table, with new MAR calculated from an age model based on bio- and magnetostratigraphy, with updated ages to match GTS2012.

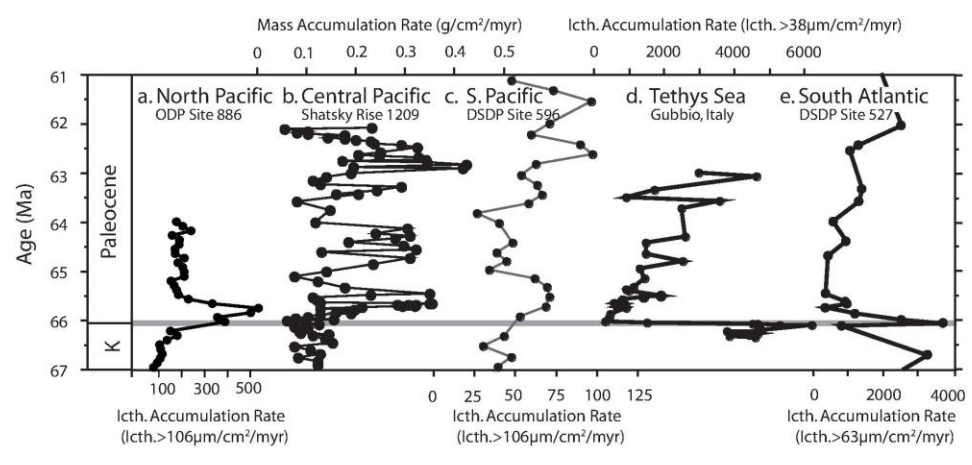
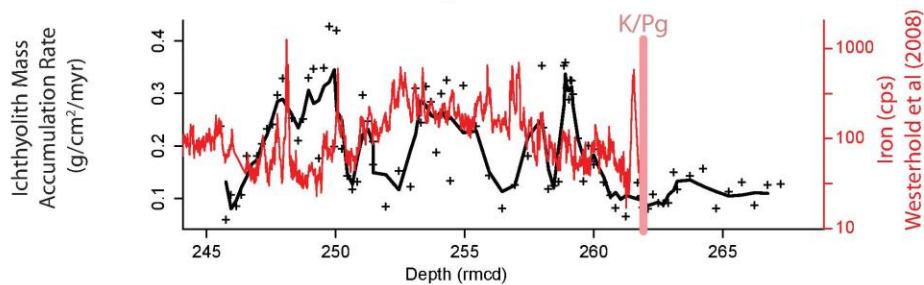


Figure S15. Fish MAR at Shatsky Rise compared to iron counts of Westerhold et al. (2008). Plotted on a depth scale to be independent of age. MAR Calculations based on (a) Age model Solution 1 of Westerhold et al. (2008) and (b) Hilgen et al. (2010). It appears that fish is independent of iron concentrations regardless of age model used. Small plus signs (+) indicate actual fish MAR, while solid black line is a 3-point running mean. Red is iron counts from Westerhold et al. (2008).

a MAR Calculated with Westerhold et al. (2008) age model solution 1



b MAR Calculated with Hilgen et al. (2010) age model

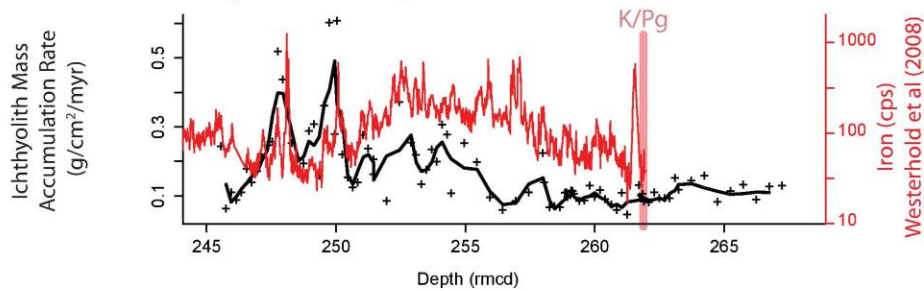
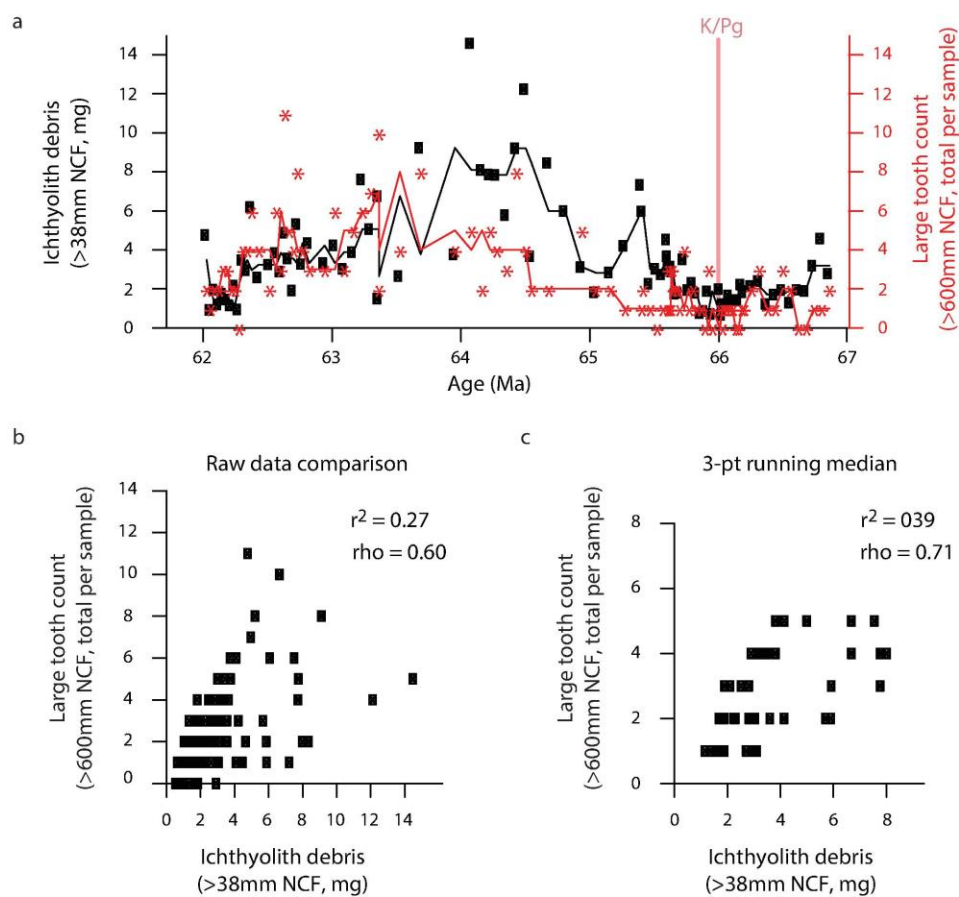


Figure S16 (a) Sample ichthyolith mass (measured as >38mm non-carbonate fraction, black circles) and sample large tooth count (counted for all teeth >600mm, red stars) against time. 11-point running median for both series shown as lines of corresponding colors. Pairwise comparison of (b) sample ichthyolith mass and large tooth count, and (c) 3-point running median of sample ichthyolith mass and large tooth count. In (b) and (c) correlations were tested with Pearson's product-moment correlation and Spearman's rank correlation and found to be significant ($p < 0.01$) (correlations in figure).



Chapter 3, in full, is a reprint of materials as it appears in Sibert, E. C., Hull, P. M., and Norris, R. D. (2014). “Resilience of Pacific Pelagic Fish following the Cretaceous/Palaeogene Mass Extinction” in *Nature Geoscience*, v. 7, no. 9, p. 667-670. DOI:10.1038/ngeo2227. The dissertation author was the primary investigator and author of this manuscript.

CHAPTER 4

No evidence for productivity-driven dwarfing in pelagic fish communities following the Cretaceous-Paleogene Mass Extinction

4.1 Abstract

Survivors of mass extinctions are often smaller than their pre-extinction predecessors, a response thought to be adaptive to poor resource conditions known as the “Lilliput Effect”. Extinction models for the Cretaceous-Paleogene mass extinction posit a sharp drop in resources after the extinction and, indeed, there is a Lilliput Effect in many fossil groups, including pelagic foraminifera, nannoplankton and shallow marine invertebrates. We investigated changes in size of pelagic fish through the P/Pg event using microfossil fish teeth (ichthyoliths) preserved in deep-sea sediment cores from two different geographic locations which had contrasting post-extinction productivity regimes: the South Atlantic (ODP 1262), which had significant declines in production, and the tropical Pacific (ODP 1209), which did not. We find that the size structure of the fish tooth assemblage is relatively unaffected in either basin across the extinction. Indeed, rather than a decrease in tooth sizes, fish in our Atlantic site show a statistically-significant increase in tooth size in the early recovery suggesting that some Paleocene fish were either larger or consuming larger, more active prey than those in the Cretaceous. Fish in both sites show an increase in the relative abundance of large teeth around 62 Ma. While this corresponds to an increase in fish flux in both basins, the Pacific shows several peaks in fish accumulation prior to 62 Ma, suggesting that absolute production is not the driving factor behind the changes in size structure. This suggests that fishes thrived in the post-extinction oceans, potentially facilitating their subsequent taxonomic dominance in the Cenozoic.

4.2 Introduction

The Cretaceous-Paleogene (K/Pg) mass extinction ~66 million years ago is associated with >90% extinction in calcareous plankton groups (Coxall et al., 2006), and a disruption of the pelagic food web (D'Hondt, 2005; Hull and Norris, 2011; Hull et al., 2011). Traditional models of the extinction have interpreted a collapse in the $\delta^{13}\text{C}$ isotope gradient as either a uniform global collapse of primary productivity – the ‘Strangelove Ocean’ (Hsu and McKenzie, 1985) – or a shift to tiny phytoplankton and a microbial loop system, a so-called ‘living ocean’ (D'Hondt, 2005). These resource-limited conditions favored smaller organisms in the immediate aftermath of the extinction event for many fossil groups, including the calcareous plankton, a so-called “Lilliput Effect” (Harries and Knorr, 2009; Schulte et al., 2010; Urbanek, 1993).

The size structure and abundance of fishes is a function of both the underlying size distribution and abundance of primary producers and zooplankton (Iverson, 1990). In a resource-stressed post-extinction world with a decrease in primary productivity or a shift to smaller-celled phytoplankton as proposed by D'Hondt et al., (1998) and Hsu and McKenzie (1985), fishes would be expected to decline in total abundance, biomass, or both, in response to the reduction in available fixed carbon. However, fish production across the extinction in the open ocean follows a similar geographic pattern to other export production proxies (Alegret and Thomas, 2009; Hull and Norris, 2011), with declines in the Atlantic, but stable or increased fish production in the Pacific (Sibert et al., 2014). Further, the K/Pg extinction caused a global restructuring of the marine vertebrate community, with the abundance of ray-finned fishes increasing compared to the sharks, suggesting that some aspects of fish community composition are decoupled from total

production after the extinction (Sibert and Norris, 2015). Indeed, molecular evidence suggests that the lineages of modern large pelagic fishes diversified in the post-extinction pelagic ecosystem (Miya et al., 2013). The vast majority of diversity in ray-finned fishes developed during the Early Paleogene (Friedman and Sallan, 2012; Near et al., 2012), suggesting that fishes may have responded differently to the K/Pg extinction than other lineages.

Here, we evaluate how oceanic fishes adapted to the post-extinction world by comparing the size structure of pre- and post-extinction fish communities between the South Atlantic, which shows a significant decline in both export and total fish production at the boundary, and the Pacific, which did not. A difference in the size structure of pre- or post-extinction fish communities between the Atlantic and Pacific Oceans could help explain the observed different responses in fish production between the basins. For example, it is possible that in regions with decreased productivity (e.g. the South Atlantic), there would be a demographic shift in the consumer population favoring smaller individuals with lower metabolic demands or individuals with smaller teeth optimized for handling smaller prey. Alternatively, it is possible that following the extinction of large-bodied Cretaceous predators (D'Hondt, 2005; Friedman, 2009; Ward et al., 1991), fishes were ecologically released and increased their body size and/or tooth size to handle newly available prey (Sibert and Norris, 2015), potentially counteracting any resource limitation in one or both productivity regimes.

4.3 Methods

We use ichthyoliths preserved in deep-sea sediment cores from two pelagic ocean sites which show different responses in fish production across the event: Ocean Drilling Program (ODP) Site 1262 in the South Atlantic and ODP Site 1209 in the North Pacific. Both sites are well-studied, deep-sea carbonate cores with established cyclostratigraphic timescales for the Paleocene (Hilgen et al., 2010; Westerhold et al., 2008) and well-preserved K/Pg boundary intervals. ODP Site 1209 has a sedimentation rate of 0.67 cm/kyr in the Cretaceous that declines to 0.3 cm/kyr in the earliest Paleocene. Sedimentation returns to pre-boundary levels by approximately 62.5 Ma. ODP Site 1262 has a sedimentation rate of ~2.0 cm/kyr in the Cretaceous and drops to 0.5 cm/kyr at the boundary. Sedimentation rate increases to 1.0 cm/kyr at 63 Ma, but does not return to pre-boundary rates during the study interval. At both sites, 10-15cc samples of carbonate ooze, sampled approximately every 20-50 kyr from 67 to 62 Ma, were dried to a constant mass at 50°C, weighed, dissolved in weak (5-10%) acetic acid, and washed over a 38µm sieve with DI water to remove the carbonate and concentrate ichthyoliths. Ichthyoliths were examined and picked out using a high-power dissection microscope. Teeth were grouped into “small” (<63µm) and “large” (>63µm) size classes for analysis. Fish teeth were differentiated from elasmobranch denticles.

To account for variations in sedimentation rate and density, we calculated ichthyolith accumulation rate (IAR; in units of ichthyoliths/cm²/kyr), using an established cyclostratigraphic age model for the Paleocene (Hilgen et al., 2010). For ODP Site 1209, the Cretaceous chronology was supplemented by shipboard biostratigraphy (Bralower et al., 2002). For ODP Site 1262, two different Cretaceous age models were considered, a

latest Cretaceous cyclostratigraphy (Westerhold et al., 2008) and the C29r/C30n boundary (Bowles, 2006). Both age models yielded nearly identical IAR values, and the cyclostratigraphic framework was used in the main analysis. All sites used shipboard variable dry-bulk-density in the accumulation rate calculation. Calculated IAR data do not meet the assumption of normality, so the Mann-Whitney U test, a non-parametric, rank-based statistical test, was used to compare IAR between sites and across the extinction event. We evaluated the size-structure of the tooth assemblage by comparing the proportion of large ($>63\mu\text{m}$) teeth within an assemblage between sites and across the extinction at each site. Differences in the assemblage composition were also evaluated using the Mann-Whitney U test. All analyses were carried out using the R statistical package.

4.4 Results and Discussion

The absolute value of ichthyolith accumulation was relatively constant in both the South Atlantic and the Central Pacific during the latest Cretaceous (Figure 4-1). The South Atlantic had slightly but significantly higher IAR in the latest Cretaceous, approximately $3.5 \text{ ich/cm}^2/\text{kyr}$ (± 1.0), compared to the Central Pacific, which had 2.6 (± 0.64) $\text{ich/cm}^2/\text{kyr}$ ($p < 0.001$). The Pacific showed a small (though statistically significant) decline in IAR during the first million years of the Paleocene, from a Cretaceous rate of 2.6 (± 0.64) $\text{ich/cm}^2/\text{kyr}$ to an early Paleocene rate of 2.0 (± 0.75) $\text{ich/cm}^2/\text{kyr}$ ($p = 0.004$). In the South Atlantic, the extinction event caused a significant 50% decline in IAR, to 1.7 (± 0.61) $\text{ich/cm}^2/\text{kyr}$ ($p < 10^{-12}$). The IAR in the South Atlantic remained depressed for 2 million years before slowly rising toward pre-extinction levels of production (Figure 4-1),

while Pacific IAR increased during the early Paleocene, exceeding pre-extinction fish production by 64 Ma, and remained elevated throughout the rest of the record, with several peaks reaching 12-14 ich/cm²/kyr – a nearly 5-fold increase over the low but stable Cretaceous IAR (Figure 4-1). South Atlantic IAR first surpasses Cretaceous levels two million years later than the Pacific does, in the interval after 62 Ma. However, as our record does not extend past this initial increase, it is unclear whether this represents a sustained recovery or a transient peak in total accumulation similar to those observed in the Pacific during the interval of 64-61 Ma.

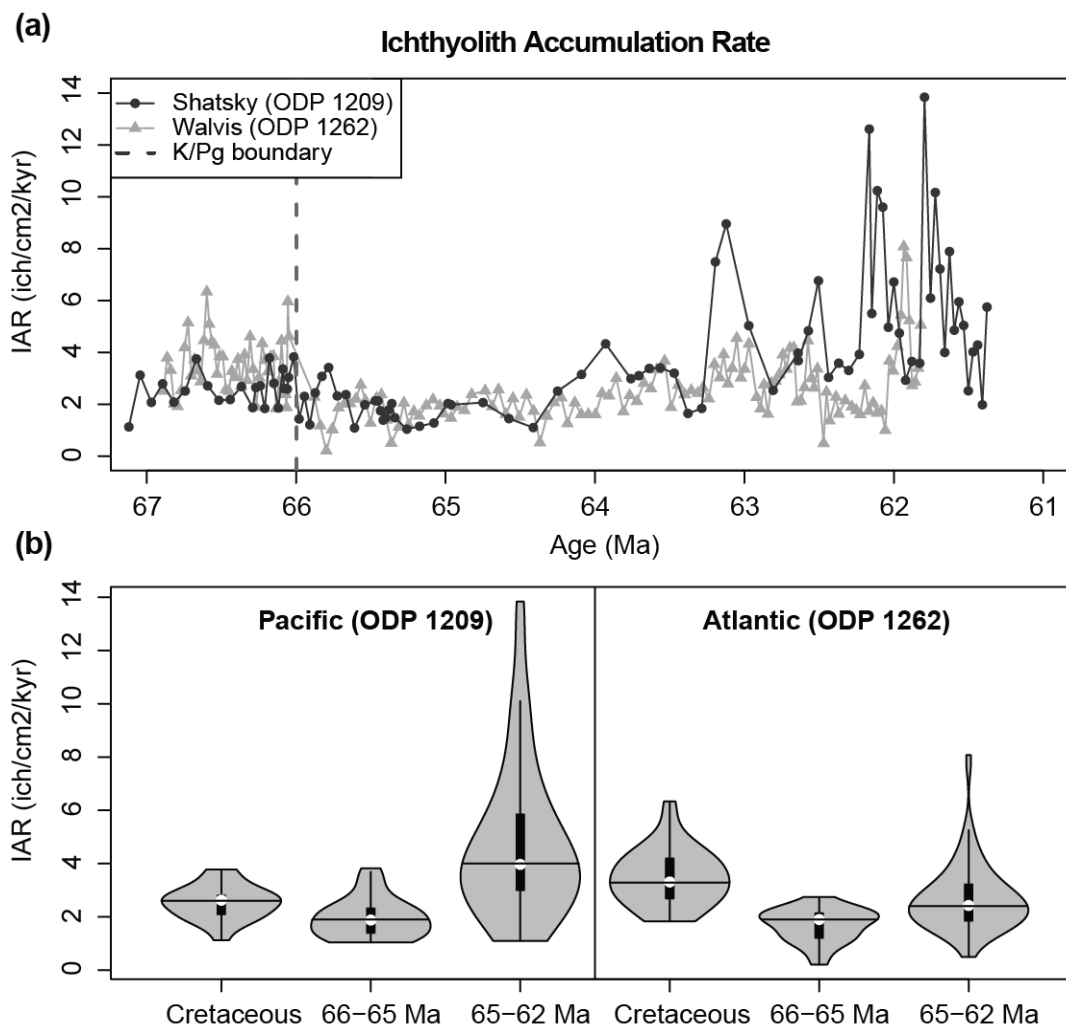


Figure 4-1: Ichthyolith accumulation rate (IAR) for ODP Site 1209 and ODP Site 1262. (a) A time-series of IAR, with the Pacific shown in black circles and the Atlantic shown in gray triangles. (b) Violin plots (combines box- and kernel density plots) of ichthyolith accumulation rate for the Cretaceous, Earliest Paleocene, and later Paleocene; left Pacific, right Atlantic. The horizontal black line is the median, black box is first and third quartiles, and the shaded gray shows the relative abundance of IAR values.

While total IAR suggests that Pacific fish did not experience a large-magnitude decline in abundance following the extinction event as they did in the Atlantic (Sibert et al., 2014), it is possible that post-extinction fishes decreased in size, but not abundance, to accommodate a decrease in prey size or availability (e.g. exhibited a Lilliput Effect). In

this case, tooth size distribution should shift toward a higher relative abundance of small teeth, particularly in the Atlantic, where the total production declined significantly. To test this, we examined the size structure of teeth in both oceanic records. In the Cretaceous, both the Atlantic and Pacific sites have ~22% of teeth $>63\mu\text{m}$; In the Paleocene, this increases to 26-27% in both ocean basins (Figure 4-2), and there is no significant difference between the ocean basins for either of these time periods, suggesting that fishes filled similar ecological roles (at least as measured by tooth size) in both basins (Figure 4-2a, b). Further, this increase in the relative abundance of larger teeth in the Paleocene is only statistically significant at the Atlantic site, and not in the Pacific (Figure 4-2c, d). These results suggest that the size structure of the tooth assemblage was relatively stable across the K/Pg extinction event. Further, there is no evidence for dwarfing in either basin. Further, a slight increase in the abundance of large teeth, suggests that the fish community structure was driven by something other than net productivity in the aftermath of the event.

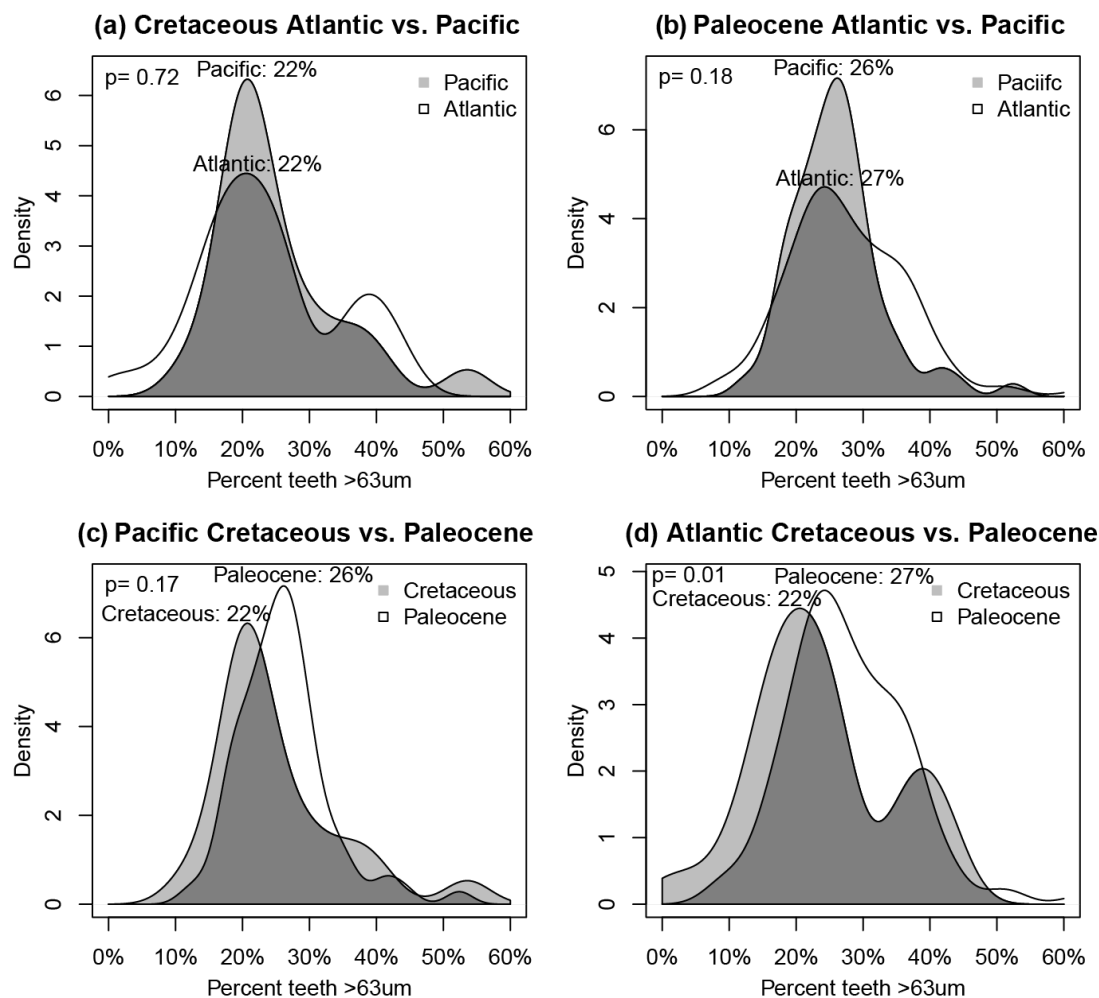


Figure 4-2: Kernel density plots showing the percent large (>63 μ m) teeth in each assemblage, split by site and time bin. The percentage reported on the figure is the median percentage of large teeth in an assemblage.

It is possible that the differences in fish productivity in the basins could be due to differences in early Paleocene fish biology or life history. For example, surviving species in the early Paleocene Pacific may have simply produced more teeth per capita than the average Cretaceous fish or those in the Atlantic, either by having more teeth in their jaws, faster shedding of teeth during life, or having a shorter generation time. Additionally, as

the post-extinction ecological regime in the Paleogene gyres was distinct from that of the Cretaceous, it is also possible that the post-extinction fauna in the different ocean basins adopted different ecological strategies. Indeed, it is likely that the size structure of the fish tooth assemblage is governed by interactions between fish and their prey: changes in prey type and size, fish mouth size, prey capture strategy, and trophic level, all likely play a part in determining the overall size structure of the fish tooth community.

Following the recovery of the open ocean $\delta^{13}\text{C}$ gradient, 3-4 million years after the extinction event, there was a wave of diversification of planktonic foraminifera, suggesting a shift in the structure of the pelagic ecosystem (Coxall et al., 2006). There is some evidence for a concurrent change in size structure regime for open-ocean fish as well. Indeed, both our Pacific and Atlantic sites show a substantial increase in the relative abundance of larger teeth near the end of their records, rising to over >50% large teeth in the assemblages at both sites, beginning around 62 Ma (Figure 4-3). This corresponds temporally with an interval of increased abundance of extremely large teeth observed in the South Pacific following the extinction event (Sibert and Norris, 2015), suggesting that fishes, too, may have expanded their roles in the pelagic ecosystem at this time. The size structure shift at ~62Ma corresponds approximately with a step-increase of IAR to above pre-extinction values in the South Atlantic, but is preceded by several peaks in IAR in the Pacific (Figure 4-3), further suggesting that tooth assemblage size structure is driven by the evolution of the prey community, rather than IAR.

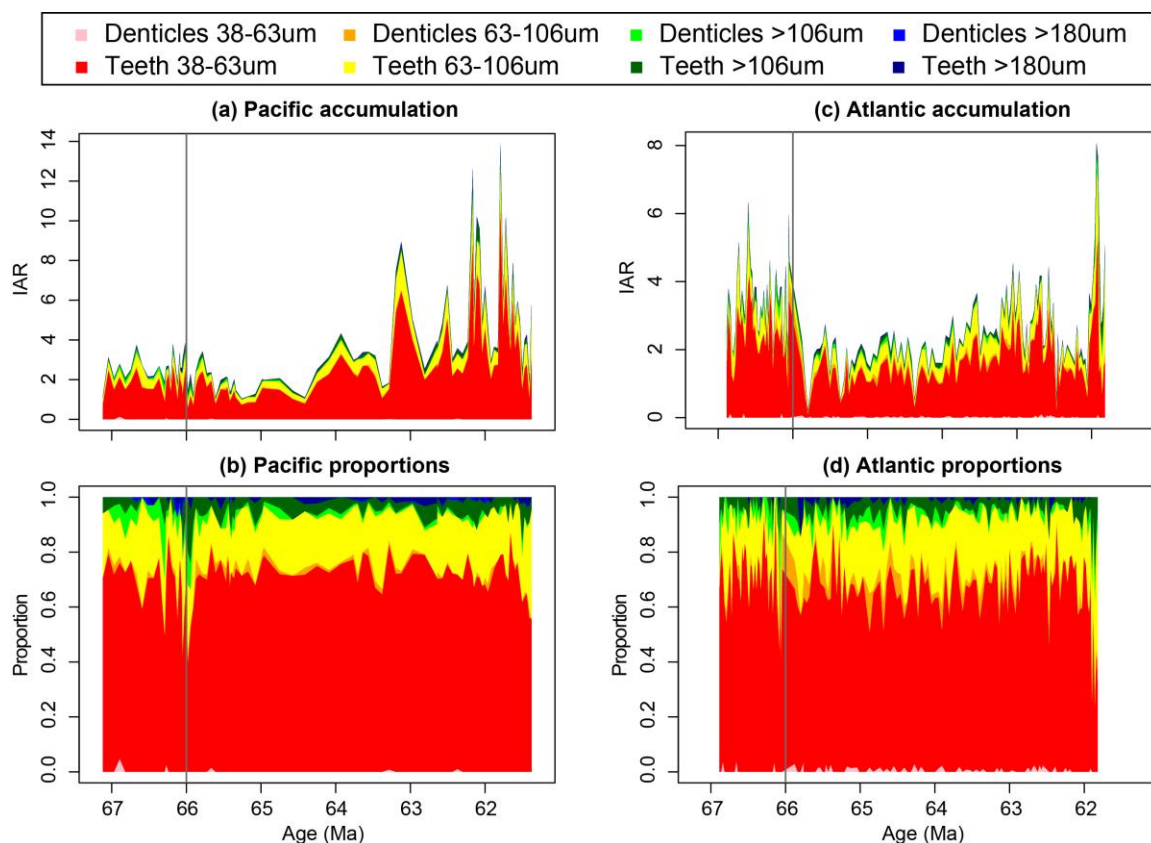


Figure 4-3: Absolute (top; a,c) and relative (bottom; b,d) abundance of each size class of ichthyoliths found in the Pacific (1209; top; a-b) and Atlantic (1262; top; c-d). Colors represent the different size classes of ichthyoliths. Note the slight increase in the yellow and green at the end of the records, approximately 62 Ma for both 1209 and 1262. Vertical gray line is the K/Pg boundary.

4.5 Conclusion

Fishes have exhibited dwarfing following other mass extinction events throughout the Phanerozoic (Sallan and Galimberti, 2015), and suffered a selective extinction of predators at the K/Pg in coastal regions (Friedman, 2009). However, in the open ocean, early Paleocene fish communities do not show any evidence for post-extinction size decreases. Indeed, there is a modest increase in overall tooth size in the immediate aftermath of the event in both the Central Pacific and South Atlantic oceans. A significant

increase in the proportion of large teeth around 62 Ma suggests that as the ocean basins recovered from the extinction event, fishes were able to more fully take advantage of newly vacated niche space following the K/Pg extinction, fundamentally expanding their ecological roles in the open ocean (Miya et al., 2013; Sibert and Norris, 2015). These trends are observed in both the Atlantic and the Pacific, even though these basins have distinctly different post-extinction productivity regimes, suggesting that the fish community structure was driven by factors other than net primary productivity, such as prey type and capture strategy. As changes in size structure of the fish tooth assemblage correspond with evolutionary events in the plankton, rather than shifts in export productivity or total IAR, this suggests that the size structure of the fish tooth assemblage was more related to prey type and availability than it is to absolute production during the Paleocene. Fishes were able to maintain Cretaceous-like roles and production in the aftermath of the extinction, while other pelagic consumers, such as ammonites went extinct. This resilience paved the way for a rapid ecological expansion in the group as the open ocean ecosystem recovered from the event, facilitating their subsequent diversification in the modern open ocean.

4.6 References

- Alegret, L., and Thomas, E., 2009, Food supply to the seafloor in the Pacific Ocean after the Cretaceous/Paleogene boundary event: *Marine Micropaleontology*, v. 73, no. 1-2, p. 105-116.
- Bowles, J., 2006, Data Report: Revised Magnetostratigraphy and Magnetic Mineralogy of Sediments from Walvis Ridge, Leg 208, *in* Kroon, D., Zachos, J.C., and Richter, C. , ed., *Proceedings of the Ocean Drilling Program, Scientific Results, 208, Volume 208*: College Station, TX (Ocean Drilling Program), p. 1-24.

- Bralower, T. J., Premoli Silva, I., Malone, M. J., Arthur, M. A., Averyt, K., Bown, P. R., Brassell, S. C., Channell, J. E. T., Clarke, L. J., Dutton, A., Eleson, J. W., Frank, T. D., Gylesjo, S., Hancock, H., Kano, H., Leckie, R. M., Marsaglia, K. M., McGuire, J., Moe, K. T., Petrizzo, M. R., Robinson, S. A., Roehl, U., Sager, W. W., Takeda, K., Thomas, D., Williams, T., Zachos, J. C., and Premoli-Silva, I., 2002, Site 1209: Proceedings of the Ocean Drilling Program, Part A: Initial Reports, v. 198, p. 105.
- Coxall, H. K., D'Hondt, S., and Zachos, J. C., 2006, Pelagic evolution and environmental recovery after the Cretaceous-Paleogene mass extinction: *Geology*, v. 34, no. 4, p. 297-300.
- D'Hondt, S., 2005, Consequences of the Cretaceous/Paleogene mass extinction for marine ecosystems: *Annual Review of Ecology, Evolution, and Systematics*, v. 36, p. 295-317.
- D'Hondt, S., Donaghay, P., Zachos, J. C., Luttenberg, D., and Lindinger, M., 1998, Organic carbon fluxes and ecological recovery from the Cretaceous-Tertiary mass extinction: *Science*, v. 282, no. 5387, p. 276-279.
- Friedman, M., 2009, Ecomorphological selectivity among marine teleost fishes during the end-Cretaceous extinction: *Proceedings of the National Academy of Sciences of the United States of America*, v. 106, no. 13, p. 5218-5223.
- Friedman, M., and Sallan, L. C., 2012, Five hundred million years of extinction and recovery: a Phanerozoic survey of large-scale diversity patterns in fishes: *Palaeontology*, v. 55, no. 4, p. 707-742.
- Harries, P. J., and Knorr, P. O., 2009, What does the 'Lilliput Effect' mean?: *Palaeogeography, Palaeoclimatology, Palaeoecology*, v. 284, no. 1-2, p. 4-10.
- Hilgen, F. J., Kuiper, K. F., and Lourens, L. J., 2010, Evaluation of the astronomical time scale for the Paleocene and earliest Eocene: *Earth and Planetary Science Letters*, v. 300, no. 1-2, p. 139-151.
- Hsu, K. J., and McKenzie, J. A., 1985, A "Strangelove" ocean in the earliest Tertiary: *Geophysical Monograph*, vol.32, p. 487-492.
- Hull, P. M., and Norris, R. D., 2011, Diverse patterns of ocean export productivity change across the Cretaceous-Paleogene boundary: New insights from biogenic barium: *Paleoceanography*, v. 26, no. 26, p. 3205.
- Hull, P. M., Norris, R. D., Bralower, T. J., and Schueth, J. D., 2011, A role for chance in marine recovery from the end-Cretaceous extinction: *Nature Geoscience*, v. 4, p. 856-860.

- Iverson, R. L., 1990, Control of Marine Fish Production: *Limnology and Oceanography*, v. 35, no. 7, p. 1593-1604.
- Miya, M., Friedman, M., Satoh, T. P., Takeshima, H., Sado, T., Iwasaki, W., Yamanoue, Y., Nakatani, M., Mabuchi, K., and Inoue, J. G., 2013, Evolutionary origin of the scombridae (tunas and mackerels): members of a paleogene adaptive radiation with 14 other pelagic fish families: *Plos One*, v. 8, no. 9, p. e73535.
- Near, T. J., Eytan, R. I., Dornburg, A., Kuhn, K. L., Moore, J. A., Davis, M. P., Wainwright, P. C., Friedman, M., and Smith, W. L., 2012, Resolution of ray-finned fish phylogeny and timing of diversification: *Proceedings of the National Academy of Sciences of the United States of America*, v. 109, no. 34, p. 13698-13703.
- Sallan, L., and Galimberti, A. K., 2015, Body-size reduction in vertebrates following the end-Devonian mass extinction: *Science*, v. 350, no. 6262, p. 812-815.
- Schulte, P., Alegret, L., Arenillas, I., Arz, J. A., Barton, P. J., Bown, P. R., Bralower, T. J., Christeson, G. L., Claey's, P., Cockell, C. S., Collins, G. S., Deutsch, A., Goldin, T. J., Goto, K., Grajales-Nishimura, J. M., Grieve, R. A. F., Gulick, S. P. S., Johnson, K. R., Kiessling, W., Koeberl, C., Kring, D. A., MacLeod, K. G., Matsui, T., Melosh, J., Montanari, A., Morgan, J. V., Neal, C. R., Nichols, D. J., Norris, R. D., Pierazzo, E., Ravizza, G., Rebolledo-Vieyra, M., Reimold, W. U., Robin, E., Salge, T., Speijer, R. P., Sweet, A. R., Urrutia-Fucugauchi, J., Vajda, V., Whalen, M. T., and Willumsen, P. S., 2010, The Chicxulub Asteroid Impact and Mass Extinction at the Cretaceous-Paleogene Boundary: *Science*, v. 327, no. 5970, p. 1214-1218.
- Sibert, E. C., Hull, P. M., and Norris, R. D., 2014, Resilience of Pacific pelagic fish across the Cretaceous/Palaeogene mass extinction: *Nature Geosci*, v. 7, no. 9, p. 667-670.
- Sibert, E. C., and Norris, R. D., 2015, New Age of Fishes initiated by the Cretaceous–Paleogene mass extinction: *Proceedings of the National Academy of Sciences*, v. 112, no. 28, p. 8537-8542.
- Urbanek, A., 1993, Biotic crises in the history of Upper Silurian graptoloids: a palaeobiological model: *Historical Biology*, v. 7, no. 1, p. 29-50.
- Ward, P. D., Kennedy, W. J., Macleod, K. G., and Mount, J. F., 1991, Ammonite and inoceramid bivalve extinction patterns in Cretaceous Tertiary boundary sections of the Biscay region (southwestern France, northern Spain): *Geology*, v. 19, no. 12, p. 1181-1184.

Westerhold, T., Roehl, U., Raffi, I., Fornaciari, E., Monechi, S., Reale, V., Bowles, J., and Evans, H. F., 2008, Astronomical calibration of the Paleocene time: *Palaeogeography, Palaeoclimatology, Palaeoecology*, v. 257, no. 4, p. 377-403.

4.7 Acknowledgements

ECS is supported by an NSF Graduate Research Fellowship. All samples were provided by the International Ocean Discovery Program. Data are available at Pangea.de. The authors would like to thank L. Waterhouse for assistance with statistical analyses, and P. Hull, K. Cramer, and L. Levin for comments on a draft version of this manuscript.

Chapter 4, in full, is in preparation for publication as: Sibert, E. C., and Norris, R. D. “No evidence for productivity-driven dwarfing in pelagic fish communities following the Cretaceous-Paleogene Mass Extinction”. The dissertation author was the primary investigator and author of this manuscript.

CHAPTER 5

New Age of Fishes initiated by the Cretaceous– Paleogene mass extinction



New Age of Fishes initiated by the Cretaceous–Paleogene mass extinction

Elizabeth C. Sibert¹ and Richard D. Norris

Scripps Institution of Oceanography, University of California, San Diego, La Jolla, CA 92037

Edited by Neil H. Shubin, The University of Chicago, Chicago, IL, and approved May 15, 2015 (received for review March 11, 2015)

Ray-finned fishes (Actinopterygii) comprise nearly half of all modern vertebrate diversity, and are an ecologically and numerically dominant megafauna in most aquatic environments. Crown teleost fishes diversified relatively recently, during the Late Cretaceous and early Paleogene, although the exact timing and cause of their radiation and rise to ecological dominance is poorly constrained. Here we use microfossil teeth and shark dermal scales (ichthyoliths) preserved in deep-sea sediments to study the changes in the pelagic fish community in the latest Cretaceous and early Paleogene. We find that the Cretaceous–Paleogene (K/Pg) extinction event marked a profound change in the structure of ichthyolith communities around the globe: Whereas shark denticles outnumber ray-finned fish teeth in Cretaceous deep-sea sediments around the world, there is a dramatic increase in the proportion of ray-finned fish teeth to shark denticles in the Paleocene. There is also an increase in size and numerical abundance of ray-finned fish teeth at the boundary. These changes are sustained through at least the first 24 million years of the Cenozoic. This new fish community structure began at the K/Pg mass extinction, suggesting the extinction event played an important role in initiating the modern “age of fishes.”

Cretaceous–Paleogene boundary | ichthyoliths | fossil fish | age of fishes | mass extinction

Ray-finned fishes are a dominant and exceptionally diverse member of modern pelagic ecosystems; however, both the fossil record and molecular clocks suggest that the vast majority of living ray-finned fishes developed only recently, during the last 100 million years (1–3). It has been proposed that the explosion in actinopterygian diversity in the Late Mesozoic and Early Cenozoic represents a new “age of fishes” in contrast to the initial diversification of fish clades in the Devonian (2, 3). However, the mechanisms and timing of this Mesozoic–Cenozoic radiation and rise to dominance by ray-finned fishes are not well constrained in current molecular phylogenies or from the relatively sparse fossil record. While the Cretaceous–Paleogene (K/Pg) mass extinction occurred ~66 million years ago (Ma), in the middle of this radiation, there is little clear phylogenetic evidence linking any changes in fish diversity directly to this event (1), although a recent phylogenetic study on pelagic fish families suggested that open ocean fishes radiated during the early Paleogene following the extinction (4).

The K/Pg extinction had a dramatic effect on open ocean marine ecosystems (5–7), although the severity of the extinction varied around the globe (7–9). Major groups at both the base and top of the food web were decimated (5, 6, 10). While the traditional model of mass extinction due to primary productivity collapse (11) has been generally discredited due to the continued productivity of select consumer groups (12, 13), it is likely that upheaval among primary producers reverberated up the food web to cause extinctions at higher trophic levels. In the open ocean, calcifying plankton such as foraminifera and calcareous nanofossils suffered >90% species-level extinctions (9, 14). These changes in the structure of the base of the food web likely helped to cause the extinctions of pelagic consumers such as ammonites and marine reptiles (10). The trophic link between the plankton and large consumers in pelagic ecosystems is small pelagic fish, which would be expected to be similarly decimated by changes in food web

structure. However, recent work has shown that while there was a collapse of small pelagic fish production in the Tethys Sea, in the Pacific Ocean, these midlevel consumers maintained Cretaceous-like or higher levels of production in the earliest Danian (15).

Changes in abundance do not tell the whole story of how pelagic fishes responded to the extinction event. Indeed, despite dramatic levels of extinction, a few species of planktonic foraminifera thrived in the postextinction oceans, reaching abundances in the ~500,000 y following the event that far exceed those of typical high-diversity Cretaceous assemblages (7). This foraminifer response shows that taxonomic diversity and biological production can be decoupled in postdisaster ecosystems like those of the earliest Danian. Fishes are highly diverse and occupy a range of ecological niches, from the smallest plankton feeders through predatory sharks. This means that different groups could exhibit differential responses to the extinction (16). Work on well-preserved body fossils has found that there was a selective extinction of shallow marine predatory fishes at the K/Pg extinction, and a radiation during the early Cenozoic (17, 18). Additionally, a low level of extinction (<33%) of sharks and rays has been inferred across the event (19, 20). However, the magnitude of pelagic fish extinction is poorly known, although a relatively modest ~12% extinction has been documented for fish tooth morphotypes between the Late Cretaceous and the early Paleocene (21).

Here we use ichthyoliths, the isolated teeth and dermal scales (denticles) of sharks and ray-finned fishes found in deep-sea sediments, to investigate the response of sharks and fishes to the K/Pg extinction. Calcium phosphate ichthyoliths are found in nearly all marine sediments, even red clays (22), where other microfossils have been dissolved by corrosive bottom water conditions. Therefore, ichthyoliths are relatively unaffected by the preservation biases typically found in other microfossil groups. Teeth and denticles are

Significance

Ray-finned fishes are the most diverse and ecologically dominant group of vertebrates on the planet. Previous molecular phylogenies and paleontological studies have shown that modern ray-finned fishes (crown teleosts) radiated sometime in the Late Cretaceous or early Paleogene. Our data suggest that crown teleosts came into their current dominant ecological role in pelagic ecosystems immediately following the Cretaceous–Paleogene mass extinction 66 million years ago by filling newly vacated ecological niches and marking the beginning of an “age of ray-finned fishes.” Our study is, to our knowledge, the first geographically comprehensive, high-resolution study of marine vertebrate communities across the extinction.

Author contributions: E.C.S. and R.D.N. designed research; E.C.S. performed research; E.C.S. contributed new methods; E.C.S. analyzed data; and E.C.S. and R.D.N. wrote the paper.

The authors declare no conflict of interest.

This article is a PNAS Direct Submission.

Data deposition: Supplementary data are available at <http://dx.doi.org/10.1594/PANGAEA.846789>.

¹To whom correspondence should be addressed. Email: esibert@ucsd.edu.

This article contains supporting information online at www.pnas.org/lookup/suppl/doi:10.1073/pnas.1504985112/-DCS/Supplemental.

reasonably common, with 10s to 100s found in a few grams of sediment, allowing studies of the fish community rather than isolated individuals. The abundance of ichthyoliths also allows for high-temporal resolution sampling similar to other microfossils. The well-resolved ichthyolith records stand in sharp contrast to those for the comparatively rare body fossil record, and can provide a complimentary analysis of abrupt biotic events such as mass extinctions or transient climate changes. In addition, the abundance, assemblage, and morphological composition of ichthyoliths record the productivity and biodiversity of the pelagic fish community.

We investigate how the pelagic fish community responded to the K/Pg extinction at six deep-sea sites in the Pacific, Atlantic, and Tethys Oceans. We use ichthyolith community metrics, including the relative abundance of microfossils from sharks and ray-finned fishes, and the size structure of the tooth assemblage to assess the changes in the pelagic fish community across the K/Pg mass extinction around the world. This represents, to our knowledge, the first geographically comprehensive, high-resolution study of pelagic marine vertebrate communities across the extinction.

Results

The K/Pg Boundary was identified in each site based on the global iridium anomaly layer, as well as the presence of tektites, impact ejecta, and slump deposits associated with the impact horizon (23–29). Site-specific chronologies were developed based on cyclostratigraphy, cobalt accumulation rates, strontium isotopes, biostratigraphy, and magnetostratigraphy, depending on the lithology at each site (see *Materials and Methods* and *SI Materials and Methods* for additional details).

Ichthyoliths are fundamentally divided into two broad taxonomic groups: teeth, which can belong to ray-finned fish as well as sharks, and dermal denticles, the tooth-like placoid scales that cover nearly all sharks and rays. We looked at the relative abundance of actinopterygian fishes to sharks before and after the extinction event, as interpreted by the relative abundance of teeth to shark denticles in an assemblage of microfossils retained on a 106- μ m sieve. A tooth/denticle ratio of >1 means actinopterygian fish teeth dominated the $>106\text{-}\mu\text{m}$ ichthyolith assemblage, while a ratio of <1 means shark denticles dominated the $>106\text{-}\mu\text{m}$ ichthyolith assemblage. It is worthwhile to note that this metric considers only the numerical abundance of microfossils at a constant size fraction ($>106\text{ }\mu\text{m}$) and not individuals or biomass of these groups.

Actinopterygian fish typically have two distinct sets of teeth, oral teeth, which are found in the jaw, and the far more abundant but significantly smaller pharyngeal teeth. The $>106\text{ }\mu\text{m}$ fraction generally contains mostly oral teeth, while smaller fractions are dominated by pharyngeal teeth and tooth fragments. Rates of tooth loss and regeneration of actinopterygian fishes are poorly constrained and vary with taxon, although teeth are replaced continuously throughout the life of the individual (30). However, in at least some taxa, many teeth are resorbed, rather than shed, during tooth replacement, so the number of teeth in the sedimentary record is likely an underrepresentation of teeth produced (30, 31).

Sharks can have 2–3 orders of magnitude more denticles—which scale numerically with body surface area—than sharks or ray-finned fish have oral or pharyngeal teeth. This means that the absolute value of the ratio of teeth to denticles in the $>106\text{-}\mu\text{m}$ size fraction, considered in this study, is not the true ratio of ray-finned fish versus shark biomass or numerical abundance. However, when considering the ratio of teeth to denticles at a constant size fraction, the metric allows for consistent comparison between assemblages, and can be interpreted as changes in relative abundances of sharks and ray-finned fish. We consider the $>106\text{-}\mu\text{m}$ fraction in this study as a uniform metric across all sample sites but note that the abundance of smaller teeth is correlated with the

abundance of larger teeth, and the absolute value of the tooth/denticle ratio increases at smaller size fractions.

An additional consideration is that teeth in the $>106\text{ }\mu\text{m}$ fraction likely include some shark teeth as well as those of ray-finned fishes. We note that shark teeth are often flattened, triangular forms with multiple cusps at the base and a cutting edge that may be ornamented with serrations. Such teeth represent $<1\%$ of the total tooth ichthyoliths in our $>106\text{ }\mu\text{m}$ samples, and were not present in a majority of assemblages. Indeed, despite constant tooth replacement, sharks will still produce several orders of magnitude more denticles in a lifetime than teeth, depending on their body size. Hence, it is unsurprising that shark teeth are rare in our assemblages, compared with the abundance of denticles. Numerical simulations show that the presence of a few shark teeth in our tooth samples does not significantly bias our results (please see *SI Materials and Methods* for more information).

We find that in the Cretaceous Pacific Ocean, the accumulation of actinopterygian teeth is consistently lower than the accumulation of shark denticles, suggesting that sharks were more dominant in the Cretaceous pelagic vertebrate community than they were in the Paleocene (Fig. 1A). The tooth to denticle ratio in the Cretaceous was $\sim 0.71:1$ in the North Pacific [Ocean Drilling Program (ODP) Site 886] Maastrichtian, and $0.76:1$ in the South Pacific [Deep Sea Drilling Project (DSDP) Site 596]. The accumulation rate of teeth increases notably after the K/Pg extinction, leading to a tooth/denticle ratio of 1:1 at both Pacific locations in the first 500,000 y of the Paleocene before increasing toward 2:1 by the mid-Paleocene (Fig. 1B). This change is significant at both sites (two-sided *t* test, $P < 0.0001$). The community change occurs at the K/Pg boundary, and cannot be explained by background variability, since the tooth/denticle ratio is nearly constant in the Cretaceous (Fig. 1B). The main reason for the increase in the tooth/denticle ratio is the increased accumulation of ray-finned fish teeth in the Paleocene, and it does not represent a large decline in sharks (Fig. 1A).

While low ichthyolith abundances $> 106\text{ }\mu\text{m}$ in the Atlantic [International Ocean Discovery Program (IODP) U1403, DSDP 386, and ODP 1262] and Tethys Sea (Gubbio) preclude similar time series analysis, grouped assemblages of ichthyoliths from the latest Cretaceous and earliest Paleocene show the same pattern as in the Pacific, with a preextinction tooth/denticle ratio between 0.7 and 1, and a postextinction ratio between 2 and 3.5 (Fig. 2). These global results suggest that the relative abundance of ray-finned fish in marine vertebrate assemblages increased dramatically at the extinction all over the world. Notably, these changes in the tooth/denticle ratio occur despite local decreases in ichthyolith accumulation in the Tethys Sea and Atlantic sites (15). In the South Pacific, we find that the ratio of ray-finned fish teeth to shark dermal denticles in the assemblage continues to rise into the Eocene, from values of $\sim 2:1$ in the earliest Paleocene to values of seven teeth per denticle in the Eocene (Fig. 3A). Hence, the increase in tooth/denticle ratio is initiated at the K/Pg boundary and continues to increase, at least in the South Pacific, for at least 24 million years after the extinction.

The size structure and accumulation rate of the tooth assemblages also changed at the K/Pg boundary in the Pacific Ocean. Tooth size was measured as the longest dimension through the centroid of each tooth (Feret's Diameter) $> 106\text{ }\mu\text{m}$ using the open source image processing program ImageJ (32). Shark denticles were excluded from this analysis, as many denticles are preserved as fragments. Both Cretaceous and Paleocene tooth assemblages are dominated by small teeth, with lengths of $<0.8\text{ mm}$, and a median size of $\sim 0.43\text{ mm}$ (Fig. 1C). In the early Paleocene, the largest increases in tooth accumulation and relative abundance occur in the largest tooth size fraction ($>0.8\text{ mm}$; Fig. 1C). This increase in the abundance of large teeth begins at the K/Pg extinction in both Pacific sites, but it is most apparent in the South Pacific starting at 64 Ma and lasting until 58–59 Ma (Figs. 1C and 3B). A Cretaceous-like

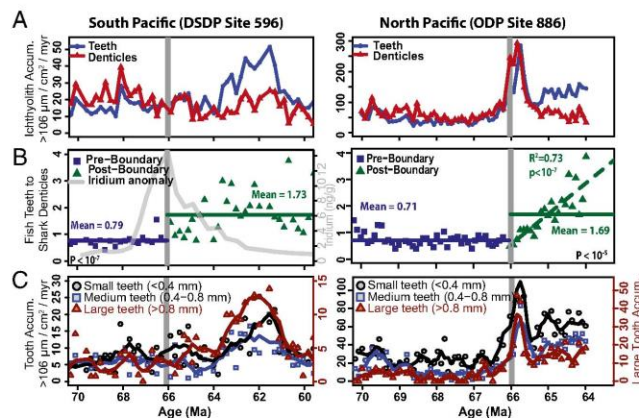


Fig. 1. South Pacific [Left; DSDP Site 596 (38)] and North Pacific [Right; ODP Site 886 (25)] across the Cretaceous–Paleogene boundary (horizontal gray line). (A) Ichthyolith accumulation. Blue circles are teeth, interpreted as ray-finned fish, and red triangles are denticles, interpreted as sharks and rays. Units are in ichthyoliths per square centimeter per million years. (B) Ratio of fish teeth to shark denticles. Solid lines are mean values for Cretaceous (blue) and Paleocene (green). The dotted green line (Right) is a regression fit to the Paleocene dataset. Iridium anomaly data are from ref. 23. (C) Accumulation rates of three size classes of fish teeth. Small teeth (black circles) have maximum length of <0.4 mm, medium teeth (blue squares) are 0.4–0.8 mm, and large teeth (red triangles) are >0.8 mm. Large tooth accumulation is on the secondary axis and is scaled to twice that of the small and medium teeth to show pattern. Solid lines are three-point running means.

size structure is partly restored after 58 Ma in the South Pacific (Fig. 3B), despite an increase in the overall abundance of teeth in each sample. This suggests that the high abundance of large teeth in the early Paleocene is due to a change in community structure and is not just an effect of having more teeth in a given sample and therefore preserving more of the rare, larger teeth. In the North Pacific, all tooth size classes see increases in their accumulation rate, but there is no unusual increase in the largest teeth relative to smaller teeth (Fig. 1C). However, the North Pacific record is only preserved to 64 Ma, about the time that the large teeth become particularly prominent in the South Pacific.

While the median tooth length in the early Paleocene does not differ significantly from that of the latest Cretaceous (~0.43 mm or 430 μm), the 75th quartile tooth length in each assemblage increases from ~0.6 mm to 0.9 mm during the early Paleocene, suggesting that the largest teeth got larger and more abundant, without much change among the remainder of the tooth assemblage (Fig. 3C). Additionally, the maximum tooth size of a given assemblage tripled at the K/Pg boundary, from an average of 1 mm

(maximum of 2.5 mm) in the Cretaceous to an average of 3 mm (maximum of >6 mm) in the Paleocene and Early Eocene. Large teeth are present in nearly every sample following the extinction for at least 24 Ma, suggesting a permanent change in the range of fish tooth size following the extinction (Fig. 3D).

Discussion

Our data show that the pelagic marine vertebrate community was profoundly affected by the K/Pg mass extinction. During the Late Cretaceous, dermal denticles make up over half of every >106- μm ichthyolith assemblage, and there is very low variability in assemblage composition (Fig. 1B), suggesting that the shift was not simply a result of a background trend that began during the latest Cretaceous. After the K/Pg boundary, teeth dominate the ichthyolith assemblages and become 2 to 3 times as abundant as denticles—a trend that is not reversed within the first 24 million years of the Cenozoic (Figs. 2 and 3). This change in the tooth/denticle ratio occurs at the peak iridium anomaly marking the boundary, even in the face of likely sediment mixing in slowly accumulating red clay sediments (Fig. 1B), implying that the Chicxulub impact was the driver for the ecological change (24). The increase in teeth relative to denticles is unlikely to reflect an artifact of misattribution of shark teeth to ray-finned fish teeth, since the absolute abundance of shark dermal denticles is nearly unchanged through the study time period and denticles are produced in vastly larger numbers than teeth in modern elasmobranchs, overwhelming any signal of elasmobranch teeth.

We interpret the change in the ratio of teeth to denticles in ichthyolith assemblages as an increase in the ecological importance of the ray-finned fishes that dominate the modern pelagic open ocean. We might expect that an increase in the population size of ray-finned fish would lead to an increase in sharks, since sharks rely on the biomass of lower trophic levels, commonly assumed to be ray-finned fish. However, the absolute abundance of shark fossils is nearly unchanged, or even decreases following the extinction (Fig. 1A), even as the ray-finned teeth increase, suggesting that increased ray-finned fish populations did not power an increase in the sharks. Instead, sharks appear to have

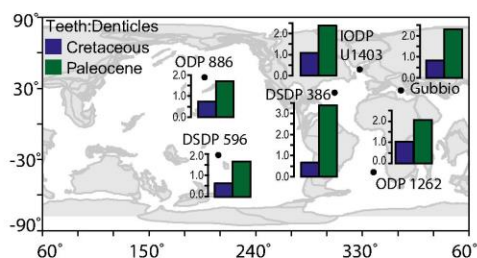


Fig. 2. Paleomap showing the ratio of fish teeth to shark denticles from the Cretaceous (blue) and Paleocene (green) from six sites around the world's ocean. Paleomap image created from the Ocean Drilling Stratigraphic Network Plate Tectonic Reconstruction Service. All histograms are plotted on the same vertical axis.

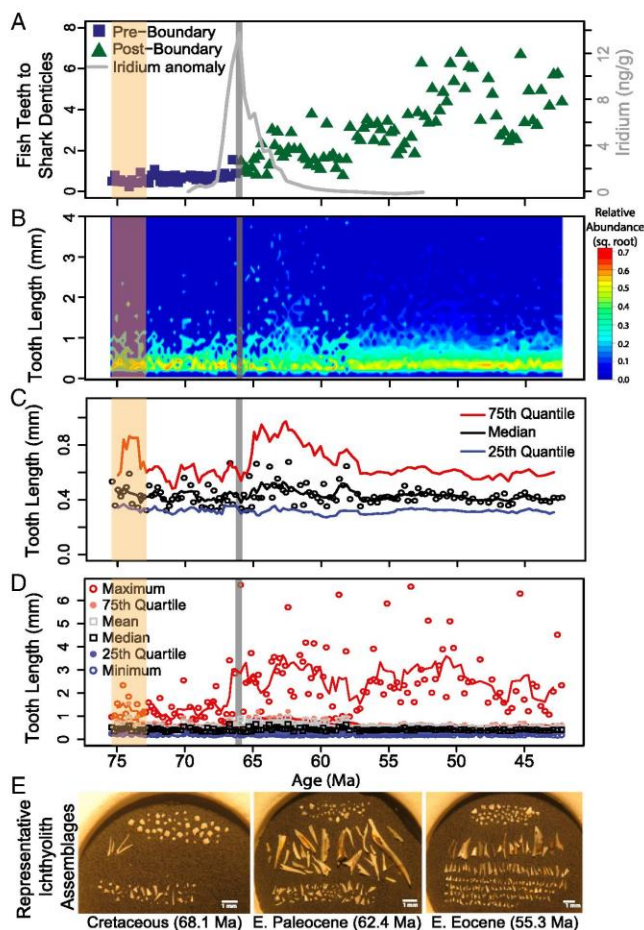


Fig. 3. An extended record from the South Pacific Ocean (DSDP Site 596) of various ichthyolith community metrics; K/Pg boundary is vertical gray line. (A) Ratio of fish teeth to shark denticles. (B) Square root of relative abundance of ichthyolith size classes. Reds and yellows denote higher relative abundance at that tooth length, while blues denote relatively rare. (C) Black circles are individual assemblage tooth length medians, and solid lines are five-point running averages, with median (black), 25th quartile (blue), and 75th quartile (red). (D) Full size structure of tooth assemblages; solid lines are five-point running means. Maximum tooth size shown as open red circles. (E) Representative photos of ichthyolith assemblages > 106 μ m from the Cretaceous, Paleocene, and Eocene from DSDP Site 596. Denticles (shark scales) are at the top of each assemblage, large teeth are in the middle, and smaller teeth are at the bottom of each photograph. Note the high abundance of “large” teeth in the Paleocene. Tan shading represents region of low tooth abundance. (Scale bar, 1 mm.)

remained stuck at similar abundances in the Paleocene as they had in the Cretaceous, suggesting that they were unable to exploit newly opened niches after the extinction, or that they traded niches to maintain an overall constant level of abundance.

Since ray-finned fish teeth are rare in the Cretaceous relative to shark denticles, fish may have been kept at low levels of abundance due to predation or were ecologically outcompeted in Cretaceous pelagic systems. The rapid increase in tooth abundance, but not in shark denticles, at the extinction suggests that the ray-finned fish seized the opportunity to diversify and colonize newly vacated niches in the open ocean that had been previously unavailable to them. Perhaps competition or predation by

ammonites and squids or other rarely fossilized groups suppressed ray-finned fish populations in the Cretaceous, allowing fish to be ecologically released by the extinction of the ammonites during the K/Pg event. At least some species of ammonite were likely planktivores, perhaps competing directly with many pelagic fish groups for trophic resources (33). In other cases, fish may have been prey for cephalopods, analogous to the ravages of the modern Humboldt squid, *Dosidicus*, in midwater fishes with the expansion of the oxygen minimum zone in the eastern Pacific (34). Finally, the increase of ray-finned fish teeth in our assemblages may be due to a change in the rate of tooth loss in fishes rather than an increase in the number of ray-finned fish individuals

from the Cretaceous to the Paleogene. There are examples of fish increasing their tooth production through changes in gene regulation, such as certain species of stickleback fish having more teeth in freshwater systems than in brackish or marine waters (35). However, the increase in tooth size and change in community structure suggest that this mechanism alone is unlikely to account for all of the changes seen in the ichthyolith community at the K/Pg boundary and maintained through the Paleocene and Eocene.

While the ratio of ray-finned fish to shark ichthyoliths appears to be relatively stable around the globe during the Cretaceous, the Paleocene ratios are more varied (Fig. 2). The productivity of pelagic ecosystems is known to have fallen abruptly in the Atlantic and Tethys Oceans while remaining relatively unchanged in the Pacific (7, 8, 12, 15). Hence, geographic variation in the fish-to-shark ratio may reflect spatial differences in dynamics of primary producers and export production in the post-K/Pg pelagic marine ecosystems (7, 8, 12) that could have supported different groups and abundances of fish in different regions (15). This is consistent with geographically heterogeneous patterns of recovery seen in other pelagic marine lineages (7).

The Paleocene increase in the size and accumulation rate of the largest teeth strongly suggests that the K/Pg event initiated a wholesale change in the fish community. Fish tooth size does not necessarily scale allometrically with body size, especially in the open ocean and deep sea: Some very large fish have only small teeth, while other very small fish have much larger teeth; hence we cannot directly interpret tooth size as a direct indication of body size. However, we suggest that the size structure of the ichthyolith assemblage does reflect the range of ecological niche space taken up by the fishes present in the system. Therefore, we infer that the large range of tooth sizes in the Paleocene indicates an expansion of the collective range of habitats and ecologies that fishes were able to exploit, somewhat analogous with the postextinction increase in the size diversity of Cenozoic mammals (36).

In addition to the increase in maximum tooth size, there is also a temporary increase in the accumulation rate, length, and relative abundance of the largest teeth (75th quartile or larger). The peak in accumulation rate and size of this largest group of teeth lasts only from the K/Pg boundary until about 60 Ma. The prominence of large teeth in the South Pacific suggests that ray-finned fishes explored a novel community structure for the first 6–7 million years of the Paleocene, in which large teeth were unusually abundant compared with those in Cretaceous and later Paleocene assemblages. The overall size structure of tooth assemblages in the later Paleocene and Eocene shows a lower relative abundance of large teeth. However, the constant presence of at least a few teeth in each sample that are significantly larger than the largest Cretaceous teeth (Fig. 3D) suggests that the decrease in relative abundance of large teeth represents a “filling in” of ecological niche space between the smallest and largest tooth sizes rather than a disappearance of large-toothed fishes in later Paleocene and Eocene fish assemblages.

A major advantage of our deep-sea ichthyolith records is that they can allow assessment of variability in marine vertebrate assemblages up to and across major events. Our Pacific records show that the latest Cretaceous vertebrate community was very stable, both in terms of the ratio of fish to sharks and the size structure of the tooth community (Fig. 3). Indeed, our South Pacific record of tooth/denticle ratios and tooth size “flatlines” for the last 10 million years of the Cretaceous. The stability of Cretaceous assemblages suggests that the changes observed at the K/Pg boundary and early Paleocene were abrupt, likely caused by the extinction event, and are not part of a background trend or the result of random chance. This change in fish community structure appears to have been caused by the Chicxulub impact (24) rather than being a long-term response to a prolonged period of volcanism during the Latest Cretaceous. Indeed, in parallel with the mammals on land (36), the K/Pg extinction event appears to have

initiated major changes in the marine vertebrate community that lead to the great diversification and ecological rise to dominance of the ray-finned fishes in our oceans today.

Conclusions

While there were relatively low levels of extinction of pelagic fish at the K/Pg boundary, we find that the extinction event marked an ecological turning point for the pelagic marine vertebrates. Most open ocean, gyre-inhabiting, Cretaceous fishes were likely small and relatively rare—like the terrestrial mammals of their time—compared with their counterparts of the Paleocene and Eocene. In the Paleogene, ecological changes such as the increase in relative abundance of ray-finned fish compared with sharks and the persistence of large-toothed fishes are both permanent changes in the fish community that were initiated by the extinction. The presence of a novel “disaster fauna” of large-toothed fishes, at least in the South Pacific, suggests that rapid evolution occurred in the pelagic fish community following the extinction (4), before a more delayed filling in of niche space occurred in the later Paleocene and Eocene. The extinction event changed the fundamental ecosystem structure of the pelagic marine vertebrate community, allowing the ray-finned fishes to rapidly diversify in the early Cenozoic pelagic oceans. The extreme stability of Cretaceous ichthyolith accumulation rates, assemblage structure, and tooth sizes suggests that, without the extinction, it is unlikely that the system would have reset so dramatically in favor of ray-finned fishes. The K/Pg extinction appears to have been a major driver in the rise of ray-finned fishes and the reason that they are dominant in the open oceans today.

Materials and Methods

Sample Preparation. Samples were obtained from Integrated Ocean Drilling Program (now International Ocean Discovery Program, IODP), ODP, and Deep Sea Drilling Project sites, from the North Pacific (ODP Site 886), South Pacific (DSDP Site 596), North Atlantic (IODP Site U1403), Central Atlantic (DSDP Site 386), and South Atlantic (ODP Site 1262). Gubbio samples were obtained from the limestone outcrop on Contessa Highway north of Gubbio, Italy (37). DSDP Sites 386 and 596 and ODP Site 886 are red clay, while ODP Site 1262 and IODP Site U1403 are primarily carbonate ooze. Sample processing varied based on lithology (see *SI Materials and Methods*). All samples were dried to constant weight in a 50 °C oven. Ichthyoliths were isolated from the samples by disaggregation with deionized water in the case of clays, and by dissolution in weak (5–10%) acetic acid in the case of carbonates. All particles > 38 μm were retained, and ichthyoliths > 106 μm were hand-picked from the residue using a dissection microscope and archived in cardboard micropaleontology slides using gum tragacanth glue to hold in place.

Ichthyolith Assemblage Analysis. Ichthyoliths were classified into denticles (shark scales) and teeth (assumed to be mostly ray-finned fish teeth, <1% shark teeth; see *SI Materials and Methods* for more discussion). All Pacific assemblages were photographed using a Canon Powershot 55 IS microscope-mounted camera. The resulting image was processed and analyzed using ImageJ (32) to count and measure the size and shape of the ichthyoliths. The other sites considered in this study were simply grouped into “preboundary” and “postboundary” assemblages for analysis. Size structure analysis was restricted to teeth, since about 20–40% of the denticles were partially fragmented.

Age Models and Accumulation Rates. While ichthyolith assemblage metrics are independent of age model beyond preboundary and postboundary, ichthyolith accumulation rate (reported as ichthyoliths per square centimeter per million years) is, by definition, age-model dependent, since the calculation depends on sedimentation rates and accurate age datums. The age model for DSDP Site 596 is based on a cobalt accumulation rate stratigraphy (38), and tied to the K/Pg boundary by a prominent iridium anomaly at that site (23). The age model has been shifted to hang on the Geologic Time Scale 2012 (GTS2012) K/Pg boundary age of 66.04 Ma (39). The ODP Site 886 age model is based on a compilation of radiolarian biostratigraphy and strontium isotope stratigraphy, and is also tied to the K/Pg boundary by an iridium anomaly (25) and given the GTS2012 age of 66.04 Ma. For the other sites, where accumulation rate is not considered, samples were grouped into preboundary and postboundary, based on prominent impact horizons in each location.

ACKNOWLEDGMENTS. All DSDP/ODP/ODP samples were generously provided through the International Ocean Discovery Program. We thank L. Levin, P. Hastings, and two anonymous reviewers for insightful comments on this manuscript. E.C.S. is supported by a National Science Foundation Graduate

Research Fellowship. R.D.N. is supported by the National Science Foundation-Ocean Sciences. Field collection of Gubbio samples was made possible by a field grant from the American Philosophical Society's Lewis and Clark Fund for Astrobiology Field Work to E.C.S. in 2012.

- Near TJ, et al. (2013) Phylogeny and tempo of diversification in the superradiation of spiny-rayed fishes. *Proc Natl Acad Sci USA* 110(31):12738–12743.
- Near TJ, et al. (2012) Resolution of ray-finned fish phylogeny and timing of diversification. *Proc Natl Acad Sci USA* 109(34):13698–13703.
- Friedman M, Sallan LC (2012) Five hundred million years of extinction and recovery: A Phanerozoic survey of large-scale diversity patterns in fishes. *Palaeontology* 55(4): 707–742.
- Miya M, et al. (2013) Evolutionary origin of the Scombridae (tunas and mackerels): Members of a paleogene adaptive radiation with 14 other pelagic fish families. *PLoS ONE* 8(9):e73535.
- Coxall HK, D'Hondt S, Zachos JC (2006) Pelagic evolution and environmental recovery after the Cretaceous-Paleogene mass extinction. *Geology* 34(4):297–300.
- D'Hondt S (2005) Consequences of the Cretaceous/Paleogene mass extinction for marine ecosystems. *Annu Rev Ecol Syst* 36:295–317.
- Hull PM, Norris RD, Bralower TJ, Schueth JD (2011) A role for chance in marine recovery from the end-Cretaceous extinction. *Nat Geosci* 4(12):856–860.
- Hull PM, Norris RD (2011) Diverse patterns of ocean export productivity change across the Cretaceous-Paleogene boundary: New insights from biogenic barium. *Paleoceanography* 26(3):PA3205.
- Jiang SJ, Bralower TJ, Patzkowsky ME, Kump LR, Schueth JD (2010) Geographic controls on nanoplankton extinction across the Cretaceous/Paleogene boundary. *Nat Geosci* 3(4):280–285.
- Ward PD, Kennedy WJ, Maceoed KG, Mount JF (1991) Ammonite and inoceramid bivalve extinction patterns in Cretaceous Tertiary boundary sections of the Biscay region (southwestern France, northern Spain). *Geology* 19(12):1181–1184.
- Hsu KJ, McKenzie JA (1985) A "Strangelove" ocean in the earliest Tertiary. *The Carbon Cycle and Atmospheric CO₂: Natural Variations Archaean to Present*, Geophysical Monograph Series, eds Sundquist ET, Broecker WS (Am Geophys Union, Washington, DC) Vol 32, pp 487–492.
- Alegret L, Thomas E, Lohmann KC (2012) End-Cretaceous marine mass extinction not caused by productivity collapse. *Proc Natl Acad Sci USA* 109(3):728–732.
- Sepúlveda J, Wendler JE, Summons RE, Hinrichs KU (2009) Rapid resurgence of marine productivity after the Cretaceous-Paleogene mass extinction. *Science* 326(5949): 129–132.
- Smit J (1982) Extinction and evolution of planktonic foraminifera after a major impact at the Cretaceous/Tertiary boundary. *Geol Soc Am Spec Pap* 190:329–352.
- Sibert EC, Hull PM, Norris RD (2014) Resilience of Pacific pelagic fish across the Cretaceous/Paleogene mass extinction. *Nat Geosci* 7(9):667–670.
- Cavin L (2002) *Effects of the Cretaceous-Tertiary Boundary Event on Bony Fishes*. Geological and Biological Effects of Impact Events, Impact Studies, eds Buffetaut E, Koerber C (Springer, Berlin), pp 141–158.
- Friedman M (2009) Ecomorphological selectivity among marine teleost fishes during the end-Cretaceous extinction. *Proc Natl Acad Sci USA* 106(13):5218–5223.
- Friedman M (2010) Explosive morphological diversification of spiny-finned teleost fishes in the aftermath of the end-Cretaceous extinction. *Proc R Soc B* 277(1688): 1675–1683.
- Kriwet J, Benton MJ (2004) Neoselachian (Chondrichthyes, Elasmobranchii) diversity across the Cretaceous-Tertiary boundary. *Paleogeogr Palaeoclimatol Palaeoecol* 214 (3):181–194.
- Guinot G, Adnet S, Cappetta H (2012) An analytical approach for estimating fossil record and diversification events in sharks, skates and rays. *PLoS ONE* 7(9):e46632.
- Doyle PS, Riedel WR (1979) *Ichthyoliths: Present Status of Taxonomy and Stratigraphy of Microscopic Fish Skeletal Debris* (Scripps Inst Oceanogr, La Jolla, CA).
- Doyle PS, Riedel WR (1985) *Cenozoic and Late Cretaceous Ichthyoliths* (Cambridge Univ Press, Cambridge, UK).
- Zhou L, Kyte FT, Bohor BF (1991) Cretaceous/Tertiary boundary of DSDP Site 596, South Pacific. *Geology* 19(7):694–697.
- Schulte P, et al. (2010) The Chicxulub asteroid impact and mass extinction at the Cretaceous-Paleogene boundary. *Science* 327(5970):1214–1218.
- Snoeckx H, Rea D, Jones C, Ingram B (1995) Eolian and silica deposition in the central North Pacific: Results from Sites 885/886. *Proc Ocean Drill Program Sci Results* 145:219–230.
- Norris RD, et al. (2014) Site U1403. *Proceedings of the Integrated Ocean Drilling Program* (Integ Ocean Drill Program Intl, Tokyo), Vol 342, p 98.
- Norris RD, Firth J, Blusztajn JS, Ravizza G (2000) Mass failure of the North Atlantic margin triggered by the Cretaceous-Paleogene bolide impact. *Geology* 28(12): 1119–1122.
- Alvarez LW, Alvarez W, Asaro F, Michel HV (1980) Extraterrestrial cause for the cretaceous-tertiary extinction. *Science* 208(4448):1095–1108.
- Westerhold T, et al. (2008) Astronomical calibration of the Paleocene time. *Paleoogeogr Palaeoclimatol Palaeoecol* 257(4):377–403.
- Trapani J, Schaefer S (2001) Position of developing replacement teeth in teleosts. *Copeia* 2001(1):35–51.
- Bemis WE, Giuliano A, McGuire B (2005) Structure, attachment, replacement and growth of teeth in bluefish, *Pomatomus saltatrix* (Linnaeus, 1776), a teleost with deeply socketed teeth. *Zoology (Jena)* 108(4):317–327.
- Rasband WS (1997–2014) ImageJ (US Nat Inst Health, Bethesda, MD).
- Kruta I, Landman N, Rouget J, Cecca F, Tafforeau P (2011) The role of ammonites in the Mesozoic marine food web revealed by jaw preservation. *Science* 331(6013): 70–72.
- Zeldberg LD, Robison BH (2007) Invasive range expansion by the Humboldt squid, *Dosidicus gigas*, in the eastern North Pacific. *Proc Natl Acad Sci USA* 104(31): 12948–12950.
- Cleves PA, et al. (2014) Evolved tooth gain in sticklebacks is associated with a cis-regulatory allele of *Bmp6*. *Proc Natl Acad Sci USA* 111(38):13912–13917.
- Alroy J (1999) The fossil record of North American mammals: Evidence for a Paleocene evolutionary radiation. *Syst Biol* 48(1):107–118.
- Alvarez W, et al. (1977) Upper Cretaceous-Paleocene magnetic stratigraphy at Gubbio, Italy. 5. Type section for Late Cretaceous-Paleocene geomagnetic reversal time scale. *Geol Soc Am Bull* 88(3):383–388.
- Zhou L, Kyte FT (1992) Sedimentation history of the South Pacific pelagic clay province over the last 85 million years inferred from the geochemistry of Deep Sea Drilling Project Hole 596. *Paleoceanography* 7(4):441–465.
- Gradstein FM, Ogg JG, Schmitz M, Ogg GM (2012) *The Geologic Time Scale* (Elsevier, Amsterdam).
- Arthur MA, Fischer AG (1977) Upper Cretaceous-Paleocene magnetic stratigraphy at Gubbio, Italy. 1. Lithostratigraphy and sedimentology. *Geol Soc Am Bull* 88(3): 367–371.
- Tucholke BE, et al. (1979) Site 386: Fracture valley sedimentation on the central Bermuda Rise. *Initial Rep Deep Sea Drill Proj* 43:195–321.
- Menard HW, et al. (1987) Site 596: Hydraulic piston coring in an area of low surface productivity in the Southwest Pacific. *Initial Rep Deep Sea Drill Proj* 91:245–267.
- Rea DK, et al. (1993) Sites 885/886. *Proc Ocean Drill Program Initial Rep* 145:303–334.
- Zachos JC, et al. (2004) Site 1262. *Proc Ocean Drill Program Initial Rep* 208:192.
- Silva IP (1977) Upper Cretaceous-Paleocene magnetic stratigraphy at Gubbio, Italy II. Biostratigraphy. *Geol Soc Am Bull* 88(3):371–374.

Supporting Information

Sibert and Norris 10.1073/pnas.1504985112

SI Materials and Methods

Sample Preparation. Excepting the samples from Gubbio, Italy, which were collected from the Contessa Highway outcrop north of the town (40), all samples were obtained through the International Ocean Discovery Program. To isolate the ichthyoliths, which are relatively rare in marine sediments, a series of methods were used based on the lithology. Before processing, all samples were dried at 50 °C, sometimes taking months, as in the case of red clays, to achieve a constant weight. Samples were processed with the goal of concentrating the ichthyoliths as much as possible without being destructive to the fossils.

Carbonate ooze samples (ODP Site 1262, IODP Site U1403) were disaggregated in deionized (DI) water and then dissolved using 5–10% acetic acid. The amount of acid varied per site, but ranged from 600 mL to 1,000 mL of 5–10% acid per 20-g sample. Samples were left in acid until they stopped reacting, about 2–4 h, and then washed over a 38- μ m sieve using DI water. Red clays (DSDP Sites 386 and 596 and ODP Site 886) were simply disaggregated in DI water. Samples were then washed over a 38- μ m sieve. The limestone samples from Gubbio were processed by first manually breaking the samples into ~1-cm pieces with a hammer. Samples were then soaked in 10% acid bath for 24-h periods and then washed through 150- μ m and 38- μ m sieves. Material > 150 μ m was returned to the acid bath, while <150- μ m material was decanted onto Whatman P5 filter paper. Limestone samples (Gubbio) took between 4 and 12 wash cycles to completely disaggregate. Ichthyoliths were then manually picked out of the coarse fraction of the residue (>106 μ m) and mounted on micropaleontology slides and classified into denticles and teeth, corresponding to sharks and ray-finned fish, respectively. Although diagnostic shark teeth are present, they typically account for <1% of teeth in the >106 μ m assemblages (and significantly less at the smaller size fractions).

Ichthyolith Assemblage Analysis. Images of ichthyolith assemblages from ODP Site 886 and DSDP Site 596 were processed and analyzed using ImageJ (32) to count and measure the size and shape of the ichthyoliths. This was done by converting photographs into black and white threshold-based images of the ichthyolith assemblages and then measuring the resulting particles using the “analyze particles” tool in ImageJ. The other sites considered in this study had small numbers of large (>106 μ m) ichthyoliths, and were not sufficiently abundant enough to look at the size structure of the tooth assemblage. For these, we grouped individual samples into Cretaceous preboundary and Paleocene postboundary groups to compare the relative abundance of teeth and denticles. A summary data table is presented in Table S1.

For ODP Site 886, where the K/Pg boundary ichthyolith counts were very high, the tooth/denticle metric was substantially biased by these samples, and the average ratio for the time interval of the Paleocene (66–63.8 Ma for ODP Site 886) was significantly different from the ratio calculated by binning the samples as was done for the other sites. The tooth/denticle ratio did not appear to be biased by unusual ichthyolith abundance for the other sites, regardless of sample size. We suspect that there may have been sedimentary changes at site ODP 886 during the K/Pg interval. For ODP Site 886, we report four methods to account for this bias: method 1, by binning all samples from the post K/Pg interval, as in other sites; method 2, by averaging the ratios reported for each assemblage; method 3, by removing the five samples with abnormally high numbers of ichthyoliths found immediately adjacent to the K/Pg boundary, which dominated the signal; and

method 4, by reducing the relative importance of these five samples by halving their numerical abundances, bringing them to a more comparable level to the other samples considered in the study, before calculating as for option 1. We note that compared with the other sites in our study, all of these estimates for the Paleocene are likely artificially low at ODP Site 886, since it accounts for the least amount of time in the Paleocene. Given the increasing trend of the tooth/denticle ratio during the first 2 million years of the Paleocene in the North Pacific (Fig. 1B) and the long-term increasing trend from the South Pacific (Fig. 3B), it is likely that the ratio in the North Pacific also increased through the Paleocene. On Fig. 2, we present the tooth/denticle value calculated by option 2, the mean ratio for all 23 Paleocene samples from Site 886 as a compromise between these biases.

The size structure of each tooth assemblage was analyzed using R statistical package. Many ichthyolith samples have clay mineral or oxide clumps in them that retain small teeth on the 106- μ m sieve, and are picked out for completion. We simulated a 106- μ m sieve to exclude these small teeth that would not have otherwise been retained by removing all teeth with at least two maximum dimensions < 106 μ m before analyzing the tooth assemblages. A histogram with equal bins (0.1 mm increments from 0 mm to 7 mm) was generated for each assemblage, and the relative abundance of each bin was considered in our analyses of the size structure across the K/Pg extinction (Figs. S1 and S2). We find that the patterns observed in the South Pacific (DSDP Site 596), of an increase in relative abundance of large teeth and a decrease in relative abundance of smaller teeth, is present in ODP Site 886 (Fig. S2).

In the case of tooth fragments, where it was apparent that the tooth length was not compromised by the fragmentation, the tooth was considered in the analysis. Accumulation rates of tooth size structure were calculated using sediment accumulation rate on three tooth size classes: small (<0.4 mm maximum length), medium (0.4–0.8 mm), and large (>0.8 mm).

Treatment of Shark Teeth. While our manuscript generally treats denticles as sourced from sharks and triangular teeth as derived from ray-finned fish, we acknowledge that shark teeth are occasionally present in some our samples, especially in the larger size fractions, which can slightly bias the interpretation of the ratio of teeth to denticles reported in the manuscript. The only sites with any obvious shark teeth were DSDP 596 and ODP 886. The other sites considered in this study (DSDP 386, ODP 1262, U1403, and Gubbio) had small numbers of teeth > 106 μ m to begin with, and revealed no shark-like teeth. We note that shark teeth are generally larger and more solid than the ray-finned fish teeth. They often have multiple cusps at the base, and often have an edge that is somewhat pointed, serrated, or otherwise indicative of slicing. Please see Fig. S1 for an example of a shark tooth in a Paleocene assemblage.

For DSDP Site 596 and ODP Site 886, there are zero to two shark teeth in any given sample assemblage, with >50% of samples not having any obvious shark teeth. Our Cretaceous samples generally have significantly fewer teeth and denticles than those of the Paleocene, and the samples in the Eocene are the largest. The presence of a shark tooth in a sample would cause the ratio to decrease considerably more in the Cretaceous than it would in the Paleocene or Eocene, and therefore push the relative abundance of sharks even higher in the Cretaceous, while not causing a major change to the larger samples of the Paleocene or Eocene.

To quantify the effect of shark teeth in our assemblages, we performed a series of bootstrap analyses, assuming a particular

abundance of shark teeth present in the samples from DSDP Site 596, and recalculated the Cretaceous and Paleocene ratios based on these numbers. The simulations were carried out using R Statistical Package. For simulations 3–7, the number of shark teeth per for each sample set in the time series was randomly chosen from a uniform integer distribution, and the resulting pre- and post-K/Pg ratios were calculated. Each simulation was run with 5,000 bootstrap replicates. In our simulated calculations, if a shark tooth was present, it was removed from the tooth part of the assemblage, and instead counted as part of the shark (denticle) assemblage. These simulations (except for scenarios 1 and 2) are deliberately significantly more extreme than the visual check of our samples suggests, allowing for a greater range of potential shark teeth in the assemblages, and test the robustness of the sample set and conclusions.

Simulations are as follows: simulation 1, 1% of teeth (rounded up) or at least one tooth per sample are shark teeth; simulation 2, 5% of teeth (rounded up) or at least one tooth per sample are shark teeth; simulation 3, a minimum of 0 and a maximum of 10 teeth (up to 50%) of each sample are shark teeth; simulation 4, a minimum of 1 and a maximum of 10 teeth (up to 50%) of each sample are shark teeth; simulation 5, a minimum of 0 and a maximum of 20 teeth (up to 50%) of each sample are shark teeth; simulation 6, a minimum of 1 and a maximum of 20 teeth (up to 50%) of each sample are shark teeth; and simulation 7, a minimum of 1 and a maximum of 40 teeth (up to 50%) of each sample are shark teeth.

The results from these experiments are summarized in Table S2, and the bootstrapped histograms from simulation 6 are shown in Fig. S3. For all simulations, the ratio of Paleocene actinopterygian to shark fossils is twice or more than the ratio in the Cretaceous. Additionally, none of our simulations shows any instances where the Paleocene ratio is less than the Cretaceous (change factor is <1). While the absolute value of the ratio is, by definition, sensitive to a number of variables, including the number of shark teeth (as well as the size fraction considered in the analysis), the overall conclusion, that the ratio of ray-finned fish versus shark fossils increases by a factor of two from the Cretaceous to the Paleocene, is robust to the presence of shark teeth.

Age Models and Time Series Analysis.

DSDP Site 386. DSDP Site 386 is an Atlantic red clay site off Bermuda Rise at 4,793 m water depth (41). Due to the lack of microfossils, the age constraints are poor at the site; however, there is a distinct K/Pg boundary slump deposit (27). Thirty-gram

samples were taken from the 2 m below and above the boundary to assess the fish community before and after the impact and extinction event. Due to the low abundance of >106- μm ichthyoliths in the core, samples were grouped as pre- and post-K/Pg boundary for analysis.

DSDP Site 596. DSDP Site 596 is a red clay site from the South Pacific Gyre at 5,711 m water depth (42). Five- to 12-gram sediment samples were processed at 5-cm intervals (~200-ky resolution) from 75.1 Ma to 42.2 Ma. The K/Pg boundary is identifiable by a prominent iridium anomaly (see Fig. 1B), and an age model developed based on the accumulation of cobalt in marine sediments was used to calculate ichthyolith accumulation rate during the study interval (23, 38). The chronology was shifted to a K/Pg boundary age of 66.04 Ma after GTS2012 (39).

ODP Site 886. ODP Site 886C is a red clay site from the North Pacific Gyre, at 5,713 m water depth (43). The age model used to calculate ichthyolith accumulation is based on strontium stratigraphy of fish teeth and tied to the K/Pg boundary using the GTS2012 age of 66.04 Ma (39) by an iridium anomaly (25). Five- to 15-gram samples of red clay were processed at 5 cm intervals (~100-ky resolution) from 70.0 Ma to 63.9 Ma. Unfortunately, a hiatus in the core precluded further analysis into the Paleocene.

ODP Site 1262. ODP Site 1262 is from Walvis Ridge in the South Atlantic at 4,759 m water depth and is mostly carbonate and clay (44). Twenty-gram carbonate samples were processed at 20 cm intervals (~20-ky resolution) from 66.8 Ma to 62.1 Ma with the cyclostratigraphic age model (29) tied to the GTS 2012 K/Pg Boundary age of 66.04 Ma (39). Due to the low numbers of large teeth (>106 μm), samples were clumped into pre- and post-K/Pg extinction for analysis.

IODP Site U1403. IODP Site U1403 is a carbonate ooze site drilled at 4,956 m water depth off of Newfoundland in the North Atlantic Ocean (26). Twenty-gram carbonate samples were processed every 20 cm (~30-ky resolution) from 66.4 Ma and 64.7 Ma. Preboundary and postboundary assemblages were considered based on an impact horizon layer identified in the shipboard site report (26).

Gubbio, Italy. One-hundred-gram samples of limestone were processed from the Scaglia Rosa formation on the Contessa Road Outcrop at Gubbio, Italy (28, 37). Samples were taken at 10- to 40-cm intervals across the K/Pg boundary between 66.3 Ma and 62.9 Ma based on a biostratigraphic age model (45) updated to GTS2012 dates (39). Samples were grouped into preboundary and postboundary assemblages for analysis.

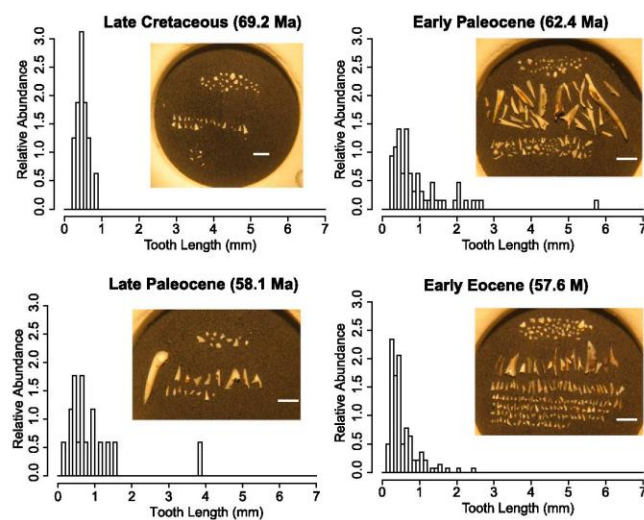


Fig. 51. Representative tooth-size histograms and ichthyolith assemblages from the South Pacific (DSDP Site 596). Histograms represent relative abundance of each tooth size class from the Late Cretaceous to the early Eocene. Note that the relative abundance of small teeth (<1 mm) decreases from the Late Cretaceous to the early Paleocene, and again from the late Paleocene to the early Eocene. The presence (and abundance) of large teeth (>1 mm) increases at the K/Pg boundary; into the early Eocene, small teeth become more abundant, and the large teeth are still present. (White scale bar, 1 mm.)

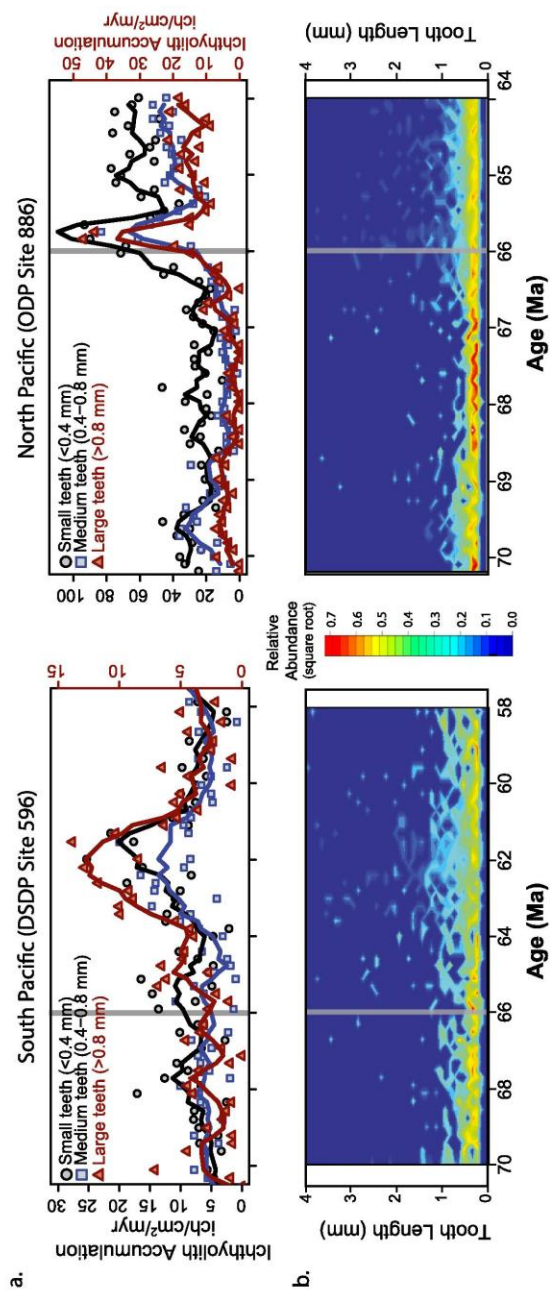


Fig. 52. Size structure of ichthyoliths at South Pacific (DSDP Site 596) and North Pacific (ODP Site 886). (A) Accumulation of small (black circles, <0.4 mm), medium (blue squares, 0.4-0.8 mm), and large (red triangles, >0.8 mm) teeth. The red axis is scaled to 2x the small and medium teeth accumulation, to account for the relatively low numbers of large teeth present. Solid lines are three-point running means. (B) Relative abundance (square root) of tooth sizes across the K/Pg boundary. Note the decrease in relative abundance (from yellow to green at Site 596 and from red to yellow at Site 886) of the mode tooth size at both sites that is accompanied by an increase in the presence and abundance of larger teeth (from dark blue to light blue) in the early Paleocene.

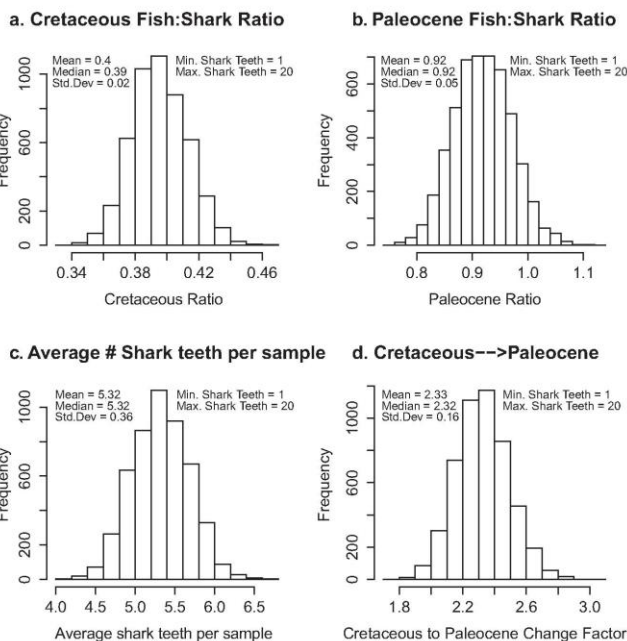


Fig. 53. Results of bootstrapped shark tooth simulation 6, showing the spread of ratios calculated for each of 5,000 simulations. (A) Cretaceous ratios in each simulation. (B) Paleocene ratios in each simulation. (C) Average number of shark teeth present in each assemblage for each simulation. (D) Factor of change between the Cretaceous ratio and the Paleocene ratio calculated in each simulation. Note that there is no value < 1, so the ratio observed in the Paleocene is always greater than the ratio observed in the Cretaceous.

Table S1. Global ichthyolith assemblage ratios used for Fig. 2

Site	Cretaceous					Paleocene				
	Age, Ma	No. of samples	Teeth > 106 μ m	Denticles > 106 μ m	Ratio	Age, Ma	No. of samples	Teeth > 106 μ m	Denticles > 106 μ m	Ratio
DSDP 386	Maastricht	9	18	27	0.67	Danian	10	122	36	3.39
DSDP 596	76–66	42	605	935	0.65	66–56	36	1,051	631	1.67
ODP 886 ¹	70.2–66 ¹	43 ¹	1,002 ¹	1,403 ¹	0.71 ¹	66–63.8 ¹	23 ¹	1,592 ¹	1,217 ¹	1.31 ¹
ODP 886 ²	70.2–66 ²	43 ²	1,002 ²	1,403 ²	0.73 ²	66–63.8 ²	23 ²	1,592 ²	1,217 ²	1.69 ²
ODP 886 ³	70.2–66 ³	43 ³	1,002 ³	1,403 ³	0.71 ³	65.6–63.8 ³	20 ³	1,157 ³	653 ³	1.77 ³
ODP 886 ⁴	70.2–66 ⁴	43 ⁴	1,002 ⁴	1,403 ⁴	0.71 ⁴	66–63.8 ⁴	23 ⁴	1,374.5 ⁴	935 ⁴	1.47 ⁴
ODP 1262	66.9–66	45	52	50	1.04	66–62.1	117	447	218	2.05
IODP 1403	66.4–66	21	29	27	1.07	66–64.7	121	121	51	2.37
Gubibo	66.3–66	10	63	77	0.82	66–62.9	26	320	139	2.30

Different metrics for ODP Site 886 are explained in *SI Materials and Methods*, with superscript referring to the method used to calculate each ratio.

Chapter 5, in full, is a reprint of materials as it appears in Sibert, E. C., and Norris, R. D. (2015). “New Age of Fishes initiated by the Cretaceous/Paleogene Mass Extinction” in the Proceedings of the National Academy of Sciences, v.112, no. 28, p. 8537-8542. DOI:10.1073/pnas.1504985112. The dissertation author was the primary investigator and author of this manuscript.

CHAPTER 6

A two-pulsed radiation of pelagic fishes following the K/Pg mass extinction

6.1 Abstract

The Cretaceous-Paleogene (K/Pg) mass extinction disrupted marine ecosystems and caused considerable extinction of higher order predators, including ammonites and marine reptiles. However, we know much less about how fish diversity responded to the K/Pg event and its aftermath, due to the low-temporal resolution achievable with the whole-body fish fossil record. Here we present a novel scheme for quantifying morphological variation in fish teeth (ichthyoliths) as a measure of taxonomic and ecological diversity, and use this to define a series of ichthyolith morphotypes present in the South Pacific Ocean between 73 and 42 million years ago (Ma). We find that there is essentially no change in trends of ichthyolith diversity in the late Cretaceous (73-66 Ma), or across the K/Pg boundary. Rather, it was two pulses of tooth morphological origination that restructured Paleogene fish diversity following the K/Pg, at 62 Ma and 58 Ma. The first pulse produced a number of short-lived, extreme morphotypes, a “disaster-fauna” restricted to the early Paleocene (66-60 Ma), while the second pulse produced the tooth morphotypes which persisted at least into the Middle Eocene. Tooth diversity reached its maximum around the Paleocene/Eocene boundary. Molecular phylogenies suggest the major radiation of pelagic fishes occurred in the vicinity of the K/Pg boundary. Our results illuminate the dynamics of this radiation, showing that the main oceanic fish radiation occurred rapidly, possibly due to the low levels of extinction in fishes across the K/Pg, with new morphotypes replacing Late Cretaceous survivors over the course of the Paleocene. While ichthyolith abundance peaks in the Early Eocene at nearly 10-fold Paleocene levels, there is little diversification in the tooth morphology during this interval. Together, these results suggest that the evolutionary trajectory of the

open ocean fish communities changed in the Paleocene, leading to the distinct structure of Cenozoic communities that we still observe today. The multiple pulses of Paleocene innovation in fish has parallels with radiations in other groups in which there is the appearance of an early group of ‘founders’ during the immediate phase of recovery from the extinction, and a later pulse of origination as Paleocene faunas are established. Together, these results suggest that the K/Pg extinction event changed the evolutionary trajectory of the open ocean fish community, allowing for fishes to take on more ecological roles within the open ocean ecosystem.

6.2 Introduction

Fishes are the most diverse clade of vertebrates living on the planet today. They dominate the world’s lakes, rivers, and oceans, and have over 30,000 described species (Nelson, 2006). Yet while fishes have populated the oceans for over 450 million years, the majority of modern fish diversity developed only recently, within one clade, the ray-finned fishes (Actinopterygii), which contains the vast majority of extant fish diversity (>27,000 species), and represents the largest known radiation of fishes in the fossil record (Friedman and Sallan, 2012). While the ray-finned fish lineage reaches back over 400 million years ago (Ma), they diversified relatively recently, with most crown-group lineages originating significantly less than 100 Ma (Friedman and Sallan, 2012; Near et al., 2013; Near et al., 2012). Recent fossil and genetic evidence suggests that open ocean fishes expanded their ecological and taxonomic bounds following the Cretaceous-Paleogene (K/Pg) mass extinction 66 Ma, which may have been a catalyst for the great diversity of fishes present in our present oceans (Miya et al., 2013; Sibert and Norris,

2015). However, the temporal uncertainty associated with molecular clock studies of diversification, compounded with the inability to capture the diversity of entirely extinct clades, make it difficult to resolve the relationship of the KPg boundary mass extinction to the ray-finned fish radiation. The body fossil of fishes also suggests a large scale turnover and radiation across the KPg boundary, but with a temporal uncertainty of millions of years. In addition, the open ocean record of fishes is particularly sparse, leaving the dynamics of open ocean clades in particular question.

Although the precise timing is unclear, there are reasons to suspect that the KPg mass extinction may have directly allowed for a Cenozoic radiation of ray-finned fishes. Mass extinction events during the Phanerozoic have helped to shape the diversity of life on the planet (Jablonski, 2005; Wagner et al., 2006), by removing the dominant flora and fauna, and allowing survivors to diversify in the aftermath of the event (Sahney et al., 2010). Following most mass extinctions, there is an interval of hundreds of thousands or millions of years during of unusual ecosystems (often low diversity and high dominance), which are eventually replaced by ecosystems with pre-event-like levels ecosystem structure and complexity (Erwin, 1998; Hull et al., 2011). Ray-finned fishes have a history of bouncing back from mass extinctions (Friedman and Sallan, 2012), often diversifying in the aftermath of ecological disaster. The Cretaceous/Paleogene event caused a selective extinction of large- and fast-jawed predatory fishes (Friedman, 2009) but ray-finned fishes radiated following the extinction event as well (Alfaro et al., 2009; Friedman, 2010; Miya et al., 2013). While it appears that open ocean ray-finned fishes thrived following the extinction, while other marine vertebrates did not (Sibert and Norris,

2015), the processes governing the radiation and success of ray-finned fishes in the aftermath of the extinction are poorly understood.

There are several climatic events in the Early Cenozoic that may also have played an important part in the diversification of ray-finned fishes in the aftermath of the K/Pg extinction. For example, the Paleocene-Eocene Thermal Maximum (PETM) was a period of rapid greenhouse-induced global warming and ocean acidification 56 Ma (McInerney and Wing, 2011), and the Early Eocene Climate Optimum (EECO), 52-50 Ma, was an extended period of extreme greenhouse warmth, with the ocean reaching its warmest in the past 90 million years (Zachos et al., 2008). In the open South Pacific Ocean, while the K/Pg may have caused a small increase in total fish abundance, fish production reached peak values more than 5 times higher than the Paleocene or Cretaceous during the EECO (Sibert et al., 2016). The EECO had both the warmest climate and highest fish production levels during the entire Cenozoic in the South Pacific, suggesting that this climate extreme event may have been a cradle for the development of open ocean fish diversity in the Cenozoic.

Here, we use a unique fossil resource, microfossil fish teeth preserved in a well-dated deep-sea sediment core, to address changes in open ocean fish morphological diversity across the K/Pg mass extinction, and through the EECO, spanning the interval of 73 Ma to 43 Ma. Fish teeth have distinct shapes that carry information about taxonomic and ecological diversity. For example, we recognize teeth whose distinctive shapes are similar to those of living myctophids and dragon fish, suggesting that some taxonomic groups, or at least their ecological roles are represented in the Paleogene fish biota. While taxonomic identification of Paleogene fish teeth is not always possible at

present, we suggest that the morphological diversity of teeth is a likely a reflection of diversity at a relatively high taxonomic level (family or order, rather than species) and could therefore be useful in defining the timing of radiations in pelagic fish lineages.

6.3 Methods

6.3.1 *DSDP Site 596 lithology and ichthyolith isolation*

Ichthyoliths were isolated from discrete sediment samples taken from Deep Sea Drilling Program (DSDP) Site 596. DSDP Site 596 is located in the South Pacific Gyre, located at 23°51.20'S, 165°39.27'W, in approximately 5710 meters water depth (Menard et al., 1987). DSDP Site 596 is almost completely pure pelagic red clay, and has remained within the South Pacific Gyre for its >85 million year history (Zhou and Kyte, 1992). A sedimentation history for DSDP Site 596 using a constant cobalt-flux model reveals a relatively low and constant sedimentation rate of approximately 0.2 to 0.27 m/myr throughout the interval considered in this study, approximately 73 to 42 Ma. There is a prominent iridium anomaly at the site at the K/Pg boundary (Zhou et al., 1991), as well as several ichthyolith biostratigraphic tie points that confirm this sedimentation rate (Winfrey and Doyle, 1984). DSDP Site 596 was sampled every 5 cm down-core, from 15 meters below seafloor (mbsf) to 22 mbsf. The 5 to 10-gram samples of red clay were dried to a constant weight in a 50°C oven to remove excess water. Samples were then disaggregated in de-ionized water, and washed over a 38µm sieve to concentrate and retain the ichthyoliths (Sibert et al., In review). As the majority of the sediment is red clay, preserved well below the CCD, the coarse fraction is composed nearly exclusively

of ichthyoliths, with occasional manganese nodules or other non-biogenic sediment grains. The coarse fraction residues were inspected under a high-power dissection microscope, and a fine paintbrush was used to transfer the ichthyoliths to cardboard microfossil slides (Figure 6-1) for storage and further analysis. Ichthyolith accumulation rate was calculated using the cobalt-accumulation model produced by Zhou and Kyte (1992). Picked ichthyolith assemblages were imaged at high resolution (~1 micron/pixel), and a semi-3D extended-depth-of-focus (EDF) image was created. These images were processed and analyzed using the Hull Lab Imaging System at Yale University. Tooth outlines were evaluated, and a minimum-bounding-box was used to calculate the maximum length, width, and aspect ratio of the teeth (Figure 6-2).



Figure 6-1: Example tooth assemblage from DSDP Site 596. Ichthyoliths in the upper $\frac{1}{4}$ of the image are denticles, while the remainder are teeth

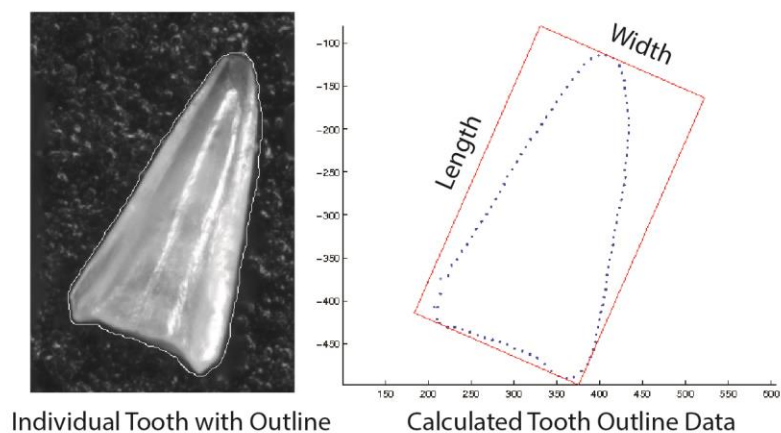


Figure 6-2: Example tooth with outline and measurements. Image taken and processed with the Hull Lab Imaging System, Yale University.

6.3.2 *Fish Tooth Morphology and Morphotypes*

While it is difficult to identify teeth to traditional taxonomic levels, a character-based coded system which quantifies morphological traits in a non-hierarchical manner can be used to quantify the morphological variation in these microfossils and create a non-hierarchical, ‘taxon-free’ morphological classification (Doyle et al., 1974; Doyle and Riedel, 1979b; Doyle and Riedel, 1985; Johns et al., 2006; Tway, 1977; Tway, 1979; Tway and Riedel, 1991). In this manuscript, we employ a new ichthyolith morphological coding system that is loosely based on the system developed by Doyle, Kennedy, and Riedel (1974). Our system differs from prior ichthyolith classification schemes in several important ways. First, it differentiates between teeth and denticles: as these ichthyolith subgroups are produced by different clades of organisms and have entirely different functional purposes (teeth versus scales), we consider them completely independently. Second, our system uses only reflected light microscopy, reducing the complexity of the mounting and analysis of teeth in transmitted-light slides, and leaving the teeth free to be

used in future analyses, such as advanced imaging (eg. microCT or Scanning Electron Microscopy) or geochemistry. Third, our coding system considers the same set of characters as potential descriptors for all teeth, removing the need for nested, hybrid character states, or for complicated nomenclature syntax, as was used in prior ichthyolith morphological coding schemes. Our system retains the flexibility built into the original ichthyolith classification schemes: it is straightforward to include additional characters or character-states to the system as novel tooth morphotypes are found and classified (Doyle et al., 1974; Tway, 1979). While our system is still a work in progress, and currently only includes traits for the teeth included in this study (South Pacific Gyre, Cretaceous to Eocene), it represents a considerable step forward in the field of ichthyolith morphometrics. Details of the characters, character states, and identified morphotypes are included in Appendix I, and summarized in Figure 6-3.

Character States for Ichthyolith Morphological description:
Teeth from S.Pacific Red Clays, Cretaceous-Eocene

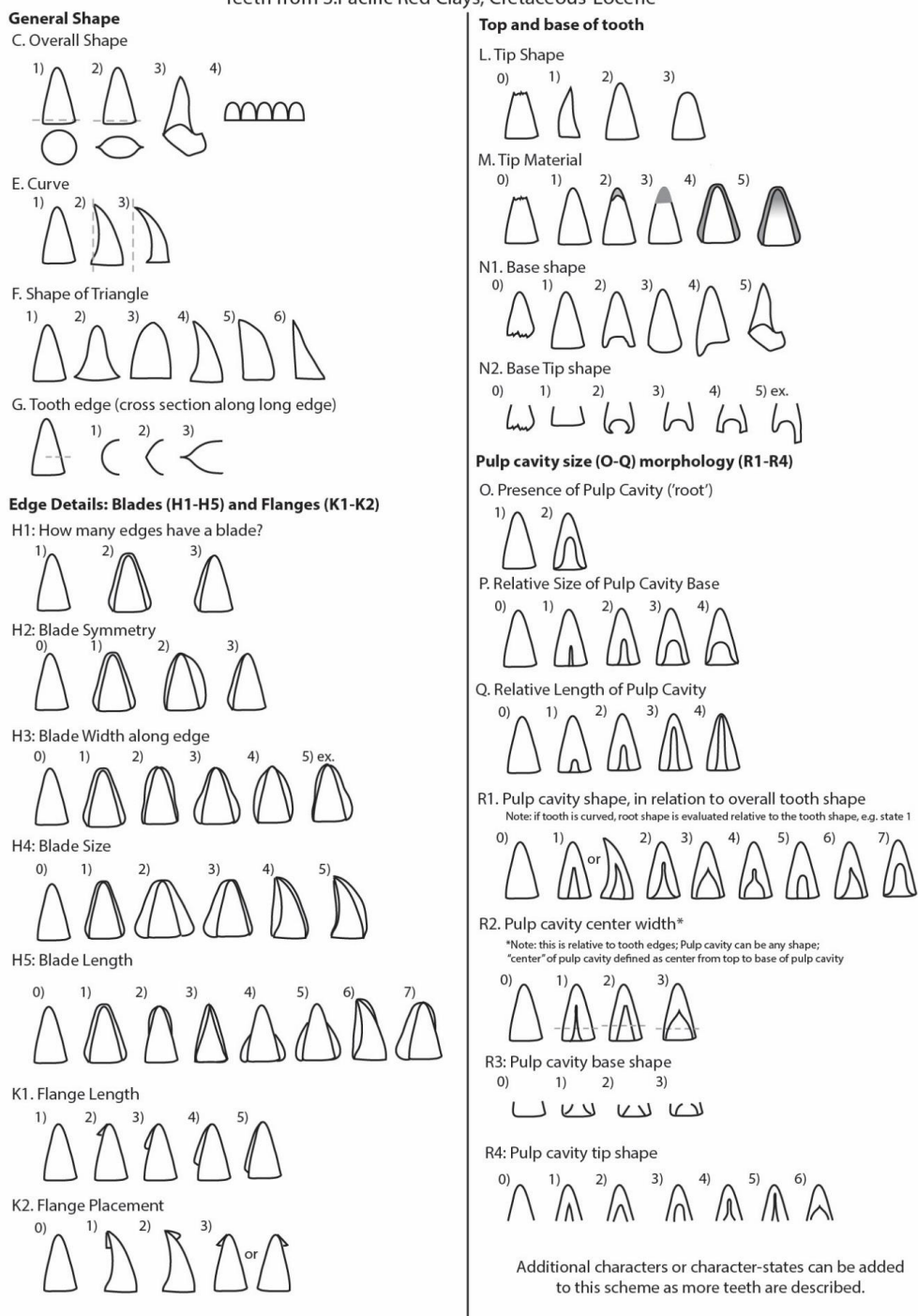


Figure 6-3: A schematic representation of the different character-states described in our tooth morphology system. We use a generic triangular tooth for simplicity in this figure, however note that because our traits are described relative to overall tooth shape, this can be applied to a variety of tooth shapes, including in this study. Extended notes and descriptions of each character and character state are available in Appendix I.

We identified 22 unique discrete characters that are easily visually distinguished, including the general shape and structure of the tooth, the size and structure of any extensions (eg. ridges), the nature of the tip, and the shape and structure of the pulp cavity (please see Appendix I for details). We used this system to code each whole or otherwise identifiable tooth from the sample set, from 74 unique samples, for a total of 1897 identified teeth, ranging in age from 42 to 73 Ma. For this study, we defined any tooth that has a unique set of character-states as a distinct morphotype: 136 unique tooth morphotypes were identified in the set. We note, however, that certain characters are correlated, so morphotypes which cluster are likely closer, either taxonomically or ecologically, than those with greatly different morphologies. As this character-coding system is, by definition, non-hierarchical, we felt this was the most reasonable way to consider tooth types without introducing a potentially false hierarchy that has no biological meaning into the system. To address the issue of small sample size, particularly in the Cretaceous and Paleocene samples, which sometimes had fewer than 20 teeth in a single sample, we grouped the samples into ~1 myr time bins, so that each time bin included sufficient teeth for analysis (34-241 teeth per time bin, average = 90.3).

To address the potential of reworked teeth artificially extending the range of a particular morphotype, we selectively removed individual occurrences of particular teeth from the analysis following a specific set of rules, described in full in Appendix II. Using our conservative set of rules, we removed 9 teeth (0.5% of total teeth described) from the analysis due to suspected reworking (1887 teeth total, ranging from 34-241 teeth per time bin, average = 89.9). Following a more liberal set of rules, we removed an additional 14 teeth (1% of total teeth described) from the analysis (1873 total teeth, 34-241 teeth per

time bin, average = 89.2). We conducted all successive analyses on all three of these datasets, and note that while the liberal dataset consistently yields slightly higher estimates for speciation and extinction rates, as it has the shortest ranges, overall, the patterns observed are robust regardless of dataset analyzed, suggesting that the effect of reworking on the overall tooth record is minimal. We present results from all three datasets where possible, however when only one dataset is represented in the figures, we use the “conservative mixing” dataset.

6.3.3 *Morphospace Analyses*

To assess changes in tooth morphology through time, we evaluated morphological disparity of the tooth morphotypes present in our samples. All analyses were carried out in R using our own scripts. We calculated distances between tooth types by assigning weights to all characters and evaluating a weighted distance between each pair of teeth based on the character-states they displayed. Traits within a character were considered to be equally distant unless there was an obvious hierarchy, in which case we created distance matrices for the character states. The characters were weighted either equally, or paired to combine several traits to have the same weight (e.g. the 4 pulp cavity morphology traits were reduced to $\frac{1}{2}$ weight each, so that they did not overpower other characters which were more easily described). For teeth which had good length, width, and aspect ratio measurements (see Figure 6-2 for an example), we combined these discrete character states with the continuous measurements by discretizing the continuous measurements into normalized bins and treating each bin as a discrete state. Distances for all traits available to compare for each pair of teeth were then averaged, to get an average

pairwise distance value. Since the traits are discrete, rather than continuous, the resulting distance matrix was analyzed using nonmetric multidimensional scaling (NMDS) to create a morphospace and evaluate the regions occupied by teeth throughout the interval.

6.3.4 *Estimation of evolutionary rates*

To assess the turnover of tooth morphotypes, we calculated origination and extinction rates. While we recognize that these fish teeth are not identifiable as individual taxa, and indeed, likely represent ecological groups or ontogenetic stages, they do have unique morphologies that have distinct stratigraphic ranges, mostly used for crude biostratigraphy (Doyle and Riedel, 1979b; Johns et al., 2006), and thus exhibit evolutionary change through time. This bias means our calculations cannot be compared in absolute terms to traditional taxonomic-unit based evolutionary rates, but it is informative in assessing the changing ecological roles of fishes in the open ocean. Our approach is similar to other ‘taxon-free’ morphological approaches that have been used to describe evolution in many now-extinct groups, including trilobites and blastoids (Foote, 1993). Since ichthyoliths are present in such high abundances, and at high temporal resolution, they represent a unique dataset with which to assess evolutionary patterns across major global change events. Here we use two different metrics to calculate per-capita origination and extinction rates for fish tooth morphotypes: Boundary Crossers (Foote, 2000) and maximum likelihood-based capture-mark-recapture (CMR).

CMR models use a time-series-based set of presence/absence observations for individuals in a population and a maximum-likelihood approach to calculate detection probability (p) and survival. For our analyses, we used Pradel-recruitment and Pradel-

lambda models, which provide estimates of recruitment or population growth (λ), respectively, in addition to the survival and detection probability parameters. These CMR models best fit the assumptions of the fossil record (Liow and Nichols, 2010), and the parameters they estimate can be transformed to extinction rate ($1 - \text{survival}$) and origination rate (recruitment for Pradel-Recruitment and λ [growth] minus survival for Pradel-Lambda). Models were fit allowing for the parameters to vary within each time bin, to be fixed over the whole interval, or to vary during each of the three geologic time periods, and the best-fit models were evaluated using AIC. The CMR timeseries reported in this manuscript are weighted model averages combining all permutations considered. CMR has a distinct advantage over other traditional rate metrics: it inherently assumes that the observed first and last occurrences of a taxon may not be the birth or death of an individual. The likelihood model that is fit assumes that the observation of an individual is a function of the likelihood that the individual was alive (survival) and the probability that it was detected (p). Thus, the parameters estimated by CMR include error for all observed stratigraphic ranges, negating the need for additional confidence interval calculations (e.g. Marshall, 1997). The CMR analysis was carried out using the MARK software (Cooch and White, 2006; White and Burnham, 1999) through the RMark package (Laake, 2013) in R (R Core Team, 2014).

Only two morphotypes disappeared at the K/Pg boundary: (1) Straight, half-length flange and (2) Clear, convex tooth, dome root, small blades (Figure 6-5). Both of these morphotypes were incredibly common in the late Cretaceous, often dominating the tooth assemblages, but disappear after the extinction event. Cretaceous teeth which were less common persisted through the event, suggesting that the mass extinction served to disrupt a previously stable, incumbent, Cretaceous fauna (Erwin, 1998; Erwin, 2001; Hull et al., 2015).

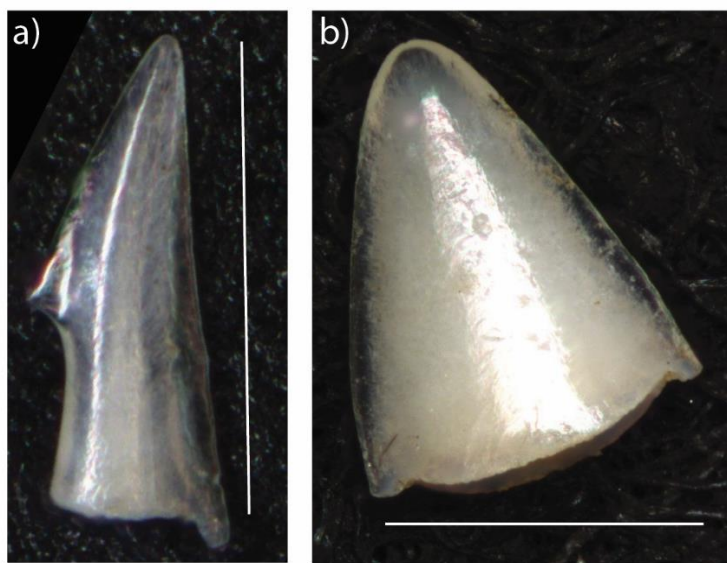


Figure 6-5: Morphotypes that went extinct at the K/Pg: a) Straight, half-length flange, b) Clear, convex tooth, dome root, small blades. Scale bars are 500 μ m, but both of these morphotypes can have a range of sizes. Images taken on the Hull lab Imaging System, Yale University.

The average length of time that a tooth morphotype existed throughout the interval sampled was 12.6 million years (all teeth). If teeth which are likely reworked are excluded, this reduces to 12.0 million years (conservative levels of reworking) or 11.1 million years (liberal levels of reworking). As there are a considerable number of morphotypes in our record which extend in range beyond the observed interval (out of

136 described morphotypes, ~24 likely extend deeper in the Cretaceous, ~34 into the Eocene, with at least 5 morphotypes spanning the entire interval), it is likely that this is an underestimate of average morphotype duration: Cretaceous morphotypes, which have the longest potential observed range, have a mean of approximately 20 million years, while those in the Paleocene and Eocene are considerably shorter (Figure 6-6). This interval is considerably longer than the estimated species duration for freshwater fish, approximately 3 million years (McKinney, 1997), or the duration of marine invertebrate species, which range from 5 to 12 million years (Raup, 1981). However, it is not surprising that tooth morphotypes, which likely represent relatively high level taxonomic groups of fish (genera or families), or taxonomic-free ecotypes, would have longer persistence through time than is seen in species-level taxonomies. Further, the wide variation in morphotype duration may be due to different morphotypes representing different taxonomic specificity: it is probable that certain families of fish have identical teeth across all individuals, while others have considerable differences within the genera or species (Streelman et al., 2003).

In any case, nearly every time bin has novel morphotypes which persist through the remaining observed record, as well as those that are short-lived, suggesting that there is considerable variation in the overall duration of individual morphotypes. A possible exception to this is that the morphotypes which evolved in the latest Cretaceous did not persist as long into the early Cenozoic as those which arose earlier. However, it is worth noting that the number of novel morphotypes in each time bin throughout the interval is relatively small (0-25, median=5), so the short ranges in the latest Cretaceous may simply be an artifact (Figure 6-6).

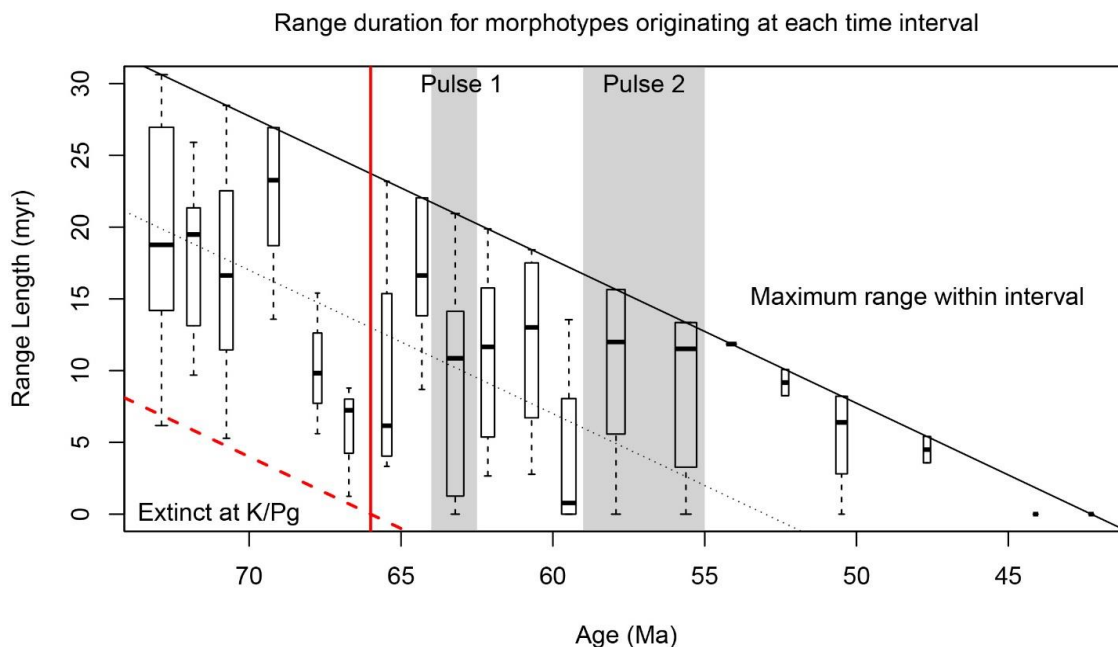


Figure 6-6: Range duration for morphotypes which originated at each time bin. Red vertical line notes the K/Pg boundary. The solid black line is the maximum observable range duration for each time bin. Points below the red dashed line denote morphotypes which were victims of the K/Pg extinction, and the dotted black line represents a trajectory of mean range duration. The size of the boxes is related to the number of novel morphotypes at each time bin. Shaded regions denote the periods of elevated diversification rate. Figure uses data from the “conservative reworking” dataset. The “original” and “liberal” datasets are very similar, maintaining the shorter-than-expected range lengths in the youngest two Cretaceous samples.

6.4.2 *Ichthyolith abundance and sampling*

There is a significant increase in total tooth abundance in the Early Eocene, centered at the Early Eocene Climate Optimum, 52-50 Ma (Sibert et al., 2016), while the K/Pg extinction does not appear to have a significant impact on the abundance of teeth (Figure 6-7).

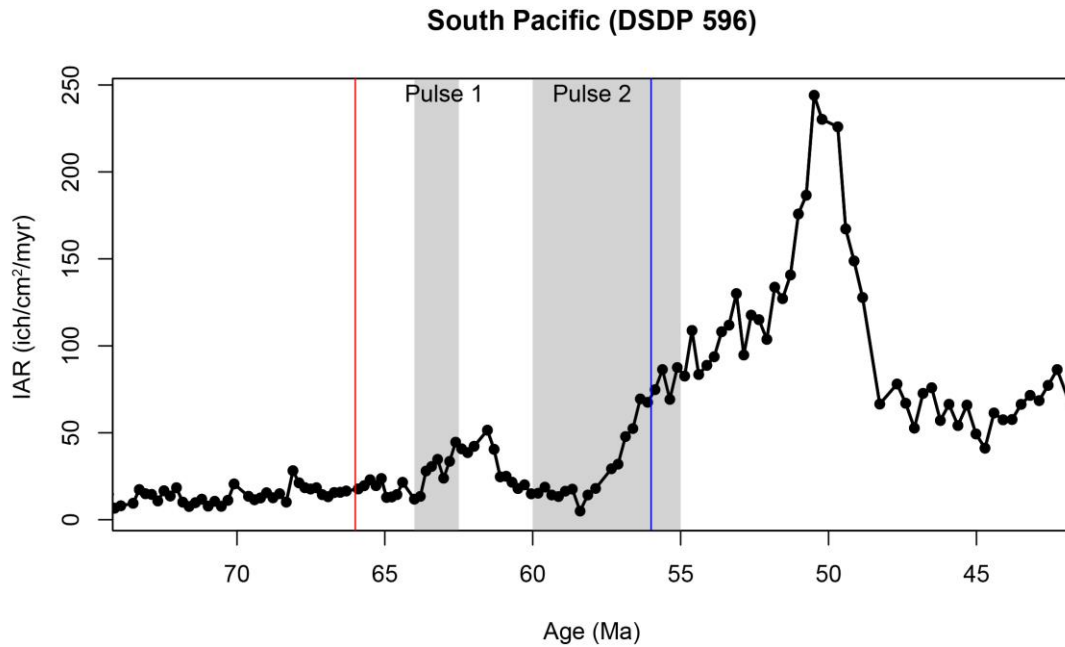


Figure 6-7: Total tooth accumulation at DSDP Site 596. (Data from Sibert et al., 2016). Red line is K/Pg mass extinction; blue line is Paleocene/Eocene boundary. Gray boxes denote the two periods of origination observed in the dataset.

Despite this, the estimated number of morphotypes (standing morphotype diversity) peaks around the Paleocene-Eocene boundary, corresponding with the peak in novel morphotypes observed, nearly 5 million years prior to the 5-fold increase in absolute abundance (Figures 6-7 and 6-8). There are two peaks in novel morphotype appearance (Figure 6-8a): 63.2 Ma, and 58-55 Ma. The time bins with the largest numbers of teeth described in this study (sampling intensity) occur after these peaks in novel morphotypes, at 62.1 Ma and 50.5 Ma, respectively, suggesting that the observed morphotype origination is not simply due to an increase in sampling intensity, but is a real, biological signal.

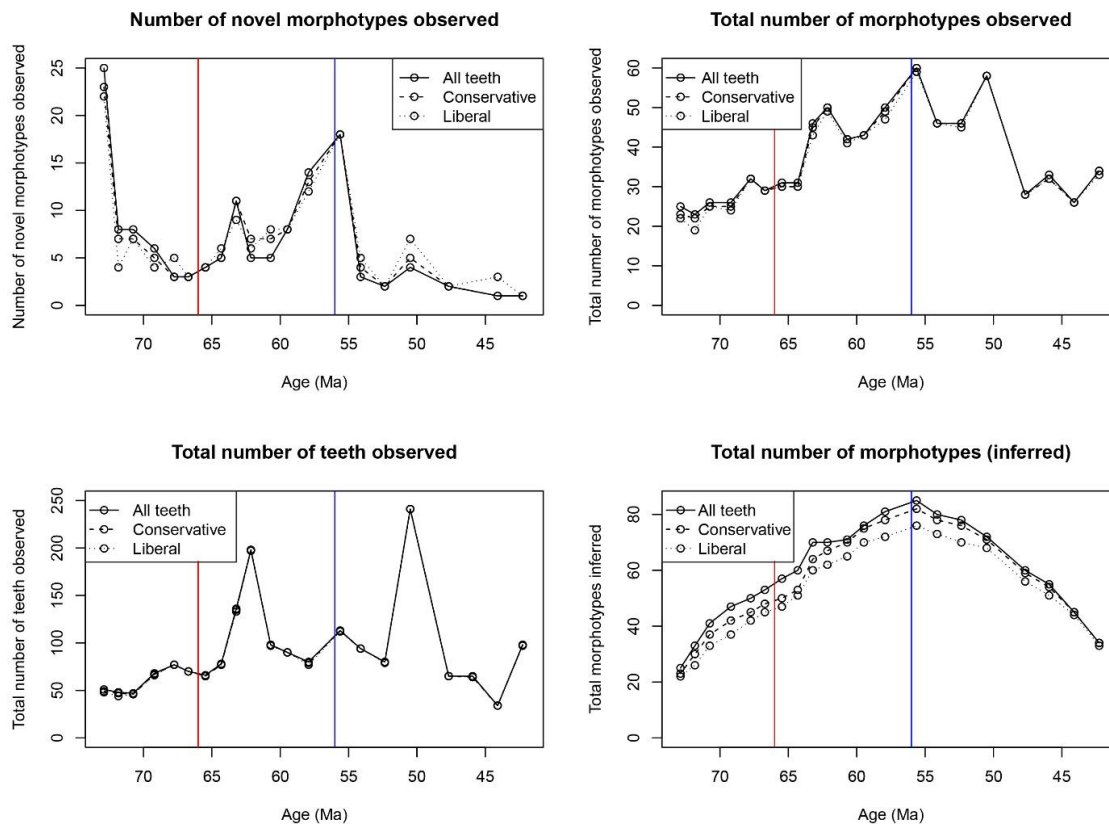


Figure 6-8: Plots comparing sampling intensity to morphotype observation. Plots showing the absolute abundance of a) novel morphotypes observed in each sample; b) number of total morphotypes observed in each sample; c) the total number of teeth counted in each sample; and d) the total number of morphotypes inferred for each sample. Note that the peaks in tooth observed fall after the peaks in novel morphotypes. Red line is the K/Pg mass extinction; Blue line is the Paleocene/Eocene boundary.

6.4.3 Origination and extinction rates

Throughout the Cretaceous and Paleocene, estimated tooth morphotype origination rate exceeded the extinction rate, however beginning in the Eocene, the estimates converge (Figure 6-9). While both estimators (Boundary Crossers [BC], and Capture-Mark-Recapture [CMR]) yield similar patterns in both origination and extinction, the absolute value for the rates is different, with the CMR method yielding absolute values for origination approximately twice the BC estimates. Estimated extinction rate is

comparable between the methods, with both yielding a constant extinction rate of approximately 0.05 (5% of extant morphotype extinction per million years) throughout the interval. The three datasets, which account for various levels of potential reworking yield strikingly similar patterns, and the variance between datasets is considerably less than the variance between time bins. Thus, reworking of teeth through bioturbation is not a significant factor in the estimates of tooth morphotype origination and extinction rates.

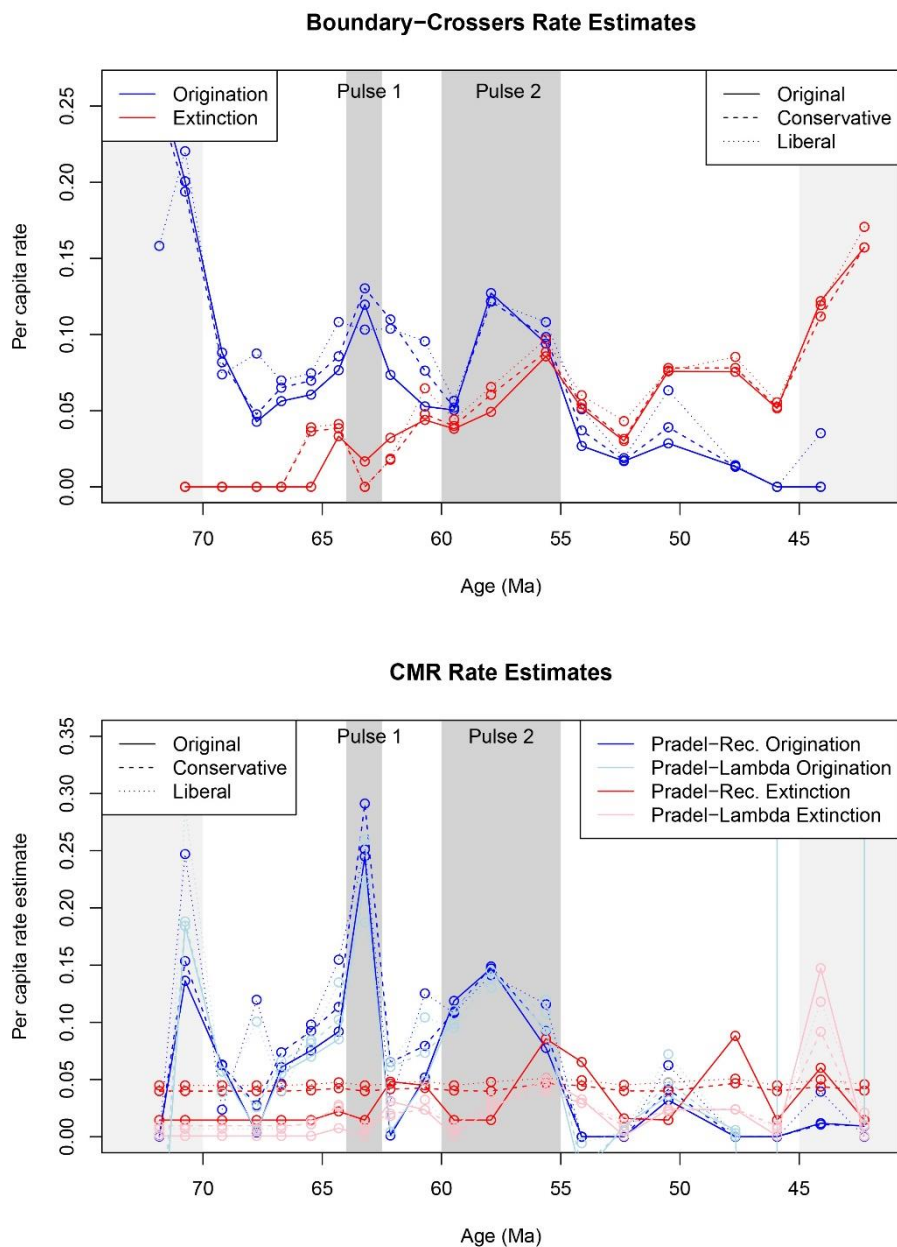


Figure 6-9: Origination and extinction rate estimates using the Boundary Crosser calculations (top; Foote 2000) and a set of capture-mark-recapture models (bottom). Dark gray shaded regions represent the two non-zero pulses of origination observed. Light-gray shaded areas represent regions of possible edge effects in our sampling. Red is extinction, while blue is origination. The different shades represent different configurations of the CMR models, while the different line dashes represent the three levels of reworking assumed in the data.

While both methods are biased by edge and sampling effects, the BC method has the largest biases, and as such, we discard the oldest 2 origination rate estimates and the youngest 2 extinction rate estimates within the time-series because they algebraically yield highly inflated estimates (Foote, 2000). Extinction rate is zero through the latest Cretaceous, while there is a low but constant per capita origination rate of 7%. Following the K/Pg extinction event, extinction rate increases, and remains at 4-7% per capita throughout the Paleocene and early Eocene. This suggests that the stable late Cretaceous ecosystem was disrupted by the K/Pg event. Further, while origination is relatively constant in the Cretaceous, at approximately 5-7% per capita, there are two distinct peaks in origination rate, showing levels nearly double the background Cretaceous average. These peaks, at 63.2 Ma, and 58-55 Ma, correspond approximately to the peaks in novel morphotype origination (Figure 6-8). Following this period of elevated origination in the Paleocene, origination declines to near zero in the Eocene (Figure 6-9), even while total fish production increases 7-fold (Figure 6-7). The BC method ignores single occurrences of taxa, and as such may underestimate the true extinction and origination rates for our dataset, as there are considerable morphotypes which occur only once, particularly during the early Paleocene (Figure 6-4).

The CMR estimates follow a similar pattern to the BC estimates, and broadly agree between datasets and across models. However, the relative magnitude of the first origination pulse and duration of the second are slightly different when using the CMR approach, possibly due to the high abundances of single-occurrence morphotypes in those intervals, which are discounted in the BC metric. The first pulse, at 63.2 Ma was significantly larger than the second, longer-lived pulse. The absolute value of the first

pulse (0.30 novel morphotypes per extant morphotype) is nearly twice that of the BC estimate (0.15). The second pulse has a similar maximum value of 0.15, but the timing of the beginning of the second pulse differs slightly between the two methods, with CMR estimating an earlier beginning (~60 Ma) and longer duration (~5 myr) than the BC method. However, both methods agree that the highest estimation of origination rate is at approximately 58 Ma, which corresponds to the time of lowest tooth abundance in the record (Figure 6-7). CMR also estimates origination declining considerably in the Eocene, to levels below estimated extinction. The Pradel-Lambda model can yield extremely small (<0.99) or large (>0.99) origination rates when the true value is close to zero, as it does for the samples at 45.9 Ma and 44.1 Ma, explaining the extreme parameter values estimated in that interval (Figure 6-9b).

The CMR extinction rates do not agree precisely across models and datasets (Figure 6-9b). The rates presented here represent an averaging of a series of models fitted using MARK, weighted based on AICc and model fit. We allowed the parameters to vary through time, to be constant through time, or to be constant within each time bin (Cretaceous, Paleocene, Eocene). In nearly all cases of the Pradel-recruitment model, extinction was best fit with a constant-through-time model, with extinction equal to ~4% throughout the interval. However the Pradel-lambda model, and the Pradel-recruitment model fit on the full dataset with no reworking assumed, yielded estimates with a similar pattern to that observed by the BC method. Together, these estimates suggest that extinction was extremely low in the Late Cretaceous, and increased slightly in the Paleocene and Eocene. There was net origination in the Cretaceous and Paleocene, and some evidence for net extinction in the Early Eocene.

6.4.4 *Changes in Morphospace Occupation*

We used multidimensional scaling to analyze the changes in morphospace occupation in the Cretaceous and Paleogene. For this analysis, morphotypes are binned more coarsely (into four time intervals: Cretaceous [>66 Ma], Early Paleocene/Pulse 1 [66-60 Ma], Late Paleocene/Pulse 2 [60-55 Ma] and Eocene [<55 Ma]) than in the analysis of origination and extinction rates. The K/Pg extinction event did not cause a substantial decrease in fish tooth morphospace occupation (Figure 6-10). One of the morphotypes which went extinct (Straight, half-length flange, Figure 6-5a) did leave a vacant part of the morphospace which did not re-fill until the Eocene, while the other victim of the K/Pg was not morphologically distinctive. The Early Paleocene sees the origination of several unique morphotypes which are distinct, morphologically, from the Cretaceous fauna (Figures 6-10 and 6-11). These extreme and morphologically unique morphotypes were short-lived, with the majority going extinct within the Early Paleocene, and only a few persisting to the Late Paleocene (Figure 6-11).

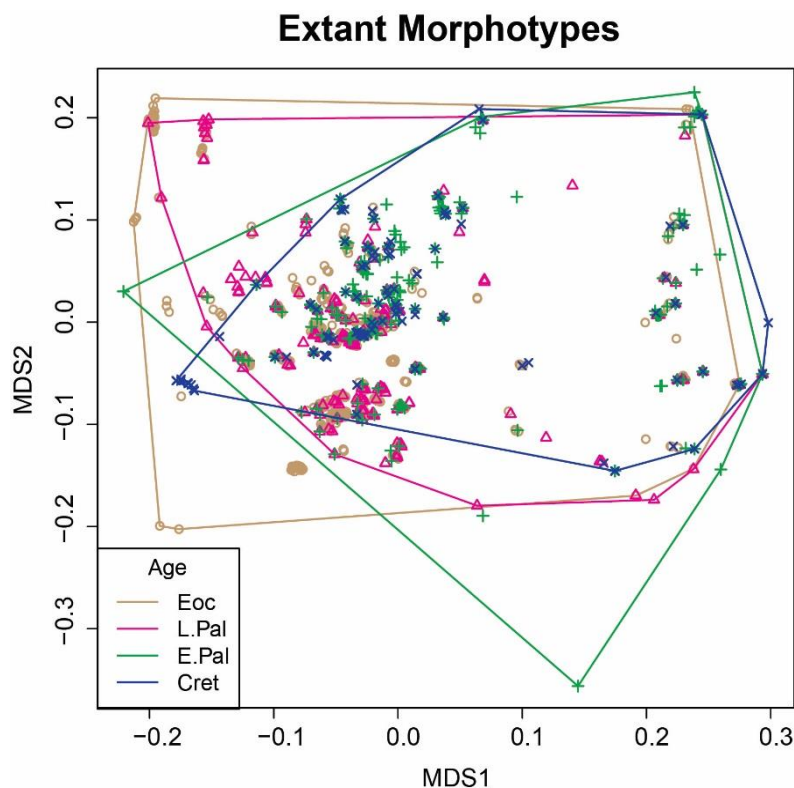


Figure 6-10: A fish tooth NMDS morphospace showing the extant morphotypes within four time bins: the Cretaceous (>66 Ma; blue), the Early Paleocene, (66-60 Ma; green), the Late Paleocene (55-60 Ma; pink), and the Eocene (55-42 Ma; brown). Each individual tooth observed in our dataset is plotted within the morphospace, and the convex hull for each time bin is outlined, representing morphospace occupied during that each time period.

While the Early Paleocene was a period of origination for many short-lived novel morphotypes (as seen previously in “Pulse 1” of the origination rate data; Figure 6-9), the Late Paleocene and Eocene fish teeth expanded into novel morphospace which persisted for the much of the remainder of the record (Figure 6-11). Overall, there is considerable overlap in the standing assemblages of teeth in each time period (Figure 6-10), with the vast majority of teeth falling within the regions established in the Cretaceous.

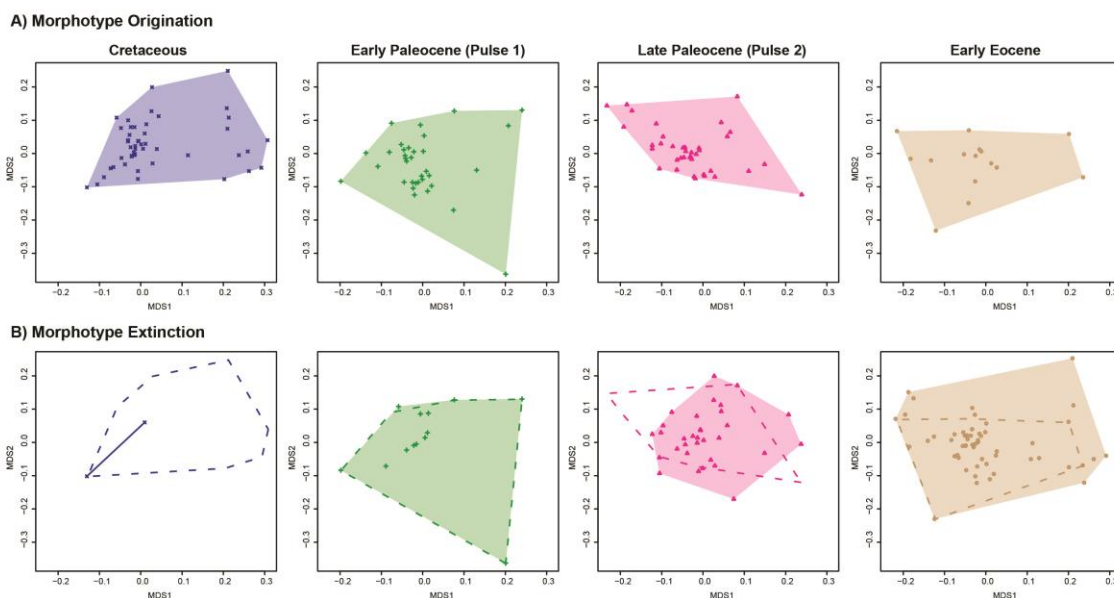


Figure 6-11: NMDS-based Morphospace occupation of tooth morphotypes which either (a) originated or (b) went extinct during each time bin: the Cretaceous (>66 Ma; blue), the Early Paleocene, pulse 1 (66-60 Ma; green), the Late Paleocene, pulse 2 (60-56 Ma; pink), and the Eocene (56-42 Ma; brown). Dotted outlines on lower (extinction) figures denote the morphospace occupation of morphotypes which originated during the same interval (the top row). Morphotypes persisting beyond our record into the Middle Eocene are plotted in gray.

6.5 Discussion

The Cretaceous-Paleogene mass extinction disrupted the stable Latest-Cretaceous pelagic fish community, which was dominated by three tooth morphotypes, while many others were present at low abundances. The Cretaceous had extremely low levels of extinction: all of the morphotypes which were present in the Cretaceous persisted to the K/Pg boundary, with most persisting into the Paleocene or Eocene. The estimated extinction rate in the Cretaceous is close to 0. Similar to the fossil plankton groups (e.g. calcareous nannofossils, Pospichal (1994)) and many other groups, there is no evidence for “stressed” fish communities in the latest Cretaceous (Schulte et al., 2010), suggesting

that any environmental change during the Latest Cretaceous was not a significant factor in fish tooth diversity or community structure. At the K/Pg, the extinction rate increased, and did not return to the Cretaceous values for the duration of the record, suggesting that the post-extinction fish community had more turnover. Furthermore, while there was very little morphotype extinction (2 out of 48), the two morphotypes that disappeared both represented the incumbent dominant fauna (Figure 6-4). Hence, it is plausible that the removal of these incumbents contributed to the subsequent diversification and expansion of ray-finned fishes in the open ocean in the Paleocene (Miya et al., 2013; Sibert and Norris, 2015).

The vast majority of teeth in all assemblages occupy a central region of the morphospace, and this does not change considerably during the study interval (Figure 6-10). However, there are evolutionarily interesting innovations in novel morphospace regions during the Paleocene and Early Eocene, which represent forms beyond the “typical” tooth, suggesting that fishes already had representatives in most possible ecological roles by the Latest Cretaceous – the vast majority of origination in the Paleocene and Eocene occurred within the established morphospace regions.

Novel morphotypes, which occupied considerably different morphospace regions than the incumbent Cretaceous fauna appeared during the first pulse of origination following the K/Pg extinction at approximately 63 Ma, however these were generally short-lived, with the majority of morphologically novel forms going extinct within the same time interval (Figure 6-11), though new morphotypes which fell within the same regions of morphospace as the Cretaceous fauna lasted longer into the Paleocene. This first origination pulse corresponds roughly to the period of elevated relative abundance of

large teeth in the system (Sibert and Norris, 2015). This suggests that there was a post-extinction “disaster fauna” of fishes which evolved in the early Paleocene while the ecosystem was recovering from the extinction event. However, these novel morphotypes were still a relatively small proportion of the total teeth, suggesting that their ecological roles were not a dominant part of the earliest Paleocene ecosystems.

The second pulse was a longer period of elevated origination rates, spanning 60 to 55 Ma. The majority of novel morphotypes which originated during this pulse fell within the morphospace bounds of a “typical fish tooth”, with fairly low disparity from the Cretaceous morphotypes, with little expansion in the morphospace occupied in the Late Paleocene beyond the range occupied by the Cretaceous Fauna (Figure 6-10). However, the late Paleocene radiation is associated with the development of a group of curved, flanged teeth (Figure 6-12) which have considerable morphological disparity, both within the morphotype group, and compared to the rest of the tooth morphotypes. Unlike most of the other extreme tooth forms which developed in the Paleocene, these flanged teeth persisted throughout the Early Eocene as some the most common morphotypes within assemblages, and apparently represent a radiation of truly novel fish during the development of the Eocene greenhouse world.



Figure 6-12: An example of the novel Late Paleocene/Early Eocene curved flanged tooth morphotype group.

Both the Cretaceous and Paleocene are periods of net origination, but origination rates drop to near 0 in the Eocene, while extinction rates remain elevated, leading to net extinction during the Early Eocene (Figure 6-9). Tooth diversity reaches a peak at the Paleocene/Eocene boundary, and decreases through the Early Eocene (Figure 6-8), even while the absolute abundance of teeth increases (Figure 6-7). The Early Eocene was a time of extreme global warmth (Zachos et al., 2008), and while tooth abundance appears to increase and decrease in concert with global temperature (Sibert et al., 2016), diversity declined during the entire interval, suggesting that taxonomic and ecological diversity of fish was decoupled from global temperature trends. It appears that the extreme warmth of the Early Eocene favored a rise in abundance, but not diversification of most groups of

fishes, favoring those best suited to survival in the greenhouse ecosystem, while others languished. However, the rates of extinction are not significantly higher in the Eocene than during the rest of the record: the extreme greenhouse conditions are only associated with reduced origination.

The morphotypes which went extinct in the Early Eocene had a much larger spread in the morphospace than those which survived into the middle Eocene (Figure 6-11). Many of the morphotypes that went extinct in the Early Eocene were more extreme forms that evolved in the Paleocene at the edges of the “typical tooth” morphospace area, whereas the persistent morphotypes, which survived into the middle Eocene are forms that were extant or very similar to those from the Cretaceous. Hence, it appears that the persistent extinction but low origination in the Eocene served to stabilize the open ocean fish community following the periods of extreme origination.

Both pulses of origination began prior to increases in total ichthyolith accumulation (Figure 6-7), suggesting that novelty preceded abundance in open ocean fishes during the Paleocene. Further, there is no change in morphological variance or community disparity during the record (Figure 6-13), across the K/Pg extinction or the during either of the pulses seen in origination data, suggesting that the extreme outliers in the tooth morphospace, while evolutionarily interesting, did not have a profound effect on the overall structure of the fish community.

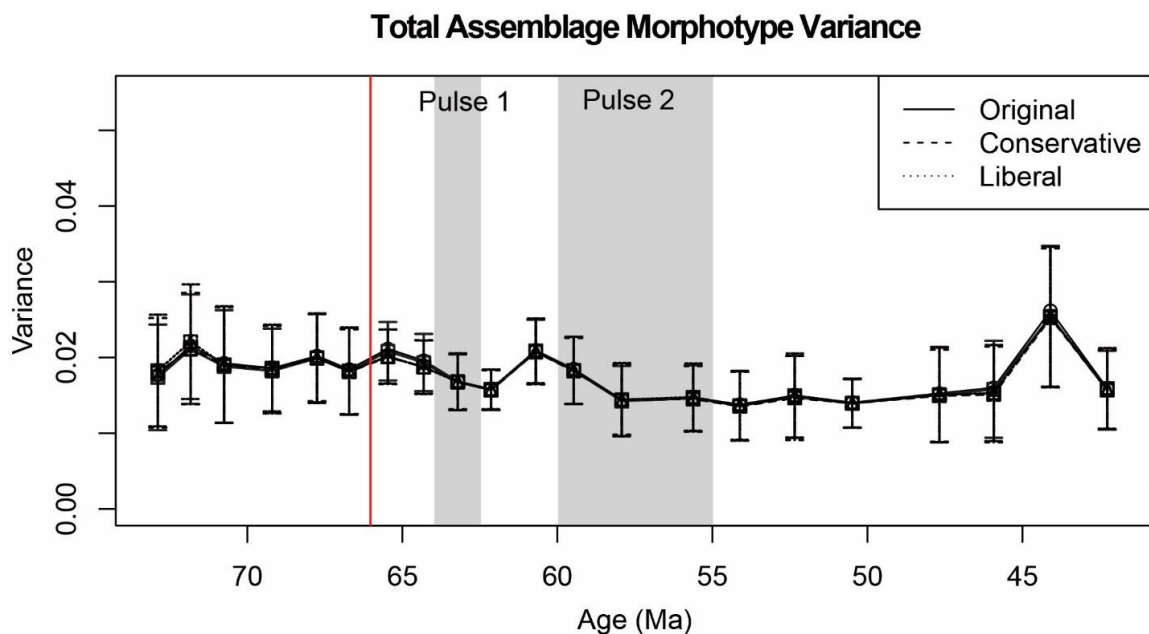


Figure 6-13: Multivariate variance of tooth disparity through time. Red vertical line is the K/Pg boundary, and error bars represent 95% confidence intervals based on bootstrap sampling.

These results suggest that the vast majority of evolutionary novelty in open ocean fishes following the K/Pg extinction developed during the Paleocene, hit its maximum diversity at the Paleocene/Eocene boundary, and stabilized during the Early Eocene. This is in contrast to the patterns observed in other open ocean plankton groups, such as planktonic foraminifera which have an initial radiation of extreme novelty in the early Paleocene, but do not hit peak diversity until the Early/Middle Eocene (Aze et al., 2011). However, the patterns of extinction for these clades are nearly opposite: while the fish saw an extinction of only two morphotypes of 48, only two planktonic foraminifera species out of 50 are thought to have survived the event. Calcareous nannofossils, which also suffered considerable extinction at the K/Pg reach peak diversity in the Middle to Late Eocene (Aubry, 1998). It is possible that while fishes were able to rapidly expand

their existing ecological niche space immediately following the extinction event, while planktonic foraminifera and calcareous nannofossils had to effectively start from scratch, thus taking a longer time to develop to their full ecological and evolutionary potential.

Further, this suggests that the evolutionary radiations of open-ocean taxa following the K/Pg extinction were led by the fish, a consumer group, rather than by the plankton, suggesting that the food web supporting fish in the Early Cenozoic was either relatively undamaged by the extinction event, or that fishes were readily able to adapt to the novel, post-disaster food web structure of the early Cenozoic.

6.6 Conclusion

The K/Pg extinction disrupted the stable Latest Cretaceous open ocean fish community, causing the extinction of the few dominant tooth morphotypes, and allowing for the diversification of the previously less abundant surviving groups. Further, the K/Pg extinction event changed the rates of origination and extinction in the group. In the aftermath of the extinction, there were two distinct pulses of origination during the Paleocene. The first, approximately 3 million years after the extinction event (63 Ma), included a number of extreme morphotypes, which were very different from the Cretaceous fauna, however these extreme forms did not persist. The second, longer-lasting pulse, occurred from 60-55 Ma, was composed mostly of diversification within existing morphologies, with one novel group persisting through the Eocene, even as the standing number of tooth morphotypes declined. Tooth morphotype diversity reached a peak in at the Paleocene/Eocene boundary, while total tooth abundance reached a peak nearly 5 million years later. The low levels of extinction in fishes at the K/Pg boundary,

and the rapid pace of their diversification, which was well ahead of most other pelagic groups, suggests that overall, the K/Pg mass extinction reset the open ocean fish community, allowing for fishes to diversify into novel ecological roles faster than groups which were harder hit, and laying the foundation for the high Cenozoic levels of diversity in the clade.

6.7 References

- Alfaro, M. E., Santini, F., Brock, C., Alamillo, H., Dornburg, A., Rabosky, D. L., Carnevale, G., and Harmon, L. J., 2009, Nine exceptional radiations plus high turnover explain species diversity in jawed vertebrates: Proceedings of the National Academy of Sciences, v. 106, no. 32, p. 13410-13414.
- Aubry, M.-P., 1998, Early Paleogene calcareous nannoplankton evolution: a tale of climatic amelioration: Late Paleocene Early Eocene climatic and biotic events in the marine and terrestrial records, edited by: Aubry, MP, Lucas, SG, and Berggren, WA, p. 158-203.
- Aze, T., Ezard, T. H., Purvis, A., Coxall, H. K., Stewart, D. R., Wade, B. S., and Pearson, P. N., 2011, A phylogeny of Cenozoic macroperforate planktonic foraminifera from fossil data: Biological Reviews, v. 86, no. 4, p. 900-927.
- Cooch, E., and White, G., 2006, Program MARK: a gentle introduction: Available in pdf format for free download at <http://www.phidot.org/software/mark/docs/book>.
- Doyle, P., Kennedy, G. G., and Riedel, W. R., 1974, Stratigraphy: Initial Reports of the Deep Sea Drilling Project, v. 26, Durban, South Africa to Fremantle, Australia; Sept.-Oct. 1972, p. 825-905.
- Doyle, P. S., Boillot, G., Winterer, E. L., Meyer, A. W., Applegate, J., Baltuck, M., Bergen, J. A., Comas, M. C., Davies, T. A., Dunham, K. W., Evans, C. A., Girardeau, J., Goldberg, D., Haggerty, J. A., Jansa, L. F., Johnson, J. A., Kasahara, J., Loreau, J.-P., Luna, E., Moullade, M., Ogg, J. G., Sarti, M., Thurow, J., and Williamson, M. A., 1988, Remarks on Cretaceous-Tertiary ichthyolith stratigraphy in the Atlantic, Ocean Drilling Program Leg 103: Proceedings of the Ocean Drilling Program, Scientific Results, v. 103, p. 445-458.
- Doyle, P. S., Dunsworth, M. J., and Riedel, W. R., 1977, Reworking of ichthyoliths in eastern tropical Pacific sediments: Deep-Sea Research, v. 24, no. 2, p. 181-198.

- Doyle, P. S., and Riedel, W. R., 1979a, Cretaceous to Neogene Ichthyoliths in a Giant Piston Core from the Central North Pacific: *Micropaleontology*, v. 25, no. 4, p. 337-364.
- Doyle, P. S., and Riedel, W. R., 1979b, Ichthyoliths: present status of taxonomy and stratigraphy of microscopic fish skeletal debris, La Jolla, CA, Scripps Institution of Oceanography, University of California, San Diego, Scripps Institution of Oceanography Reference Series.
- Doyle, P. S., and Riedel, W. R., 1985, Cenozoic and Late Cretaceous ichthyoliths, Cambridge, United Kingdom (GBR), Cambridge Univ. Press, Cambridge, Plankton stratigraphy.
- Doyle, P. S., Riedel, W. R., Thiede, J., Vallier, T. L., Adelseck, C. G., Boersma, A., Cepek, P., Dean, W. E., Fujii, N., Koporulin, V. I., Rea, D. K., Sancetta, C. A., Sayre, W. O., Seifert, K. E., Schaaf, A., Schmidt, R. R., Windom, K. E., and Vincent, E., 1981, Ichthyoliths at Site 464 in the Northwest Pacific, Deep Sea Drilling Project Leg 62: Initial Reports of the Deep Sea Drilling Project, v. 62, p. 491-494.
- Edgerton, C. C., Doyle, P. S., and Riedel, W. R., 1977, Ichthyolith age determinations of otherwise unfossiliferous Deep Sea Drilling Project cores: *Micropaleontology*, v. 23, no. 2, p. 194-205.
- Erwin, D. H., 1998, The end and the beginning: recoveries from mass extinctions: Trends in Ecology & Evolution, v. 13, no. 9, p. 344-349.
- Erwin, D. H., 2001, Lessons from the past: Biotic recoveries from mass extinctions: Proceedings of the National Academy of Sciences, v. 98, no. 10, p. 5399-5403.
- Foote, M., 1993, Discordance and concordance between morphological and taxonomic diversity: *Paleobiology*, v. 19, no. 02, p. 185-204.
- Foote, M., 2000, Origination and extinction components of taxonomic diversity: general problems: *Paleobiology*, v. 26, no. sp4, p. 74-102.
- Friedman, M., 2009, Ecomorphological selectivity among marine teleost fishes during the end-Cretaceous extinction: Proceedings of the National Academy of Sciences of the United States of America, v. 106, no. 13, p. 5218-5223.
- Friedman, M., 2010, Explosive morphological diversification of spiny-finned teleost fishes in the aftermath of the end-Cretaceous extinction: Proceedings of the Royal Society B-Biological Sciences, v. 277, no. 1688, p. 1675-1683.

- Friedman, M., and Sallan, L. C., 2012, Five hundred million years of extinction and recovery: a Phanerozoic survey of large-scale diversity patterns in fishes: *Palaeontology*, v. 55, no. 4, p. 707-742.
- Hull, P. M., Darroch, S. A. F., and Erwin, D. H., 2015, Rarity in mass extinctions and the future of ecosystems: *Nature*, v. 528, no. 7582, p. 345-351.
- Hull, P. M., Norris, R. D., Bralower, T. J., and Schueth, J. D., 2011, A role for chance in marine recovery from the end-Cretaceous extinction: *Nature Geoscience*, v. 4, p. 856-860.
- Jablonski, D., 2005, Mass extinctions and macroevolution: *Paleobiology*, v. 31, no. sp5, p. 192-210.
- Johns, M. J., Barnes, C. R., and Narayan, Y. R., 2005, Cenozoic and Cretaceous ichthyoliths from the Tofino Basin and western Vancouver Island, British Columbia, Canada: *Palaeontologia Electronica*, v. 8, p. no. 2, 202.
- Johns, M. J., Barnes, C. R., and Narayan, Y. R., 2006, Cenozoic ichthyolith biostratigraphy; Tofino Basin, British Columbia: *Canadian Journal of Earth Sciences = Revue Canadienne des Sciences de la Terre*, v. 43, no. 2, p. 177-204.
- Kozarek, R. J., 1978, Biostratigraphic analysis of ichthyoliths Master's]: University of Oregon.
- Kozarek, R. J., Orr, W. N., Donnelly, T. W., Francheteau, J., Bleil, U., Borella, P. E., Gartner, S., Juteau, T., Kelts, K., Quisefit, J. P., Rusinov, V., Salisbury, M., Sinton, J. M., Smith, B. M., Swift, S. A., Ui, T., Bryan, W. B., Robinson, P. T., Bollinger, C., Byerly, G., Emmermann, R., Hamano, Y., Levi, S., Miles, G. A., Pertsev, N., Ricou, L. E., Siesser, W. G., Stephen, R. A., Swanson, D. A., White, S., Flower, M. F. J., Bohrer, D., Hobart, M., Johnson, D., Mathez, E., Mevel, C., Pritchard, R. G., Puchelt, H., Rigotti, P. A., and Staudigel, H., 1980, Ichthyoliths, Deep Sea Drilling Project Legs 51 through 53: Initial Reports of the Deep Sea Drilling Project, v. Vol. 51, 52, 53, no. Part 2, p. 857-895.
- Laake, J. L., 2013, RMark: an R interface for analysis of capture-recapture data with MARK, US Department of Commerce, National Oceanic and Atmospheric Administration, National Marine Fisheries Service, Alaska Fisheries Science Center.
- Liow, L. H., and Nichols, J. D., 2010, Estimating rates and probabilities of origination and extinction using taxonomic occurrence data: capture-mark-recapture (CMR) approaches: *Alroy and Hunt*, p. 81-94.

- Marshall, C. R., 1997, Confidence intervals on stratigraphic ranges with nonrandom distributions of fossil horizons: *Paleobiology*, p. 165-173.
- McInerney, F. A., and Wing, S. L., 2011, The Paleocene-Eocene Thermal Maximum: A Perturbation of Carbon Cycle, Climate, and Biosphere with Implications for the Future: *Annual Review of Earth and Planetary Sciences*, v. 39, no. 1, p. 489-516.
- McKinney, M. L., 1997, Extinction Vulnerability and Selectivity: Combining Ecological and Paleontological Views: *Annual Review of Ecology and Systematics*, v. 28, p. 495-516.
- Menard, H. W., Natland, J. H., Jordan, T. H., Orcutt, J. A., Adair, R. G., Burnett, M. S., Kim, I. I., Lerner-Lam, A., Mills, W., Prevot, R., Riedesel, M. A., Ritzwoller, M. H., Rosencrantz, E. J., Shaw, P. R., Shearer, P. M., Smith, D. K., Toy, K. M., Trowell, S., Van Bruggen, C., Whitmarsh, R. B., and Willoughby, D. F., 1987, Site 596; hydraulic piston coring in an area of low surface productivity in the Southwest Pacific: *Initial Reports of the Deep Sea Drilling Project*, v. 91, p. 245-267.
- Miya, M., Friedman, M., Satoh, T. P., Takeshima, H., Sado, T., Iwasaki, W., Yamanoue, Y., Nakatani, M., Mabuchi, K., and Inoue, J. G., 2013, Evolutionary origin of the scombridae (tunas and mackerels): members of a paleogene adaptive radiation with 14 other pelagic fish families: *Plos One*, v. 8, no. 9, p. e73535.
- Near, T. J., Dornburg, A., Eytan, R. I., Keck, B. P., Smith, W. L., Kuhn, K. L., Moore, J. A., Price, S. A., Burbrink, F. T., Friedman, M., and Wainwright, P. C., 2013, Phylogeny and tempo of diversification in the superradiation of spiny-rayed fishes: *Proceedings of the National Academy of Sciences*, v. 110, no. 31, p. 12738-12743.
- Near, T. J., Eytan, R. I., Dornburg, A., Kuhn, K. L., Moore, J. A., Davis, M. P., Wainwright, P. C., Friedman, M., and Smith, W. L., 2012, Resolution of ray-finned fish phylogeny and timing of diversification: *Proceedings of the National Academy of Sciences of the United States of America*, v. 109, no. 34, p. 13698-13703.
- Nelson, J. S., 2006, *Fishes of the World*, New York, NY, Wiley, 600 p.:
- Pospichal, J. J., 1994, Calcareous nannofossils at the KT boundary, El Kef: No evidence for stepwise, gradual, or sequential extinctions: *Geology*, v. 22, no. 2, p. 99-102.
- R Core Team, 2014, *R: A language and environment for statistical computing*. Vienna, Austria: R Foundation for Statistical Computing; 2013.

- Raup, D. M., 1981, Extinction: bad genes or bad luck?: *Acta geológica hispánica*, v. 16, no. 1, p. 25-33.
- Riedel, W. R., 1978, Systems of morphologic descriptors in paleontology: *Journal of Paleontology*, v. 52, no. 1, p. 1-7.
- Sahney, S., Benton, M. J., and Ferry, P. A., 2010, Links between global taxonomic diversity, ecological diversity and the expansion of vertebrates on land: *Biology Letters*, v. 6, no. 4, p. 544-547.
- Schulte, P., Alegret, L., Arenillas, I., Arz, J. A., Barton, P. J., Bown, P. R., Bralower, T. J., Christeson, G. L., Claeys, P., Cockell, C. S., Collins, G. S., Deutsch, A., Goldin, T. J., Goto, K., Grajales-Nishimura, J. M., Grieve, R. A. F., Gulick, S. P. S., Johnson, K. R., Kiessling, W., Koeberl, C., Kring, D. A., MacLeod, K. G., Matsui, T., Melosh, J., Montanari, A., Morgan, J. V., Neal, C. R., Nichols, D. J., Norris, R. D., Pierazzo, E., Ravizza, G., Rebolledo-Vieyra, M., Reimold, W. U., Robin, E., Salge, T., Speijer, R. P., Sweet, A. R., Urrutia-Fucugauchi, J., Vajda, V., Whalen, M. T., and Willumsen, P. S., 2010, The Chicxulub Asteroid Impact and Mass Extinction at the Cretaceous-Paleogene Boundary: *Science*, v. 327, no. 5970, p. 1214-1218.
- Sibert, E. C., Cramer, K. L., Hastings, P. A., and Norris, R. D., In review, Methods for isolation and quantification of microfossil fish teeth and elasmobranch dermal denticles (ichthyoliths) from marine sediments.
- Sibert, E. C., and Norris, R. D., 2015, New Age of Fishes initiated by the Cretaceous–Paleogene mass extinction: *Proceedings of the National Academy of Sciences*, v. 112, no. 28, p. 8537-8542.
- Sibert, E. C., Norris, R. D., Cuevas, J. M., and Graves, L. G., 2016, 85 million years of Pacific Ocean Gyre ecosystem structure: long-term stability marked by punctuated change: *Proceedings of the Royal Society B: Biological Sciences*, no. In press.
- Streelman, J., Webb, J., Albertson, R., and Kocher, T., 2003, The cusp of evolution and development: a model of cichlid tooth shape diversity: *Evolution & Development*, v. 5, no. 6, p. 600-608.
- Tway, L. E., 1977, Pennsylvanian ichthyoliths from the Shawnee Group of eastern Kansas [Master's]: University of Oklahoma.
- Tway, L. E., 1979, A coded system for utilizing ichthyoliths of any age: *Micropaleontology*, v. 25, no. 2, p. 151-159.

- Tway, L. E., and Riedel, W. R., 1991, Prototype expert system to assist in ichthyolith identifications, *in* Emry, R. J., and Sues, H.-D., eds., *Journal of Vertebrate Paleontology*, Volume 11: Norman, University of Oklahoma, p. 58-59.
- Wagner, P. J., Kosnik, M. A., and Lidgard, S., 2006, Abundance distributions imply elevated complexity of post-Paleozoic marine ecosystems: *Science*, v. 314, no. 5803, p. 1289-1292.
- White, G. C., and Burnham, K. P., 1999, Program MARK: survival estimation from populations of marked animals: *Bird study*, v. 46, no. S1, p. S120-S139.
- Winfrey, E. C., and Doyle, P. S., 1984, Preliminary ichthyolith biostratigraphy, Southwest Pacific, DSDP sites 595 and 596, *Eos, Transactions, American Geophysical Union*, Volume 65: Washington, American Geophysical Union, p. 949.
- Zachos, J. C., Dickens, G. R., and Zeebe, R. E., 2008, An early Cenozoic perspective on greenhouse warming and carbon-cycle dynamics: *Nature*, v. 451, no. 7176, p. 279-283.
- Zhou, L., and Kyte, F. T., 1992, Sedimentation history of the South Pacific pelagic clay province over the last 85 million years inferred from the geochemistry of Deep Sea Drilling Project Hole 596: *Paleoceanography*, v. 7, no. 4, p. 441-465.
- Zhou, L., Kyte, F. T., and Bohor, B. F., 1991, Cretaceous/Tertiary boundary of DSDP Site 596, South Pacific: *Geology*, v. 19, no. 7, p. 694-697.

6.8 Appendix I: A novel coding scheme for quantifying the morphological variation of tooth-type ichthyoliths

6.8.1 Introduction

The identification and description of ichthyoliths has been a particular challenge to micropaleontologists working on the fossil group. As they are difficult or impossible to classify taxonomically, a non-hierarchical character/state coding system is appropriate for working with ichthyolith morphology. One such system was developed for ichthyoliths by Doyle Kennedy and Riedel (1974), and used extensively in the 1970s and 1980s to identify ichthyoliths in marine sediments (Doyle et al., 1974; Doyle et al., 1988; Doyle et al., 1977; Doyle and Riedel, 1979a, b; Doyle and Riedel, 1985; Doyle et al., 1981; Edgerton et al., 1977; Johns et al., 2005; Johns et al., 2006; Kozarek, 1978; Kozarek et al., 1980; Riedel, 1978; Tway, 1979; Winfrey and Doyle, 1984). This ichthyolith coding and classification scheme had incredible flexibility, in that it could be modified for use with novel ichthyolith morphotypes and assemblages, simply by the addition of characters or traits (e.g. Riedel, 1978; Tway, 1979). However, the system has a number of limitations, which precluded it from gaining traction in the scientific community.

First, the coding system failed to differentiate between teeth and dermal scales (denticles). While both of these microfossils are composed of calcium phosphate, they are from different clades of animals (denticles are restricted to chondrichthyans, while teeth are found in all marine vertebrates), and have different ecological and functional roles: teeth are found on the inside of the mouth, used in prey handling, while denticles form an overlapping skin that enhances the hydrodynamics of the organisms. Further, teeth and

denticles have different morphological traits, and combining them in the same classification scheme needlessly increases the complexity of the system.

Second, the existing ichthyolith coding systems are based on transmitted-light microscopy, with ichthyoliths mounted in optical medium on glass slides. As ichthyoliths are not radially symmetrical, and the vast majority of ichthyoliths have a three-dimensional structure, the orientation of ichthyoliths on the slide can change the interpretation of particular characters. Additionally, certain structures and traits are missed when transmitted light microscopy, such as the shape of the base of the tooth, or the shape and structure of blades present on certain regions of the fossil. Further, ichthyoliths fixed in optical medium for transmitted light microscopy are unusable for future study, such as advanced imaging (eg. Scanning Electron Microscopy), or geochemical analysis.

Finally, existing ichthyolith morphological character code schemes generate long alpha-numeric “names”, which, while helpful in defining the morphological variation of a particular ichthyolith, are difficult to remember or ascribe meaning. The code included syntax to allow for multiple character-states to be present within one trait, further complicating the system. A series of “colloquial names”, 3-4 keyword word combinations that helped to describe the individual ichthyoliths was introduced as well (Doyle et al., 1974), however the alpha-numeric codes remained the primary way to identify ichthyolith subtypes in the literature.

Here we use a new ichthyolith classification coding scheme, and apply it to microfossil teeth from the South Pacific Gyre, spanning the Cretaceous through the Eocene. We build upon the prior classification schemes of (Doyle and Riedel, 1979b;

Doyle and Riedel, 1985; Johns et al., 2005; Johns et al., 2006; Tway, 1979), addresses some of the challenges presented by these methods. The ichthyolith classification scheme used in this manuscript considers only tooth-type ichthyoliths, and uses reflected light microscopy. We considerably simplify the trait-coding system by having only one level of characters which apply to all teeth, rather than a series of successively nested characters that apply to specific groups of teeth. Further, while our system does generate an alpha-numeric string that uniquely identifies a particular ichthyolith, we have also assigned colloquial names to each morphotype, drawing on the character-state vocabulary used in the coding system. While our system currently applies only to a subset of microfossil teeth (Cretaceous-Eocene, South Pacific), it can easily be modified to include additional characters or traits as novel tooth morphotypes are identified and coded, simply by adding additional character-states or even characters if necessary. This system lends itself to straightforward computational analysis, as each tooth trait character is coded numerically, with the same characters for all tooth morphotypes – where a character is not present, it is coded as a 0. While the system is still a work in progress, it represents a substantial step forward in the field of ichthyolith morphological systematics.

6.8.2 Coding System

We define 22 traits for tooth morphology, within 6 trait groups: general shape/structure, blades (if any), flange (if any), tip shape, base shape, and pulp cavity. While general shape is important for differentiating broad groups of teeth, the majority of variation is within the shape of the pulp cavity, the size and structure of the blades, and composition of the tip, all traits that are distinguishable with reflected light microscopy

and high resolution imaging. Using this system, we identified a series of 136 ichthyolith morphotypes in our dataset, where each individual ichthyolith morphotype is defined as a unique set of character-states within the system. Similarly to prior ichthyolith coding schemes, we define a set of characters, each with a series of character-states. While this system is currently designed for handling ichthyoliths from the South Pacific Cretaceous to Eocene, it is straightforward to add novel character states or even whole characters into the analysis. Our ichthyolith coding scheme, with illustrations, follows. Throughout, tooth character-groups are denoted in bold, individual traits are denoted as underline, and any specific notes clarifying identification or differentiation of a particular character state are noted in italics. Pictorial representations of these traits are shown in Figure 6-3.

Section 1: General Ichthyolith Classification and identifiers:

Trait A: Ichthyolith type. *While our system currently only has coded traits for teeth, denticles are present and common in our ichthyolith assemblages, and are quantified here.*

1 = Tooth

2 = Denticle

3 = Other

Trait B: Degree of Fragmentation. *Level of fragmentation determines whether the outline-based morphometrics (length/width/aspect ratio; traits LEN, WID, AR) are included in the morphospace analysis, while outline data is not. However, in future studies, tooth outlines may be used, and as such, the teeth are classified to include a differentiation here.*

1 = No fragmentation; entire ichthyolith is preserved. *Outline and LEN/WID/AR appropriate for analysis*

2 = Small amounts of fragmentation, whole ichthyolith is identifiable.

LEN/WID/AR appropriate for analysis

3 = Fragmentation is considerable, but most traits are discernable; ichthyolith is identifiable to morphotype. *Only qualitative descriptors, no measurement data used in final analysis*

4 = Fragmentation is too great to identify morphological characters, but the ichthyolith is identifiable to tooth or denticle

Section 2: Tooth Morphological Characters

Notes: Throughout, the “base” and “bottom” of the tooth refers to the part of the tooth which connects to the jawbone, and the “tip” and “top” refers to the part of the tooth opposite the base, most often a pointed end.

2.1. General ichthyolith shape

Trait C: Overall shape of ichthyolith: *There are many additional potential generic ichthyolith shapes, however none of these were present in this sample set. As such, we include the note that for very different shapes, character-states can be added to this system.*

1 = Cone (tooth starts wide, goes to a small tip, eg. triangular in shape; has round base in cross-section)

2 = Triangle (tooth starts wide, goes to small tip, eg. triangular in shape; has flattened base cross-section)

3 = Asymmetrical triangle with flared base (approximately triangular in shape, has base which flares out from tooth and is not symmetrical)

4 = Flat, cusped

Trait E: Degree of curvature

1 = Straight; Tip centered above base

2 = Small curve: tip does not pass edge of tooth base

3 = Large curve: tip extends past base edge

Trait F: Shape of triangle

1 = Straight (tip centered above base)

2 = Concave edges (tip centered above base)

3 = Convex edges (tip centered above base)

4 = Curved (concavo-convex; tip not centered)

5 = plano-convex (right angle from base to tip, convex hypotenuse; tip not centered)

6 = Right Triangle (right angle from base to tip; hypotenuse straight)

Trait G: Shape of edges

1 = No obvious edge (eg. tooth is cone-shaped [Trait C1])

2 = Defined edge, no extended edge/blade

3 = Has a blade or extended edge

Edge Details: Blades (H1-H5) and Flanges (K1-K2)

Notes: “blades” are defined as edge-details which extend from the side of a tooth, lengthwise, and do not have abrupt beginnings or endings. They can reach the top or

bottom of the tooth, but it is not necessary. “Flanges” are edge details which extend from the side of a tooth, and begin at the tip, and which have an abrupt ending partway down the tooth. If the tooth has no blade or no flange, this is encoded with values of 1 in Trait H1 and Trait K1 respectively. All other traits are coded as 0, and not considered in the morphological analysis for those teeth.

Trait H1: Number of blades: *note that the numeric coding does not correspond directly with the absolute number of blades for this trait.*

1 = no blades

2 = both sides have blades (2 blades)

3 = One side has a blade only

Trait H2: Blade symmetry:

0 = no blades

1 = Blades are symmetrical

2 = Blades are asymmetrical (but two are present)

3 = One blade only

Trait H3: Blade width along edge: *while some blades are approximately the same size along the tooth, others flare at the top or bottom.*

0 = no blades

1 = equal sized along length

2 = wider at the top

3 = wider at the bottom

4 = widest in the middle

5 = different each blade; *Note that asymmetrical blades may fall into any H3 character state, as it simply describes the overall shape of the blades.*

Trait H4: Blade size: *describes the relative size of blades present, compared to the tooth proper*

0 = no blades

1 = small blades, both sides (blades combined $< 1/4$ of width of tooth)

2 = large blades, both sides (blades combined $> 1/4$ of width of tooth)

3 = One small, one large

4 = Concave large, convex/straight small (for non-straight teeth)

5 = convex large, concave/straight small (for non-straight teeth)

Trait H5: Blade length: *note: additional character states are possible for novel tooth morphotypes*

0 = no blades

1 = Blade runs length of tooth, from tip to base

2 = Top $1/3$ of tooth only

3 = Top $2/3$ of tooth only

4 = Bottom $1/3$ of tooth only

5 = bottom $2/3$ of tooth only

6 = concave whole length; convex upper part only

7 = large blade runs whole length; small blade runs upper part only

Trait K1: Flange length: *relative to the total tooth size*

1 = no flange

2 = small ($< 1/4$ of tooth length)

3 = medium (1/4-1/2 of tooth length)

4 = long (>1/2 of tooth length)

5 = very long (>80% length)

Trait K2: Flange location:

0 = no flange

1 = concave only

2 = convex or straight side

3 = one side (for an otherwise symmetrical tooth)

Tip (L, M) and base (N1, N2) characters

Trait L: Tip shape

0 = tip not preserved

1 = Pointed tip

2 = smoothed point

3 = rounded

Trait M: Tip material: *note that many actinopterygian teeth have a small layer of acrodin,*

a modified bone material, as a slight cap on their teeth. Here we assess whether teeth

have tips made of different material than the rest of the tooth.

0 = tip not preserved

1 = same material as rest of tooth

2 = thin layer just over the tip

3 = Whole tip, with flat bottom

4 = Tip and blades

5 = More than tip/blades

Trait N1: Base shape

0 = base not preserved

1 = flat base

2 = concave base (*often has 'base tips', trait N2*)

3 = convex base

4 = asymmetrical base with base tip(s)

5 = flared base (*often correlates with Trait C-3*)

Trait N2: Base tip shape: *if only one tip, assess the single one*

0 = no base preserved

1 = no tips

2 = curved tip(s)

3 = pointed tip(s) (straight)

4 = flat/square tip(s)

5 = asymmetrical tips (two, different)

Pulp cavity size (O-Q) and morphology (R1-R4): *nearly all teeth have some sort of pulp cavity, however some teeth are fully solid and have no obvious pulp cavity. The pulp cavity is often best viewed using transmitted light microscopy, but is visible in high-magnitude reflected light microscopy as well. As pulp cavity morphology is highly variable, we have defined four characters which, when considered together, describe an overall structure for the pulp cavity. While there are some characters that often link together, there are many which can be combined in different permutations to create*

unique pulp cavity shapes. If there is no pulp cavity, Trait O the only one which counts in the morphospace analysis. The rest are considered a value of 0, which discounts them from the analysis.

Trait O: Is there a pulp cavity?

1 = no pulp cavity present

2 = pulp cavity present

Trait P: Pulp cavity base size: *this is measured relative to the base of the whole tooth*

0 = no pulp cavity

1 = small (<1/3 of base width)

2 = medium (1/3 – 2/3 of base width)

3 = large (>2/3 of base width)

4 = whole base (base of pulp cavity extends to both edges of the tooth)

Trait Q: Pulp cavity length: *measured relative to the whole tooth*

0 = no pulp cavity

1 = short (<1/3 of tooth length)

2 = medium (1/3 – 2/3 of tooth length)

3 = large (>2/3 of tooth length)

4 = full length (pulp cavity stretches to the tip of the tooth)

Trait R1: Pulp cavity approximate shape, in relation to tooth shape: *if tooth is curved, a curved pulp cavity which mirrors the curve of the tooth is considered 'straight', etc.*

0 = no pulp cavity

1 = straight

2 = concave (curves in from the tooth edges)

3 = convex (curves out from the tooth edges)

4 = funnel (convex at the bottom, concave at the top)

5 = parallel (pulp cavity edges are parallel to each other, not to the tooth edges)

6 = asymmetrical (pulp cavity combines any two other pulp cavity shape

descriptors)

7 = vase-shaped (concave at base, rounded at top)

Trait R2: Pulp cavity center width, in relation to the tooth edges: *here “center” is defined as the middle, length-wise, of the pulp cavity, not the tooth.*

0 = no pulp cavity

1 = small, pulp cavity center width is $<1/3$ of tooth width

2 = medium, pulp cavity center width is $1/3$ to $3/4$ of tooth width

3 = large, pulp cavity center width is $>3/4$ of tooth width

Trait R3: Pulp cavity base shape

0 = no pulp cavity

1 = curve out towards edges of tooth

2 = flat (no change from the rest of the pulp cavity shape)

3 = curve in, away from edges of tooth

Trait R4: Pulp cavity tip shape

0 = no pulp cavity

1 = pointed *goes to obvious angular point*

2 = rounded point *pointed, but no angular tip*

3 = very rounded *nearly semi-circular in many cases*

4 = pinched tip (rounded, wide) *can see area in the tip*

5 = pinched tip (extended, thin) *often appears to be single line at the top*

6 = rounded with tip *similar to state #3, but with an angular tip*

The final traits included in our morphospace analysis are LEN, WID, and AR. These traits are measured as the “length”, “width”, and “aspect ratio” of the minimum bounding box that surrounds a tooth, when the tooth is placed flat so its widest surface is facing up. These traits are only included in the analysis if the image and tooth are of sufficient quality to obtain appropriate measurements.

6.8.3 Morphotype Designation

Individual morphotypes were defined as teeth with unique combinations of traits. As our ichthyolith morphological scheme is currently in development, and there is no taxonomic identification for these teeth, we believe that it would be premature to develop and apply a formal naming scheme to the different tooth morphotypes. However, as strings of alpha-numeric codes are cumbersome and do not easily convey information, we have developed a series of working names for the tooth morphotypes identified in this study. These names are a combination of character-trait keywords which capture the essence of the tooth, and facilitated repeated visual identification of morphotypes. We fully expect that these names will change as the morphological scheme continues to expand and develop to include other morphotypes. A morphotype was considered “distinct” when it had a unique set of coded characters, regardless of how large or small the differences were.

6.9 Appendix II: Rules used for removing potentially reworked teeth from analysis.

Red clays are very useful for working with ichthyoliths, since their slow sedimentation rate concentrates the microfossils. However, they are susceptible to bioturbation, which can move teeth up or down 10 or more centimeters in the sediment column. There is not evidence for large amounts of bioturbation (within the record), but it is likely that some of the individual teeth have been moved up or down the sediment column, either through bioturbation, or by sticking to the drill pipe during the recovery process. As such, we considered three scenarios by which to analyze our data and calculate the evolutionary rate and NMDS metrics: the original dataset, with all tooth occurrences included, a dataset which makes some conservative assumptions about the occurrences of teeth which may have been reworked and removes them from the analysis, which was used in the main figures and a dataset which makes some more liberal assumptions about occurrences of teeth which may have been reworked and therefore removed from the analysis. While all three datasets yield the same major conclusions, the average range length is shortest, and extinction rate is highest in for the liberal set, since it removes the unlikely singleton occurrences that greatly extend range duration as zombie taxa. A comparison of the range charts for all three datasets is shown in Figure 6-14.

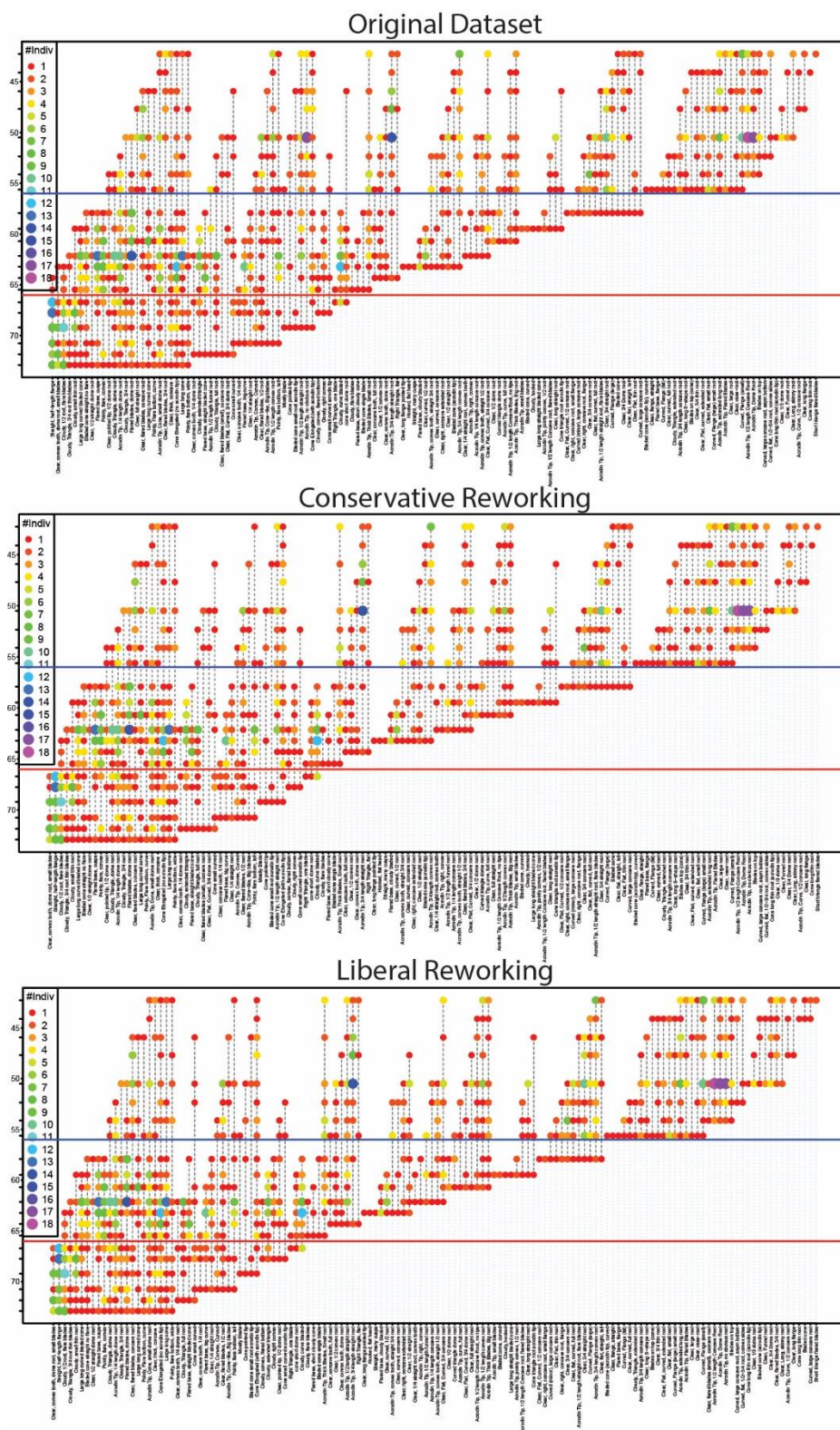


Figure 6-14: Stratigraphic range charts of all ichthyolith morphotypes for each of the three levels of reworking considered. Full legend in Figure 6-4.

6.9.1 Conservative reworking rules

Remove a data point if:

1. Suspected zombie taxa: if abundance decreases from >3 per time bin to 1 per time bin and lasts <1 million years across a known geologic boundary (either the K/Pg or the P/E)
2. Suspected reworking: if there is an interval of >5 myr between a singleton occurrence of a morphotype, before or after an interval where the morphotype is not rare (eg. present in at least 2 time bins in a row)
3. Suspected reworking: if there is an interval of >8 myr, only single occurrence, assume reworking of the morphotype away from most common time intervals which it is present (not necessary to be present in two consecutive time bins, as in rule 2)

Table 6-1: Teeth removed from analysis under conservative reworking dataset rules (10 total).

Tooth Morphotype Name	Tooth Object ID	Action	Rule
Straight, half-length flange	P136.084.1.obj00024 P137.085.1.obj00022	remove upper 2 samples	1
Clear, convex tooth, dome root, small blades	P127.075.1.obj00076	remove upper 1 sample	1
Clear, full straight root	P175.123.1.obj00031	Remove lower 1 sample	2/3
Clear, flared blades, 3/4 root	P173.121.1.obj00002	Remove lower 1 sample	2/3
Acrodin Tip, 1/2 length funnel root	P169.117.1.obj00011	Remove lower 1 sample	3
Acrodin Tip, 1/2 length convex root	P163.111.1.obj00004	Remove lower 1 sample	2/3
Acrodin Tip, no obvious root	P158.106.1.obj00012	remove lower 1 sample	2/3
cone short dome root	P065.013.1.obj00019	Remove upper 1 sample	2
Clear, 3/4 Dome root	P109.057.1.obj00033	remove lower 1 sample	2

6.9.2 Liberal reworking rules

Remove teeth from the dataset if they meet the criteria for conservative cuts OR the following:

4. If common during range (>2 per time bin, no long intervals), singleton present >3 myr before common range (mixed down)
5. If common during range (>2 per time bin, no long intervals), any individuals >5 myr above common range (mixed up)
6. If the morphotype is rare (eg. present as a singleton occurrence throughout range, with intervals of non-presence <5myr), any gaps >12 million years, remove singleton at end of gap.

Table 6-2: Teeth removed from analysis under liberal reworking dataset rules (14 total).

Tooth Morphotype Name	Tooth Object ID	Action	Rule
Clear, pointed tip, 1/2 dome root	P175.123.1.obj00008	Remove lower 1 sample	4
Clear, flared blades, 3/4 root	P116.064.1.obj00037; P124.072.1.obj00090	Remove next lowest 2	4
Cloudy, extended triangle	P168.116.1.obj00022	Remove lower 1 sample	4
Cloudy, Triangle, full root	P085.033.1.obj00031; P098.046.1.obj00102	Remove upper 2 sample	5
Clear, flared blades (small), concave root	P168.116.1.obj00019	remove 1 lower sample	6
Clear, Flat, Curved, 3/4 dome root	P170.118.1.obj00006	remove 1 lower sample	6
Acrodin Tip, 1/2 length straight root	P156.104.1.obj00012	remove 1 lower sample	4
Bladed cone (acrodin tip)	P129.077.1.obj00023	remove lower 1 sample	6
Acrodin Tip, 3/4 length convex root	P131.079.1.obj00076	remove 1 lower sample	4
Bladed cone	P105.053.1.obj00019	remove 1 lower sample	6
Clear, Flat, thin root	P053.001.1.obj00070	remove 1 upper sample	5
Curved, large concave root	P105.053.1.obj00057	remove 1 lower sample	6

6.10 Acknowledgements

E. C. S. was funded by an NSF predoctoral fellowship and a Smithsonian Institution Peter Buck Predoctoral Fellowship at the Smithsonian National Museum of Natural History. Special thanks to P. Hull and L. Elder for help with image processing, M. Friedman for morphotype discussion, G. Hunt, for direction with evolutionary rate modeling, and the SIO Department for research travel funding.

Chapter 6 is in preparation for publication as Sibert, E. C., Friedman, M., Hull, P. M., Hunt, E., and Norris, R. D. “A two-pulsed radiation of pelagic fishes following the K/Pg mass extinction”. The dissertation author was the primary investigator and author of this manuscript.

CHAPTER 7

**85 million years of Pacific Ocean gyre ecosystem structure: long-term stability
marked by punctuated change**

PROCEEDINGS B

rspb.royalsocietypublishing.org

CrossMark
click for updates

Research

Cite this article: Sibert E, Norris R, Cuevas J, Graves L. 2016 Eighty-five million years of Pacific Ocean gyre ecosystem structure: long-term stability marked by punctuated change. *Proc. R. Soc. B* **283**: 20160189. <http://dx.doi.org/10.1098/rspb.2016.0189>

Received: 27 January 2016

Accepted: 20 April 2016

Subject Areas:

palaeontology, evolution, ecology

Keywords:

fish, elasmobranch, shark, pelagic ecosystem evolution, ichthyoliths

Author for correspondence:Elizabeth Sibert
e-mail esibert@ucsd.edu

Electronic supplementary material is available at <http://dx.doi.org/10.1098/rspb.2016.0189> or via <http://rspb.royalsocietypublishing.org>.

THE ROYAL SOCIETY
PUBLISHING

Eighty-five million years of Pacific Ocean gyre ecosystem structure: long-term stability marked by punctuated change

Elizabeth Sibert¹, Richard Norris¹, Jose Cuevas² and Lana Graves¹¹Scripps Institution of Oceanography, University of California San Diego, La Jolla, CA 92037, USA²Department of Environmental and Ocean Sciences, University of San Diego, San Diego, CA 92110, USA

ES, 0000-0003-0577-864X

While the history of taxonomic diversification in open ocean lineages of ray-finned fish and elasmobranchs is increasingly known, the evolution of their roles within the open ocean ecosystem remains poorly understood. To assess the relative importance of these groups through time, we measured the accumulation rate of microfossil fish teeth and elasmobranch dermal denticles (ichthyoliths) in deep-sea sediment cores from the North and South Pacific gyres over the past 85 million years (Myr). We find three distinct and stable open ocean ecosystem structures, each defined by the relative and absolute abundance of elasmobranch and ray-finned fish remains. The Cretaceous Ocean (pre-66 Ma) was characterized by abundant elasmobranch denticles, but low abundances of fish teeth. The Palaeogene Ocean (66–20 Ma), initiated by the Cretaceous/Palaeogene mass extinction, had nearly four times the abundance of fish teeth compared with elasmobranch denticles. This Palaeogene Ocean structure remained stable during the Eocene greenhouse (50 Ma) and the Eocene–Oligocene glaciation (34 Ma), despite large changes in the overall accumulation of both groups during those intervals, suggesting that climate change is not a primary driver of ecosystem structure. Dermal denticles virtually disappeared from open ocean ichthyolith assemblages approximately 20 Ma, while fish tooth accumulation increased dramatically in variability, marking the beginning of the Modern Ocean. Together, these results suggest that open ocean fish community structure is stable on long timescales, independent of total production and climate change. The timing of the abrupt transitions between these states suggests that the transitions may be due to interactions with other, non-preserved pelagic consumer groups.

1. Introduction

Ray-finned fishes (Actinopterygii) are a ubiquitous part of nearly all modern marine ecosystems. Both molecular and fossil studies have shown that while the actinopterygian lineage originated over 400 Ma, the great diversity of modern ray-finned fish in marine environments developed relatively recently, during the past 100 million years (Myr) [1–3]. Shark diversity, conversely, developed much earlier, with the vast majority of family-level diversity established between 250 and 100 Ma [4–6]. Yet, the structure and function of pelagic ecosystems are not only defined solely by the taxonomic diversity of organisms present, but also involve the roles and relative abundance of these taxa within pelagic food webs. The abundance of top predators, including pelagic sharks, fish such as tunas and billfish, seabirds and marine mammals, depends upon an efficient food chain and enough primary productivity to support large biomass, high trophic-level organisms [7,8], as well as how that energy is distributed between competing taxa [9].

We assess the ecological importance of pelagic ray-finned fish and elasmobranchs (sharks, skates and rays), by using the microfossil record of ichthyoliths, the mineralized teeth and dermal scales (denticles) of ray-finned fish and

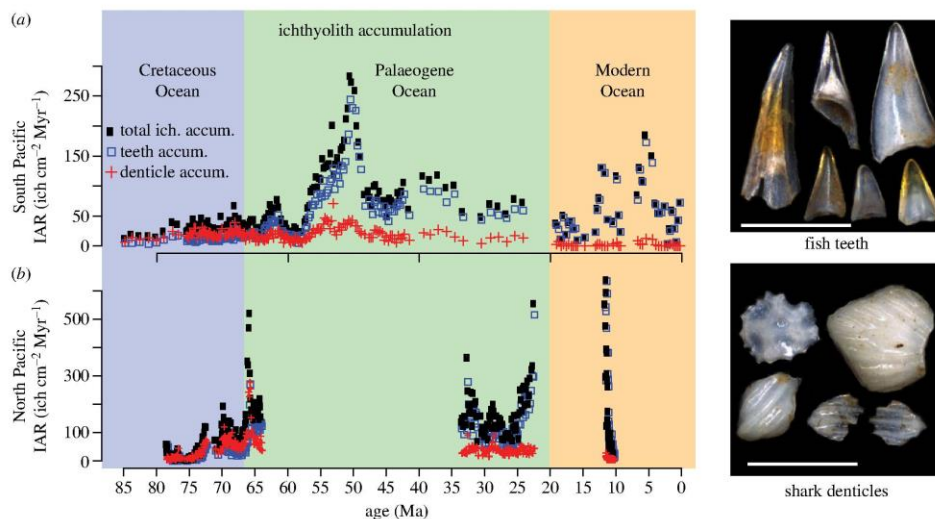


Figure 1. Eighty-five million year accumulation records from (a) DSDP Site 596 in the South Pacific and (b) ODP Site 886 in the North Pacific, showing total ichthyolith accumulation (black filled squares) split into tooth accumulation (blue open squares) and denticle accumulation (red plus signs). The three ocean ecosystem states are indicated by shaded boxes (Cretaceous is blue, Palaeogene is green and Modern is orange). Note the peak in ichthyolith accumulation in the Early Eocene, and the high variability of the Modern Ocean. Images are of representative Eocene-age fish teeth and elasmobranch denticles. Scale bar, 500 μm .

elasmobranchs, respectively (figure 1). Their calcium phosphate composition makes ichthyoliths highly resistant to dissolution; they are among the most robust fossils of any kind, and are often preserved even when all other microfossils are dissolved [10,11]. The history of open ocean fish and elasmobranch communities is recorded by ichthyoliths in deep-sea sediments at high temporal resolution, delivered to the seafloor either shed by live or dead individuals, or as indigestible elements in faecal matter. This allows for the study of fish production and community structure through geologic time [12,13]. Nearly, all teeth in our samples are small (less than 300 μm), and most lack the multiple cusps and serrations that would identify large teeth as those of sharks rather than ray-finned fish [13].

We evaluated the ichthyolith record for the last 85 Myr from two red-clay deep-sea sediment cores: Deep Sea Drilling Program (DSDP) Site 596 in the South Pacific gyre and Ocean Drilling Program (ODP) Site 886 in the North Pacific gyre. Both ocean basins exhibit the same three distinct, stable ecosystem states during this interval, each lasting tens of millions of years. Open ocean gyres are the largest habitats on the planet and have very low net primary production per unit area, yet they support complex and diverse food webs [14]. The characteristics of the Pacific Ocean gyres are governed by the global wind-field, making their geographical location and size relatively stable on geologic timescales, and ideal for studying millions of years of ecosystem evolution. While the exact locations of these sites have migrated with the Pacific Plate, both DSDP 596 and ODP 886 are pure pelagic red clay, and have remained well within the boundaries of the South and North Pacific gyres, sufficiently far from the land to have no terrigenous input beyond wind-blown dust, for the entirety of the 85 Myr record [15,16].

The absolute number of elasmobranch scales or fish teeth is not directly translatable to an absolute standing stock of individuals during a given time period, since ichthyolith

numbers can be affected by changes in the sedimentation rate as well as changes in the biological community. We have accounted for variations in the sedimentation rate by calculating the flux of teeth and denticles (ichthyolith accumulation rate (IAR): $\text{ich cm}^{-2} \text{Myr}^{-1}$, see the electronic supplementary material, methods and figures S1–S8) to the seafloor using independent timescales for each drill core [15,16]. IAR represents a metric of relative changes in biomass over a fixed time interval, which we call ‘fish (or elasmobranch) production’. We acknowledge that variation in IAR may also reflect changes in the mix of species with different population turnover rates or tooth abundances, such as the relative abundance of long-lived species and short-lived ‘forage fish’. This same caveat also applies to the comparison of tooth accumulation rate (AR) to denticle AR where the relative fluxes are probably only meaningful as a general indication of the relative abundance and importance of ray-finned fish and elasmobranchs within the pelagic ecosystem. In the present day ocean, primary production in the North Pacific Gyre is somewhat higher than that of the South Pacific basin [17]. The absolute value of North Pacific IAR is significantly higher than that in the South Pacific throughout our record, suggesting that IAR may be related to productivity, and if so, that the North Pacific has been a more biologically productive region of the ocean than the South Pacific for at least 75 Myr.

2. Cretaceous Ocean

During the Cretaceous, ichthyolith assemblages in both the North and South Pacific gyres were dominated by denticles. Elasmobranch denticles are approximately 1.4 times as abundant as fish teeth (0.06 standard error of the mean (s.e.m.)) in

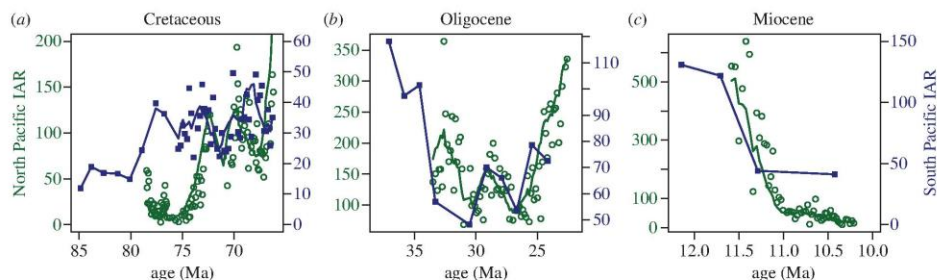


Figure 2. Direct comparison of North Pacific (open circles; left axes) and South Pacific (closed squares; right axes) ichthyolith accumulation for (a) the Cretaceous, (b) the Oligocene and (c) the Miocene. For (a,b), the solid lines are 1 Myr moving averages. For (c), the solid lines are 0.2 Myr moving averages. (Online version in colour.)

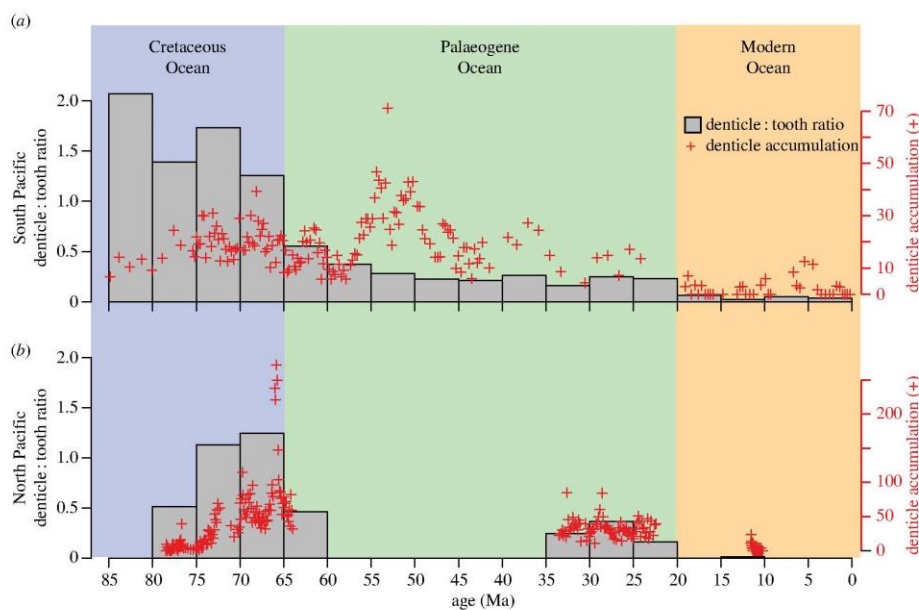


Figure 3. Eighty-five million year relative and absolute abundance of elasmobranch dentites. Bar plot is the relative abundance, or ratio of dentites to teeth; plus signs (+) are the absolute abundance, in dentites per cm^2 per million years. The three ocean ecosystem states are indicated by shaded boxes. (Online version in colour.)

the North Pacific and 1.5 times more abundant (0.10 s.e.m.) in the South Pacific. During the oldest part of our records, before 75 Ma, ichthyoliths of all kinds are rare in both the North and South Pacific gyres, suggesting that both elasmobranchs and ray-finned fish were uncommon in the Cretaceous open ocean gyre habitat. IAR in the North Pacific was $21.5 \pm 14.6 \text{ ich cm}^{-2} \text{ Myr}^{-1}$, while IAR in the South Pacific was $23.0 \pm 9.2 \text{ ich cm}^{-2} \text{ Myr}^{-1}$ (figures 1 and 2a). The Pacific open ocean gyres became significantly more favourable to both elasmobranchs and ray-finned fish by approximately 75 Ma (figures 1 and 2a), when IAR increased to $97.5 \pm 30.4 \text{ ich cm}^{-2} \text{ Myr}^{-1}$ in the North Pacific, and $34.6 \pm 9.1 \text{ ich cm}^{-2} \text{ Myr}^{-1}$ in the South Pacific, both significantly different from the pre-75 Ma values (two-sided *t*-test, $\mu_1 \neq \mu_2$, $p < 10^{-16}$ for North Pacific, $p = 0.003$ for South Pacific). Despite the increase in the overall IAR, the relative

abundance of dentites to teeth remained unchanged until the end of the Cretaceous (two-sided *t*-test, $\mu_1 = \mu_2$, $p > 0.5$ for both North and South Pacific) [13].

3. Palaeogene Ocean

The Cretaceous/Palaeogene extinction (K/Pg, 66 Ma) ended the over 10-million year period of stable pelagic ecosystem structure of the Late Cretaceous [13]. The relative abundance elasmobranchs to ray-finned fish fossils fell to 0.63 denticles for every tooth in the Palaeocene in both the North and South Pacific gyres (figure 3), reflecting a dramatic post-extinction change in ecological importance of elasmobranchs compared with ray-finned fish [13]. Additionally, both fossil and molecular studies suggest that pelagic lineages of

ray-finned fishes diversified following the extinction [2,18,19] while no such pelagic radiation is evident in shark molecular phylogenies [5], and an analysis of fossil shark diversity does not show increased origination following the extinction [6]. Ray-finned fish appear to have been ecologically released by the extinction of competitors or predators, possibly including ammonites and marine reptiles like mosasaurs and plesiosaurs [12,13]. Elasmobranchs, on the other hand, did not increase in relative or absolute abundance following the extinction event, suggesting that they either did not see the extinction of competitors, or that most of the newly available resources were subsumed by the ray-finned fishes. The ratio of elasmobranch fossils to fish fossils decreased through the Palaeocene, as the new pelagic ecosystem state developed, but remained relatively stable at approximately one denticle for every four teeth, from 56 Ma to approximately 20 Ma (North Pacific: 0.29 ± 0.11 s.d., South Pacific: 0.27 ± 0.10 s.d.).

Extreme climate change during the Palaeogene did not affect the ecosystem structure. However, absolute abundance of both elasmobranchs and ray-finned fish increased to the highest values in our 85-million record between 53 and 50 Ma (figure 1), at the peak of the Early Eocene Climate Optimum (EECO). Fish accumulation began an exponential increase approximately 58 Ma, reaching peak levels of $285 \text{ ich cm}^{-2} \text{ Myr}^{-1}$ at 52 Ma in the South Pacific gyre, a fivefold increase from the maximum Palaeocene values ($41.45 \pm 19.2 \text{ ich cm}^{-2} \text{ Myr}^{-1}$), and indeed nearly twice the maximum accumulation in the South Pacific of any other time in the past 85 Myr. Denticle AR displays a nearly identical fivefold increase during this time, albeit from a much lower baseline than fish, from 14.5 ± 5.9 denticles $\text{cm}^{-2} \text{ Myr}^{-1}$ in the later Palaeocene to nearly 71 denticles $\text{cm}^{-2} \text{ Myr}^{-1}$ in the Early Eocene (figures 1 and 3).

Some fishes are known to increase their tooth production in under differing environmental conditions [20,21], so it is possible that individual fish may have increased their rates of tooth production during the EECO. However, as both ray-finned fish teeth and elasmobranch denticles increase and decrease synchronously, it is unlikely that this mechanism explains the patterns observed. Alternatively, it is possible that the nearly identical rate of increase across elasmobranchs and fish reflects an increase in overall primary productivity or ecosystem efficiency in the warm Early Eocene ocean, as an increase in fish abundance may represent an increase in elasmobranch prey. Finally, changes in ichthyolith accumulation could reflect a variation in turnover rate of populations, and therefore more generations and biomass present over a fixed interval of time. For example, the warmer waters of the EECO may have increased metabolic rates, and thus shortened generation time, driving an increase in IAR.

Models of fish production in a warmer future ocean predict that the gyres will become more oligotrophic and less productive of fish and elasmobranchs as thermal stratification shifts primary production fully into long, bacterioplankton-based food chains [22]. Our results, in contrast, suggest that fish production in the gyres was much more efficient during the Early Eocene 'Greenhouse' than during cooler climates of the Palaeocene or later Cenozoic. Eocene fish and elasmobranch production was apparently supported by more efficient and/or shorter food chains, possibly because an overall warmer ocean may efficiently recycle organic matter and return nutrients to surface primary producers [23,24].

Coincident with the establishment of a permanent Antarctic icecap 34 Ma, South Pacific tooth accumulation fell by nearly 40%, from the Middle to Late Eocene value of 87.8 ± 20.6 to 52.6 ± 6.1 teeth $\text{cm}^{-2} \text{ Myr}^{-1}$ ($\mu_1 \neq \mu_2$, $p = 0.003$). Denticle accumulation also showed a decrease, from 16.1 ± 6.0 denticles $\text{cm}^{-2} \text{ Myr}^{-1}$ in the ice-free Eocene to 6.5 ± 3.1 denticles $\text{cm}^{-2} \text{ Myr}^{-1}$ in the Oligocene South Pacific; however, this decrease is not significant ($p = 0.058$), possibly due to low abundances of denticles in the samples. The North Pacific IAR is $152 \pm 60.4 \text{ ich cm}^{-2} \text{ Myr}^{-1}$ in the Early Oligocene, approximately double the contemporary values of the South Pacific, and slightly lower than those of the Palaeocene North Pacific ($177.3 \pm 21.5 \text{ ich cm}^{-2} \text{ Myr}^{-1}$; $\mu_1 \neq \mu_2$, $p = 0.006$), mirroring the observed difference in fish production between the Early Palaeocene and the Oligocene observed in the South Pacific (figure 2b). The Eocene–Oligocene transition is a time of increased diatom production in the Southern Ocean, which is thought to have driven an increase in food web efficiency, small forage fish abundance and the diversification of marine mammals and seabirds [25–29], which would prey on the small pelagic fish represented in our ichthyolith records. However, it appears that increased production of large phytoplankton at high latitudes did not drive an increase in ray-finned fish and elasmobranch production in the gyres, as the beginning of 'Icehouse Earth' was associated with a decrease in both fish and elasmobranch production.

4. Modern Ocean

At 20 Ma, both the relative and absolute abundance of pelagic elasmobranch fossils declined dramatically and suddenly, to one denticle for every 50 or more teeth (North Pacific: 0.013 ± 0.03 denticles per tooth; South Pacific: 0.033 ± 0.05 denticles per tooth), marking the beginning of the Modern Ocean ecosystem state (figure 3). The decline in the ratio of elasmobranch AR to fish AR between the Palaeogene and Modern Ocean states is highly significant (two-sided *t*-test, $\mu_1 \neq \mu_2$, $p < 10^{-16}$ for both gyres). In the Palaeogene Ocean, denticle accumulation was approximately 24.3 ± 12.4 denticles $\text{cm}^{-2} \text{ Myr}^{-1}$ in the South Pacific and 32.8 ± 12.9 denticles $\text{cm}^{-2} \text{ Myr}^{-1}$ in the North Pacific. The Modern Ocean saw an abrupt decrease in these ARs, which we interpret as a decline in the abundance of elasmobranchs, to 2.1 ± 3.2 denticles $\text{cm}^{-2} \text{ Myr}^{-1}$ in the South Pacific and 2.0 ± 4.3 denticles $\text{cm}^{-2} \text{ Myr}^{-1}$ in the North Pacific (two-sided *t*-test, $\mu_1 \neq \mu_2$, $p < 10^{-16}$ for both gyres). Since there is no parallel decline in tooth accumulation at this time, this represents a real decrease in elasmobranchs, rather than a change in sedimentation or other sedimentary bias. This decline in elasmobranch production and abundance when compared with ray-finned fish reflects a dramatic difference in the ecological roles of elasmobranchs between the Palaeogene and Modern ecosystem states.

The exact timing of the decline in elasmobranch abundance is not pinpointed in our record due to sedimentary gaps in both gyres, but is constrained to fall between 19 and 21 Ma. There is no apparent climate or biotic event around 20 Ma which could have driven this abrupt shift [30]. The loss of denticles from the record means that nearly all the IAR signal is driven by ray-finned fish production. South Pacific tooth IAR is highly variable on short timescales in the Neogene when compared with the Palaeogene, with a mean IAR value of $58.4 \pm 43.8 \text{ ich cm}^{-2} \text{ Myr}^{-1}$, but has a range of

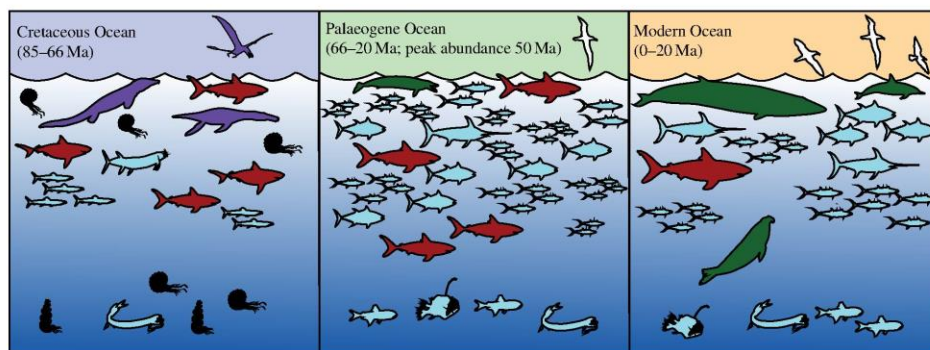


Figure 4. A cartoon illustration of the three ocean ecosystem states described in this paper, including representatives of known pelagic consumers from the intervals, showing an increase in ray-finned fish abundance (blue) into the Cenozoic and decline, after 20 Ma, in elasmobranch abundance (red). Fish responded to the extinction of pelagic reptiles (purple) and ammonites (black) in the Cretaceous Ocean, while elasmobranchs decline during the expansion of marine mammals (green) and seabirds (white) in the Neogene Ocean.

3.7–185 $\text{ich cm}^{-2} \text{Myr}^{-1}$ with rapid oscillations between these extremes. In the North Pacific, where a hiatus prevented observation of the basal Miocene there is a dramatic decline in ichthyolith accumulation between 11.6 and 11 Ma from 550 to 41 $\text{ich cm}^{-2} \text{Myr}^{-1}$, immediately preceding a rise in diatom accumulation at the site (figure 2c). The South Pacific record shows a simultaneous, short-lived drop in ichthyolith abundance, falling from 130.8 $\text{ich cm}^{-2} \text{Myr}^{-1}$ at 12 Ma to 41.1 $\text{ich cm}^{-2} \text{Myr}^{-1}$ at 11 Ma (figure 2c), suggesting that the increased variability observed in the South Pacific may be an aliased record of real, basin-wide cycles of fish production such as the one observed at high resolution in the North Pacific. Both our North Pacific Gyre record and equatorial Pacific cores show a major increase in opal production and organic matter export peaking between 10.2 and 11.3 Ma [31], suggesting that gyre fish production was inversely correlated with major bloom periods in diatoms for at least some of their history. This drop in fish tooth flux is somewhat counter-intuitive, as most modern diatom-dominated modern ecosystems have a high abundance of fish due to the more efficient food web based on the large phytoplankton.

Notably, the Early Miocene coincides with the radiations of baleen whales [25,29,32], large pelagic ray-finned fish like tunas [33], and many sea birds [26], all of which may have been competitors for resources with elasmobranchs, either directly by targeting common prey, or indirectly by targeting lower trophic levels like krill and forage fish. Pelagic elasmobranchs obviously did not become extinct, indeed, there are numerous notable pelagic shark species, including *Megalodon*, that have a prominent fossil record during the Neogene [34]. We speculate that the rise of other pelagic vertebrate competitors alongside increased variability in fish production, may have driven decreased elasmobranch production, or favoured the rise of migratory super-predators in the clade. Abundance-based evaluations of marine tetrapods during these intervals, alongside evaluations of taxonomic richness, could help to address the role of environment versus ecology in these ecosystem structural changes [35,36].

Furthermore, although we might expect increased ichthyolith accumulation towards the recent due to better preservation, the most recent 3 Myr of ichthyolith accumulation in the South Pacific fluctuate between 25 and 75 $\text{ich cm}^{-2} \text{Myr}^{-1}$, a mere

fraction of the ichthyolith accumulation of the 10 Myr prior, and indeed for most of the Cenozoic. These low but variable levels of ichthyolith accumulation suggest that fish production in general may be depressed in modern gyres, perhaps due to focusing of nutrient supply to coastal and equatorial upwelling centres or nutrient trapping in the Southern Ocean [25,29]. Indeed, it has been proposed that radiations of large whales are in response to increasingly distributed centres of productivity, requiring long distance migration [25]. Seabirds may also be part of this trend, since many coastal and pelagic species have very long foraging flight distances [27]. As modern pelagic sharks undertake large migrations across ocean basins [37], it is possible that the observed decline in denticles in our Modern Ocean system represents not a decrease in elasmobranch biomass throughout the world's oceans, but a rather decrease in the proportion of time spent in the gyre habitat, and thus in the flux of denticles to the deep ocean seafloor.

5. Conclusion

Over the past 85 Myr, there have been three distinct pelagic ecosystem structures in the Pacific Ocean gyres, defined by their relative and absolute abundances of elasmobranchs and ray-finned fish (figure 4). Abrupt transitions between the three ocean ecosystem states occur approximately simultaneously in both ocean basins, and are unrelated to major climate events during the interval. The shift from the Cretaceous Ocean to the Palaeogene Ocean was triggered by the K/Pg mass extinction [13]. The resulting Palaeocene Ocean system had remarkable stability in the relative balance of ray-finned fish and elasmobranchs, despite large changes in absolute abundance, and the imposition of numerous dramatic climate perturbations, including extreme greenhouse and hyperthermal events during the Palaeocene and Eocene [38] and the transition from a greenhouse to icehouse planet with permanent polar icecaps [39]. There is no apparent climatic or biotic driver for the transition from Palaeogene to Modern Ocean [36], since polar glaciation began more than 10 Myr prior, and there are no obvious perturbations to carbon or oxygen isotopes [30]. However, the basal Neogene is coincident with the rise and diversification of many other pelagic

groups, including radiations of pelagic diatoms [40], zooplankton [41] and pelagic vertebrates [28,32]. Hence, it is likely that the open ocean ecosystem structures of the past 85 Myr are driven by ecological thresholds triggered by changes in the pelagic resource base and dynamics of competition among pelagic consumers in the open ocean [36].

6. Methods

(a) Sampling protocol for ichthyolith extraction

Red-clay samples (5–15 g) were taken at 5 cm intervals throughout the two deep-sea sediment cores, effectively providing a continuous record downcore. For ODP Site 886, samples were 2–3 cm in length, taken at 5 cm intervals (approx. 30–50 kyr resolution). For DSDP Site 596, samples were taken at 5 cm intervals (approx. 200 kyr resolution) for the interval of 85–42 Ma, and approximately 20–25 cm intervals (approx. 1 Myr resolution) for the interval from 42 Ma to present. All samples were dried to a constant weight at 50°C, sometimes taking months to remove all water. Once dry, samples were weighed and disaggregated in 50–100 ml de-ionized water. Additionally, approximately 10–20 ml of 5% acetic acid was added to the samples to remove any residual carbonate. Samples were wet-sieved over a 38 µm sieve, and dried overnight at 50°C. All ichthyoliths more than 106 µm were picked out of the residue using a dissection microscope and very fine paintbrush, and classified as either a tooth or a denticle. They were mounted on cardboard micropalaeontological slides using gum tragacanth. Samples were processed in random order, rather than stratigraphic order, to avoid additional bias. IARs were calculated from established age models for the sites [15,16].

(b) Calculation of ichthyolith accumulation rates

While the community metric we report, the ratio of elasmobranchs to fish, is independent of timescale, the reported IARs and our

interpretation of ‘how many’ fish or elasmobranchs is dependent on the accuracy of age models and sedimentation rates of each core. Red clays are traditionally very difficult to date, as they are lacking in traditional microfossil groups for biostratigraphy, and accumulate too slowly for magnetostratigraphy. We used independently developed geochemical-based age models well established in the literature, to calculate IAR for each site. For DSDP Site 596, we employ the sedimentological framework of Zhou & Kyte [16], which is based on an inverse-AR model using cobalt concentrations in the sediments. For ODP Site 886, we work within the framework compiled by Snoeckx *et al.* [15] which includes strontium isotope stratigraphy for the oldest samples, and magnetostratigraphy, and radiolarian biostratigraphy for the youngest. ODP Site 886 has two hiatuses in the record. In addition, ODP Site 886 had several intervals in the Late Cretaceous which included manganese oxides formed around ichthyoliths, making the determination of total ichthyoliths impossible. Both sites have a prominent iridium anomaly at the Cretaceous–Palaeogene boundary [15,16,42], providing an additional tie-point for the age models. Further discussion of the age models is provided in the electronic supplementary material.

Data accessibility. All data generated in this study have been archived in the Pangea Data Repository (doi:10.1594/PANGAEA.859876) and the Dryad data repository (doi:10.5061/dryad.38537).

Authors’ contributions. E.S. and R.N. designed the study. E.S. generated DSDP 596 dataset and 886 Cretaceous/Palaeocene. L.G. generated 886 Oligocene and J.C. generated 886 Miocene datasets. E.S. and R.N. wrote the paper with input from J.C. and L.G.

Competing interests. We have no competing interests.

Funding. E.S. is supported by an NSF Graduate Research Fellowship. Samples were provided by the Integrated Ocean Drilling Program (now International Ocean Discovery Program).

Acknowledgements. Images were taken on the Hull Lab Imaging System at Yale University. The authors would like to thank L. Levin for comments on a draft version of this manuscript, and N. Pyenson and an anonymous reviewer for their thoughtful reviews of this manuscript.

References

- Friedman M, Sallan LC. 2012 Five hundred million years of extinction and recovery: a Phanerozoic survey of large-scale diversity patterns in fishes. *Palaeontology* **55**, 707–742. (doi:10.1111/j.1475-4983.2012.01165.x)
- Miya M *et al.* 2013 Evolutionary origin of the scombridae (tunas and mackerels): members of a paleogene adaptive radiation with 14 other pelagic fish families. *PLoS ONE* **8**, e73535. (doi:10.1371/journal.pone.0073535)
- Near TJ, Eytan RI, Dornburg A, Kuhn KL, Moore JA, Davis MP, Wainwright PC, Friedman M, Smith WL. 2012 Resolution of ray-finned fish phylogeny and timing of diversification. *Proc. Natl. Acad. Sci. USA* **109**, 13 698–13 703. (doi:10.1073/pnas.1206625109)
- Heinicke M, Naylor G, Hedges S. 2009 Cartilaginous fishes (Chondrichthyes). In *The timetree of life*, pp. 320–327. New York, NY: Oxford University Press.
- Sorenson L, Santini F, Alfaro ME. 2014 The effect of habitat on modern shark diversification. *J. Evol. Biol.* **27**, 1536–1548. (doi:10.1111/jeb.12405)
- Guinot G, Adnet S, Cappetta H. 2012 An analytical approach for estimating fossil record and diversification events in sharks, skates and rays. *PLoS ONE* **7**, e44632. (doi:10.1371/journal.pone.0044632)
- Iverson RL. 1990 Control of marine fish production. *Limnol. Oceanogr.* **35**, 1593–1604. (doi:10.4319/lo.1990.35.7.1593)
- Moloney CL, Field JG. 1991 The size-based dynamics of plankton food webs. I. A simulation model of carbon and nitrogen flows. *J. Plankton Res.* **13**, 1003–1038. (doi:10.1093/plankt/13.5.1003)
- Kitchell JF, Essington TE, Boggs CH, Schindler DE, Walters CJ. 2002 The role of sharks and longline fisheries in a pelagic ecosystem of the central Pacific. *Ecosystems* **5**, 202–216. (doi:10.1007/s10021-001-0065-5)
- Doyle PS, Riedel WR. 1979 Cretaceous to Neogene ichthyoliths in a giant piston core from the Central North Pacific. *Micropalaeontology* **25**, 337–364. (doi:10.2307/1485427)
- Doyle PS, Riedel WR. 1979 *Ichthyoliths: present status of taxonomy and stratigraphy of microscopic fish skeletal debris*. La Jolla, CA: Scripps Institution of Oceanography, University of California, San Diego.
- Sibert EC, Hull PM, Norris RD. 2014 Resilience of Pacific pelagic fish across the Cretaceous/Palaeogene mass extinction. *Nat. Geosci.* **7**, 667–670. (doi:10.1038/ngeo2227)
- Sibert EC, Norris RD. 2015 New age of fishes initiated by the Cretaceous–Palaeogene mass extinction. *Proc. Natl. Acad. Sci. USA* **112**, 8537–8542. (doi:10.1073/pnas.1504985112)
- Azam F, Fenchel T, Field JG, Gray J, Meyer-Reil L, Thingstad F. 1983 The ecological role of water-column microbes in the sea. *Estuaries* **10**, 257–263. (doi:10.3354/meps010257)
- Snoeckx H, Rea D, Jones C, Ingram B. 1995 Eolian and silica deposition in the central North Pacific: results from sites 885/886. *Proc. Ocean Drill. Program: Sci. Results* **145**, 219–230. (doi:10.2973/odp.proc.sr.145.123.1995)
- Zhou L, Kyte FT. 1992 Sedimentation history of the South Pacific pelagic clay province over the last 85 million years inferred from the geochemistry of Deep Sea Drilling Project Hole 596.

- Paleoceanography* **7**, 441–465. (doi:10.1029/92PA01063)
17. Falkowski PG, Barber RT, Smetacek V. 1998 Biogeochemical controls and feedbacks on ocean primary production. *Science* **281**, 200–206. (doi:10.1126/science.281.5374.200)
 18. Near TJ *et al.* 2013 Phylogeny and tempo of diversification in the superradiation of spiny-rayed fishes. *Proc. Natl Acad. Sci. USA* **110**, 12 738–12 743. (doi:10.1073/pnas.1304661110)
 19. Friedman M. 2010 Explosive morphological diversification of spiny-finned teleost fishes in the aftermath of the end-Cretaceous extinction. *Proc. R. Soc. B* **277**, 1675–1683. (doi:10.1098/rspb.2009.2177)
 20. Cleves PA, Ellis NA, Jimenez MT, Nunez SM, Schluter D, Kingsley DM, Miller CT. 2014 Evolved tooth gain in sticklebacks is associated with a cis-regulatory allele of *Bmp6*. *Proc. Natl Acad. Sci. USA* **111**, 13 912–13 917. (doi:10.1073/pnas.1407567111)
 21. Bemis WE, Giuliano A, McGuire B. 2005 Structure, attachment, replacement and growth of teeth in bluefish, *Pomatomus saltatrix* (Linnaeus, 1766), a teleost with deeply socketed teeth. *Zoology* **108**, 317–327. (doi:10.1016/j.zool.2005.09.004)
 22. Polovina JJ, Dunne JP, Woodworth PA, Howell EA. 2011 Projected expansion of the subtropical biome and contraction of the temperate and equatorial upwelling biomes in the North Pacific under global warming. *ICES J. Mar. Sci.* **68**, 986–995. (doi:10.1093/icesjms/fsq198)
 23. Lyle AO, Lyle MW. 2006 Missing organic carbon in Eocene marine sediments: is metabolism the biological feedback that maintains end-member climates? *Paleoceanography* **21**, PA2007. (doi:10.1029/2005pa001230)
 24. Norris R, Turner SK, Hull P, Ridgwell A. 2013 Marine ecosystem responses to Cenozoic global change. *Science* **341**, 492–498. (doi:10.1126/science.1240543)
 25. Berger W. 2007 Cenozoic cooling, Antarctic nutrient pump, and the evolution of whales. *Deep Sea Res. Part II* **54**, 2399–2421. (doi:10.1016/j.dsr2.2007.07.024)
 26. Ando T, Fordyce RE. 2014 Evolutionary drivers for flightless, wing-propelled divers in the Northern and Southern Hemispheres. *Palaeoogeogr. Palaeoecol.* **400**, 50–61. (doi:10.1016/j.palaeo.2013.08.002)
 27. Warheit KI, Schreiber E, Burger J. 2002 The seabird fossil record and the role of paleontology in understanding seabird community structure. In *Biology of marine birds* (eds EA Schreiber, J Burger), pp. 17–55. Boca Raton, FL: Taylor & Francis Group.
 28. Pyenson ND, Kelley NP, Parham JF. 2014 Marine tetrapod macroevolution: physical and biological drivers on 250 Ma of invasions and evolution in ocean ecosystems. *Palaeoogeogr. Palaeoecol.* **400**, 1–8. (doi:10.1016/j.palaeo.2014.02.018)
 29. Marx FG, Uhen MD. 2010 Climate, critters, and cetaceans: Cenozoic drivers of the evolution of modern whales. *Science* **327**, 993–996. (doi:10.1126/science.1185581)
 30. Cramer BS, Toggweiler JR, Wright JD, Katz ME, Miller KG. 2009 Ocean overturning since the Late Cretaceous: inferences from a new benthic foraminiferal isotope compilation. *Paleoceanography* **24**, PA4216. (doi:10.1029/2008pa001683)
 31. Lyle M, Baldauf J. 2015 Biogenic sediment regimes in the Neogene equatorial Pacific, IODP Site U1338: burial, production, and diatom community. *Palaeoogeogr. Palaeoecol.* **433**, 106–128. (doi:10.1016/j.palaeo.2015.04.001)
 32. Steeman ME *et al.* 2009 Radiation of extant cetaceans driven by restructuring of the oceans. *Syst. Biol.* **58**, 573–585. (doi:10.1093/sysbio/syp060)
 33. Santini F, Sorenson L. 2013 First molecular timetree of billfishes (Istiophoriformes: Acanthomorpha) shows a Late Miocene radiation of marlins and allies. *Ital. J. Zool.* **80**, 481–489. (doi:10.1080/11250003.2013.848945)
 34. Pimiento C, Clements CF. 2014 When did *Carcharodes megalodon* become extinct? A new analysis of the fossil record. *PLoS ONE* **9**, e111086. (doi:10.1371/journal.pone.0111086)
 35. Pyenson ND, Irmis RB, Lipps JH. 2010 Comment on 'Climate, critters, and cetaceans: Cenozoic drivers of the evolution of modern whales'. *Science* **330**, 178. (doi:10.1126/science.1189866)
 36. Benton MJ. 2009 The red queen and the court jester: species diversity and the role of biotic and abiotic factors through time. *Science* **323**, 728–732. (doi:10.1126/science.1157719)
 37. Bonfil R, Mejer M, Scholl MC, Johnson R, O'Brien S, Oosthuizen H, Swanson S, Kotze D, Paterson M. 2005 Transoceanic migration, spatial dynamics, and population linkages of white sharks. *Science* **310**, 100–103. (doi:10.1126/science.1114898)
 38. Zachos JC, McCarren H, Murphy B, Röhl U, Westerhold T. 2010 Tempo and scale of late Paleocene and early Eocene carbon isotope cycles: implications for the origin of hyperthermals. *Earth Planet. Sci. Lett.* **299**, 242–249. (doi:10.1016/j.epsl.2010.09.004)
 39. Liu Z, Pagani M, Zinniker D, DeConto R, Huber M, Brinkhuis H, Shah SR, Leckie RM, Pearson A. 2009 Global cooling during the Eocene–Oligocene climate transition. *Science* **323**, 1187–1190. (doi:10.1126/science.1166368)
 40. Finkel ZV, Sebbo J, Feist-Burkhardt S, Irwin A, Katz M, Schofield O, Young J, Falkowski P. 2007 A universal driver of macroevolutionary change in the size of marine phytoplankton over the Cenozoic. *Proc. Natl Acad. Sci. USA* **104**, 20 416–20 420. (doi:10.1073/pnas.0709381104)
 41. Lipps JH. 1970 Plankton evolution. *Evolution* **24**, 1–22. (doi:10.2307/2406711)
 42. Zhou L, Kyte FT, Bohor BF. 1991 Cretaceous/Tertiary boundary of DSDP Site 596, South Pacific. *Geology* **19**, 694–697. (doi:10.1130/0091-7613(1991)019<0694:ctbods>2.3.co;2)

7.9 Supplementary Methods

The accumulation of red clays is extremely slow, usually <1 meter per million years, and assumed to have low variability. Since they accumulate below the CCD, the main source of sediment is wind-blown dust, and therefore sedimentation rate is not as effected by changes in planktonic productivity or shifts in ocean carbonate chemistry. Over the long timescales we consider in this study, our IAR estimates are unlikely to be highly biased by significant fluctuations in sedimentation rate. Additionally, paleo-reconstructions of plate movement for both sites show that they have remained within their respective open ocean gyres for at least the past 85 million years (Snoeckx et al., 1995; Zhou and Kyte, 1992), further supporting the relative stability of the sedimentary environment through the record, and suggesting that the changes observed in fish accumulation are not due to the sedimentary column moving across biome boundaries.

Accounting for variable sediment MAR: Neogene DSDP Site 596. The age model for DSDP Site 596 is based off of a cobalt accumulation inverse model developed by Zhou and Kyte (1992), who calculate sediment mass accumulation rates (MAR) for the entire interval. While the sedimentation rate and MAR of sediments during the interval from 85-22 Ma at DSDP 596 is low and relatively constant, there is a change in the depositional environment around 20 Ma, and the upper interval displays considerable variability in sediment MAR that consistently higher than the older regime (Figure S1[7-5], table 5 from Zhou and Kyte (1992)).

To calculate ichthyolith accumulation rate (IAR), sediment mass accumulation rate (MAR) was linearly interpolated. However, in the Neogene sediment MAR for DSDP 596 is considerably more variable than the Cretaceous and Paleogene record. We

evaluated two different IAR options (1) using variable MAR by interpolating the raw MAR values as calculated by Zhou and Kyte, and (2) average MAR, using the average MAR value for the Neogene of 28.44 (the gray line in Figure S1[7-5]). While the IAR values between the two options are slightly offset from each other, they are not considerably different (Figure S2[7-6]). We have chosen to present the IAR calculated by interpolation from the Zhou and Kyte age model in the main figures, and note that the sediment MAR does not have a large effect on the calculated IAR for the Neogene. Indeed, ichthyolith AR and sediment AR are independent for both DSDP Site 596 and DSP Site 886 (Figure S3[7-7]), suggesting that the IAR values calculated are a biological signal, rather than a function of sediment accumulation.

There is an inflection in the cobalt accumulation curve and age-depth model (Figure S4[7-8]) between the low, constant MAR of the Cretaceous and Paleogene, and the high and variable MAR of the Neogene. This section of the core has intermediate sediment MAR values reported by Zhou and Kyte (Zhou and Kyte, 1992). We have discounted the data-points in this region in our final interpretation (shaded gray box in figures S1-S2 & S4-S6 [7-5, 7-6, 7-8, 7-9, 7-10]), as they produce improbably high IAR values. Indeed, the abrupt beginning and ending of the interval, and denticle AR values more than twice as high as any values seen during the rest of the record, even when sharks dominated the assemblages (Figure S5[7-9]), suggest that this is likely a sedimentary artifact, and not a biological feature. We note that the raw ichthyoliths per gram of this section is elevated as well (Figure S6[7-10]), though not enough to explain the extremely high MAR. While it is possible that the 4 million year interval from 23-19 Ma is a time of extremely high ichthyolith accumulation, it is more likely that the

elevated ichthyolith concentrations and increased cobalt accumulations are a post-deposition sedimentary feature of the core.

ODP Site 886 MAR. ODP Site 886 has two major hiatuses in its record, separating the record into three distinct sedimentation regimes (Snoeckx et al., 1995), with the lowest sedimentation rates during the Cretaceous, and the highest in the Miocene, however within each of the three regimes, sedimentation rate is constant (Figure S7[7-11]). Similar to DSDP Site 596, IAR is driven mostly by the raw ichthyoliths/gram sediment found in the samples, and thus is independent of sedimentary regime (Figure S8[7-12]).

Supplementary References

- Snoeckx, H., Rea, D., Jones, C., and Ingram, B., 1995, Eolian and silica deposition in the central North Pacific: Results from Sites 885/886: Proceedings of the Ocean Drilling Program. Scientific results, v. 145, p. 219-230.
- Zhou, L., and Kyte, F. T., 1992, Sedimentation history of the South Pacific pelagic clay province over the last 85 million years inferred from the geochemistry of Deep Sea Drilling Project Hole 596: *Paleoceanography*, v. 7, no. 4, p. 441-465.

Figure S1: Sediment MAR at DSDP Site 596

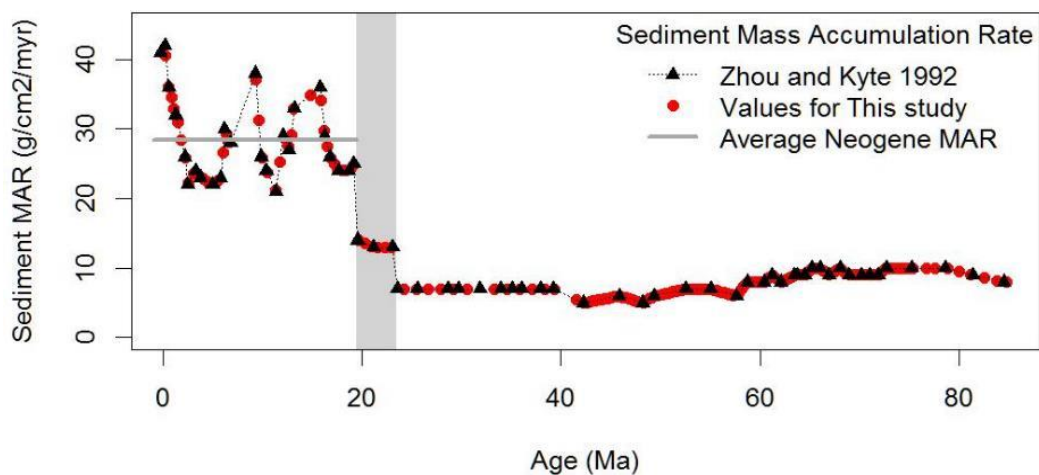


Figure 7-5: Figure S1: Sediment mass accumulation rate for DSDP Site 596, based on Zhou and Kyte 1992 (black triangles). Red dots are the interpolated sediment MAR values for the samples used in this study. The gray horizontal line is the average sediment MAR for the variable Neogene, used to calculate an alternate MAR (see Figure S2). Vertical gray band indicates the discounted interval due to age model breakdown.

Figure S2: IAR for DSDP Site 596

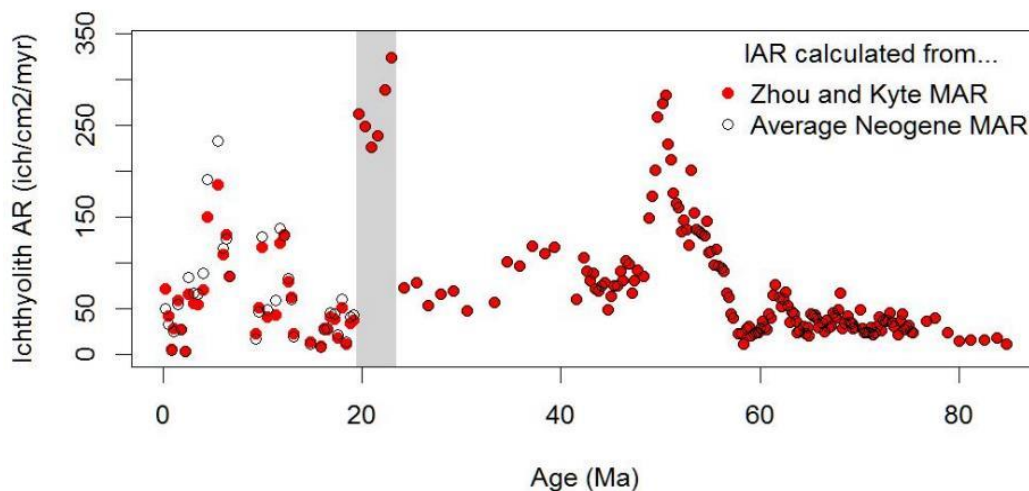


Figure 7-6: Figure S2: Ichthyolith Accumulation Rate calculated for DSDP Site 596 using the interpolated sediment MAR values (red dots), and the Neogene average MAR value (open black circles). Vertical gray band represents discounted datapoints.

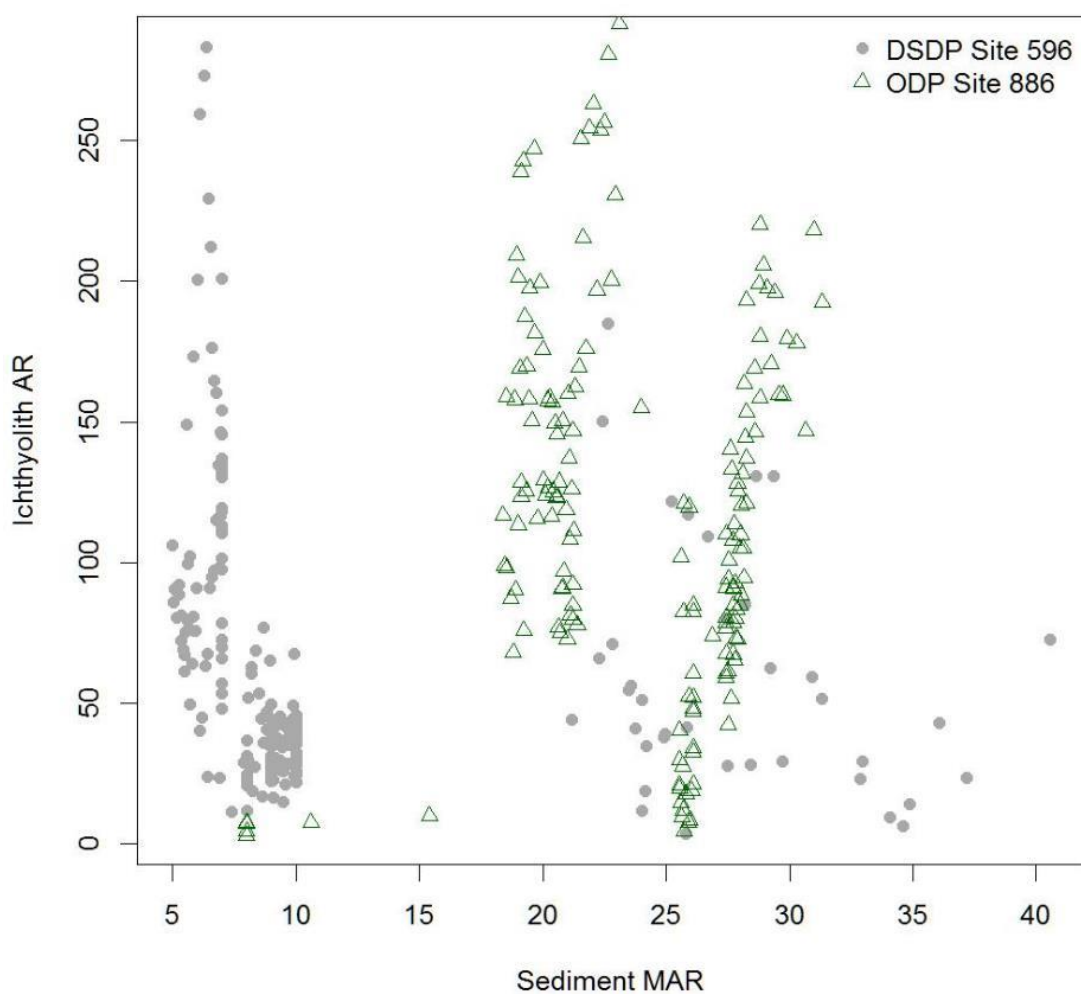
Figure S3: Sediment MAR vs. Ichthyolith AR

Figure 7-7: Figure S3: Sediment MAR versus Ichthyolith accumulation. There is no relationship between these two values, suggesting that IAR is independent of sedimentation. Gray dots are DSDP Site 596, and green triangles are ODP Site 886.

Figure S4: Age-Depth for DSDP Site 596

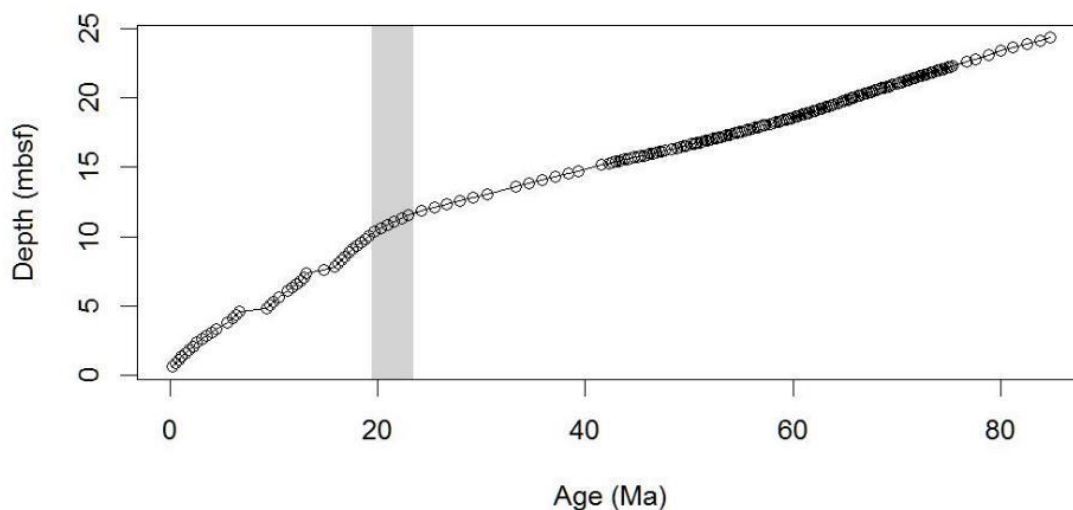


Figure 7-8: Figure S4: Age-depth plot for DSDP Site 596. Note the increased sedimentation rate beginning at approximately 23 Ma. Vertical gray band represents discounted datapoints.

Figure S5: IAR for DSDP Site 596

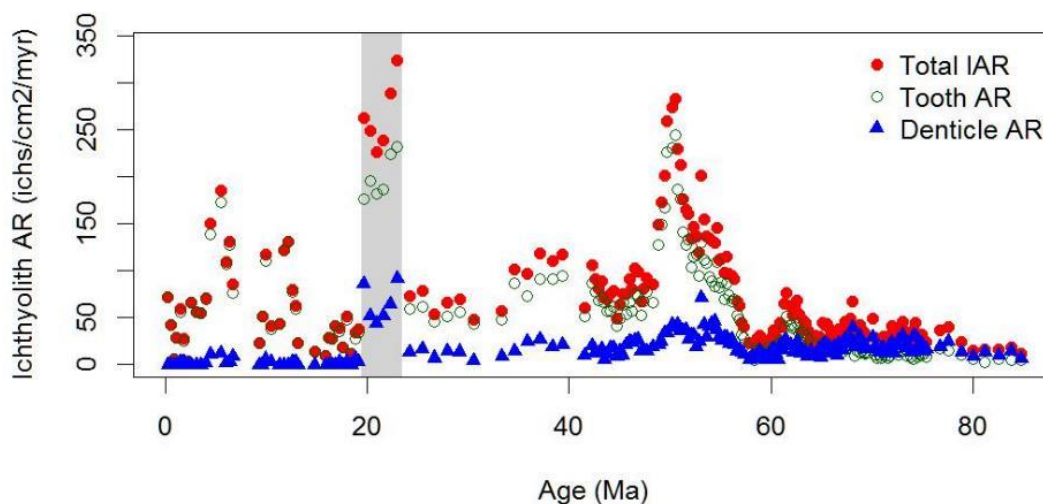


Figure 7-9: Figure S5: Total ichthyolith (red dots), tooth (green open circles), and denticle (blue solid triangles) accumulation rates for DSDP Site 596, showing the abnormally high values during the interval of 23-19 Ma. Horizontal gray band represents discounted datapoints.

Figure S6: Ichthyoliths per gram sediment at DSDP Site 596

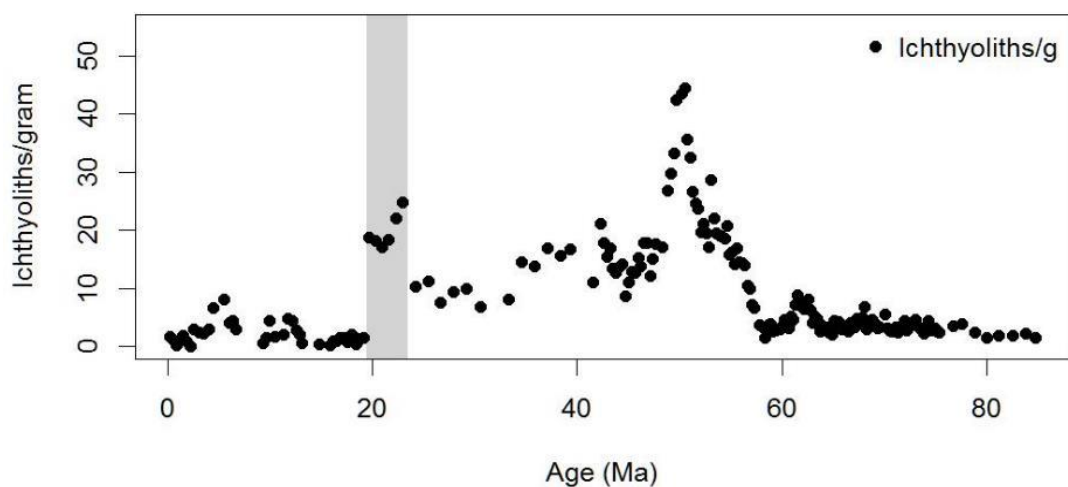


Figure 7-10: Figure S6: Ichthyoliths per gram for DSDP Site 596. Vertical gray bar represents discounted datapoints.

Figure S7: Age-depth plot for ODP Site 886

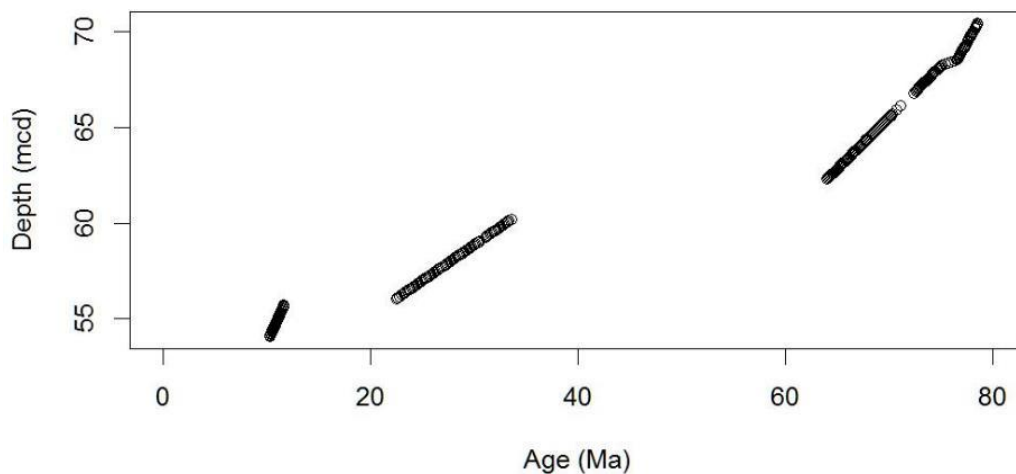
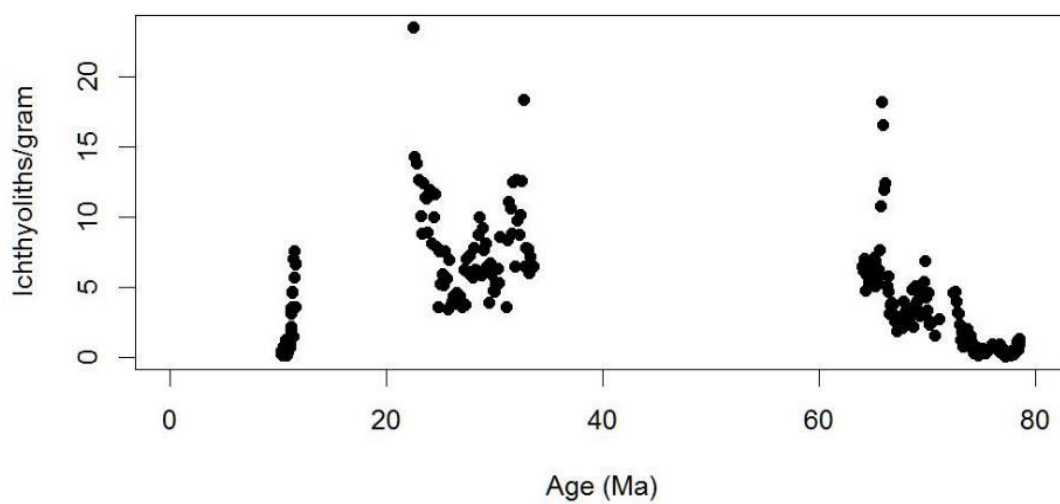


Figure 7-11: Figure S7: Age-depth model for ODP Site 886, showing constant sedimentation rate, with two major hiatuses in the record.

Figure S8: Ichthyoliths per gram sediment at ODP Site 886**Figure 7-12: Figure S8: Total ichthyoliths per gram sediment at ODP Site 886.**

7.10 Acknowledgements

Chapter 7, in full, is a reprint of materials as it appears in as: Sibert E, Norris R, Cuevas J, Graves L. (2016) “Eighty-five million years of Pacific Ocean gyre ecosystem structure: long-term stability marked by punctuated change” in the Proceedings of the Royal Society B, v.283: 20160189. <http://dx.doi.org/10.1098/rspb.2016.0189>. The dissertation author was the primary investigator and author of this manuscript.

CHAPTER 8

Conclusion to the Dissertation

8.1 Major Findings

In this dissertation, I have laid the foundations for using ichthyoliths, a novel microfossil preserved in nearly all marine sediments, as a paleontological and paleoecological proxy for fish production and evolution. I first developed a series of methods to effectively and efficiently isolate ichthyoliths from deep-sea sediments (Chapter 2), including a novel protocol for staining ichthyoliths with Alizarin Red S, that makes it possible to efficiently count and pick ichthyoliths from a variety of deep sea sediment samples, including those containing abundant biogenic silica and terrestrially-derived sediments. I then used this proxy to assess the response of fishes to global change events in Earth's history (Chapters 3-7).

Fishes are an integral part of marine ecosystems, and the most diverse group of vertebrates on the planet (Nelson, 2006), yet their fossil record is relatively sparse, as the preservation of body fossils is rare, and mostly limited to coastal or freshwater species which can be preserved in land-based outcrops. Ichthyoliths preserved in deep-sea sediment cores provide a temporally robust fossil record of open ocean fishes, yet their small size and poorly understood taxonomic affinity has caused them to be overlooked by both the paleoceanographic and paleontological communities. Before my work, ichthyoliths were used largely by two communities of earth scientists: research studying radiogenic isotopes preserved within mineral coatings on tooth phosphate (Huck et al., 2016; Martin and Haley, 2000; Scher and Martin, 2004; Thomas et al., 2014), and work to establish a tooth-based biostratigraphy for otherwise unfossiliferous pelagic red clay sediments (Doyle, 1983; Doyle and Riedel, 1979; Doyle and Riedel, 1985; Doyle et al.,

1985; Johns et al., 2006), however this is the first work to consider ichthyoliths as fossils which represent fish biological and ecological processes in their own right.

It is clear that the fish microfossil record can greatly improve our understanding of how vertebrate consumers have responded to global change events, and assess the variability of those communities through geologic time. The abundance of ichthyoliths in deep-sea sediment cores allows us to assess the impact of environmental changes on fish diversity, community structure, and production, at a temporal resolution of 10s of thousands of years, which has previously been impossible using the traditional vertebrate fossil record, which commonly has millions of years between samples, and rarely preserves the whole fish community. The abundance of teeth and denticles, when expressed as an “Ichthyolith accumulation rate” can be broadly thought of as a measure of fish productivity. Ichthyolith-based productivity joins other paleo-productivity measures derived from the abundances of other microfossil groups, elemental-based export production proxies, and measures based on organic matter fluxes as independent means of assessing the history of ocean productivity through geologic time. However, ichthyolith-based methods have a distinct value compared to most other methods: they both offer a record of the upper parts of pelagic food webs, and involve fossils that are found in virtually every type of marine sediment.

Ichthyoliths also are likely to record information of fish biodiversity. Currently, we can assign relatively few ichthyoliths to specific living groups of teleost fishes and elasmobranchs, but this biological taxonomy will surely improve as more work is done on the morphology of the teeth and denticles of living taxa. It is likely that the majority of ichthyoliths belong to pelagic fish groups such as vertical migrators or large pelagic

fishes, however at present, their taxonomic affinity is poorly understood. The biological identification of ichthyoliths will open up a new window into the evolution of vertebrate biodiversity in the open oceans, potentially making it feasible to calibrate molecular clocks, assess ecological evolution and changes in life history characteristics of open ocean fish, and evaluate the fine-grained response of fish to global change events in the geologic record.

I have investigated fish and marine ecosystem evolution using ichthyoliths at three scales of interpretation: (1) fish/ecosystem production based on ichthyolith abundances, (2) community structure based on ichthyolith assemblage composition, and (3) fish evolution, based on changes in individual ichthyolith morphology. These approaches provide considerable insight into the dynamics of upper trophic level consumers and their evolutionary and ecological patterns in the open ocean. I have shown that fishes were remarkably resilient to global change events, and that fish evolution and community assemblage changes are decoupled from changes in absolute production. This suggests that fishes, as a group, were consistently able to adapt to changing climates and environments throughout the latest Cretaceous and Paleogene.

The quantification of productivity in open ocean ecosystems is a long-standing problem in biological oceanography and paleoceanography. While there are many ways to assess paleo export production in open ocean ecosystems, including carbon isotope gradients (D'Hondt et al., 1998; Hsu and McKenzie, 1985) and biogenic barium export (Hull and Norris, 2011; Lyle and Baldauf, 2015), these metrics are limited to measuring the relative production of fixed carbon which is exported to the seafloor.

The paleo-production of higher order organisms is poorly understood. Biological oceanographers have asked the question “how many fish are in the sea” in many forms (Iverson, 1990). While fishes do not represent a large proportion of standing biomass in the ocean when compared to the primary producers, the relative abundance of fishes is controlled by both the total amount of primary productivity, and the trophic efficiency of the food web (Moloney and Field, 1991). The relative abundance of ichthyoliths in open ocean sediments is a function of these, as well as the number of teeth that any given fish produces in its lifetime, and how fast those fish turn over. While this may not always be directly translatable into a biomass which can be compared to our modern standing stock, the changes in ichthyolith accumulation can reveal changes in ecosystem productivity through time. The ichthyolith record yields distinct, and repeatable findings in accumulation rate, suggesting that the signals preserved have biological significance and are not simply due to random chance. For example, I have found broadly similar patterns in the timing and magnitude of change patterns of ichthyolith accumulation rate (IAR) between disparate ocean basins around the world. Apparent cycles in IAR between, for instance, the North Pacific and the South Pacific suggest that the flux of fish remains to the sea floor is a repeatable measure. The abundance of ichthyoliths in relatively small samples of deep sea sediment also means that I have been able to generate the first records of vertebrate abundance that have resolutions comparable to those of other marine microfossils, typically a few thousand years to ~50 kyr between samples, compared to the traditional vertebrate record, which often has gaps of millions of years.

In this dissertation, I have found that fish production in the Late Cretaceous was low and had low variability, compared to the Cenozoic, suggesting that either fishes did

not play a large part in the Cretaceous marine ecosystem, or that the levels of primary or secondary production in the Cretaceous were consistently lower than in the Cenozoic. It is possible that Cretaceous fishes were significantly longer-lived, or did not shed their teeth as rapidly as those in the Cenozoic, or that fishes were sharing trophic resources with many additional pelagic consumer groups, such as ammonites, marine reptiles, or other, non-fossilized Cretaceous fauna.

Fish production across the Cretaceous-Paleogene Mass Extinction remained stable in the Pacific, but declined in the Atlantic (Sibert et al., 2014). This follows the same pattern as export production (Hull and Norris, 2011), suggesting that ichthyolith accumulation, to a first approximation, is related to net primary productivity. Presently this pattern of relatively stable or increasing IAR in the Pacific and decreasing IAR in the Atlantic following the K/Pg is supported by observations from seven deep sea drill sites, and one terrestrially uplifted, formerly open ocean outcrop, suggesting it is a robust pattern. Further all of these sites show a shift in the relative abundance of teeth to denticles in the ichthyolith assemblage, with Cretaceous samples having approximately equal numbers of teeth and denticles, but Paleocene samples having nearly twice the number of teeth as denticles, suggesting that the shift in assemblage composition was independent from any changes in productivity at the extinction.

I have also produced a few longer IAR records through later parts of the Paleogene and Neogene and these show the promise for future work on Cenozoic record of open ocean fish. For example, my longest record, to date comes from the South Pacific gyre (DSDP 596) where I obtained a record over the past 85 million years of IAR and ichthyolith morphology. In the South Pacific record, fish production increased to its

maximum in the past 85 million years during the warmest time in the record, the Early Eocene Climate Optimum, approximately 52-50 million years ago. The abundance of ichthyoliths follows global temperature as it increases and then decreases throughout the Paleogene, suggesting a link between ecosystem productivity and global ocean temperature. Further, the relative abundance of teeth and denticles stays constant throughout the entire interval, suggesting that the assemblage composition is not related to total production or global climate.

During the past 20 million years, fish production in the Pacific gyres has been incredibly variable with time, a distinct difference from the stable, low-variability regimes of the Cretaceous and Paleogene. Parts of this story of changing IAR are borne out by patchy records from other deep sea sites. For example, in the North Pacific (from ODP 886) there are broadly similar trends in IAR compared to the South Pacific DSDP 596 record. Both records show that fish production increased from the Cretaceous to the Paleocene, decreased across the Eocene-Oligocene transition (as polar glaciation began) and had large swings in production in the Neogene. This latter finding suggests that the modern open ocean may have patchier nutrient input, in time and/or space than earlier systems.

Yet fish production does not tell the whole story of how the marine ecosystem has responded to global change: an ecosystem is defined both by total production, and by the presence and abundance of the organisms within it. In this dissertation, I developed metrics to assess the structure of the fish community, including the relative abundance of elasmobranch denticles to fish teeth, and the relative abundance of different size classes of fish teeth.

The structure of fish communities as measured by the ratio of teeth to denticles and size structure of teeth is remarkably stable for periods of over 10 million years at a time, and changes independently from variations in fish production. For example, the findings highlighted in Chapter 5 (Sibert and Norris, 2015), of the global shift in relative abundance of denticles and teeth immediately after the K/Pg extinction showed that fishes responded to the extinction by rapidly expanding their relative abundance in open ocean ecosystems, disrupting a previously stable Cretaceous ecosystem structure. By using a high resolution timeseries, as is possible in deep-sea sediment cores, I was able to show that the variability of the assemblage structure leading up to the event was very low, and that the change in relative abundance was immediate, on the order of thousands of years, rather than millions, demonstrating that the K/Pg event was the cause of the change, and that the fish community was not otherwise ‘stressed’ or destabilized by environmental change leading up to the event. Further, the newly established Paleocene assemblage stayed stable for the next 40 million years, shifting abruptly near the base of the Neogene to the new, and similarly stable structure that has persisted through the Pliocene, and likely through present day (Sibert et al., 2016).

The finding that community assemblages vary independently from fish production is particularly intriguing, because it suggests that the structure of fish communities is not driven by primary production. This finding is robust across different time periods (from the Cretaceous to the modern), and holds true across the disparate community structure metrics of size structure and relative abundance of fossil types. Indeed, it suggests that the structure of fish communities may be resilient to major changes in overall primary production. It is possible that community structure only changes during periods where

extreme evolutionary pressure is driving the system, such as during the recovery from a mass extinction event.

At the finest scale of ichthyolith metrics, individual tooth morphology can reveal patterns of evolution in the group. While the taxonomic affinity is presently unknown for most teeth that I have studied, they are morphologically distinct, and likely represent different diets or ecologies of individual fish taxa or ecotypes. In this dissertation, I have developed a scheme for quantifying and analyzing variation in tooth morphology. I have found that across the K/Pg extinction, while only two morphotypes of 48 went extinct, they were dominant in the Cretaceous while the lineages which survived were rare. The surviving morphotypes rapidly diversified in the Paleocene. An initial radiation generated many novel, but short-lived “disaster” forms, and a second pulse of origination established the morphotypes which lived during the Eocene. It is important to note that my present morphological taxonomy likely captures a relatively high taxonomic level among fish (e.g. family level or non-taxonomic ecotype or functional group), and is therefore likely to detect only the largest-scale changes in the original fish community, rather than the changes in representation at the species or even genus level. Indeed, as tooth shape is governed by both taxonomy and ecology, variation in tooth morphology likely does not capture the fine-scale, species-level signals, which may be more responsive to global change.

8.2 A Cenozoic Age of Fishes

A constant thread throughout this dissertation is that following the K/Pg extinction, fish production, community structure, and diversity shifted in such a way to

greatly favor the group. Throughout the Cenozoic, fishes, particularly ray-finned fishes were able to quickly and consistently adapt to global change, either through changes in production or through diversification. The vast majority of Paleogene and extant ray-finned fish diversity developed in the Paleocene, while other clades diversified later, in the Early Eocene. However, fish production reached an all-time high during the Eocene greenhouse, even as diversity in tooth morphology in the open ocean declined. Total fish production is decoupled from shifts in diversity and community structure, suggesting that fish diversity and community structure is governed by evolutionary, rather than ecological processes. Further, the high-temporal resolution ichthyolith records in this dissertation show that the K/Pg event marked a turning point for the group, allowing fishes to expand, diversify, and thrive in the Cenozoic, arguably the true “Age of Fishes” (Friedman and Sallan, 2012; Near et al., 2012; Sibert and Norris, 2015).

8.3 The future of ichthyolith work

This dissertation has barely scratched the surface of potential for the ichthyolith record. There are many time periods and environments still to study: I have focused on the open ocean Paleogene for the majority of this dissertation, however Chapter 7 suggests that both the Cretaceous and the Neogene open ocean ecosystems are distinctly different from the Paleogene. I have worked with several students during my dissertation who have generated ichthyolith records for some of the time periods which I have not yet focused on, but which support the main findings of this dissertation: the Miocene (23-5 Ma, work by Jose Cuevas), the Eocene/Oligocene (40-25 Ma, work by Michelle Zill), and the Paleocene-Eocene Thermal maximum (PETM, 56 Ma, work by Douglas

Tomeczik). Doug's work at the PETM showed that on extremely fine timescales, not captured by my red clay record, the PETM is associated a significant increase in fish production, but no change in the fish community. Jose's work on the Miocene has revealed that there is considerable variability in fish production throughout the interval, and it may be correlated with export production proxies such as biogenic barium preserved in deep-sea sediments. Further, Michelle's work at the Eocene-Oligocene boundary showed that the transition had a geographically and temporally heterogeneous effect on absolute fish productivity, with Antarctic sites declining before sites located farther to the north. Further, Michelle's work confirmed an observation made in Chapter 7 of the dissertation from ODP Site 886, that fish production, measured by IAR appears to be inversely related to diatom abundance during the Oligocene and Miocene. In addition, this dissertation was largely limited to gyre sediments, but there is considerable potential for future work comparing the dynamics of onshore and offshore ecosystems through time and across climate events.

A particularly important "next step" in the field of ichthyolith micropaleontology is to ground-truth the proxy in the modern, both from a biological production, and a taxonomic and ecological standpoint. Comparisons of ichthyolith abundance and community structure in sediments from different habitats will improve our understanding of past fish production. Further, to better understand changes in the fish community, a system which provides some taxonomic or ecological context to the shapes and structures of the ichthyoliths is paramount. If we can identify different taxonomic clades or ecological guilds of fishes in the ichthyolith record, we can study the evolution of fish ecology at fine-scale resolution.

Indeed, ichthyoliths have many potential applications, from paleoceanography and paleobiology, to conservation biology, historical ecology, and even archaeology. In this dissertation, I have demonstrated that ichthyoliths are a viable and significant fossil group, and developed methods of analysis for the ichthyolith fossil record. Yet this dissertation truly represents a beginning in the field. Nearly every ichthyolith-based discovery has been somewhat surprising, pointing to more questions and ideas about how fish have evolved and interacted with the open ocean ecosystem, and the field of ichthyolith research will only continue to expand and diversify in the years to come.

8.4 References

- D'Hondt, S., Donaghay, P., Zachos, J. C., Luttenberg, D., and Lindinger, M., 1998, Organic carbon fluxes and ecological recovery from the Cretaceous-Tertiary mass extinction: *Science*, v. 282, no. 5387, p. 276-279.
- Doyle, P. S., 1983, Ichthyolith stratigraphy in the Pacific, *Eos, Transactions, American Geophysical Union*, Volume 64: Washington, American Geophysical Union, p. 741-742.
- Doyle, P. S., and Riedel, W. R., 1979, Cretaceous to Neogene Ichthyoliths in a Giant Piston Core from the Central North Pacific: *Micropaleontology*, v. 25, no. 4, p. 337-364.
- Doyle, P. S., and Riedel, W. R., 1985, *Cenozoic and Late Cretaceous ichthyoliths*, Cambridge, United Kingdom (GBR), Cambridge Univ. Press, Cambridge, Plankton stratigraphy.
- Doyle, P. S., Riedel, W. R., Heath, G. R., Burckle, L. H., D'Agostino, A. E., Bleil, U., Horai, K.-i., Jacobi, R. D., Janecek, T. R., Koizumi, I., Krissek, L. A., Monechi, S., Lenotre, N., Morley, J. J., Schultheiss, P. J., and Wright, A. A., 1985, Ichthyolith biostratigraphy of western North Pacific pelagic clays, *Deep Sea Drilling Project Leg 86: Initial Reports of the Deep Sea Drilling Project*, v. 86, p. 349-366.

- Friedman, M., and Sallan, L. C., 2012, Five hundred million years of extinction and recovery: a Phanerozoic survey of large-scale diversity patterns in fishes: *Palaeontology*, v. 55, no. 4, p. 707-742.
- Hsu, K. J., and McKenzie, J. A., 1985, A "Strangelove" ocean in the earliest Tertiary: *Geophysical Monograph*, vol.32, p. 487-492.
- Huck, C. E., van de Flieddt, T., Jiménez-Espejo, F. J., Bohaty, S. M., Röhl, U., and Hammond, S. J., 2016, Robustness of fossil fish teeth for seawater neodymium isotope reconstructions under variable redox conditions in an ancient shallow marine setting: *Geochemistry, Geophysics, Geosystems*, p. n/a-n/a.
- Hull, P. M., and Norris, R. D., 2011, Diverse patterns of ocean export productivity change across the Cretaceous-Paleogene boundary: New insights from biogenic barium: *Paleoceanography*, v. 26, no. 26, p. 3205.
- Iverson, R. L., 1990, Control of Marine Fish Production: *Limnology and Oceanography*, v. 35, no. 7, p. 1593-1604.
- Johns, M. J., Barnes, C. R., and Narayan, Y. R., 2006, Cenozoic ichthyolith biostratigraphy; Tofino Basin, British Columbia: *Canadian Journal of Earth Sciences = Revue Canadienne des Sciences de la Terre*, v. 43, no. 2, p. 177-204.
- Lyle, M., and Baldauf, J., 2015, Biogenic sediment regimes in the Neogene equatorial Pacific, IODP Site U1338: Burial, production, and diatom community: *Palaeogeography, Palaeoclimatology, Palaeoecology*.
- Martin, E., and Haley, B., 2000, Fossil fish teeth as proxies for seawater Sr and Nd isotopes: *Geochimica Et Cosmochimica Acta*, v. 64, no. 5, p. 835-847.
- Moloney, C. L., and Field, J. G., 1991, The size-based dynamics of plankton food webs. I. A simulation model of carbon and nitrogen flows: *Journal of plankton research*, v. 13, no. 5, p. 1003-1038.
- Near, T. J., Eytan, R. I., Dornburg, A., Kuhn, K. L., Moore, J. A., Davis, M. P., Wainwright, P. C., Friedman, M., and Smith, W. L., 2012, Resolution of ray-finned fish phylogeny and timing of diversification: *Proceedings of the National Academy of Sciences of the United States of America*, v. 109, no. 34, p. 13698-13703.
- Nelson, J. S., 2006, *Fishes of the World*, New York, NY, Wiley, 600 p.:
- Scher, H. D., and Martin, E. E., 2004, Circulation in the Southern Ocean during the Paleogene inferred from neodymium isotopes: *Earth and Planetary Science Letters*, v. 228, no. 3-4, p. 391-405.

- Sibert, E. C., Hull, P. M., and Norris, R. D., 2014, Resilience of Pacific pelagic fish across the Cretaceous/Palaeogene mass extinction: *Nature Geosci*, v. 7, no. 9, p. 667-670.
- Sibert, E. C., and Norris, R. D., 2015, New Age of Fishes initiated by the Cretaceous–Paleogene mass extinction: *Proceedings of the National Academy of Sciences*, v. 112, no. 28, p. 8537-8542.
- Sibert, E. C., Norris, R. D., Cuevas, J. M., and Graves, L. G., 2016, 85 million years of Pacific Ocean Gyre ecosystem structure: long-term stability marked by punctuated change: *Proceedings of the Royal Society B: Biological Sciences*, no. In press.
- Thomas, D. J., Korty, R., Huber, M., Schubert, J. A., and Haines, B., 2014, Nd isotopic structure of the Pacific Ocean 70–30 Ma and numerical evidence for vigorous ocean circulation and ocean heat transport in a greenhouse world: *Paleoceanography*, v. 29, no. 5, p. 2013PA002535.